A STUDY OF THE SYNTHESIS, CHARACTERIZATION AND CYTOTOXICITY OF TROPONES AND TROPONIMINES AND ITS RHENIUM(I) COORDINATION COMPOUNDS

by

LEANDRI JANSEN VAN VUUREN

A dissertation submitted in fulfilment of the requirements in respect

of the Master's Degree

MAGISTER SCIENTIAE

in the

DEPARTMENT OF CHEMISTRY

in the

FACULTY OF NATURAL AND AGRICULTURAL SCIENCES

at the

UNIVERSITY OF THE FREE STATE

SUPERVISOR: DR MARIETJIE SCHUTTE-SMITH

CO-SUPERVISOR: PROF. HENDRIK GIDEON VISSER

February 2020

Acknowledgements

The glory and honour all belong to my Heavenly Father for his unfailing love, grace and the talents and gifts He has given me.

I would like to express my humble and sincere gratitude towards everyone who assisted and supported me in any way throughout the year.

Marietjie, for your unwavering motivation, support and guidance as a supervisor and a friend. Thank you for believing in me and teaching me hard work and determination. Your passion and love for life are inspiring.

Deon, thank you for your input in my work and the support and guidance you give.

All my colleagues in the Inorganic Chemistry group, for your support and assistance, especially with crystallography. A special thanks to Christo, Jeaneme, Lucy and Ursula for the camaraderie.

Dr Eleanor Müller at the Chemistry Department (UFS), thank you for the time and effort you put into my cytotoxicity studies. I appreciate it.

Prof. Ted Kroon at the Physics Department (UFS), thank you for the use of your laboratory and photoluminescence equipment and for your assistance. I appreciate all your time and effort.

The National Research Foundation (NRF) for funding.

All my friends and family, for your care, support and love. I am blessed with so many wonderful people in my life. A special thank you to my future parents-in-law, Hennie and Marika. Thank you for your support, welcoming me into your family and loving me as your own.

To my parents, Ben and Hantie. I can't thank you enough for the sacrifices you've made to give me the best life possible. Thank you for your support and unconditional love every day. I love and appreciate you very much. My siblings, Cornél, Jan, Jami and Benji, thank you for your love and your friendship.

Rikus, thank you for being by my side every step of the way and for your unfaltering love, especially through the tough times. I am privileged to have you in my life. Thank you for the wonderful example you set with your ambition, determination and love for life.

"Be thankful for what you have. Work hard for what you don't have."

TABLE OF CONTENTS

TABLE OF CONTENTS

TABLE OF CONTENTS

TABLE OF CONTENTS

TABLE OF CONTENTS

TABLE OF CONTENTS

SYMBOLS AND ABBREVIATIONS

Å	angstrom
α	alpha
β	beta
γ	gamma
B_0	magnetic field strength
c	Speed of light in a vacuum
δ	chemical shift
h	Planck's constant
ℓ	overall spin
λ	Wavelength
ν	Frequency
$\bar{\nu}$	Wavenumber
E	Energy
σ	Sigma
θ	Theta
ω	angular frequency
AA	Atomic Absorption
ACRAMTU	1-[2-(acridin-9-ylamino)ethyl]-1,3-dimethylthiourea
ACS	The American Cancer Society
ADME-Tox	Absorption, Distribution, Metabolism, Excretion and Toxicity
AgNPs	Silver nanoparticles
AIDS	Acquired immune deficiency syndrome
APL	Acute promyelocytic leukemia
ATIH	Aminotroponimine
ATO	Arsenic trioxide
ATRA	All-*trans*-retinoic acid
AuNPs	Gold nanoparticles
Bisim	Bisimine
CML	Chronic myelogenous leukemia
CO	Carbonyl
DAD	1,4-diazabutadiene
DAPTA	1,4-diacetyl-1,3,7-triaza-5-phosphabicyclo[3.3.1]nonane
DAR	Darinaparsin
DNA	Deoxyribonucleic acid
Dox	Doxorubicin

SYMBOLS AND ABBREVIATIONS

en	Ethane-1,2-diamine
fac	*facial*
FDA	Food and Drug Administration
FID	free induction decay
GC	Gas Chromatography
HDAC	Histone deacetylase
HPV	Human Papilloma Virus
HSAB	'Hard and Soft Acid and Base'
IC_{50}	Half maximal inhibitory concentration
ICP	Inductively Coupled Plasma
IR	Infrared absorption
KP1019	Indazolium *trans*-[tetrachloridobis(1H-indazole)ruthenate(III)]
MLCT	Metal-to-ligand-charge-transfer
MDR	Multidrug resistance
MS	Mass Spectrometry
N_4	Tetraamide
NKP-1339	Sodium *trans*-[tetrachloridobis(1H-indazole)ruthenate(III)]
NMR	Nuclear Magnetic Resonance
NMSC	Non-melanoma skin cancer
NO	Nitric oxide
$^1O_2$	Singlet oxygen
$^3O_2$	Molecular oxygen
O_2^-	Superoxide anion
OH	Hydroxyl radical
PACT	Photoactivated chemotherapy
PT-ACRAMTU	$[PtCl(en)\text{-}(ACRAMTU)](NO_3)_2$
PTA	1,3,5-triaza-7-phosphaadamantane
PDT	Photodynamic therapy
ppb	parts per billion
PS	Photosensitizer
RNA	Ribonucleic acid
ROS	Reactive oxygen species
SubH	Suberoyl-bis-hydroxamic acid

SYMBOLS AND ABBREVIATIONS

TAMs	Tumor associated macrophages
*t*Bu$_2$bp	4,4'-di-*tert*-butyl-2,2'-bipyridine
THP	tris(hydroxymethyl)phosphine
US	United States
UV/Vis	Ultraviolet-visible
XRD	X-ray Diffraction

In Re(I) tricarbonyl complexes:

TropNMe	2-(Methylamino)troponato anion
TropNEt	2-(Ethylamino)troponato anion
TropNEtF	2-(2-Fluoroethylamino)troponato anion
TropNEtPh	2-(Phenethylamino)troponato anion
TropNHBn	2-(Benzylamino)troponato anion
(Me)$_2$ATI	*N*-Methyl-2-(methylamino)troponiminato anion
(Et)$_2$ATI	*N*-Ethyl-2-(ethylamino)troponiminato anion
(EtF)$_2$ATI	*N*-2-Fluoroethyl-2-(2-fluoroethylamino)troponiminato anion
(EtPh)$_2$ATI	*N*-Phenethyl-2-(phenethylamino)troponiminato anion
(Bn)$_2$ATI	*N*-Benzyl-2-(benzylamino)troponiminato anion
(Me,Bn)ATI	*N*-Methyl-2-(benzylamino)troponiminato anion
(Et,Bn)ATI	*N*-Ethyl-2-(benzylamino)troponiminato anion
(EtF,Bn)ATI	*N*-2-Fluoroethyl-2-(benzylamino)troponiminato anion
(EtPh,Bn)ATI	*N*-Phenethyl-2-(benzylamino)troponiminato anion

ABSTRACT

Rhenium(I) tricarbonyl complexes have gained much interest over the past years for its possible applications in radiopharmacy, chemotherapy and photodynamic therapy (PDT). In order to defeat cancer worldwide, it is imperative that scientists develop better, and improve current treatment methods. In this study the aim is to expand the knowledge on Re(I) tricarbonyl complexes and its potential in anticancer research, with the focus on good cytotoxicity and photoluminescent properties.

Five *N,O* bidentate 2-(alkylamino)tropone ligand systems were successfully synthesized in yields between 22 % and 66 %. Nine *N,N'* bidentate aminotroponimine ligand systems were successfully synthesized in yields ranging from 22 % to 74 %. Five Re(I) tricarbonyl complexes of the type *fac*-[$Re(CO)_3(H_2O)$(*N,O*)] (*N,O* = different *N,O* bidentate ligands) and nine of the type *fac*-[$Re(CO)_3(H_2O)$(*N,N'*)] (*N,N'* = different *N,N'* bidentate ligands) were synthesized successfully in yields of 66 % - 75 % and 53 % - 94 %, respectively.

The crystal structures of 2-tosyloxytropone (TropOTs), 2-(methylamino)tropone (TropNHMe) and 2-(2-fluoroethylamino)tropone (TropNHEtF) were obtained, solved and reported in this study. The structures of these molecules have interesting packing patterns in their unit cells. TropNHMe has three molecules in the asymmetric unit and TropOTs and TropNHEtF have only one. Hydrogen bonding interactions are observed in all three the structures and in TropNHMe these interactions form one-dimensional infinite chains. In the structures of TropOTs and TropNHMe π-π interactions are observed, but not in TropNHEtF, where hydrogen bonding interactions are possibly responsible for the packing pattern observed in the unit cell.

The *in vitro* cytotoxicity of all the ligands and four of the *fac*-[$Re(CO)_3(H_2O)$(*N,O*)] (*N,O* = different *N,O* bidentate ligands) complexes was determined. The results include IC_{50} values ranging from 0.45 μM - 36.1 μM for the ligands and 47.0 μM - 77.4 μM for the complexes. Four of the *N,N'* bidentate ligands, namely [(EtPh,Bn)ATI]H, [(Me,Bn)ATI]H, [(Et,Bn)ATI]H and [$(EtPh)_2$ATI]H have IC_{50} values of 0.45, 0.66, 1.10 and 2.4 μM, respectively, which are lower than that of cisplatin, the control in this study, with an IC_{50} value of 3.26 μM.

ABSTRACT

Selected ligands and complexes were evaluated for its photoluminescent properties and the results are reported in this study. The excitation wavelengths of the ligands and complexes range from 257 nm - 377 nm and the emission wavelengths from 405 nm - 517 nm. The intensity of the emissions ranges from 2.37 x 10^3 to 21.5 x 10^3 arbitrary units with $[(Me)_2ATI]H$ having an exceptionally high intensity value of 218.0 x 10^3 arbitrary units. The 2-(alkylamino)tropone ligands and its complexes have longer excitation wavelengths than that of the aminotroponimine ligands and its complexes with *fac*-$[Re(CO)_3(H_2O)(TropNEtPh)]$ being the exception. TropNHEtF, TropNHBn and TropNHEtPh and their Re(I) tricarbonyl complexes *fac*-$[Re(CO)_3(H_2O)(TropNEtF)]$, *fac*-$[Re(CO)_3(H_2O)(TropNBn)]$ and *fac*-$[Re(CO)_3(H_2O)(TropNEtPh)]$ are the three ligand-complex pairs that exhibit red shifts in their emissions from the ligand to the complex. The quantum yields of the compounds could unfortunately not be determined successfully due to the low intensities of the emissions.

Key terms:

Re(I) tricarbonyl, cytotoxicity, photoluminescence, X-ray crystallography, 2-(alkylamino)tropone, aminotroponimine, chemotherapy, photodynamic therapy, *N,O* bidentate, *N,N'* bidentate

1

GENERAL BACKGROUND AND AIM

1.1 Introduction to the current challenges and opportunities in cancer research

The term ‘cancer’ refers to a group of diseases that involves the abnormal growth and division of cells in the body. The cells are able to metastasize and spread to other tissue and organs in the body, forming malignant tumors. Tumors that do not metastasize are called benign.[1] Cancer is primarily caused by genetic mutations in cells due to lifestyle, environmental and hereditary factors.[2]

Although cancer represents diseases with frightening statistics and consequences, there are some breakthroughs in the fight against it. The American Cancer Society (ACS) conducted research that shows that the cancer mortality rate in the United States (US) decreased with 27 % from 1991 to 2016 due to less smoking, better screening and diagnosis and more successful treatment of cancer.[3] Although this seems like a promising prospective there is an increase in cancer incidence rates linked to obesity among adults under 50 years of age. Another alarming fact is that younger generations such as millennials (born around 1985) have twice the risk to develop six types of cancer than baby boomers (born around 1950) when they were the same age.[3] Cancer rates are also increasing due to people living longer and having a higher risk of developing cancer at a higher age. The manifestation of certain types of cancer such as cancer induced by the Human Papilloma Virus (HPV), gastrointestinal cancers and skin cancer are also increasing due to the lifestyle of people constantly changing for the worst.[4]

---

[1] Cancer. (2019). Retrieved 20 October 2019, from https://www.who.int/en/news-room/fact-sheets/detail/cancer.

[2] Anand, P., Kunnumakara, A. B., Sundaram, C., Harikumar, K. B., Tharakan, S. T., Lai, O. S., Sung, B. & Aggarwal, B. B. (2008). *Pharmaceutical Research*, **25**(9), 2097-2116.

[3] Why Are More Young Adults Getting Cancer? Obesity May Be to Blame. (2020). Retrieved 3 January 2020, from https://www.mskcc.org/blog/why-are-more-young-adults-getting-cancer-obesity-may-be-blame.

[4] Center, D. (2020). The Three Reasons So Many People are Getting Cancer (Op-Ed). Retrieved 3 January 2020, from https://www.livescience.com/51099-the-three-reasons-cancer-rates-are-rising.html

Another major factor contributing to the battle to keep cancer incidence and mortality rates down is the number of cancer victims in rural areas around the world without access to adequate health care.[5] For example, in Africa, especially Sub-Saharan Africa, cancer does not receive high priority for health care services due to the overwhelming burden and incidence of the acquired immune deficiency syndrome (AIDS) as well as diseases such as hypertension and diabetes. The less affluent patients can often not afford any form of health care services regarding cancer and those in rural areas will also not have access to the services and therefore cancer is often diagnosed at a late stage and/or not treated adequately.[5] According to Levin *et al.* only 50 % of the population in Africa have access to radiation oncology services.[6]

The methods for the diagnosis and treatment of cancer are diverse and some are very invasive. Cancer treatments can be curative or palliative and includes surgery, chemotherapy, radiation therapy, hormonal therapy, targeted therapy and palliative care, depending on the type, progress and location of the tumor, as well as the patient's overall health and their preference.[7]

1.2 Chemotherapy

Chemotherapy utilizes chemicals in the form of drugs to inhibit the growth of and kill the fast-growing cancer cells in the body. Cancer cells are highly chemo sensitive and very responsive to chemotherapeutic agents which consist of cytotoxic chemical compounds. These compounds consist of organic molecules or metal complexes and interfere with the biological processes in the cells to inhibit their growth or kill them.[8] Chemotherapy is not only used for the treatment of cancer, but also for bone marrow and immune system diseases. Although it is a very effective treatment method, it is invasive and toxic, implicating many side effects, some of which are

[5] Jamison, D., Feachem, R., Makgoba, M., Bos, E., Rogo, K., Baingana, F. & Hofman, K. (2006). *Disease and Mortality in Sub-Saharan Africa* (2nd ed.). Washington, D.C: World Bank.

[6] Levin, C., El Gueddari, B. & Meghzifene, A. (1999). *Radiotherapy and Oncology*, **52**(1), 79-83.

[7] Cancer - Diagnosis and treatment - Mayo Clinic. (2019). Retrieved 20 October 2019, from https://www.mayoclinic.org/diseases-conditions/cancer/diagnosis-treatment/drc-20370594

[8] Lundqvist, E., Fujiwara, K. & Seoud, M. (2015). *International Journal of Gynecology & Obstetrics*, **131**, S146-S149.

mild and treatable and others being severe. These side effects limit the use of chemotherapeutic drugs and the exploration of alternative therapy is therefore crucial.[8]

1.3 Photodynamic therapy

The ongoing research conducted towards cancer yields new and improved diagnostic and therapeutic methods and ways to prevent cancer. A major challenge remains the discovery of methods that are non-invasive and have lower systemic toxicity and which are still selective towards cancer cells.[9] One of the alternative forms of therapy developed over the years is photodynamic therapy (PDT). PDT utilizes chemical compounds called photosensitizers to target specific cells or tissues which are destroyed upon exposure to light of a certain wavelength due to the reactive oxygen species (ROS) formed in the process.[10,11,12] These chemical compounds usually only become cytotoxic when exposed to light and renders this form of therapy less invasive than chemotherapy.

PDT has been used as an alternative treatment due to its lower toxicity and the lack of drug resistance associated with it.[13] The drug resistance is mainly overcome by PDT as a result of the photodamage caused by PDT to the cellular components where drug resistance originates.[13]

1.4 Rhenium(I) tricarbonyl complexes in cancer research

Although cisplatin, carboplatin and oxaliplatin are excellent platinum-based anticancer agents, they induce severe systemic toxicity and are prone to drug-resistance, two of the major challenges faced in cancer research. These

[9] Zhu, R., He, H., Liu, Y., Cao, D., Yan, J., Duan, S., Chen, Y. & Yin, L. (2019). *Biomacromolecules*, **20**(7), 2649-2656.
[10] Macdonald, I. & Dougherty, T. (2001). *Journal of Porphyrins and Phthalocyanines*, **5**(02), 105-129.
[11] Tampa, M., Sarbu, M., Matei, C., Mitran, C., Mitran, M., Caruntu, C., Constantin, C., Neagu, M. & Georgescu, S. (2019). *Oncology Letters*, **17**, 4085-4093.
[12] Matei, C., Tampa, M., Poteca, T., Panea-Paunica, G., Georgescu, S. R., Ion, R. M., Popescu, S. M. & Giurcaneanu, C. (2013). *Journal of Medicine and Life*, **6**(1), 50-54.
[13] Spring, B., Rizvi, I., Xu, N. & Hasan, T. (2015). *Photochemical and Photobiological Sciences*, **14**(8), 1476-1491.

compounds have sparked interest in the development of new possible drug candidates containing metal centers.[14]

This also led to the investigation of rhenium complexes, which are rapidly gaining interest as anticancer agents. These complexes have generally desired properties such as high stability, structural diversity and rich spectroscopic properties.[15] Many research studies prove their *in vitro* anticancer activity, highlighting compounds that are even more potent than cisplatin in certain cancer cell lines and that can overcome the challenge of drug resistance by inducing cell death *via* distinct mechanisms from cisplatin.[14,16,17,18,19] Compounds containing the stable rhenium(I) tricarbonyl core have been broadly investigated as possible imaging and therapeutic agents.[16,18,19,20,21]

1.5 Tropolone-derived ligand systems

Tropolone and its derivatives are non-benzenoid compounds collectively called troponoids or tropolonoids and many of these natural compounds have

[14] Konkankit, C., King, A., Knopf, K., Southard, T. & Wilson, J. (2019). *ACS Medicinal Chemistry Letters*, **10**(5), 822-827.
[15] Lee, L., Leung, K. & Lo, K. (2017). *Dalton Transactions*, **46**(47), 16357-16380.
[16] Gantsho, V., Dotou, M., Jakubaszek, M., Goud, B., Gasser, G., Visser, H. & Schutte-Smith, M. (2020). *Dalton Transactions*, **49**(1), 35-46.
[17] Shtemenko, N. I., Chifotides, H. T., Domasevitch, K. V., Golichenko, A. A., Babiy, S. A., Li, Z., Paramonova, K. V., Shtemenko, A. V. & Dunbar, K. R. (2013). *Journal of Inorganic Biochemistry*, **129**, 127-134.
[18] He, L., Pan, Z., Qin, W., Li, Y., Tan, C. & Mao, Z. (2019). *Dalton Transactions*, **48**(13), 4398-4404.
[19] Collery, P., Mohsen, A., Kermagoret, A., Corre, S., Bastian, G., Tomas, A., Wei, M., Santoni, F., Guerra, N., Desmaële, D. & D'angelo, J. (2015). *Investigational New Drugs*, **33**(4), 848-860.
[20] Hostachy, S., Policar, C. & Delsuc, N. (2017). *Coordination Chemistry Reviews*, **351**, 172-188.
[21] Suntharalingam, K., Awuah, S. G., Bruno, P. M., Johnstone, T. C., Wang, F., Lin, W., Zheng, Y., Page, J. E., Hemann, M. T. & Lippard, S. J. (2015). *Journal of The American Chemical Society*, **137**(8), 2967-2974.

antimicrobial,[22] antiviral[23] and anticancer[24,25,26,27,28] activities. These compounds are versatile ligands used in inorganic and organometallic chemistry.[29,30] The functionality of these ligands is usually attributed to the carbonyl oxygen (O) or imine nitrogen (N) and the vicinal coordinating substituent, generally also oxygen or nitrogen, which both impart a metal chelating ability to these types of ligand systems. Another characteristic of these ligand systems is the conjugated ten π-electron backbone which stabilizes the ligand.[31]

1.6 Aim of this study

The aims set for this study are as follows:

- The synthesis and characterization of five *N,O* bidentate ligand systems - (2-alkylamino)tropones:
    - 2-(Methylamino)tropone (TropNHMe)
    - 2-(Ethylamino)tropone (TropNHEt)
    - 2-(2-Fluoroethylamino)tropone (TropNHEtF)
    - 2-(Phenethylamino)tropone (TropNHEtPh)
    - 2-(Benzylamino)tropone (TropNHBn)

[22] Saleh, N. A., Zfiefak, A., Mordarski, M. & Pulverer, G. (1988). *Zentralblatt fuer Bakteriologie, Mikrobiologie und Hygiene, Series A: Medical Microbiology, Infectious Diseases, Virology, Parasitology*, **270**, 160-170.
[23] Tavis, J. E. & Lomonosova, E. (2015). *Antiviral Research*, **118**, 132-138.
[24] Liu, S. & Yamauchi, H. (2006). *Biochemical and Biophysical Research Communications*, **351**(1), 26-32.
[25] Haney, S. L., Allen, C., Varney, M. L., Dykstra, K. M., Falcone, E. R., Colligan, S. H., Hu, Q., Aldridge, A. M., Wright, D. L., Wiemer, A. J. & Holstein, S. A. (2017). *Oncotarget*, **8**(44), 76085-76098.
[26] Jayakumar, T., Liu, C., Wu, G., Lee, T., Manubolu, M., Hsieh, C., Yang, C. & Sheu, J. (2018). *International Journal of Molecular Sciences*, **19**(4), 939-952.
[27] Balsa, L., Ruiz, M., Santa Maria de la Parra, L., Baran, E. & León, I. (2020). *Journal of Inorganic Biochemistry*, **204**, 110975.
[28] Ononye, S., VanHeyst, M., Oblak, E., Zhou, W., Ammar, M., Anderson, A. & Wright, D. (2013). *ACS Medicinal Chemistry Letters*, **4**(8), 757-761.
[29] Roesky, P. (2000). *Chemical Society Reviews*, **29**(5), 335-345.
[30] Schutte-Smith, M., Roodt, A. & Visser, H. (2019). *Dalton Transactions*, **48**(27), 9984-9997.
[31] Nishinaga, T., Aono, T., Isomura, E., Watanabe, S., Miyake, Y., Miyazaki, A., Enoki, T., Miyasaka, H., Otani, H. & Iyoda, M. (2010). *Dalton Transactions*, **39**, 2293-2300.

- The synthesis and characterization of nine *N,N'* bidentate ligand systems - aminotroponimines:
    - *N*-Methyl-2-(methylamino)troponimine ([$(Me)_2$ATI]H)
    - *N*-Ethyl-2-(ethylamino)troponimine ([$(Et)_2$ATI]H)
    - *N*-2-Fluoroethyl-2-(2-fluoroethylamino)troponimine ([$(EtF)_2$ATI]H)
    - *N*-Phenethyl-2-(phenethylamino)troponimine ([$(EtPh)_2$ATI]H)
    - *N*-Benzyl-2-(benzylamino)troponimine ([$(Bn)_2$ATI]H)
    - *N*-Methyl-2-(benzylamino)troponimine ([(Me,Bn)ATI]H)
    - *N*-Ethyl-2-(benzylamino)troponimine ([(Et,Bn)ATI]H)
    - *N*-2-Fluoroethyl-2-(benzylamino)troponimine ([(EtF,Bn)ATI]H)
    - *N*-Phenethyl-2-(benzylamino)troponimine ([(EtPh,Bn)ATI]H)
- The synthesis and characterization of five *fac*-Re(I) tricarbonyl complexes of the type *fac*-[$Re(CO)_3(H_2O)$(*N,O*)]:
    - *fac*-[$Re(CO)_3(H_2O)$(TropNMe)]
    - *fac*-[$Re(CO)_3(H_2O)$(TropNEt)]
    - *fac*-[$Re(CO)_3(H_2O)$(TropNEtF)]
    - *fac*-[$Re(CO)_3(H_2O)$(TropNEtPh)]
    - *fac*-[$Re(CO)_3(H_2O)$(TropNBn)]
- The synthesis and characterization of nine *fac*-Re(I) tricarbonyl complexes of the type *fac*-[$Re(CO)_3(H_2O)$(*N,N'*)]:
    - *fac*-[$Re(CO)_3(H_2O)$($(Me)_2$ATI)]
    - *fac*-[$Re(CO)_3(H_2O)$($(Et)_2$ATI)]
    - *fac*-[$Re(CO)_3(H_2O)$($(EtF)_2$ATI)]
    - *fac*-[$Re(CO)_3(H_2O)$($(EtPh)_2$ATI)]
    - *fac*-[$Re(CO)_3(H_2O)$($(Bn)_2$ATI)]
    - *fac*-[$Re(CO)_3(H_2O)$((Me,Bn)ATI)]
    - *fac*-[$Re(CO)_3(H_2O)$((Et,Bn)ATI)]
    - *fac*-[$Re(CO)_3(H_2O)$((EtF,Bn)ATI)]
    - *fac*-[$Re(CO)_3(H_2O)$((EtPh,Bn)ATI)]
- The solid-state crystal structure determination of ligands and compounds
- The cytotoxicity evaluation of the ligands and compounds
- The photoluminescence studies of the ligands and compounds and the determination of the quantum yields

Chapter 1

To be able to achieve the goals set for this study, a thorough background of the chemical workings of possible oncological treatment methods relevant to this research is necessary. It is also needful to gain knowledge on the chemical compounds already involved in these treatment methods as well as the prospective compounds chosen for this study and their mechanisms of action by which they cripple cancer cells. These subjects will be discussed amply in Chapter 2.

2
LITERATURE STUDY

2.1 Cancer

By the time a person dies they would have dealt with cancer at least once in their life. Whether it be a friend, a family member or oneself, some currently has it or had it in the past. This disease has existed through all human history.[1] Cancer is a group of diseases that involves the abnormal division and growth of cells that can also metastasize, in other words spread to other parts of the body. Tumors of this sort are called malignant and those that do not metastasize are called benign.[2] About 90 - 95 % of cancer cases are caused by genetic mutations due to environmental and lifestyle factors. The remaining 5 - 10 % are as a result of inherited genetics.[3]

Cancer is usually diagnosed due to the appearance of symptoms, which does not happen in all cases, or through routine screening. A definitive diagnosis cannot be made immediately, and further examinations are required, such as physical examinations, laboratory tests, biopsies, and imaging tests.[4] Various treatment options are available for cancer patients, whether it be curative or palliative. The primary treatments include surgery, chemotherapy, radiation therapy, hormonal therapy, targeted therapy, and palliative care. The treatment that is used will depend on the type, location and progress of the cancer as well as the patient's overall health and, of course, preference.[4]

Cancer is expected to be ranked as the leading cause of death worldwide in the 21st century. The incidence and mortality rates are growing rapidly worldwide. The reasons for this are complicated but do reflect ageing, population growth and

[1] Hajdu, S. (2010). *Cancer*, **117**(5), 1097-1102.
[2] Cancer. (2019). Retrieved 20 October 2019, from https://www.who.int/en/news-room/fact-sheets/detail/cancer.
[3] Anand, P., Kunnumakara, A. B., Sundaram, C., Harikumar, K. B., Tharakan, S. T., Lai, O. S., Sung, B. & Aggarwal, B. B. (2008). *Pharmaceutical Research*, **25**(9), 2097-2116.
[4] Cancer - Diagnosis and treatment - Mayo Clinic. (2019). Retrieved 20 October 2019, from https://www.mayoclinic.org/diseases-conditions/cancer/diagnosis-treatment/drc-20370594

changes in the occurrence and distribution of the main risk factors for cancer, of which many are related to socioeconomic development.[5]

In their Global cancer statistics of 2018,[5] Bray *et al.* estimated that there would be 18.1 million new cases of cancer (17.0 million excluding non-melanoma skin cancer (NMSC)) and 9.6 million deaths due to cancer (9.5 million excluding NMSC) worldwide in 2018. There are more than 100 types of cancers affecting humans.[2] Table 2.1 shows the cancer types with the highest incidence and mortality rates (% of total cases) in both sexes combined.[5]

Table 2.1: The cancer types with the highest incidence and mortality rates worldwide.

Incidence	Mortality
Lung cancer (11.6 %)	Lung cancer (18.4 %)
Female breast cancer (11.6 %)	Colorectal cancer (9.2 %)
Prostate cancer (7.1 %)	Stomach cancer (8.2 %)
Colorectal cancer (6.1 %)	Liver cancer (8.2 %)

The cancer with the highest incidence and mortality rate, however, will vary substantially across countries depending on the degree of economic development and the associated social and lifestyle factors.[2,5]

Cancer is a worldwide problem, with limited success to its prevention, diagnosis, and treatment. The development of new and better forms of diagnosis as well as treatment is a never-ending assignment for researchers in various fields. In this research project, the focus will be on the investigation of compounds suitable for chemotherapy as well as photodynamic therapy.

2.2 Chemotherapy

Chemotherapy uses cytotoxic chemical compounds to cause cell death or cell growth inhibition *via* numerous biological mechanisms.[6] The many possible adverse effects of these compounds limit the use of these drugs, and the appropriate selection of it for specific patients is critical. Cancer cells are fast proliferating cells

[5] Bray, F., Ferlay, J., Soerjomataram, I., Siegel, R., Torre, L. & Jemal, A. (2018). *CA: A Cancer Journal for Clinicians*, **68**(6), 394-424.
[6] Lundqvist, E., Fujiwara, K. & Seoud, M. (2015). *International Journal of Gynecology and Obstetrics*, **131**, S146-S149.

that are actively going through the different stages of the cell cycle. These cells are highly chemo sensitive and are therefore more responsive to chemotherapy.[6]

According to Lind,[7] chemotherapeutic drugs can be classified into the following groups according to their mechanism and the type of compound:

- Alkylating agents: A group of chemically reactive drugs that covalently bonds with DNA to cause breaking and cross-linking of DNA strands.[7]
- Platinum compounds: These compounds are activated intracellularly to form reactive intermediates that covalently bonds with nucleotides from DNA strand cross-links.[8]
- Antimetabolites: These compounds' structures are similar to naturally occurring purines and pyrimidines.[9,10] They have two modes of action:
  - Inhibition of key enzymes involved in DNA synthesis.
  - Incorporation into DNA and RNA to form breaks in strands.
- Anthracyclines and related compounds: Originally these compounds were antibiotics produced by microorganisms.[7] Their mechanisms involve:
  - Intercalation with DNA, causing strand breaks in DNA.
  - Generation of free radicals causing oxidative damage to cellular proteins.
  - Topoisomerase (II) inhibition.
- Topoisomerase inhibitors: Topoisomerase enzymes control the three-dimensional structure of DNA. They have an important function in DNA replication and transcription.[11]
- Tubulin-binding drugs: Microtubules, of which tubulin is the basic subunit, has important functions in the cell and cell replication processes. Several classes of chemo drugs are known to interfere with the functioning of tubulin.[7]
- Tyrosine kinase inhibitors: These enzymes contain an extracellular ligand binding site. Binding of chemo drugs to this site results in the dysfunction of important processes in the cell involved with tyrosine kinases.[7]

---

[7] Lind, M. (2008). *Medicine*, **36**(1), 19-23.
[8] Belani, C. (2004). *Seminars in Oncology*, **31**, 25-33.
[9] Walling, J. (2006). *Investigational New Drugs*, **24**(1), 37-77.
[10] Rose, M., Farrell, M. & Schmitz, J. (2002). *Clinical Colorectal Cancer*, **1**(4), 220-229.
[11] Pommier, Y. (2006). *Nature Reviews Cancer*, **6**(10), 789-802.

2.2.1 Cytotoxicity

Chemotherapy, as discussed in the previous section, substantially relies on cytotoxic agents to cause damage and cell death to cancer cells, which are rapidly dividing and reproducing cells.

The term cytotoxicity refers to a quality of a compound being toxic to cells. The toxins induce a number of adverse events in the cells: [12,13]

- Necrosis due to the loss of membrane integrity. The cells die rapidly as a result of cell lysis.
- Cell viability decreases, meaning that cells cease to actively grow and divide.
- Apoptosis which is controlled cell death as a result of a genetic program.

When cells undergo necrosis, rapid swelling will occur, membrane integrity will be lost, the metabolism will shut down and the cell contents will be released into the environment. Since necrosis is such a fast process, there is not enough time for the cells to activate certain genetic programs for apoptosis to occur and therefore will not express apoptotic markers. During apoptosis, clearly defined cytological and molecular events occur, including a change in the cell's refractive index, shrinkage of the cytoplasm, nuclear condensation, and DNA cleavage. Secondary necrosis could also follow apoptosis, again leading to the metabolism shutting down, loss of membrane integrity and cell lysis.

An important part of investigating compounds as possible medicinal, especially chemotherapeutic agents, is determining the cytotoxicity and mechanism of cell death of these compounds.[12,13,14] Thus, there is a need for cheap, reliable and reproducible short-term cytotoxicity and cell viability assays. These assays are based on the various cell functions and how they are affected by the chemicals they are exposed to. Currently, there are various cytotoxicity assays being used in the fields of toxicology and pharmacology. Their methods are mostly based on the

[12] Riss, T. & Moravec, R. (2004). *ASSAY and Drug Development Technologies*, **2**(1), 51-62.

[13] Aslantürk, Ö. (2018). *Genotoxicity - A Predictable Risk to Our Actual World*. doi: 10.5772/intechopen.71923

[14] Niles, A., Moravec, R., Eric Hesselberth, P., Scurria, M., Daily, W. & Riss, T. (2007). *Analytical Biochemistry*, **366**(2), 197-206.

evaluation of, and distinction between healthy and damaged cells after administration of chemicals of a certain concentration.[12]

For researchers to compare their results and findings with others in literature, a common unit is used when referring to cytotoxicity results. The half maximal inhibitory concentration (IC_{50}) is a measure of the potency of a substance in inhibiting a specific biological or biochemical function. Therefore, IC_{50} is a useful quantitative measure of the *in vitro* cytotoxicity of a compound and is usually expressed in molar (M) concentration.[15]

2.2.2 Cytotoxicity of *N,O* and *N,N'* bidentate ligands

In many studies these days the focus is on the influence of a ligand on the antitumor activity of a metal complex.[16] Abbasi and co-workers synthesized a novel Schiff base ligand derived from 2-hydroxy-1-naphthaldehyde and 2-methoxyethylamine and its mononuclear Cu(II), Ni(II) (Figure 2.1) and V(IV) complexes.[16] They tested the anticancer activity of the ligand and the complexes on the gastric cancer cell line MKN-45. The ligand as well as the Ni(II) complex thereof showed high *in vitro* cytotoxicity with the ligand having an IC_{50} value of 5.993 ± 1.947 µM and the Ni(II) complex 6.654±0.449 µM. The IC_{50} of the positive control, 5-fluorouracil is 5±2 µM.[16]

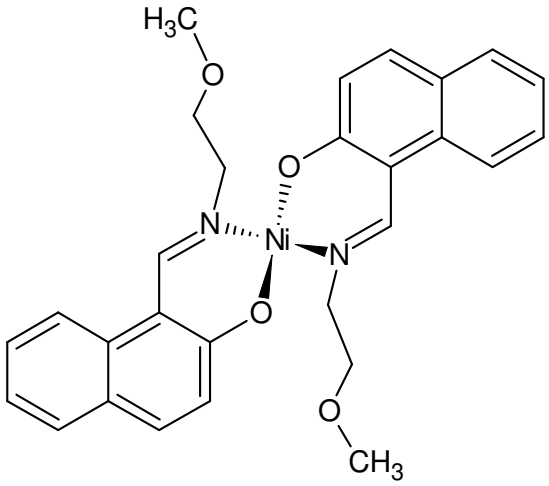

Figure 2.1: The chemical structure of the Ni(II) Schiff base complex synthesized by Abbasi and co-workers.[16]

[15] Stewart, M. & Watson, I. (1983). *British Journal of Clinical Pharmacology*, **16**(1), 3-7.
[16] Abbasi, Z., Salehi, M., Khaleghian, A. & Kubicki, M. (2018). *Journal of Molecular Structure*, **1173**, 213-220.

Hosny *et al.*[17] synthesized a novel ligand, 2-isonicotinoyl-*N*-phenylhydrazine-1-carbothioamide (H3L), as illustrated in Figure 2.2, as well as its Co(II), Cu(II), Ni(II) and Zn(II) complexes. The ligand displayed very good cytotoxicity against both human colon cancer (HCT-116) and human liver cancer (HEPG-2) cell lines with an IC_{50} value close to the standard, doxorubicin. The cytotoxicity of the Zn(II) complex was studied as a representative example and proved to be less cytotoxic than the ligand itself.

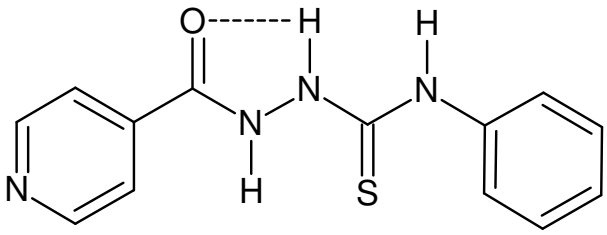

Figure 2.2: The chemical structure of 2-isonicotinoyl-*N*-phenylhydrazine-1-carbothioamide (H3L).

2.2.3 Cytotoxicity of Re(I) tricarbonyl complexes

One example of the cytotoxic evaluation of Re(I) tricarbonyl complexes from literature is a study conducted by Knopf *et al.*[18] Knopf and co-workers synthesized and studied the *in vitro* anticancer activity and *in vivo* biodistribution of a few Re(I) aqua tricarbonyl complexes of the general formula *fac*-$[Re(CO)_3(N,N')(H_2O)]^+$ where *N,N'* = 2,2'-bipyridine and derivatives thereof. An example of one of the chemical structures of these complexes is depicted in Figure 2.3. All these complexes yielded IC_{50} values less than 20 μM except for one complex. This study yielded a positive indication of the potential use of Re(I) tricarbonyl complexes as anticancer agents. A more detailed discussion follows in paragraph 2.8.2.

[17] Hosny, N., Hassan, N., Mahmoud, H. & Abdel-Rhman, M. (2019). *Applied Organometallic Chemistry*, **33**(8). doi: 10.1002/aoc.4998

[18] Knopf, K., Murphy, B., MacMillan, S., Baskin, J., Barr, M., Boros, E. & Wilson, J. (2017). *Journal of The American Chemical Society*, **139**(40), 14302-14314.

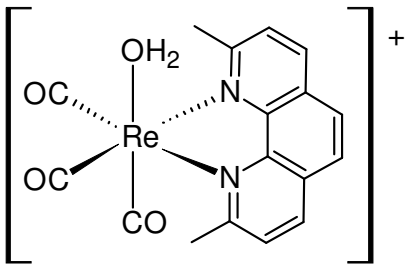

Figure 2.3: The chemical structure of *fac*-[Re(CO)$_3$(2,9-dimethyl-1,10-phenanthroline)(H$_2$O)]$^+$.[18]

2.3 Photodynamic therapy

Although the progress in cancer research has yielded many successful forms of treatments, the selectivity and sensitivity of the compounds involved remain a major challenge for researchers. The therapeutic efficacy and the undesired systemic toxicity of chemotherapeutic drugs is of great concern.[19] Alternative forms of therapy, such as photodynamic therapy (PDT) that can improve the therapeutic efficacy of chemo drugs are worth exploring. PDT is utilized to overcome some of the challenges faced in oncology such as treatment toxicity and especially drug resistance.[20] Drug-resistance originates from both intrinsic and acquired mechanisms which include drug target changes, increased drug efflux, and the activation of signaling pathways for the repair of damaged cellular components and suppression of cell death. These mechanisms are mainly overcome by the photodamage caused by PDT to antiapoptotic proteins, drug efflux pumps, and the tumor's microenvironment.

Photodynamic therapy (PDT) is a modern, non-invasive therapeutic method that can destroy various cells and tissues by using chemicals to target certain cells or tissues, just like chemotherapy.[21,22,24] Yet, the chemicals used in PDT mostly only become cytotoxic once exposed to electromagnetic radiation. The treatment process contains three components of utmost importance. A photosensitizer is administered to localize at a specific site followed by the irradiation with light and the consequent

[19] Zhu, R., He, H., Liu, Y., Cao, D., Yan, J., Duan, S., Chen, Y. & Yin, L. (2019). *Biomacromolecules*, **20**(7), 2649-2656.
[20] Spring, B., Rizvi, I., Xu, N. & Hasan, T. (2015). *Photochemical and Photobiological Sciences*, **14**(8), 1476-1491.
[21] Macdonald, I. & Dougherty, T. (2001). *Journal of Porphyrins and Phthalocyanines*, **5**(02), 105-129.

generation of reactive oxygen species (ROS) which cause cell death.[21,22] PDT has been used in several medical fields including dermatology, urology, ophthalmology, pneumology, cardiology, dentistry and immunology.[22,23] PDT is also useful as an antimicrobial and antiviral treatment for various infectious diseases, water sterilization and inactivation of pathogens in blood products.[23]

As mentioned previously, PDT requires the presence of three components simultaneously:[24]

- A photosensitizer (PS)
- A light source
- Oxygen

The process of PDT is illustrated in Figure 2.4 followed by a detailed explanation.

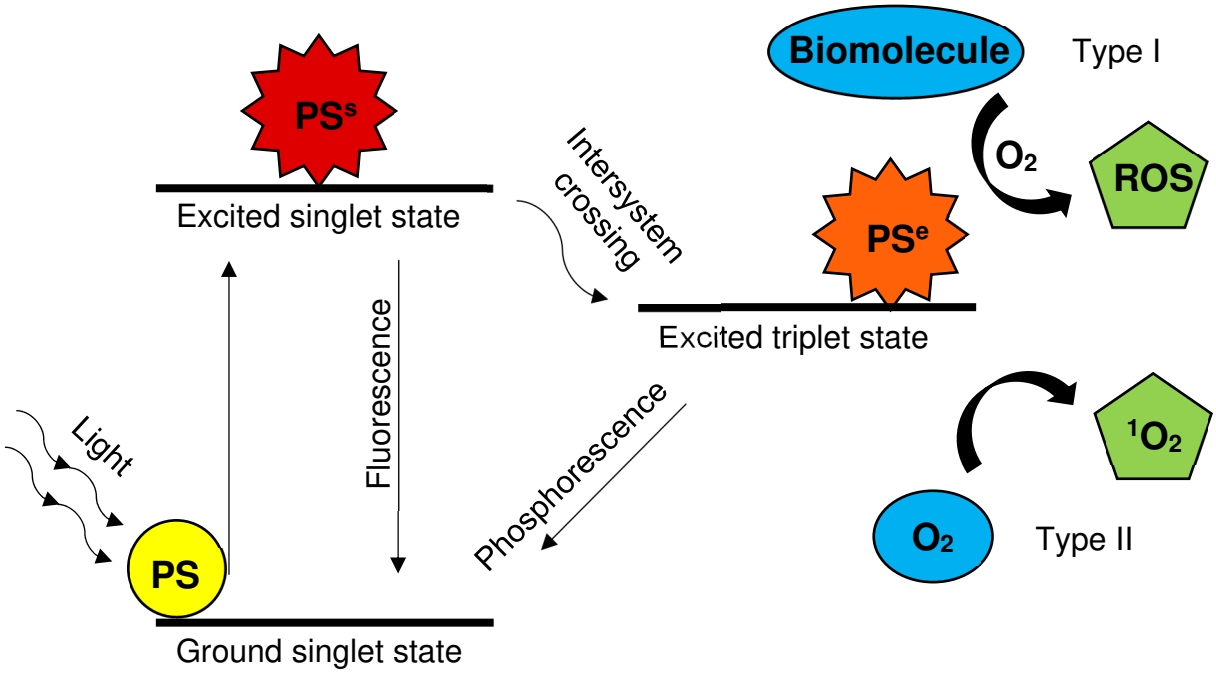

Figure 2.4: The photodynamic process and the interaction of an excited PS with surrounding molecules.

The uptake of the PS is favoured in tumor cells and macrophages due to the phagocytic activity and the scavenger-receptor photosensitizer-targeting properties

[22] Tampa, M., Sarbu, M., Matei, C., Mitran, C., Mitran, M., Caruntu, C., Constantin, C., Neagu, M. & Georgescu, S. (2019). *Oncology Letters*, **17**, 4085-4093.
[23] Benov, L. (2015). *Medical Principles and Practice*, **24**(s1), 14-28.
[24] Matei, C., Tampa, M., Poteca, T., Panea-Paunica, G., Georgescu, S. R., Ion, R. M., Popescu, S. M. & Giurcaneanu, C. (2013). *Journal of Medicine and Life*, **6**(1), 50-54.

of tumor associated macrophages (TAMs).[25] When the PS is exposed to light of a specific wavelength, it becomes activated to the excited singlet state (PS^s) which is short-lived (nanoseconds). The PS can then relax to the ground state (fluorescence) or undergo intersystem crossing to the triplet state, which is long-lived (microseconds). The PS in the triplet state interacts with surrounding molecules v*ia* two pathways:[21,22]

- Type I reactions: Free radical production, either by abstraction of a hydrogen or transfer of an electron between the PS and the substrate.
- Type II reactions: Energy transfer occurs between the PS and oxygen. This occurs when the PS interacts with molecular oxygen ($^3O_2$) and produces ROS which includes the superoxide anion (O_2^-), hydroxyl radical (OH) and singlet oxygen ($^1O_2$).

Singlet oxygen has proved to be responsible for the destructive effects of PDT.[22,24] It induces autophagy, apoptosis and necrosis by severely damaging cellular components.[24,26,27] The damage is dependent on factors such as:[22,23,24]

- Type of PS
- Dose of PS
- Localization of PS
- Intensity and wavelength of light
- Oxygen concentration

Several important events played a role in the history of PDT. Ancient civilizations already knew that numerous plants, when combined with sunlight, could treat skin diseases such as vitiligo and psoriasis.[28,29] The rediscovery and mechanism exposition of PDT only occurred at the beginning of the 1900's when Raab and Von Tappeiner observed an *in vitro* photodynamic effect and then in 1904 Tappeiner

[25] Korbelik, M. & Hamblin, M. (2015). *Photochemical and Photobiological Sciences*, **14**(8), 1403-1409.
[26] Huang, Z. (2005). *Technology in Cancer Research and Treatment*, **4**(3), 283-293.
[27] Tsay, J., Trzoss, M., Shi, L., Kong, X., Selke, M., Jung, M. & Weiss, S. (2007). *Journal of The American Chemical Society*, **129**(21), 6865-6871.
[28] Rkein, A. & Ozog, D. (2014). *Dermatologic Clinics*, **32**(3), 415-425.
[29] Sârbu, M., Georgescu, S., Tampa, M., Sârbu, A. & Simionescu, O. (2018). *Romanian Journal of Internal Medicine*, **56**(2), 75-84.

coined the term 'photodynamic'.[22,30] During the same time Niels Finsen worked on treating lupus vulgaris and other diseases with concentrated light radiation and was awarded the Nobel Prize for his contribution.[31,32] In 1929 Hans Fischer was awarded the Nobel Prize for the investigation of porphyrins[32] which led to the discovery of the hematoporphyrin derivative (HpD) by Lipson and Baldes in 1960[33] and photofrin (Figure 2.5) by Dougherty.[34] These compounds are first generation PS's which have several limitations, including a complex composition and low light absorption rate.[32]

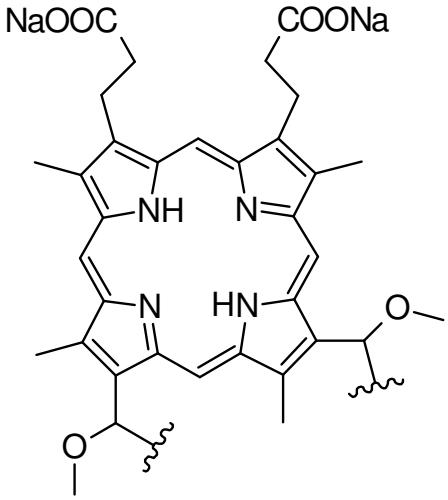

Figure 2.5: The chemical structure of porfimer sodium, also called photofrin.

As is the case in all research fields, there is always room for improvement and over the years, several improvements have indeed emerged as second-generation PS's which are less toxic than first generation PS's. These PS's are pure compounds and absorb well in the range of 650-800 nm (red to near-infrared region) because the absorption of single photons in the region above 800 nm does not provide enough energy to excite oxygen to its singlet state.[35] The main limitations include a lower selectivity for the target tissue and an insufficient depth of treatment.[23,36] These compounds mainly have a cyclic tetrapyrrolic structure (Figure 2.5) and are

[30] Hönigsmann, H. (2013). *Photochemical and Photobiological Sciences*, **12**(1), 16-21.
[31] Gøtzsche, P. (2011). *Journal of The Royal Society of Medicine*, **104**(1), 41-42.
[32] Kou, J., Dou, D. & Yang, L. (2017). *Oncotarget*, **8**(46), 81591-81603.
[33] Lipson, R. & Baldes, E. J. (1960). *Archives of Dermatology*, **82**(4), 508-516.
[34] Dougherty, T. (1984). *Critical Reviews in Oncology/Hematology*, **2**(2), 83-116.
[35] Abrahamse, H. & Hamblin, M. (2016). *Biochemical Journal*, **473**(4), 347-364.
[36] Paszko, E., Ehrhardt, C., Senge, M., Kelleher, D. & Reynolds, J. (2011). *Photodiagnosis and Photodynamic Therapy*, **8**(1), 14-29.

represented by porphyrins and its derivatives, chlorins, bacteriochlorins, phthalocyanines and metallo-phthalocyanines.[23,37,38]

To improve the outcomes of PDT even more, third generation PS's are currently investigated and this entails the intense research toward nanoparticles and gene engineering mediated PDT.[19,32]

2.3.1 Photoluminescence and organometallic complexes as luminescent probes

Photoluminescence is, in short, the emission of light from matter after the absorption of photons from electromagnetic radiation. Fluorescence and phosphorescence are two well-known forms of photoluminescence and the processes are schematically described in Figure 2.6.

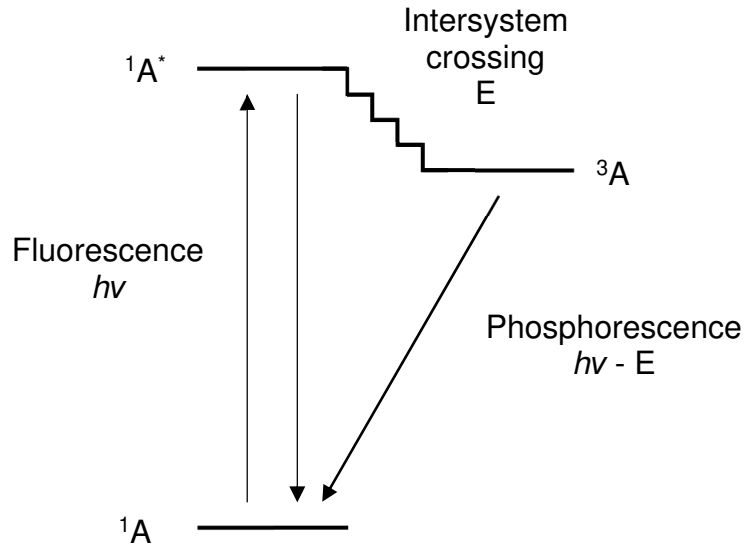

Figure 2.6: A schematic representation of the processes of fluorescence and phosphorescence.

A substance that absorbs electromagnetic radiation undergoes internal energy transitions after which it re-emits the energy in the form of light. This relaxation can

[37] Tampa, M., Matei, C. L., Popescu, S. A., Georgescu, S. R., Neagu, M. O., Constantin, C. & Ion, R. M. S. (2013). *Revista de Chimie*, **64**, 639-645.
[38] Matei, C., Tampa, M., Ion, R. M., Neagu, M. & Constantin, C. (2012). *Digest Journal of Nanomaterials and Biostructures*, **7**, 1535-1547.

result in fluorescence, which occurs fast, or phosphorescence, which is a long-lived process.[39]

Cell imaging by luminescence entails the use of non-invasive probes to study the morphological characteristics of tissue.[40,41,42] The cell, the most important component in all living organisms, could cause very serious diseases when not functioning as it should; hence, the development of luminescent probes for live cell imaging has drawn much attention in recent years. Generally, most of the commonly used fluorescent probes consist of organic dyes, which have various limitations, including small Stokes shift values and short luminescence lifetimes.[43,44]

Investigations into viable alternatives to organic fluorophores for imaging applications have yielded luminescent transition metal complexes which proved to have some advantages:[43]

- Excitation and emission maxima in the visible region can easily be tuned.
- Emission energies can be tuned by modification of the auxiliary ligands.
- They have large Stokes shifts which aid in facile separation of excitation and emission wavelengths and elimination of self-quenching.
- Relatively long phosphorescence lifetimes.
- Sufficient solubility in aqueous solution.

The first metal-to-ligand-charge-transfer (MLCT) fluorescent rhenium complexes applied in cell imaging was a series of lipophilic and hydrophilic Re(I) tricarbonyl complexes (Figure 2.7) of the type *fac*-$[Re(CO)_3L(bisim)]^+$ with bisim = bisimine prepared by Amoroso *et al*.[42] These complexes were investigated for its membrane permeabilities in liposomes and this study proved the potential use of such complexes in fluorescence microscopy cell imaging.[42] These findings alone will

[39] Atkins, P. & De Paula, J. (2010). *Physical Chemistry* (9th ed.). Oxford: Oxford University Press.
[40] Ma, D., Zhong, H., Fu, W., Chan, D. S., Kwan, H., Fong, W., Chung, L., Wong, C. & Leung, C. (2013). *Plos ONE*, **8**(2), e55751.
[41] Stephens, D. (2003). *Science*, **300**(5616), 82-86.
[42] Amoroso, A. J., Coogan, M. P., Dunne, J. E., Fernández-Moreira, V., Hess, J. B., Hayes, A. J., Lloyd, D., Millet, C., Pope, S. J. A. & Williams, C. (2007). *Chemical Communications*, **29**, 3066-3068.
[43] Yang, Y., Zhao, Q., Feng, W. & Li, F. (2013). *Chemical Reviews*, **113**(1), 192-270.
[44] Kuil, J., Steunenberg, P., Chin, P. T. K., Oldenburg, K., Jalink, J., Velders, A. & van Leeuwen, F. W. B. (2011). *ChemBioChem*, **12**, 1897-1903.

spark the interest of any researcher investigating both Re(I) complexes and bisimine ligands.

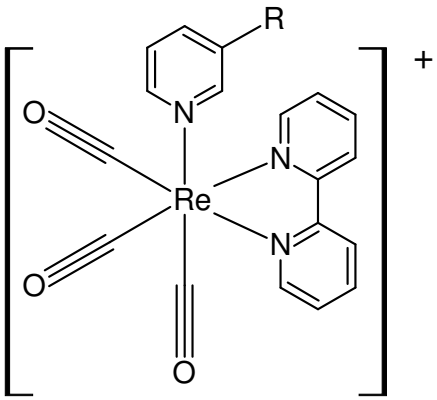

Figure 2.7: The chemical structure of *fac*-[Re(CO)$_3$L(bisim)]$^+$ with bisim = bisimine and R = octyl, merystyl, steryl, CH$_2$OH.

Trondl *et al*.[45] and Mari *et al*.[46] reported ruthenium-based anticancer drugs, which exhibit superior cytotoxicity as well as the possibility of light-activated drug candidates in both PDT and PACT (photoactivated chemotherapy).[46] Two of these compounds, NKP-1339 (sodium *trans*-[tetrachloridobis(1H-indazole)ruthenate(III)]) and KP1019 (indazolium *trans*-[tetrachloridobis(1H-indazole)ruthenate(III)]), progressed to phase I clinical trials and their chemical structures are depicted in Figure 2.8.

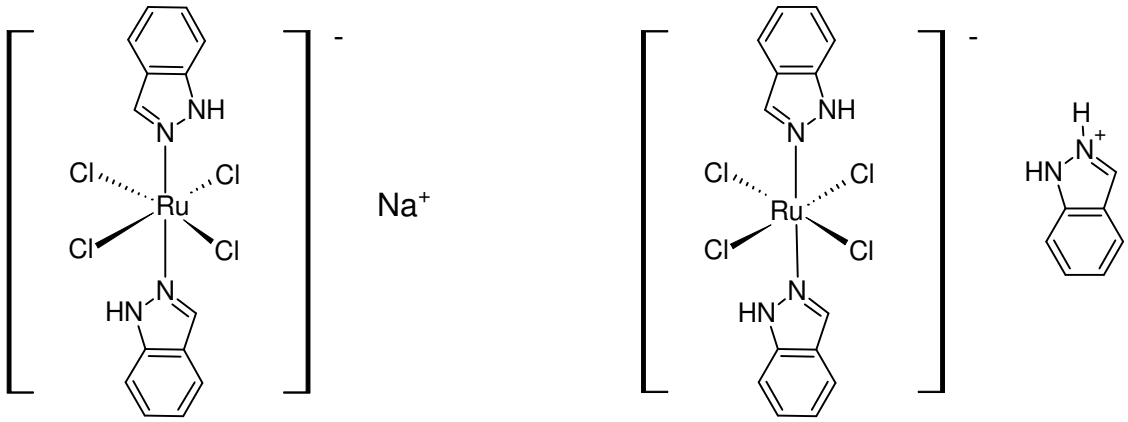

Figure 2.8: The chemical structures of NKP-1339 (left) and KP1019 (right).

[45] Trondl, R., Heffeter, P., Kowol, C., Jakupec, M., Berger, W. & Keppler, B. (2014) *Chemical Science*, **5**(8), 2925-2932.

[46] Mari, C., Pierroz, V., Ferrari, S. & Gasser, G. (2015). *Chemical Science*, **6**(5), 2660-2686.

Marker and co-workers[47] synthesized water-soluble Re(I) tricarbonyl complexes of the general formula *fac*-[Re(CO)$_3$(*N,N'*)(PR$_3$)]$^+$, where *N,N'* is a diamine ligand and PR$_3$ is 1,3,5-triaza-7-phosphaadamantane (PTA), tris(hydroxymethyl)phosphine (THP), or 1,4-diacetyl-1,3,7-triaza-5-phosphabicyclo[3.3.1]nonane (DAPTA). These compounds were all tested as photoactivated anticancer agents in human cervical (HeLa), ovarian (A2780), and cisplatin-resistant ovarian (A2780CP70) cancer cell lines.[47] The THP and DAPTA ligands display triplet-based luminescence in aqueous solutions and its Re(I) tricarbonyl complexes undergo photosubstitution of a CO ligand and sensitize the formation of singlet oxygen (^{1}O$_2$) with high quantum yields.[47] The Re(I) tricarbonyl complexes containing the PTA ligand showed no emission or photosubstitution upon irradiation with 365 nm light. The complexes containing THP and DAPTA displayed minimal toxicity in the absence of light but exhibited a very good cytotoxic response upon irradiation.[47] These findings present many opportunities for further investigations into compounds of this type.

Aminotroponimines (ATIH) containing a dansyl fluorophore substituent on one nitrogen and an alkyl substituent on the other (H^{R}DATI) have been studied for its use as a ligand in metal-based nitric oxide sensors (Figure 2.9).[48] Franz *et al*. synthesized and investigated air-stable cobalt complexes of such aminotroponimines.[49] They found that these complexes react with nitric oxide to release the fluorophore-containing ligand which yields an increase in fluorescence intensity.

[47] Marker, S., MacMillan, S., Zipfel, W., Li, Z., Ford, P. & Wilson, J. (2018). *Inorganic Chemistry*, **57**(3), 1311-1331.
[48] Balachandra, C. & Sharma, N. (2017). *Dyes and Pigments*, **137**, 532-538.
[49] Franz, K., Singh, N., Spingler, B. & Lippard, S. (2000. *Inorganic Chemistry*, **39**(18), 4081-4092.

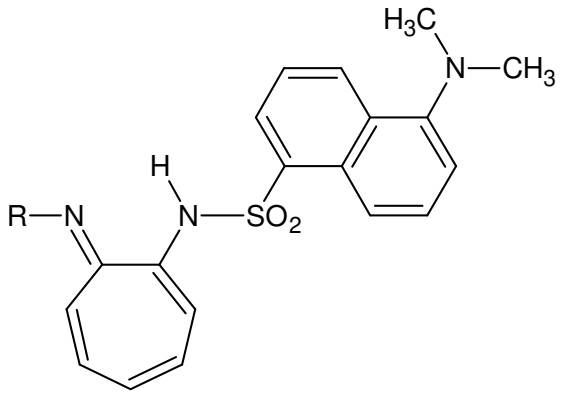

Figure 2.9: The chemical structure of H^RDATI, a fluorophore-containing aminotroponimine ligand.

2.4 Metals in medicine with focus on anticancer agents

Over the years metal complexes and their method of action have been the subject of several investigations towards developing anticancer medicine. Metals, especially nickel, chromium, arsenic, cadmium, and beryllium have been identified as carcinogenic agents.[50] Regardless of this fact, many metals have anticancer properties which have been well reported for over forty years. The research escalated from the groundbreaking contributions to research by Rosenberg, Livingstone and Williams in the 1960's and 1970's.[51,52,53] Rosenberg's discovery is the most renowned since cisplatin was the first metal complex approved for use as a chemotherapeutic agent in 1978 and is still one of the three most employed drugs in chemotherapy today. In 1989 and 1996, carboplatin and oxaliplatin were approved by the Food and Drug Administration (FDA). These two new complexes exhibited a better toxicological profile as well as a different activity spectrum.[50] These three platinum complexes are depicted in Figure 2.10.

[50] Marloye, M., Berger, G., Gelbcke, M. & Dufrasne, F. (2016). *Future Medicinal Chemistry*, **8**(18), 2263-2286.
[51] Rosenberg, B., VanCamp, L., Trosko, J. E. & Mansour, V. H. (1969). *Nature,* **222**(5191), 385-386.
[52] Livingstone, S. & Mihkelson, A. (1970). *Inorganic Chemistry*, **9(**11), 2545-2551.
[53] Williams, D. (1972). *Chemical Reviews*, **72**(3), 203-213.

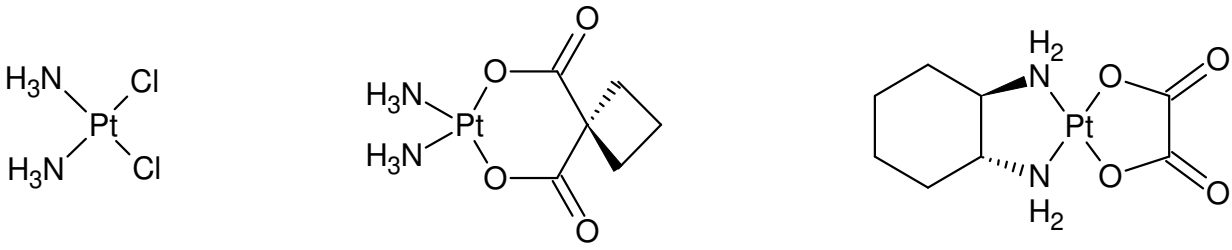

Cisplatin Carboplatin Oxaliplatin

Figure 2.10: The three most widely used platinum drugs in oncology, cisplatin, carboplatin and oxaliplatin.

Scientists are eager to investigate most d-block metals for their potential as new anticancer compounds or to improve those already endowed with anticancer properties, especially due to the growing resistance to platinum.[54] There are already advancements made in this field with several ruthenium complexes studied in clinical trials.[50,55] NKP-1339 (sodium *trans*-[tetrachloridobis(1H-indazole)ruthenate(III)]) (Figure 2.11) is the first ruthenium-based anticancer drug in clinical development and was successfully studied in a phase I clinical trial.[56] This compound is the sodium salt analogue of KP1019 (indazolium *trans*-[tetrachloridobis(1H-indazole)ruthenate(III)]) (Figure 2.11) which proved to be superior to 5-fluorouracil, the standard agent used against colorectal cancer, in its activity against a rat colon cancer model.[56] These two ruthenium compounds, illustrated in Figure 2.11, have high tumor targeting potential due to their strong binding to serum proteins like albumin and transferrin.[55,56]

[54] Konkankit, C., King, A., Knopf, K., Southard, T. & Wilson, J. (2019). *ACS Medicinal Chemistry Letters*, **10**(5), 822-827.
[55] Trondl, R., Heffeter, P., Kowol, C., Jakupec, M., Berger, W. & Keppler, B. (2014) *Chemical Science*, **5**(8), 2925-2932.
[56] Mari, C., Pierroz, V., Ferrari, S. & Gasser, G. (2015). *Chemical Science*, **6**(5), 2660-2686.

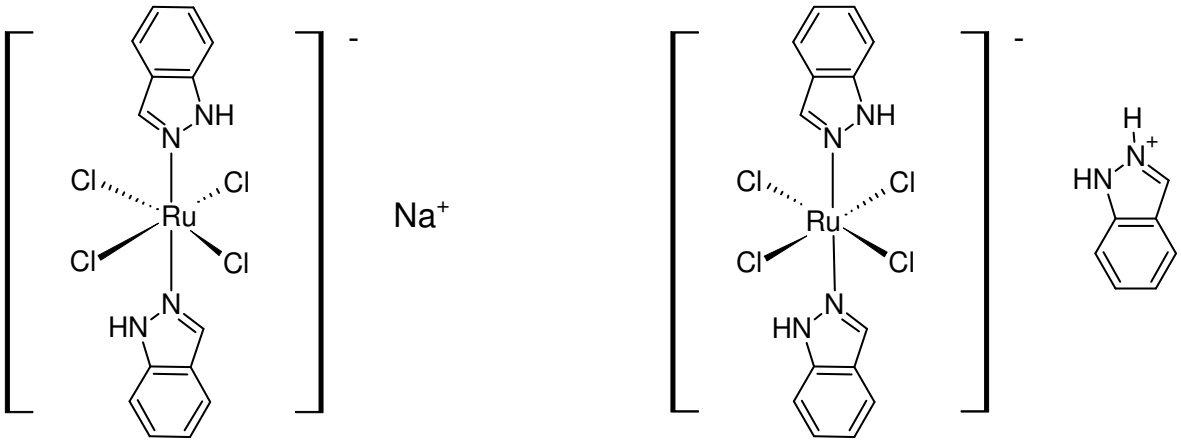

Figure 2.11: The chemical structures of two anticancer agents NKP-1339 and KP1019.

Hussain *et al*.[57] studied copper-based compounds for their anticancer and anti-inflammatory potential, as it is well known that copper's high redox activity makes it highly cytotoxic. Copper-based compounds containing benzimidazole-derived Schiff bases and secondary ligands such as 1,10-phenanthroline and 2,2′-bipyridyl were investigated and yielded promising anticancer results.[57]

To overcome the major challenges, such as severe systemic toxicity and drug-resistance brought about by platinum-based drugs, many scientists have approached the problem by designing palladium-based drugs.[58] Palladium complexes are structurally analogous to platinum complexes and have many structural and chemical properties making it an ideal candidate to replace platinum-based drugs. El-Boraey and El-Gammal synthesized a novel tetraamide (N_4) macrocyclic ligand as well as a few of its metal complexes, including palladium(II) (Figure 2.12).[59] *In vitro* anticancer evaluations against breast cancer (MCF7) and hepatocarcinoma (HepG2) cell lines indicated that the ligand as well as its metal complexes have potential anticancer activity, with the cytotoxicity of the compounds increasing with coordination to a metal centre.[59]

[57] Hussain, A., Alajmi, M. F., Rehman, M. T., Amir, S., Husain, F. M., Alsalme, A., Siddiqui, M. A., Alkhedhairy, A. A. & Khan, R. A. (2019) *Scientific Reports*, **9**(1), doi:10.1038/s41598-019-41063-x.

[58] Jahromi, E., Divsalar, A., Saboury, A., Khaleghizadeh, S., Mansouri-Torshizi, H. & Kostova, I. (2016). *Journal of The Iranian Chemical Society*, **13**(5), 967-989.

[59] El-Boraey, H. & El-Gammal, O. (2015). *Spectrochimica Acta Part A: Molecular and Biomolecular Spectroscopy*, **138**, 553-562.

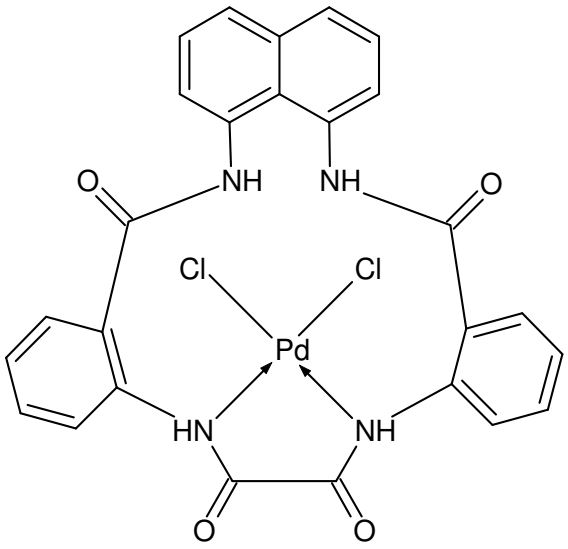

Figure 2.12: The chemical structure of the palladium(II) metal complex of naphthyl-dibenzo[1,5,9,12]tetraazacyclopen-tadecine-6,10,11,15-tetraonea.

Due to their unique characteristics, gold nanoparticles (AuNPs) are of interest in medical applications, especially anticancer treatment. In a recent review, Sztandera and co-workers elaborated on the many applications of AuNPs as well as the numerous synthetic methods for the specific applications.[60] The anticancer applications of AuNPs lies in photothermal therapy, radiofrequency therapy, as drug carriers, and as angiogenesis modulators.[60]

The anticancer properties of green synthesized silver nanoparticles (AgNPs) were investigated by Al-Sheddi *et al*.[61] This investigation demonstrated that AgNPs induce oxidative stress leading to mitochondrial membrane damage and interference with cell cycles. They prove to induce apoptosis and necrosis of human cervical cancer (HeLa) cells due to their concentration-dependent cytotoxic activity.[61] Buttacavoli *et al*. also investigated AgNPs, embedded into a specific polysaccharide (EPS) biosynthesized by *Klebsiella oxytoca* DSM 29614 under aerobic (AgNPs-EPS^{aer}) and anaerobic conditions (AgNPs-EPS^{anaer}).[62] The cytotoxic activity of these AgNPs were evaluated against human breast (SKBR3 and

[60] Sztandera, K., Gorzkiewicz, M. & Klajnert-Maculewicz, B. (2018). *Molecular Pharmaceutics*, **16**(1), 1-23.
[61] Al-Sheddi, E. S., Farshori, N. N., Al-Oqail, M. M., Al-Massarani, S. M., Saquib, Q., Wahab, R., Musarrat, J., Al-Khedhairy, A. A. & Siddiqui, M. A. (2018). *Bioinorganic Chemistry and Applications*, **2018**, 1-12.
[62] Buttacavoli, M., Albanese, N. N., Di Cara, G., Alduina, R., Faleri, C., Gallo, M., Pizzolanti, G., Gallo, G., Feo, S., Baldi, F. & Cancemi, P. (2018). *Oncotarget*, **9**(11), 9685-9705.

8701-BC) and colon (HT-29, HCT 116 and Caco-2) cancer cell lines where AgNPs-EPS^{aer} proved to be the most cytotoxic against breast cancer cells with an IC_{50} value of 5 μM for SKBR3 cells and 8 μM for 8701-BC cells.[62]

Arsenic, a metal known to us as poison and an ancient drug is used worldwide as an anticancer agent. Due to its significant cytotoxic activity, arsenic trioxide (ATO) was used in the treatment of chronic myelogenous leukemia (CML) in the 1800's.[63] As with many other metals and its complexes, the combination thereof with other compounds or treatment such as radiation, chemotherapy and molecular-targeted drugs could possibly improve its activity or mechanism of action. The combination of ATO with all-*trans*-retinoic acid (ATRA), for example, proved to induce apoptosis in acute promyelocytic leukemia (APL) cells with an improved outcome and lower toxicity than the combination of ATRA with conventional chemotherapeutics.[63]

Darinaparsin (DAR) is a novel organic molecule of arsenic consisting of demethylated arsenic (an inorganic arsenic metabolite) and glutathione (Figure 2.13).[64] It was designed to exhibit greater cytotoxicity by increasing intracellular arsenic concentration and increased apoptosis, proving to possibly be an effective treatment against leukemia, myeloma, lymphoma, and various solid tumor cell lines.[64]

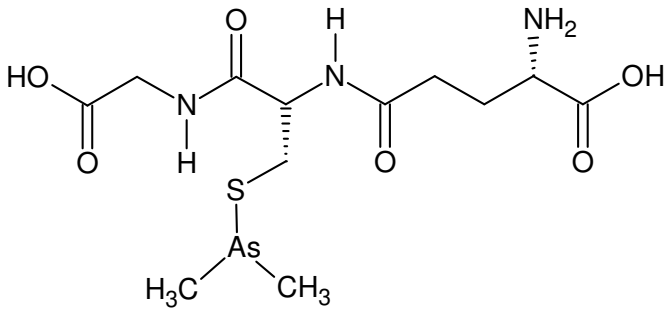

Figure 2.13: Darinaparsin (DAR), an organic form of arsenic and a potential anticancer agent.

[63] Ota, A., Wahiduzzaman, M. & Hosokawa, Y. (2018). *Current Understanding of Apoptosis - Programmed Cell Death*. doi: 10.5772/intechopen.74824

[64] Khairul, I., Wang, Q., Jiang, Y., Wang, C. & Naranmandura, H. (2017). *Oncotarget*, **8**(14), 23905-23926.

2.5 Using ligands to tune the anticancer properties of metals

Although some simple metal salts could prove to be highly toxic, they usually display poor ADME-Tox (Absorption, Distribution, Metabolism, Excretion and Toxicity) parameters.[50] As these parameters are very important for use in human medicine, it is necessary to incorporate different ligands into a metal complex to optimize these parameters. Ligands and their roles in optimizing metal complexes could be classified according to a few general properties which will be discussed in this section and are summarized in Table 2.2.[50]

Table 2.2: A summary of the different biological mechanisms that induce certain effects and tune the anticancer properties of metals.

Effect of ligand	Mechanism
Bioactivity	• DNA-intercalation • Enzyme inhibition • Disruption of mitochondrial permeability (MMP) • Stressing endoplasmic reticula
Tissue- and cell-targeting, active cellular influx	• Binding to overexpressed receptors on cancer cells to increase biological selectivity
Passive cellular influx	• Altering molecular size and charge • Modifying logP
Increased water solubility	• Modifying logP and the lipo- and hydrophilicity
Photoactive properties	• Modify ability to produce O_2^-
Reduced reactivity	• Steric hindrance around the metal • Decrease the electrophilicity of the metal
Decreased cellular efflux	• Inhibition of the efflux pump by the ligand • Decreasing the electrophilicity of the metal
Targeting organelles	• Positively charged complexes • Complexes with optimal logP and lipophilicity

2.5.1 Bioactivity

When exploring possible anticancer metal complexes, the incorporated ligands could be chosen arbitrarily or it could be one of various known bioactive ligands such as antitumor antibiotics, enzyme inhibitors or small inorganic molecules such as NO and CO.[50,65] Nitric oxide (NO) as a ligand display many biological activities, especially in the mediation of tumor-induced angiogenesis, which is an important step in the development of metastases.[65]

The incorporation of planar, aromatic and polycyclic ligands, in the same class as 1,10-phenanthroline and 2,2':6',2"-terpyridine is illustrated in the design of PT-ACRAMTU ([PtCl(en)-(ACRAMTU)]$(NO_3)_2$, en=ethane-1,2-diamine, ACRAMTU=1-[2-(acridin-9-ylamino)ethyl]-1,3-dimethylthiourea; Figure 2.14).[66] This type of platinum-acridine complexes designed by Suryadi and Bierbach have shown a 500-fold higher cytotoxicity than cisplatin in non-small cell lung cancer which is known to be aggressive and chemoresistant.[66]

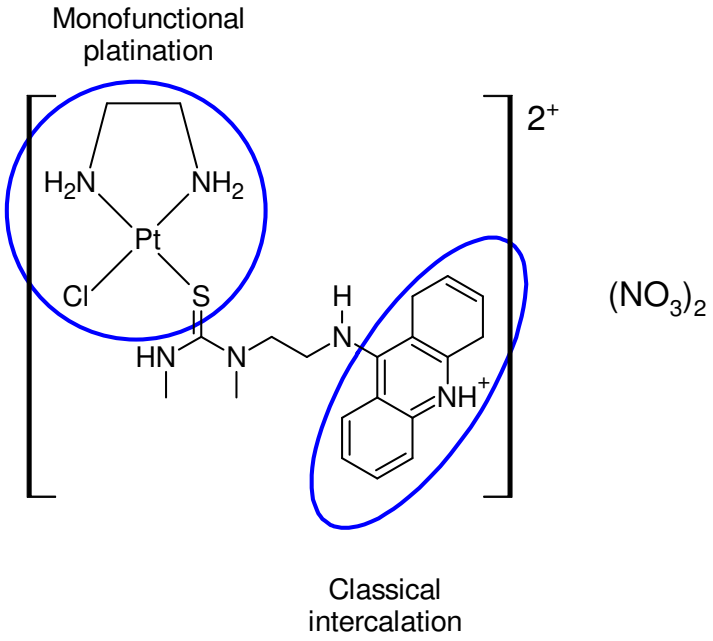

Figure 2.14: Structure and functions of the platinum-acridine hybrid agent PT-ACRAMTU.

Figure 2.14 also indicates the two functional parts of the molecule. Platination refers to the binding of the molecule to DNA and the consequent interference with its repair

[65] Hanif, M., Babak, M. & Hartinger, C. (2014). *Drug Discovery Today*, **19**(10), 1640-1648.
[66] Suryadi, J. & Bierbach, U. (2012). *Chemistry - A European Journal*, **18**(41), 12926-12934.

mechanism, leading to cell death. Intercalation involves the insertion of a molecule, ideally flat, in between the base pairs of a DNA strand which inhibits DNA replication.

Drug resistance is a major challenge in many medical disciplines and it mostly originates at the gene expression level. This is where enzyme inhibitors become promising compounds for treatment.[67] Histone deacetylase (HDAC) inhibitors are very good examples of such compounds and have important roles in controlling critical cellular functions such as cell proliferation, cell cycle regulation and apoptosis.[67] Photoactivation of platinum(IV)-azido complexes results in species that are cytotoxic and capable of causing cell death in many cells. Irradiation with ultraviolet (UV) or visible (Vis) light leads to the photoreduction of these species to bioactive platinum(II) species that can platinate DNA irreversibly. Utilizing this process in tumor cells destroys the nuclear DNA, causing cell death. Kasparkova *et al*. designed a photoactivatable platinum(IV)-diazide complex *cis,trans*-[Pt(N_3)(Sub)$_2$(*t*Bu$_2$bpy)] (Figure 2.15) with suberoyl-bis-hydroxamic acid (SubH) as axial ligands and 4,4'-di-*tert*-butyl-2,2'-bipyridine (*t*Bu$_2$bpy). SubH is an excellent HDAC inhibitor and thus has antiproliferative activity.[67]

[67] Kasparkova, J., Kostrhunova, H., Novakova, O., Křikavová, R., Vančo, J., Trávníček, Z. & Brabec, V. (2015). *Angewandte Chemie International Edition*, **54**(48), 14478-14482.

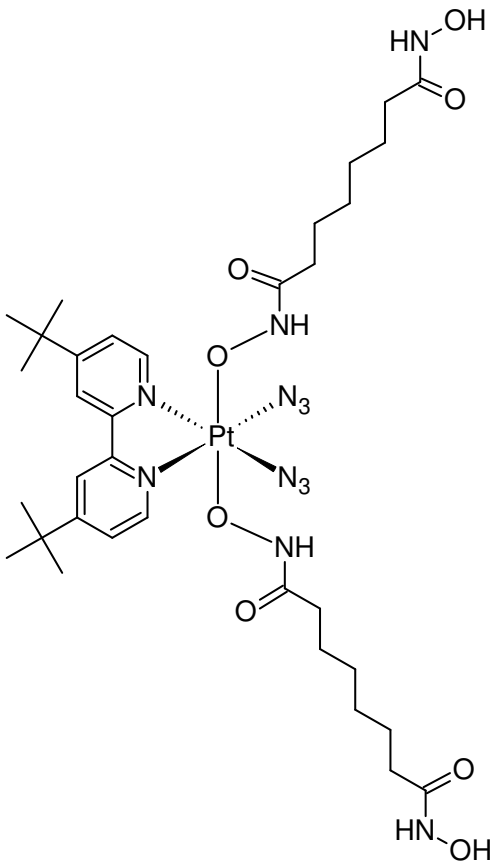

Figure 2.15: The chemical structure of the platinum(IV)-diazide complex *cis,trans*-[Pt(N_3)(Sub)$_2$(*t*Bu_2bpy)].

Doxorubicin (Dox) is a well-established, broad spectrum antitumor agent that localizes in the nucleus and inhibits Topoisomerase II by DNA intercalation.[68] This drug, as many other anthracyclines are prone to multidrug resistance (MDR). As new strategies are always explored to improve current chemotherapeutic agents, Imstepf *et al*. developed bioconjugates of two small organometallic rhenium cyclopentadienyl complexes, [(η^5-C_5H_4COOH)Re(CO)$_3$] (Cp) and [(η^5-$C_5H_4CH(NH_2)COOH$)Re(CO)$_3$] (Cp-*N*), to doxorubicin (Dox) (Figure 2.16). This resulted in the redirection of the localization of compounds from the nucleus to the mitochondria. This is no surprise as lipophilic, cationic compounds are taken up in the mitochondria due to the electrochemical gradient between the inner and outer membranes. Both Cp-Dox and Cp-*N*-Dox compounds are very lipophilic. These two complexes disrupt mitochondrial membrane potential, inducing apoptosis resulting

[68] Imstepf, S., Pierroz, V., Rubbiani, R., Felber, M., Fox, T., Gasser, G. & Alberto, R. (2016). *Angewandte Chemie International Edition*, **55**(8), 2792-2795.

in excellent toxicity toward HeLa cells with IC_{50} values of 0.34±0.03 μM for Cp-Dox and 1.65±0.26 μM for Cp-*N*-Dox.[68]

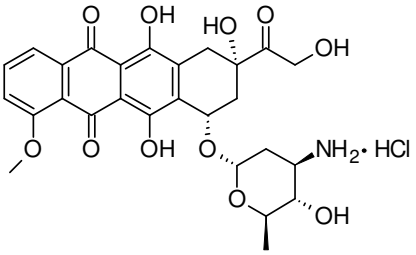

Dox

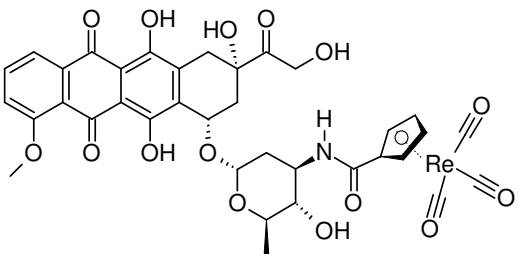

Cp-Dox

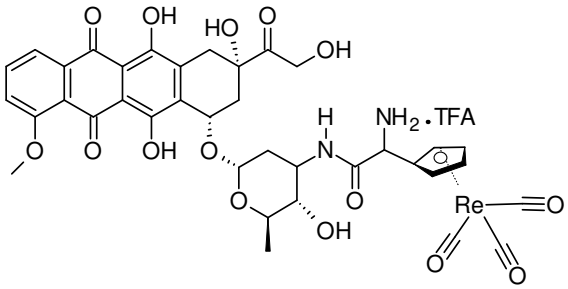

Cp-*N*-Dox

Figure 2.16: Doxorubicin and two of its bioconjugates, Cp-Dox and Cp-*N*-Dox.

2.5.2 Tissue- and cell-targeting, active cellular influx

Chemotherapy is known for the many side effects of the treatment due to their non-selectivity towards cancer cells. Ligands chosen very specifically could increase the selectivity by being the targeting moiety itself or having the targeting moiety attached to it by a cleavable bond. Tumor cells grow rapidly and are in need of more nutrients than normal cells. Cancer cells also generally overexpress a lot of receptors. These two factors could result in cancer cells being easily targeted by monoclonal antibodies and vitamins such as B12, folic acid or biotin, peptides and carbohydrates incorporated into metal complexes.[69]

2.5.3 Passive cellular influx and increased water solubility

Metal complexes can enter cancer cells by passive diffusion across membranes. For this to happen, the lipophilicity-hydrophilicity balance is important and can be altered or controlled through the coordinating ligands. Generally, the ideal logP for

[69] Gandioso, A., Shaili, E., Massaguer, A., Artigas, G., González-Cantó, A., Woods, J. A., Sadler, P. J. & Marchán, V. (2015). *Chemical Communications*, **51**(44), 9169-9172.

optimal membrane diffusion ranges from -0.4 to +5.6.[70] Modification of logP can occur with the addition of lipophilic (increase logP) or hydrophilic (decrease logP) groups. It is important to remember that an increase in lipophilicity generally leads to a decrease in water solubility.[71] Water solubility is a crucial property for the administration of a drug to a patient, either orally or parenterally.

Various metal carbonyl complexes (Re, Os, Co, Fe, Cr, Tu, Mn) have been reported with promising antiproliferative properties and they exhibit high lipophilicity.[42,50,72,73] The reported cytotoxic Re organometallic complexes were based on the *fac*-$[Re(CO)_3]^+$ core, which is easily synthesized and chemically stable. The majority of the antiproliferative Re complexes is in the form of *fac*-$[Re(CO)_3(bisimine)L]^n$ (n=0,-1) (Figure 2.17) where L is a monodentate pyridine derivative or a halide (Cl^-, Br^-) ligand.[42,72] Bisimine ligands are typically 2,2'-bipyridine or phenanthroline-based molecules.

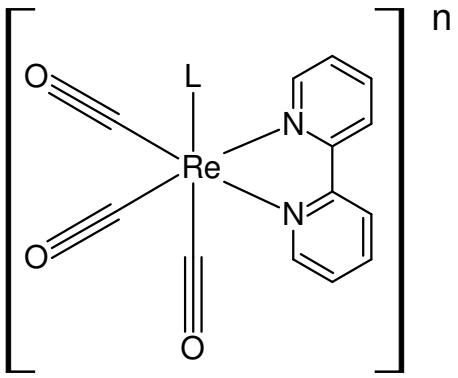

Figure 2.17: The chemical structure of *fac*-$[Re(CO)_3L(bisim)]^n$ (n=0,-1) with bisim = bisimine and L is a monodentate pyridine derivative or a halide (Cl^-, Br^-) ligand.

Although the structures seem to be similar, there is a considerable difference in cytotoxicity of the compounds and it generally increases with increase of lipophilicity, most probably due to increased cellular uptake.[72]

[70] Krämer, S., Aschmann, H., Hatibovic, M., Hermann, K., Neuhaus, C., Brunner, C. & Belli, S. (2016). *Advanced Drug Delivery Reviews*, **101**, 62-74.
[71] Bacher, F., Dömötör, O., Kaltenbrunner, M., Mojović, M., Popović-Bijelić, A., Gräslund, A., Ozarowski, A., Filipovic, L., Radulović, S., Enyedy, É. A. & Arion, V. B. (2014). *Inorganic Chemistry*, **53**(23), 12595-12609.
[72] Leonidova, A. & Gasser, G. (2014). *ACS Chemical Biology*, **9**(10), 2180-2193.
[73] Gasser, G., Ott, I. & Metzler-Nolte, N. (2011). *Journal of Medicinal Chemistry*, **54**(1), 3-25.

Molecular size and charge also play an important role in cellular uptake. A recent study of He *et al.*[74] shows that an increase in logP does not always lead to cell penetration and according to Matsson and Kihlberg[75] cell permeability sharply decreases for compounds with molecular weights of more than 1000 g/mol; the compounds with molecular masses between 500 and 1000 g/mol is virtually unexplored. The role of the charge in cellular accumulation was investigated by Simpson *et al.*[76] They have established that cations are generally more prone to enter cells, mostly through organic cation transporters.

2.5.4 Photoactive properties

Photoactivatable ligands facilitate the activation of a complex at a specific location inside cells, creating the possibility of selectively destroying tumor cells.[77] Photodynamic therapy (PDT) is based on multiple processes by which a superoxide anion (O_2^-) is generated with a chemical source called a photosensitizer.[77]

This process is seen in low-valent metal complexes containing electron-accepting ligands such as polypyridine and α,α'-diimines.[42] More sophisticated structures have also been developed over the past three decades. From these, macrocyclic ligands that can produce O_2^- with high energy such as porphyrin, chlorin and phtalocyanine have been approved by the US FDA as photosensitizers.[33,34]

The photoinduced reactions of a metal complex with DNA could lead to chemical and photochemical cleavage of the strands as well as the interruption of vital signaling processes.[21,22]

[74] He, L., Li, Y., Tan, C., Ye, R., Chen, M., Cao, J., Ji, L. & Mao, Z. (2015). *Chemical Science*, **6**(10), 5409-5418.
[75] Matsson, P. & Kihlberg, J. (2017). *Journal of Medicinal Chemistry*, **60**(5), 1662-1664.
[76] Simpson, P., Schmidt, C., Ott, I., Bruhn, H. & Schatzschneider, U. (2013). *European Journal of Inorganic Chemistry*, **2013**(32), 5547-5554.
[77] deBoer-Maggard, T. R. & Mascharak, P. K. (2014). *Ligand Design in Medicinal Inorganic Chemistry*. Chichester, UK: Wiley.

2.5.5 Reduced reactivity

The reactivity of the metal complexes with other molecules, especially biomolecules, is another important trait that can be controlled by ligands.[78,79] Three cellular molecules and the reactivity thereof are of interest:

- Water (aquation)
- Thiol-binding molecules (resistance)
- DNA-repairing enzymes (resistance)

The reactivity of the metal complex with these molecules must be reduced to avoid side effects such as aquation occurring too fast and resistance of the tumor through thiols and enzymatic repair systems. A lower reactivity could be achieved by lowering the electrophilicity and increasing the steric hindrance around the metal. This could unfortunately decrease the anticancer activity, and thus a good balance should be found.[78,79]

2.5.6 Decreased cellular efflux

The active efflux of materials out of cells could be problematic and would decrease the anticancer activity of a compound since it will be unable to achieve its full potential in the cell.[80] Specialized transporter systems are responsible for the active efflux. Metal complexes that are specifically designed to overcome this are rare and it is known that the ligands usually bind to these systems and, in that way, inhibit them.[80,81] It is also hypothesized that the presence of the metal center also inhibits transport out of the cell. Some complexes exhibit efflux pump inhibition as shown by Spoerlein-Guettler *et al*.[82]

---

[78] Brown, S., Trotter, K., Sutcliffe, O., Plumb, J., Waddell, B., Briggs, N. & Wheate, N. (2012). *Dalton Transactions*, **41**(37), 11330-11339.

[79] Babak, M. V., Meier, S. M., Legin, A. A., Adib Razavi, M. S., Roller, A., Jakupec, M. A., Keppler, B. K. & Hartinger, C. G. (2013). *Chemistry - A European Journal*, **19**(13), 4308-4318.

[80] Pati, M., Niso, M., Ferorelli, S., Abate, C. & Berardi, F. (2015). *RSC Advances*, **5**(125), 103131-103146.

[81] Barta Holló, B., Magyari, J., Armaković, S., Bogdanović, G. A., Rodić, M. V., Armaković, S. J., Molnár, J., Spengler, G., Leovac, V. M. & Mészáros Szécsényi, K. (2016). *New Journal of Chemistry*, **40**(7), 5885-5895.

[82] Spoerlein-Guettler, C., Mahal, K., Schobert, R. & Biersack, B. (2014). *Journal of Inorganic Biochemistry*, **138**, 64-72.

2.5.7 Targeting organelles

A more recent topic is the targeting of organelles, as discussed earlier as well. This method originates from the use of more sophisticated techniques such as fluorescent confocal microscopy and Inductively Coupled Plasma Mass Spectrometry (ICP-MS) in which the exact location of metal species in cellular compartments can be determined.[50] Metal complexes involved have physicochemical properties that allows it to prefer certain organelles that are important for cell growth and replication, although the exact mechanism of action is not really known or investigated. An example of this preference is Doxorubicin (Dox) and its Re-complexes where the Dox on its own will only accumulate in the nucleus, but its Re-complexes prefers to accumulate in the mitochondria.[50,68]

2.6 *N,O* and *N,N'* bidentate ligands

Tropone and tropolone compounds, also called troponoids and tropolonoids, consist of a non-benzenoid seven-membered aromatic ring system.[83] These chemical moieties are present in many naturally occurring biological products and exhibit antibacterial, anti-fungal, anti-tumor and anti-viral biological activities.[84,85,86,87,88] The tropolonoids have a unique electronic structure and photophysical absorption and emission properties. Fluorescence are observed in some bioactive tropolonoid compounds such as colchicine, which has shown fluorescence after binding with tubulin proteins.[85] The fluorescent properties of tropolone were then also investigated. Tropolone and colchicine both have very low quantum yields at room temperature, but substituted tropolone derivatives have shown fluorescence with improved quantum yields.[83]

---

[83] Balachandra, C. & Sharma, N. (2017). *Dyes and Pigments*, **137**, 532-538.
[84] Liu, N., Song, W., Schienebeck, C., Zhang, M. & Tang, W. (2014). *Tetrahedron*, **70**(49), 9281-9305.
[85] Tormos, R. & Bosca, F. (2013). *RSC Advances*, **3**(30), 12031-12034.
[86] Boguszewska-Chachulska, A., Krawczyk, M., Najda, A., Kopańska, K., Stankiewicz-Drogoń, A., Zagórski-Ostoja, W. & Bretner, M. (2006). *Biochemical and Biophysical Research Communications*, **341**(2), 641-647.
[87] Inamori, Y., Sakagami, Y., Morita, Y., Shibata, M., Sugiura, M., Kumeda, Y., Okabe, T., Tsujibo, H. & Ishida, N. (2000). *Biological and Pharmaceutical Bulletin*, **23**(8), 995-997.
[88] Barret, M., Bhatia, P., Kociok-Köhn, G. & Molloy, K. (2014). *Transition Metal Chemistry*, **39**(5), 543-551.

In the 1960's, a renowned class of ligands called aminotroponimines (ATIH) were discovered.[89,90] These bidentate nitrogen chelating ligands are the synthetic aza-derivatives of tropolone and exhibit a very interesting and rich coordination chemistry with many main-group and transition metal complexes synthesized over decades.[91,92,93] ATIH ligands are anionic, bidentate nitrogen donors and can form very stable chelated complexes.[94] In the neutral form the amine (C-N) and imine (C=N) bond lengths differ, but in the anionic form it usually exhibits perfect symmetry, indicating the delocalization of the negative charge through the seven-membered ring.[95] This results in a 10 π-electron system as depicted in Figure 2.18 with R = H, alkyl, aryl. These ligands are believed to be much more resistant towards electrophiles and nucleophiles than the well-known 1,4-diazabutadiene (DAD) ligand.[95]

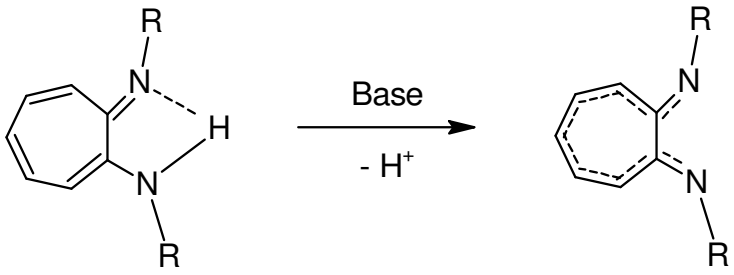

Aminotroponimine [ATI]H

10 π–electron system

Figure 2.18: A representation of the conjugated electron system of an aminotroponimine ligand.

In a study where Balachandra and Sharma synthesized a few boron aminotroponimine complexes, of which an example is illustrated in Figure 2.19, only the boron aminotroponimine complexes were fluorescent and the

[89] Brasen, W., Holmquist, H. & Benson, R. (1960). *Journal of The American Chemical Society*, **82**(4), 995-996.
[90] Brasen, W., Holmquist, H. & Benson, R. (1961). *Journal of The American Chemical Society*, **83**(14), 3125-3135.
[91] Holm, R. H. & O'Connor, M. J. (1971). *Progress in Inorganic Chemistry*, **14**, 241-401.
[92] Villacorta, G. & Lippard, S. (1986). *Pure and Applied Chemistry*, **58**(11), 1477-1484.
[93] Roesky, P. (2000). *Chemical Society Reviews*, **29**(5), 335-345.
[94] Dochnahl, M., Löhnwitz, K., Pissarek, J., Biyikal, M., Schulz, S., Schön, S., Meyer, N., Roesky, P. & Blechert, S. (2007). *Chemistry - A European Journal*, **13**(23), 6654-6666.
[95] Dias, H. V. R., Jin, W. & Ratcliff, R. E. (1995). *Inorganic Chemistry*, **34**(24), 6100-6105.

aminotroponimines showed no emission properties.[83] Observations like these create opportunities for the development of many novel fluorophores.

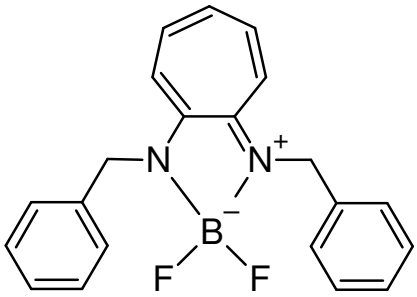

Figure 2.19: The chemical structure of boron *N*-benzyl-2-(benzylamino)troponimine.[83]

The synthesis of nitrogen containing ligands is of great value and interest to academic and industrial researchers because many natural products and pharmaceuticals contain an amine or amide moiety.[94] The exploration of this class of ligands as well as their precursors, tropolone and 2-(alkylamino)tropones has yielded compounds with applications as anticancer agents,[96] active catalysts for various important reactions such as intramolecular hydroamination, ethylene polymerization, olefin polymerization and many more.[97] It also yielded a class of compounds called tropocoronands. These ligands are versatile binucleating macrocycles that tend to bind to low oxidation state late transition metals such as Cu(I) and Rh(I).[98]

Tropolone-derived ligands exhibit some unique features:[97]

- Form a five-membered chelating ring with the metal center.
- Contain an enolic hydroxyl group analogous to a β-diketone.
- Negative charge accumulates predominantly on the nitrogen atoms of the 2-(alkylamino)tropone ligands.
- The large, planar seven-membered aromatic ring contributes substantially to the stability of a complex.

[96] Mendiguchia, B. S., Pucci, D., Mastropietro, T. F., Ghedini, M. & Crispini, A. (2013). *Dalton Transactions*, **42**, 6768-6774.
[97] Dwivedi, A. D., Binnani, C., Tyagi, D., Rawat, K. S., Li, P., Zhao, Y., Mobin, S. M., Pathak, B. & Singh, S. K. (2016). *Inorganic Chemistry*, **55**(13), 6739-6749.
[98] Villacorta, G. M., Rao, C. P. & Lippard, S. (1988). *Journal of The American Chemical Society*, **110**(10), 3175-3182.

By varying the *N*-alkyl substituents of the ligands, different properties and effects on the metal chelating and coordinating abilities of the ligands can be investigated. The substituents could be modified with regards to a few properties:[94]

- Steric effects by using alkyl groups from a smaller methyl group to sterically more demanding groups such as benzyl, cyclohexyl or *tert*-butyl groups.
- Chelation properties that could be altered by different linkers in macrocycles.
- Electronic effects that could be modified by utilizing the basicity and thus the donor strength of the ligand's nitrogen atoms.

2.7 The history and general applications of rhenium

The following paragraphs will focus and elaborate on the properties of rhenium.

Rhenium was a missing link on the periodic table (Figure 2.20) until 1925 when it was discovered and isolated from platinum ores by Walter Noddack, Ida Noddack-Tacke and Otto Berg in Germany.[99] It was independently discovered by J.G.F. Druce in England from commercial manganese salts.[99] The platinum ores from which the element was first commercially isolated were mined in the region of the Rhine River, thus deriving the element's name from the Latin term for the river, *Rhenus.* It was the last of the natural occurring elements to be discovered and is extremely rare.[99]

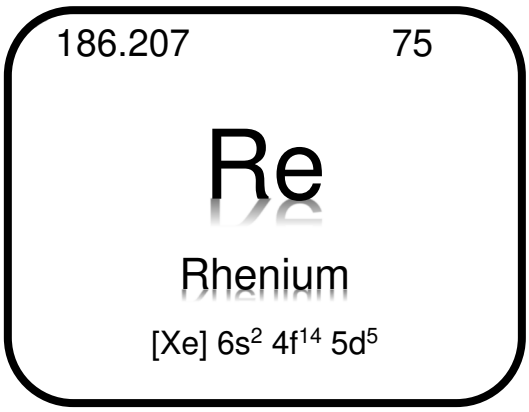

Figure 2.20: The element Rhenium as seen in the Periodic Table of Elements.

It is one of the least abundant elements in the earth's crust with a distribution of approximately 1-4 ppb and for many years it was thought that no mineral existed

[99] Weeks, M. E. (1956). *Discovery of the Elements* (6th ed.). Easton: Journal of Chemical Education.

that contained rhenium as the only cation.[100,101] In 1994 rhenium sulphide was discovered by Russian scientists at the mouth of a volcano on a remote island off the east coast of Russia.[101] Today rhenium is isolated as the by-product of the purification of molybdenum and copper.

Rhenium occurs naturally as a mixture of two stable isotopes, 37.4 % ^{185}Re and 62.6 % ^{187}Re and has the widest range of oxidation states (-3, -1, 0, +1, +2, +3, +4, +5, +6, +7) of all elements, which is one of its most important traits. As the heaviest congener of manganese, one would expect the chemistry of the two elements to be analogous, but the only resemblance is found in the organometallic compounds of the oxidation states +1 and lower. The only element rhenium resembles closely is technetium.[102]

Rhenium has the third-highest melting point (3186 ˚C) and highest boiling point (5360 ˚C) of all stable elements. It has a very high density of 21.02 g/cm^3, exceeded only by platinum, osmium, and iridium. It is a lustrous, silvery white, polyvalent transition metal with exceptional physiochemical properties, rendering it irreplaceable in some of its industrial applications.[101] Rhenium has a hexagonal close-packed crystal system which it retains up until its melting point, which imparts the ductile nature to the element. Rhenium is a key component in superalloys as it enhances the ductility, tensile strength and heat resistance of the alloys, making it a highly desirable metal in the commercial, aviation and space industry.[102] Surprisingly, rhenium is of more significance in the chemical industry than anywhere else. Its high selectivity and peculiar resistance to nitrogen, phosphorus and sulphur poisoning contributes greatly to its applications in catalytic processes such as:

- alkylation
- dealkylation
- dehydrochlorination
- dehydrogenation
- dehydro-isomerization

[100] Rouschias, G. (1974). *Chemical Reviews,* **74**(5), 531-566.
[101] Korzhinsky, M., Tkachenko, S., Shmulovich, K., Taran, Y. & Steinberg, G. (1994). *Nature*, **369**, 51-52.
[102] Dobrzańska-Danikiewicz, A. & Wolany, W. (2016). *Archives of Materials Science and Engineering,* **82**(2), 70-78.

- hydrocracking
- oxidation
- reforming
- hydrogenation

It is also well-known for its medical applications, which will be discussed in more detail in the following paragraphs.

2.8 Rationale for investigating the anticancer potential of rhenium(I) complexes

Complexes of metals with a d^6 electron configuration in their outermost shell display different properties and characteristics such as kinetic stability, charge, size, and lipophilicity. These factors in turn influence the *in vivo* stability and bioactivity of compounds. Utilizing the different properties of different ligands, the properties of the metal complexes could be altered to make compounds more appropriate for their possible medical applications.[50]

2.8.1 Properties of rhenium rendering it useful in medicine, especially oncology

In the early 1940's Walter Hiebner *et al.* studied the substitution of halogen rhenium pentacarbonyl complexes and this led to the synthesis and characterization of many organometallic Re carbonyl complexes.[103] The first cytotoxic *fac*-$[Re(CO)_3]^+$ complexes, namely *fac*-$[Re_2(\mu\text{-}OH)_3(CO)_6]^-$, *fac*-$[Re_2(\mu\text{-}OH)(\mu\text{-}OPh)_2(CO)_6]^-$, *fac*-$[Re_2(\mu\text{-}OMe)_2(\mu\text{-}dppf)(CO)_6]$, and *fac*-$[Re_2(\mu\text{-}OPh)_2(\mu\text{-}dppf)(CO)_6]$ (dppf = 1,10-bis(diphenylphosphino)-ferrocene), were reported in 2000 by Yan *et al*.[104]

Rhenium(I) complexes generally have an octahedral coordination geometry which, apart from the three carbonyls, provides three labile binding sites.[105] According to

[103] Hieber, W. & Fuchs, H. (1941). *Zeitschrift Für Anorganische Und Allgemeine Chemie*, **248**(3), 269-275.
[104] Yan, Y. K., Cho, S.E., Shaffer, K.A., Rowell, J.E., Barnes, B.J. & Hall, I.H. (2000). *Pharmacology*, **55**, 307–313.
[105] Bauer, E., Haase, A., Reich, R., Crans, D. & Kühn, F. (2019). *Coordination Chemistry Reviews*, **393**, 79-117.

Pearson's 'Hard and Soft Acid and Base' (HSAB) theory,[106] the *fac*-$[Re(CO)_3]^+$ core is considered a hard Lewis acid. This results in complex stabilities in the order *fac*-$[Re(CO)_3$(N-donor] > *fac*-$[Re(CO)_3$(S-donor] > *fac*-$[Re(CO)_3$(O-donor]. Therefore, many *fac*-$[Re(CO)_3]^+$ synthesized complexes found in literature are complexes of pyridine, bipyridine, phenanthroline and its derivatives.[107]

Transition metal complexes are known for their ability to bind to DNA either covalently or non-covalently. Non-covalent interactions can occur by intercalation, groove (major or minor) binding or external electrostatic binding.[108] The coordination chemistry of rhenium, especially compounds containing the *fac*-$[Re(CO)_3]^+$ moiety received considerable attention over many years due to its possible medical applications as β-emitters (^{186}Re and ^{188}Re isotopes) in radiopharmaceuticals. These 'hot' $^{186/188}$Re complexes together with their ^{99m}Tc analogues have shown good biosafety and have been used in clinics.[109,110] Cold Re organometallic compounds have been investigated by researchers for quite some time because of their intrinsic properties that are advantageous for chemotherapy:[105]

- One of the first and foremost is the variety of cell death mechanisms induced by these complexes such as apoptosis, paraptosis and necroptosis.
- Secondly, rhenium complexes have proved to be applicable as luminescent probes in cell imaging and in photodynamic therapy (PDT), photosensitizers in photocatalysis and photoactivatable therapy by means of CO-releasing mechanisms, which can be activated by proper irradiation in the region of a tumor. [111]

Many Re(I) tricarbonyl complexes in literature exhibit long-lived phosphorescence, large Stokes shifts and high quantum yields.[109,110]

---

[106] Pearson, R.G. (1963). *Journal of The American Chemical Society,* **85**, 3533–3539.
[107] Safi, B., Mertens, J., De Proft, F. & Geerlings, P. (2006). *The Journal of Physical Chemistry A*, **110**(29), 9240-9246.
[108] Ma, D. L., Che, C. M., Siu, F. M., Yang, M. & Wong, K. Y. (2007). *Inorganic Chemistry,* **46**, 740-749.
[109] Illán-Cabeza, N., García-García, A., Moreno-Carretero, M., Martínez-Martos, J. & Ramírez-Expósito, M. (2005). *Journal of Inorganic Biochemistry*, **99**(8), 1637-1645.
[110] Wang, F., Liang, J., Zhang, H., Wang, Z., Wan, Q., Tan, C., Ji, L. & Mao, Z. (2019). *ACS Applied Materials and Interfaces*, **11**(14), 13123-13133.
[111] Otero, C., Carreño, A., Polanco, R., Llancalahuen, F., Arratia-Pérez, R., Gacitúa, M. & Fuentes, J. (2019). *Frontiers in Chemistry*, **7**. doi: 10.3389/fchem.2019.00454

2.8.2 Recent advances in the exploration of rhenium(I) as a chemotherapeutic drug

Recently, Wang and co-workers[110] synthesized two dinuclear Re(I) tricarbonyl complexes with the general formula *fac*-[$Re_2(CO)_6(dip)_2L](PF_6)_2$ (dip = 4,7-diphenyl-1,10-phenanthroline ; L = 4,4'-azopyridine or 4,4'-dithiodipyridine) and are illustrated in Figure 2.21. The cytotoxicity of these complexes was tested on various cancer cell lines and the complexes proved to be more toxic than cisplatin toward most of the cell lines tested and possess higher anticancer activities than many reported Re-based anticancer agents.[110]

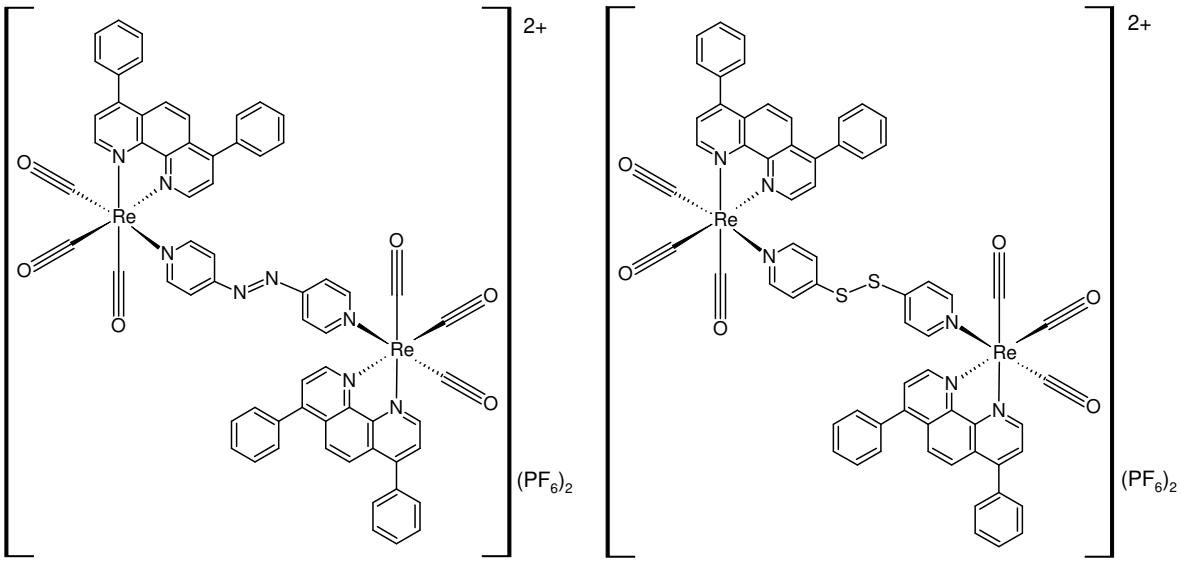

Figure 2.21: The chemical structures of two dinuclear Re(I) tricarbonyl complexes synthesized by Wang *et al.*[110]

Supporting this work, Konkankit *et al.*[54] investigated the rhenium(I) complex *fac*-[$Re(CO_3$(2,9-dimethyl-1,10-phenanthroline)$(H_2O)]^+$ (Figure 2.22) that was previously reported by Knopf *et al*. to be very potent in its *in vitro* anticancer activity in a different way than conventional platinum-based drugs.[18] The study of Konkankit *et al*. mainly concluded that *fac*-[$Re(CO)_3$(2,9-dimethyl-1,10-phenanthroline)$(H_2O)]^+$ inhibits tumor growth and thus has potential as an anticancer agent.

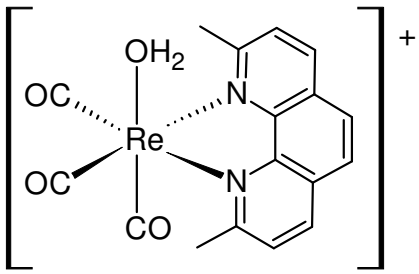

Figure 2.22: The chemical structure of *fac*-[Re(CO)$_3$(2,9-dimethyl-1,10-phenanthroline)(H$_2$O)]$^+$.[18]

This compound also proved to have higher anticancer activity towards HeLa cells than cisplatin.[18] Development of more complexes with properties like these could possibly prevent cross-resistance between compounds. In this study, the aqueous speciation, subcellular localization, and anticancer activity were studied. The *in vivo* anticancer activity was evaluated in mice and it was found that it is capable of inhibiting tumor growth. These favourable results as well as the limited detrimental effects prove that compounds of this type could possibly be used as anticancer agents.[54] This investigation also described the cellular uptake as the complex accumulates preferentially in mitochondria.

The *fac*-[Re(CO)$_3$]$^+$ core is known for its photosensitizing properties and an increased cytotoxicity upon irradiation was proven. Complexes with iminedipyridyl ligands were studied by Patra and co-workers.[112] In HeLa cells these complexes moderately inhibited growth with better cytotoxicity than cisplatin for the same cell line and proved to have a good safety profile which makes it suitable for the treatment of cervical cancer.[112]

The class of compounds based on cyrhetrene [(CO)$_3$Re(η^5-C$_5$H$_5$)] is increasingly investigated in biological studies.[113,114] Their suitable photo-physical and electrochemical properties, high stability in water and air, lipophilicity and specific

[112] Patra, M., Wenzel, M., Prochnow, P., Pierroz, V., Gasser, G., Bandow, J. & Metzler-Nolte, N. (2015. *Chemical Science*, **6**(1), 214-224.
[113] Oyarzo, J., Acuña, A., Klahn, H., Arancibia, R., Silva, C. P., Bosque, R., López, C., Font-Bardía, M., Calvis, C. & Messeguer, R. (2018). *Dalton Transactions*, **47**(5), 1635-1649.
[114] Anisimov, I., Saloman, S., Hildebrandt, A., Lang, H., Trzybiński, D., Woźniak, K., Šakić, D., Vrček, V. & Kowalski, K. (2017). *Chempluschem*, **82**(6), 859-866.

biological activities made them applicable especially as antimalarial[115,116] and anticancer agents.[42,117,118,119,120]

A detailed biological study was performed by Massi and co-workers[121] on *N*-heterocyclic carbene complexes of Re(I) and ruthenium, which are modified with indomethacin, an anti-inflammatory drug. The antiproliferative activity was tested against different pancreatic cancer cell lines and healthy HEK cells. The complexes displayed IC_{50} values in the low micromolar range, similar to cisplatin, for all the cancer cell lines tested and slightly higher values for the healthy cells. Similar complexes of ruthenium were tested and showed no activity. One structural property that proved to influence the activity of the complexes was the lability of the auxiliary bromide ligand.[121]

A series of Re(I) tricarbonyl complexes with mixed donor ligands were tested for their cytotoxicity against breast cancer cells.[122] These compounds have very low IC_{50} values in the sub micromolar range in MCF-7A, MCF-10A and MDA-MB breast cancer cell lines. The authors attributed the good results to the lipophilicity of the complexes which improves cell membrane penetration and DNA intercalation abilities. The phenanthroline-based complex seen in Figure 2.23 has the lowest IC_{50}

[115] Glans, L., Hu, W., Jöst, C., De Kock, C., Smith, P. J., Haukka, M., Bruhn, H., Schatzschneider, U. & Nordlander, E. (2012). *Dalton Transactions*, **41**(21), 6443-6450.
[116] Arancibia, R., Dubar, F., Pradines, B., Forfar, I., Dive, D., Klahn, A. & Biot, C. (2010). *Bioorganic and Medicinal Chemistry*, **18**(22), 8085-8091.
[117] Hu, W., Splith, K., Neundorf, I., Merz, K. & Schatzschneider, U. (2011). *JBIC Journal of Biological Inorganic Chemistry*, **17**(2), 175-185.
[118] Can, D., Spingler, B., Schmutz, P., Mendes, F., Raposinho, P., Fernandes, C., Carta, F., Innocenti, A., Santos, I., Supuran, C. T. & Alberto, R. (2012). *Angewandte Chemie International Edition*, **51**(14), 3354-3357.
[119] Muñoz-Osses, M., Godoy, F., Fierro, A., Gómez, A. & Metzler-Nolte, N. (2018). *Dalton Transactions*, **47**(4), 1233-1242.
[120] Concha, C., Quintana, C., Klahn, A. H., Artigas, V., Fuentealba, M., Biot, C., Halloum, I., Kremer, L., López, R., Romanos, J., Huentupil, Y. & Arancibia, R. (2017). *Polyhedron*, **131**, 40-45.
[121] Simpson, P., Casari, I., Paternoster, S., Skelton, B., Falasca, M. & Massi, M. (2017). *Chemistry - A European Journal*, **23**(27), 6518-6521.
[122] Wilder, P. T., Weber, D. J., Winstead, A., Parnell, S., Hinton, T. V., Stevenson, M., Giri, D., Azemati, S., Olczak, P., Powell, B. V., Odebode, T., Tadesse, S., Zhang, Y., Pramanik, S. K., Wachira, J. M., Ghimire, S., Mccarthy, P., Barfield, A., Banerjee, H. N., Chen, C., Golen, J. A., Rheingold, A. L., Krause, J. A., Ho, D. M., Zavalij, P. Y., Shaw, R. & Mandal, S. K. (2018). *Molecular and Cellular Biochemistry*, **441**(1-2), 151-163.

value (0.023±0.002 μM) in this study. It was also observed that the lability of the axial ligand had less of an influence on the activity than the changes in the phenanthroline moiety.

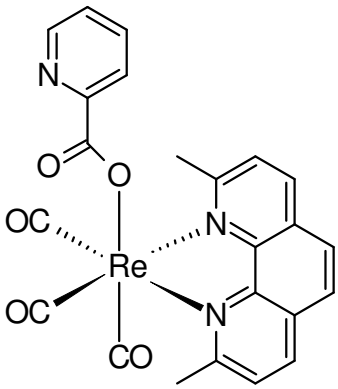

Figure 2.23: A phenanthroline-based Re(I) complex studied by Wilder *et al.*[122]

2.9 Conclusion

Research in the field of cancer treatment increased immensely over the years and have yielded many forms of treatment and subsequent improvements. Cancer is still on the increase and therefore there is a constant need for the development of new treatments and improvement of the existing chemotherapeutic drugs.

Re(I) complexes have proved to have several traits rendering it suitable for applications in various types of therapy as well as diagnosis. Ligands such as 2-(alkylamino)tropones and aminotroponimines are attractive for use in combination with Re(I) due to their proven advantageous properties. They also provide opportunities for the development of fluorophores. Synthesizing derivatives of these types of ligands and Re(I) complexes thereof with possible applications in chemotherapy and photodynamic therapy would contribute greatly to this field of research.

The next two chapters will describe the synthesis and characterization techniques of the 2-(alkylamino)tropone and aminotroponimine ligand systems as well as its Re(I) tricarbonyl complexes.

3

THE BASIC THEORY OF CHARACTERIZATION TECHNIQUES

3.1 Introduction

Characterization of reagents and products is a very important part of a research project which aids in the identification of starting materials, possible intermediates, by-products and pure products. There are various methods available for the characterization of newly synthesized chemical compounds. The methods used depend on the state of the sample being analysed, i.e. solid or solution state. The various methods are also divided into two groups, distinguishing destructive and non-destructive methods from each other. Inductively Coupled Plasma (ICP), Elemental Mass (MS) and Atomic Absorption (AA) spectrometry as well as Gas Chromatography (GC) are examples of destructive methods. Non-destructive methods are preferred when only a small quantity of sample is available and will generally use some form of radiation to identify components. Examples of these methods are Infrared absorption (IR), Ultraviolet-visible (UV/Vis) and Nuclear Magnetic Resonance (NMR) Spectroscopy as well as X-ray Diffraction crystallography (XRD).

In this research project, *N,O* and *N,N'* bidentate ligands as well as the Re(I) tricarbonyl complexes containing these ligands are characterized by means of IR, UV/Vis and NMR spectroscopy. The structures of a precursor molecule and two ligands were fully characterized with XRD and will be further evaluated in Chapter 5. The basic theory of these techniques and photoluminescence will be discussed in this chapter.

3.2 Infrared (IR) absorption spectroscopy

Spectroscopic methods are based on the measurement of the amount of radiation absorbed or emitted by the species of interest. This electromagnetic radiation or light (Figure 3.1) is a form of energy transmitted through space at an extremely fast

rate.[1] The radiation could be described as a wave and has properties such as wavelength, frequency, velocity, and amplitude and can travel readily through a vacuum. In molecular absorption spectroscopy the amount of radiation absorbed as a result of excitation is measured as a function of wavelength.[1] These absorption measurements can give qualitative and quantitative information which is of great value to the researcher.

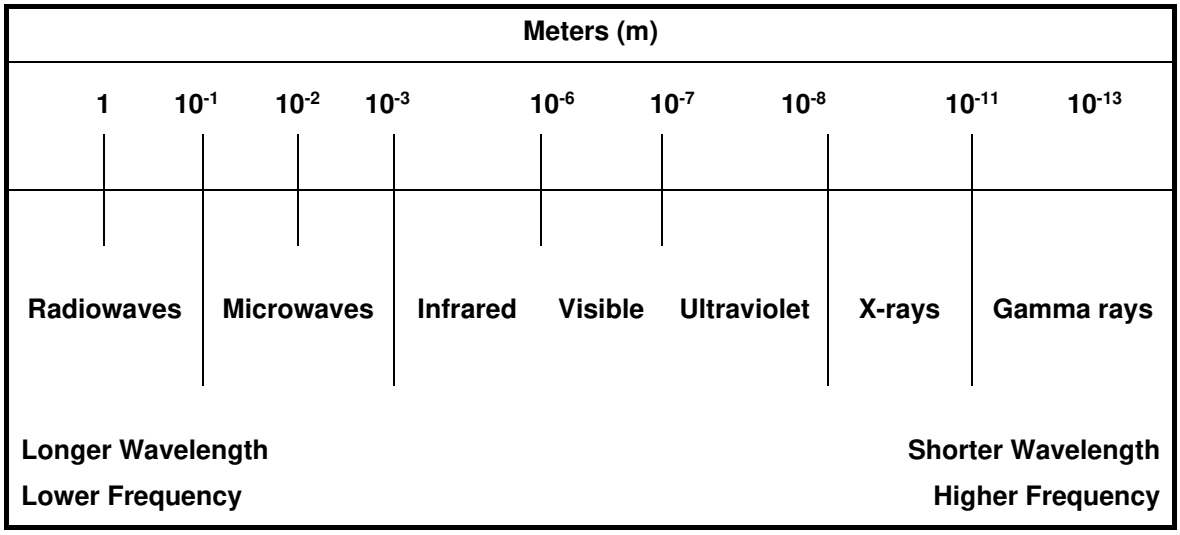

Figure 3.1: Electromagnetic wavelength spectrum.

IR spectroscopy is less efficient for quantitative analysis than UV/Vis spectroscopy due to its lower sensitivity and deviations from Beer's Law. Regardless, it is a powerful method for the analysis and characterization of organic and inorganic compounds because, excluding some homonuclear molecules such as O_2, N_2 and Cl_2, all molecular species absorb infrared radiation. Every molecular compound, except for chiral molecules, has a unique infrared absorption spectrum which is also called a molecular fingerprint. The spectrum of an analysed compound is compared to this fingerprint to determine if the desired reaction took place and consequently characterize a synthesized compound.[1,2]

The energy of infrared radiation is usually too low to cause electronic transitions but can induce vibrational and rotational transitions associated with the ground state of a molecule.[1,2] A few types of molecular vibrations are depicted in Figure 3.2.

[1] Skoog, D., West, D., Holler, J. & Crouch, S. (2014). *Fundamentals of Analytical Chemistry* (9th ed.). Belmont, California: Cengage Learning.
[2] Skoog, D., Holler, J. & Crouch, S. (2007). *Principles of Instrumental Analysis* (6th ed.). Belmont, California: Brooks/Cole.

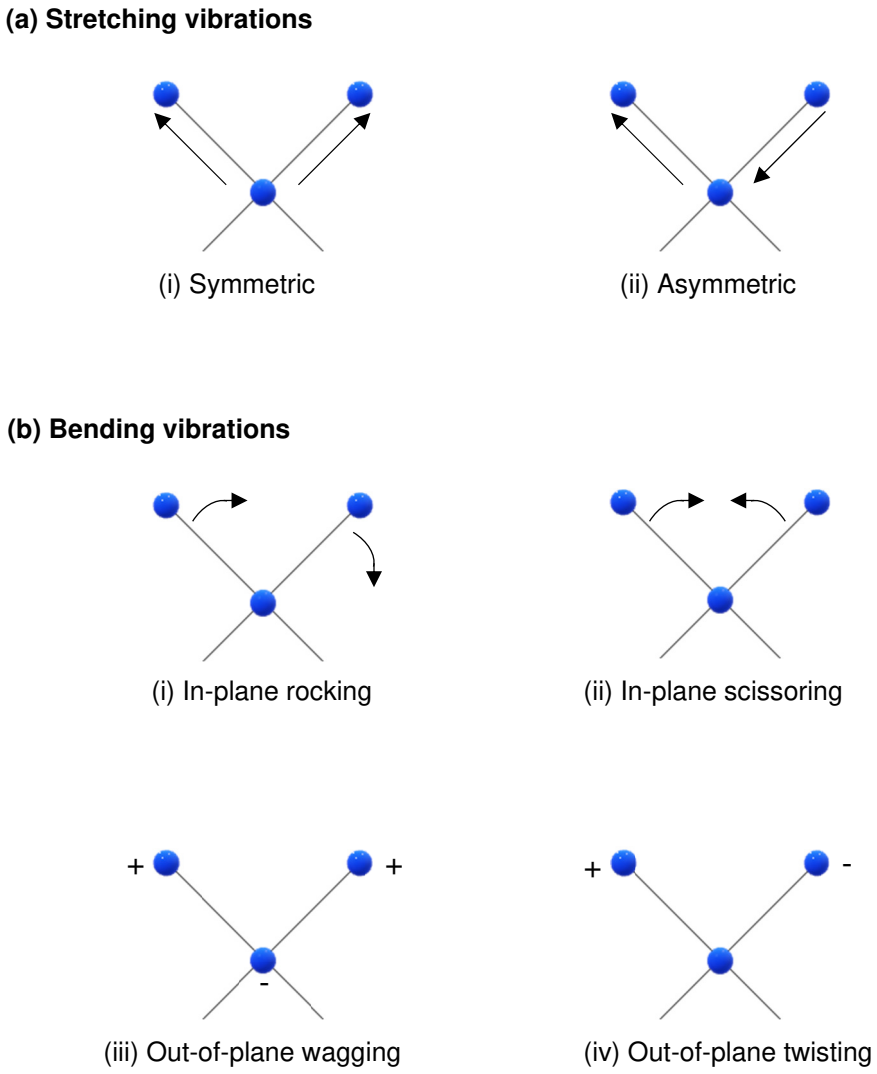

Figure 3.2: Examples of the types of molecular vibrations. The plus (+) sign indicates motion out of the page and the minus (-) sign indicates motion into the page.

For a vibrational state to absorb energy from the incident infrared radiation and thus appear on the IR spectrum, it is necessary that a net change in dipole moment occurs during the vibration.[2,3] The charge distribution in a heteronuclear molecule is not symmetric due to the difference in electron density of the atoms. When such a polar molecule vibrates, there is a regular fluctuation in its dipole moment. A field is established that can interact with the alternating electric field of the radiation. When the frequency of the radiation matches the vibrational energy of the molecule, absorption of radiation takes place and results in a change in the amplitude of the

[3] Denney, R., Jeffery, G., Bassett, J. & Mendham, J. (1989). *Vogel's Textbook of Quantitative Chemical Analysis* (5th ed.). Harlow, England: Longman Scientific & Technical.

molecular vibration. Rotation of asymmetric molecules around their centres of mass produces a similar interaction leading to absorption.[2]

These frequencies (ν, Hz) of the radiation where absorption occurs are rarely used as the abscissa in spectra because of the inconvenient size of its unit. Although the terminology is strictly incorrect, wavenumber ($\bar{\nu}$, cm^{-1}) is used as the unit instead and is referred to as the frequency.[2] The relationship between the wavenumber, frequency and energy is shown in Equations 1 and 2:

$$\bar{\nu} = \frac{1}{\lambda} = \frac{\nu}{c} \quad \ldots(1)$$

$$E = h\nu = \frac{hc}{\lambda} = hc\bar{\nu} \quad \ldots(2)$$

with $\bar{\nu}$ = wavenumber (cm^{-1}), λ = wavelength (cm), ν = frequency (s^{-1}), c = speed of light in a vacuum (3×10^{10} $cm.s^{-1}$), E = energy (Joule) and h = Planck's constant (6.63×10^{-34} J.s).

There are general trends regarding stretching frequencies of compounds or molecules. For example, the frequencies of triple bonds are higher than that of double bonds, which in turn have higher frequencies than single bonds. Another trend involves the influence of dipole moments; more polar bonds will have higher stretching frequencies. Familiarizing oneself with these trends could contribute to the usefulness of this technique.

3.3 Ultraviolet-visible (UV/Vis) spectroscopy

Ultraviolet-visible (UV/Vis) spectroscopy is a useful spectrochemical method to characterize organic, inorganic, and biochemical compounds. This type of absorption spectrometry can also be used to monitor titrations, study the composition of complex ions and follow the kinetics of chemical reactions for quantitative purposes.[1]

When a molecule is excited by ultraviolet or visible radiation it undergoes electronic, vibrational, and rotational transitions. Excitation occurs when an electron is promoted from its ground state (low energy orbital) to an excited state (high energy orbital). A very simplified diagram of this process is presented in Figure 3.3. The energy of the radiation must be exactly the same as the energy difference between these two orbitals for absorption to occur.[1,2]

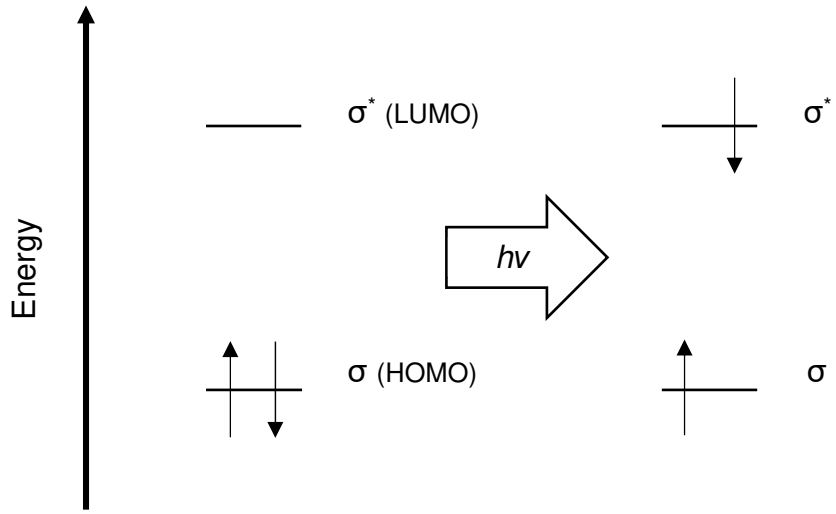

Figure 3.3: The excitation of electrons when radiated with ultraviolet or visible light.

Organic molecules absorb radiation at wavelengths in the range of 180-780 nm. This is due to the interactions between photons and bonding electrons between two atoms or electrons that are delocalized around atoms such as oxygen, sulphur, nitrogen, and halogens. The wavelength at which absorption takes place depends on how strong the bonds are:[1,2]

- Electrons in single bonds (C-C and C-H) are held firmly and require energies corresponding to wavelengths below 180 nm for excitation and absorption to take place.
- The electrons in double and triple bonds are not held as firmly as single bonds and require lower energies (at higher wavelengths) for excitation.

Thus, compounds with unsaturated bonds display absorption bands that are useful for characterization. Such organic functional groups that absorb in the ultraviolet-visible region are called chromophores.[1,2]

Inorganic compounds generally absorb broad bands of visible radiation in at least one of their oxidation states, resulting in these compounds being coloured. This type

of absorption occurs due to the transitions of electrons between filled and unfilled *d*-orbitals.[1,2] The energies corresponding to these transitions depend on the ligands coordinated to the metal. The position of the metal on the periodic table, its oxidation state and the ligand bonded to it determines the energy between the *d*-orbitals and thus the wavelength of the maximum absorption.[1,2]

3.4 Nuclear Magnetic Resonance (NMR) spectroscopy

Nuclear Magnetic Resonance (NMR) spectroscopy determines information about the molecular structure of compounds that would be difficult, if not impossible, to determine by any other method. As with other spectroscopic techniques, NMR spectroscopy is based on the interaction of matter with electromagnetic radiation. In this technique, the interactions of an oscillating radio-frequency electromagnetic field with nuclei in a strong external magnetic field are measured. These nuclei form part of atoms which form part of molecules.[4]

A particle of radiation is called a photon and is originally in the form of an oscillating electric or magnetic field. For another particle to absorb a photon, the photon must have the same energy as the motion of that particle. It is only possible for the energies to be equal if the oscillations of the photon's electric and/or magnetic fields can constructively interfere with the oscillations of the particle's electric and/or magnetic fields. As soon as these energies are equal, the system is said to be in resonance and absorption can occur. Different atoms in a molecule absorb or resonate at different radio-frequencies at a given field strength.[4,5]

Atomic nuclei spin on their own axes and thus have magnetic properties that will cause their energy levels to split on exposure to an external magnetic field. Spin-paired atoms like ^{12}C, ^{16}O and ^{32}S has no overall spin ($\ell = 0$) and cannot exhibit

[4] Macomber, R. (1998). *A Complete Introduction to Modern NMR Spectroscopy*. New York: John Wiley & Sons.

[5] Claridge, T. (2009). *High-resolution NMR Techniques in Organic Chemistry* (2nd ed.). Amsterdam: Elsevier.

resonance on an NMR spectrum. A few NMR-active nuclides are shown in Table 3.1.[2,4,6]

Table 3.1: Examples of NMR-active nuclides and their properties.

Nuclide	Element/ isotope	Spin	Natural abundance (%)	Frequency relative to ^{1}H
^{1}H	Hydrogen-1	½	99.985	1.00000
^{13}C	Carbon-13	½	1.108	0.25145
^{15}N	Nitrogen-15	½	0.37	0.10137
^{19}F	Fluorine-19	½	100	0.94094
^{31}P	Phosphorus-31	½	100	0.40481
^{2}H (or ^{2}D)	Deuterium-2	1	0.015	0.15351

The overall spin (ℓ) is an important characteristic of a nucleus and can have values equal to or greater than zero and which are multiples of ½ in order to be NMR active. It can be determined for each nucleus as follows:

- If the number of neutrons and the number of protons are both even, the nucleus has no overall spin.
- If the sum of the number of neutrons and protons is odd, then the nucleus has a half-integer spin (i.e. 1/2, 3/2, 5/2, etc.).
- If the number of neutrons and the number of protons are both odd, the nucleus has an integer spin (i.e. 1, 2, 3, etc.).

According to quantum mechanics, a nucleus of spin ℓ will have $2\ell + 1$ possible states of orientation. In the absence of an external magnetic field, these orientations are degenerate, but the energy levels will split as soon as an external field is applied.[2,4,5]

According to Heisenberg's uncertainty principle, the positive charge in an atom's nucleus prefers not to be well located. This results in the presence of a magnetic moment in an isotope's nucleus and affords it its NMR activity. When a sample is subjected to the high strength magnetic field in an NMR magnet the magnetic moments of the NMR active nuclei aligns, either partially parallel (α spin state) or

[6] Simpson, J. (2008). *Organic Structure Determination Using 2-D NMR Spectroscopy*. Amsterdam: Elsevier.

antiparallel (β spin state) with the direction of the external field.[2,6] The energies of these two spin states diverge linearly with the increasing magnetic field as indicated in Figure 3.4. This is called the Zeeman effect.

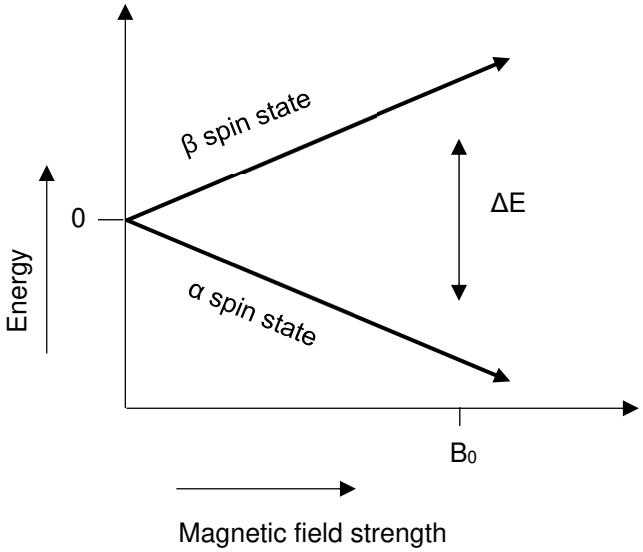

Figure 3.4: A Zeeman energy diagram displaying the divergence of the energies of the two allowed spin states for a spin-1/2 nucleus with increase in the applied magnetic field strength.

Each NMR-active nuclide will display a unique difference in energy at a given magnetic field strength. The slope for this energy divergence is expressed by the gyromagnetic ratio which is unique for every nuclide. The ratio and its equation (Equation 3) show the relationship between the difference in energy (ΔE, joule) of the two states of a spin-1/2 nucleus and the strength of the applied magnetic field (B_0, tesla).[6]

$$\Delta E = \gamma B_0 \qquad \ldots(3)$$

As mentioned previously, for the energy transitions and absorption by the excited nuclei to occur, photons from the applied radiation must have the same energy (Equation 4) as the energy gap between the two spin states.[2,6]

$$\Delta E = h\nu = \frac{h\omega}{2\pi} \qquad \ldots(4)$$

From Equation 4, *h* is Planck's constant (6.63 x 10^{-34} J.s), ν is frequency (s^{-1}) and ω is the angular frequency ($rad.s^{-1}$). A magnetic signal called a free induction decay (FID) is emitted by the excited nuclei. These signals are detected and captured electronically and digitally. It is then processed computationally to possibly reveal detailed information about the sample.[2,6]

It would seem obvious that atoms of the same kind would experience the same energy in a given applied magnetic field and consequently have one peak on the spectrum for that specific atom. This is however not the case, due to nuclear shielding and deshielding. NMR-active nuclei in a molecule are surrounded by different environments in each molecule. The electron density of the molecule can resist the applied magnetic field and thus shield the nuclei from this field to some extent. The chemical shift (δ) is defined as the alteration of the radio-frequency at which chemically distinct NMR-active nuclei resonates as a result of the shielding.[5,6]

Another effect that nuclei have on each other due to the applied magnetic field, is coupling. During spinning of the nuclei, the different spin states interact with each other through the chemical bonds of the molecule and this causes splitting of the NMR signals. Of course, this phenomenon provides even more detail with regards to the connectivity of the atoms in a molecule. It is reported as a *J*-coupling number in units of Hz and is obtained by measuring the difference between the peaks on the NMR spectrum.[4,5,6]

3.5 X-ray Diffraction (XRD) crystallography

Crystals have been of great interest to many scientists since the earliest times. A crystal is defined as a substance that is crystalline, periodic in three dimensions and is bound by plane faces. Crystallography is the study of crystals and is based on the structural determination of a compound in the solid state with two generally used methods, X-ray and neutron diffraction.[7] It is a widely used and an invaluable form of characterization of chemical compounds, especially in organometallic chemistry.[7,8]

[7] Ladd, M. & Palmer, R. (2013). *Structure Determination by X-ray Crystallography* (5th ed.). New York: Springer.

[8] Crabtree, R. (2005). *The Organometallic Chemistry of the Transition Metals* (4th ed.). Hoboken, New Jersey: John Wiley & Sons.

Chapter 3

X-ray diffraction was used as early as 1913 when William Lawrence Bragg established the three-dimensional arrangement of atoms in a crystal for the first time.[9] This was not long after Wilhelm Conrad Röntgen had discovered X-rays and Max von Laue proposed that these X-rays could by scattered by crystals.[9]

The simplest unit of a crystal structure is called the unit cell. The repetitive arrangement of the unit cell describes the three-dimensional structure of a crystal. This arrangement exists as a specific space group. In X-ray diffraction, a beam of monochromatic X-rays is passed through a single crystal of a sample. This incident beam is then diffracted at various angles and will appear as spots on a photograph. The film methods are seldomly used today and is replaced by using a computer-controlled device called a diffractometer. The angle and intensity of the set of diffracted beams is dependent on the nature and arrangement of the electron density in the unit cell and thus contain information about the location of the atoms in the unit cell. The spots on the photograph will provide information about the arrangement of the unit cell in space. Once the positions of the atoms are known precisely, the molecule's properties such as interatomic distances, bond angles, planarity of a particular group of atoms, the angles between planes and conformation angles around bonds can be calculated.[7,9]

The faces of a crystal exist as planes in three-dimensional space as depicted in Figure 3.5.

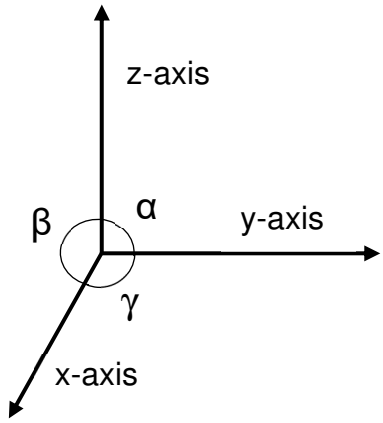

Figure 3.5: The general crystallographic axes x, y and z, as well as their interaxial angles.

[9] Glusker, J. & Trueblood, K. (2010). *Crystal Structure Analysis* (3rd ed.). Oxford: Oxford University Press.

A parametral plane is usually defined to which other planes are referenced according to the three numbers, *h*, *k* and *l*, which are called Miller indices. This notation was developed by Miller in 1839.[7,9]

3.5.1 The theory of XRD and Bragg's Law

Bragg's Law is used to explain why faces of crystals appear to reflect X-rays at certain angles of incidence. This explanation is presented in Figure 3.6 where a beam of X-rays enters a crystal with an angle θ to the atomic planes.

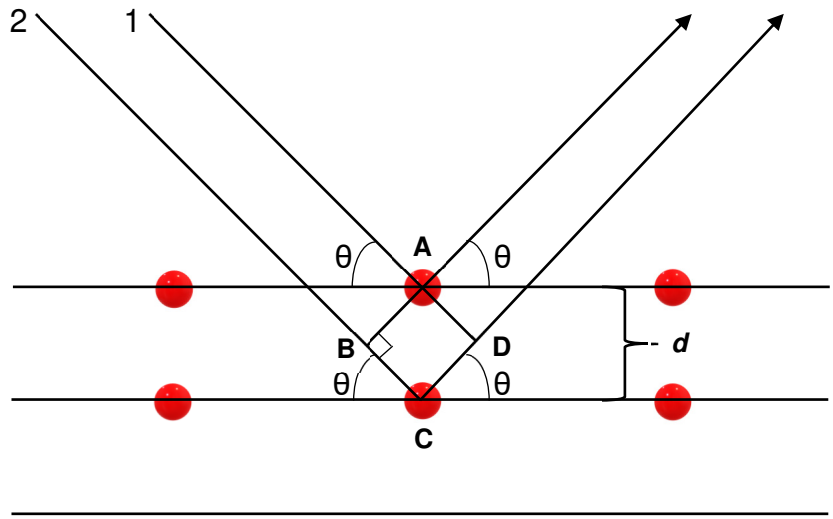

Figure 3.6: Representation of the diffraction of X-rays according to Bragg's Law.

A crystal contains evenly spaced atomic planes that reflect the waves of radiation. The orientation of the set of planes is represented by the Miller indices, *h*, *k* and *l* and the spacing between these planes is represented by *d*. X-rays that are reflected from the same planes remain in phase. Those reflecting from adjacent planes will undergo constructive interference because they are out of phase and have travelled different path lengths of which the length is an integer multiple (n) of the X-ray wavelength (λ). Bragg's Law refers to Equation 5:[7,9]

$$n\lambda = 2dsin\theta \qquad \ldots(5)$$

A reflection is 'indexed' when its Miller indices or its reciprocal lattice vector components have been identified from the diffraction angle 2θ at a given wavelength. The indexing yields the unit cell lengths and angles as well as its space group.

3.5.2 The three stages of the analysis of a crystal structure by X-ray diffraction

The three stages of the process by which a crystal structure is analysed describes the most important steps that are followed.[9]

1. Data collection. This process entails the experimental measurement of the scattering directions of the diffracted X-ray beams. From this a unit cell is selected and its dimensions measured. The intensities of as many as possible of the Bragg reflections or diffracted beams from the same crystal are recorded. As mentioned previously, these intensities are dependent on the nature of the atoms in the crystal as well as their relative positions in the unit cell.

2. *Solving a 'trial structure'*. A 'trial structure' is basically a proposed atomic arrangement in the crystal. The structure is concluded by using direct methods or the Patterson method. This arrangement of atoms measured with respect to the unit-cell axes is listed as atomic coordinates. From the coordinates the intensity of the Bragg reflections corresponding to this trial structure can be calculated. The calculated intensities are compared to the corresponding experimentally determined intensities. This serves as an indication to whether the trial structure is essentially correct and thus a 'good' structure.

3. *Refinement of the trial structure*. Refinement is a form of modification. This means that a good trial structure is modified repeatedly until the calculated and measured intensities agree with each other within certain limits of errors in the observations. A least squares refinement is generally used, although difference electron-density maps could also be used. Refinement of a structure yields information on the three-dimensional atomic coordinates in the crystal as well as atomic displacement parameters.

3.6 Theory of photoluminescence studies

Photoluminescence spectroscopy is the measurement of the emission of light from any form of matter following the absorption of photons from electromagnetic radiation. The two most important forms of photoluminescence are fluorescence and phosphorescence and it is schematically presented in Figure 3.7 followed by a brief explanation of the processes.

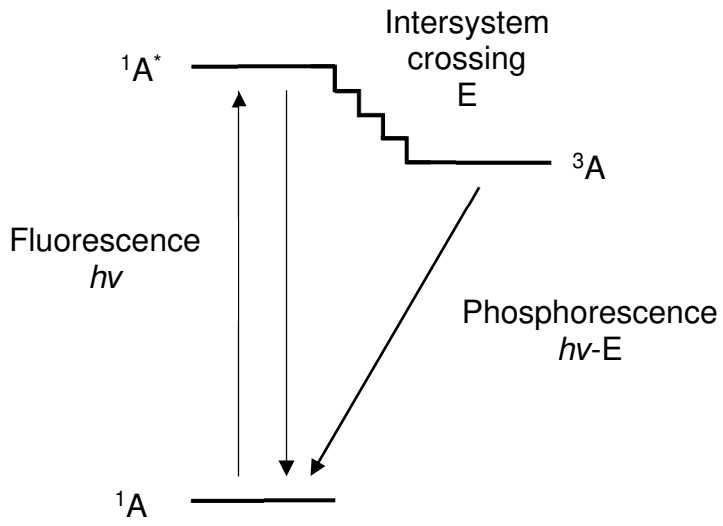

Figure 3.7: A Jablonski diagram of the excitation, intersystem crossing and relaxation of molecule A by phosphorescence.

When a substance absorbs electromagnetic radiation, it undergoes internal energy transitions before re-emitting the energy in the form of light. Electrons of the substance can change energy states by resonance, where photons of a certain wavelength are absorbed, and re-emitted photons are of equal energy. Fluorescence is a faster process than phosphorescence. Although it is fast, it discards a certain amount of the original energy to the surroundings as vibrational energy and this results in the re-emitted photons having a lower energy than what the absorbed photons initially had. The re-emitted photons of lower energy are said to be 'red-shifted', referring to the reduced energy.[1,10] In phosphorescence the excited electrons undergo intersystem crossing. This means that they enter a state with altered spin multiplicity which is usually the triplet state.[1,10] When an electron is in a triplet state, relaxation to the lower singlet state energies is forbidden according to quantum mechanics, resulting in a very slow relaxation process. This slow radiative relaxation back to the singlet state could last up to minutes or hours and this is the basis for 'glow in the dark' substances.[1,10]

Although certain aliphatic and alicyclic carbonyl compounds and highly conjugated double-bond structures show fluorescence, a greater number of cyclic aromatic compounds yield intense and very useful molecular fluorescence emission. Most

[10] Atkins, P. & De Paula, J. (2010). *Physical Chemistry* (9th ed.). Oxford: Oxford University Press.

unsubstituted aromatic hydrocarbons show fluorescence in solution and yields an increase in quantum efficiency proportional to the number of rings and their degree of condensation.[1,10] Very simple heterocycles such as pyridine, furan, thiophene, and pyrrole do not fluoresce, but fused-ring structures that contain these molecules often do. Substitution on aromatic rings brings about changes in the wavelength of absorption maxima and thus changes in the fluorescence bands. Substitution also affects the fluorescence efficiency. The luminescence of a molecule could be quenched by molecules with widely spaced vibrational levels that accept the large amount of energy.[1,10]

Photoluminescence could be used for qualitative and quantitative analysis as well as in the study of chemical equilibria and kinetics of reactions. It has become a very sought-after trait in chemical compounds due to the use of such compounds in photodynamic therapy research.[1]

4

SYNTHESIS AND CHARACTERIZATION OF *N,O* AND *N,N'* BIDENTATE LIGANDS AND ITS *fac*-RE(I) TRICARBONYL COMPLEXES

4.1 Introduction

Rhenium complexes are constantly gaining more interest as anticancer agents. These complexes have a d^6 electron configuration in its outermost shell and display highly desirable traits such as high kinetic stability, structural diversity, charge, size, lipophilicity and rich spectroscopic properties.[1,2] These properties of the complexes can be tuned to make them more suitable for their possible medical applications by implementing different types of ligand systems.[2] In terms of photodynamic therapy (PDT), many Re(I) tricarbonyl complexes exhibit long-lived phosphorescence, large Stokes shifts and high quantum yields.[3,4] These factors influence the *in vivo* stability and bioactivity of the complexes and are thus very important to consider when designing these compounds.

Rhenium(I) tricarbonyl complexes usually have three labile binding sites due to their octahedral geometry.[5] Many of these complexes found in literature contain pyridine, bipyridine, phenanthroline and its derivatives as ligand systems and complexes of this type (*fac*-[Re(CO)$_3$(*N*-donor)]) seem to be the most stable.[6] This is based on Pearson's 'Hard and Soft Acid and Base' (HSAB) theory which implicates that

[1] Lee, L., Leung, K. & Lo, K. (2017). *Dalton Transactions*, **46**(47), 16357-16380.
[2] Marloye, M., Berger, G., Gelbcke, M. & Dufrasne, F. (2016). *Future Medicinal Chemistry*, **8**(18), 2263-2286.
[3] Illán-Cabeza, N., García-García, A., Moreno-Carretero, M., Martínez-Martos, J. & Ramírez-Expósito, M. (2005). *Journal of Inorganic Biochemistry*, **99**(8), 1637-1645.
[4] Wang, F., Liang, J., Zhang, H., Wang, Z., Wan, Q., Tan, C., Ji, L. & Mao, Z. (2019). *ACS Applied Materials and Interfaces*, **11**(14), 13123-13133.
[5] Bauer, E., Haase, A., Reich, R., Crans, D. & Kühn, F. (2019). *Coordination Chemistry Reviews*, **393**, 79-117.
[6] Safi, B., Mertens, J., De Proft, F. & Geerlings, P. (2006). *The Journal of Physical Chemistry A*, **110**(29), 9240-9246.

complexes containing the *fac*-$[Re(CO)_3]^+$ core are considered hard Lewis acids.[7] They have a high affinity for *N*-donor ligand systems as these are hard bases.

The *N,O* and *N,N'* ligand systems explored in this study, namely 2-(alkylamino)tropones and aminotroponimines (Figure 4.1) are derivatives of tropolone and consist of a non-benzenoid seven-membered aromatic system with a conjugated 10 π-electron backbone that contributes to the system's stability.[8] Tropolone has been utilized as an *O,O'* bidentate ligand coordinated to a *fac*-$[Re(CO)_3]^+$ core as part of very interesting studies which include good results for substitution kinetics as well as cytotoxicity.[9,10,11] Various derivatives of tropolone exhibit antimalarial,[12] antimicrobial,[13] antiviral[14] and anticancer[15,16,17,18,19] activities and more derivatives thereof are worth exploring.

[7] Pearson, R.G. (1963). *Journal of The American Chemical Society,* **85**, 3533-3539.
[8] Balachandra, C. & Sharma, N. (2017). *Dyes and Pigments*, **137**, 532-538.
[9] Schutte, M., Kemp, G., Visser, H. & Roodt, A. (2011). *Inorganic Chemistry*, **50**(24), 12486-12498.
[10] Schutte, M., Roodt, A. & Visser, H. (2012). *Inorganic Chemistry*, **51**(21), 11996-12006.
[11] Gantsho, V., Dotou, M., Jakubaszek, M., Goud, B., Gasser, G., Visser, H. & Schutte-Smith, M. (2020). *Dalton Transactions*, **49**(1), 35-46.
[12] Sennari, G., Saito, R., Hirose, T., Iwatsuki, M., Ishiyama, A., Hokari, R., Otoguro, K., Ōmura, S. & Sunazuka, T. (2017). *Scientific Reports*, **7**(1). doi: 10.1038/s41598-017-07718-3
[13] Saleh, N. A., Zfiefak, A., Mordarski, M. & Pulverer, G. (1988). *Zentralblatt fuer Bakteriologie, Mikrobiologie und Hygiene, Series A: Medical Microbiology, Infectious Diseases, Virology, Parasitology*, **270**, 160-170.
[14] Tavis, J. E. & Lomonosova, E. (2015). *Antiviral Research*, **118**, 132-138.
[15] Liu, S. & Yamauchi, H. (2006). *Biochemical and Biophysical Research Communications*, **351**(1), 26-32.
[16] Haney, S. L., Allen, C., Varney, M. L., Dykstra, K. M., Falcone, E. R., Colligan, S. H., Hu, Q., Aldridge, A. M., Wright, D. L., Wiemer, A. J. & Holstein, S. A. (2017). *Oncotarget*, **8**(44), 76085-76098.
[17] Jayakumar, T., Liu, C., Wu, G., Lee, T., Manubolu, M., Hsieh, C., Yang, C. & Sheu, J. (2018). *International Journal of Molecular Sciences*, **19**(4), 939-952.
[18] Balsa, L., Ruiz, M., Santa Maria de la Parra, L., Baran, E. & León, I. (2020). *Journal of Inorganic Biochemistry*, **204**, 110975.
[19] Ononye, S., VanHeyst, M., Oblak, E., Zhou, W., Ammar, M., Anderson, A. & Wright, D. (2013). *ACS Medicinal Chemistry Letters*, **4**(8), 757-761.

2-(Alkylamino)tropone **Aminotroponimine**

Figure 4.1: The general chemical structure of the 2-(alkylamino)tropone and aminotroponimine ligand systems.

The carbonyl oxygen (O) or imine nitrogen (N) and the vicinal coordinating substituent, generally also oxygen or nitrogen, endow certain functionalities as well as a metal chelating ability to these ligand systems.[20] The aminotroponimine ligands are anionic, bidentate nitrogen donors which form stable complexes with metals.[21] In the anionic state the molecule usually exhibits perfect symmetry which demonstrates the delocalization of the negative charge through the conjugated system and is illustrated in Figure 4.2.[22] These ligands are favoured over the well-known 1,4-diazabutadiene (DAD) ligand as they are less susceptible to reactions with electrophiles and nucleophiles.[22]

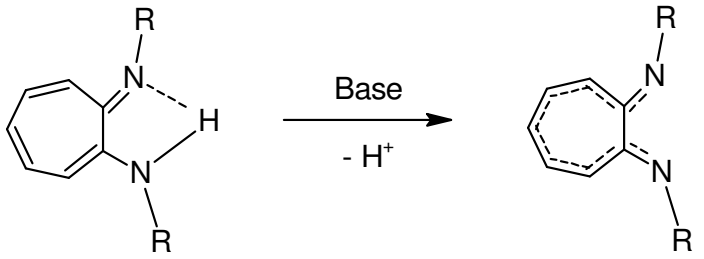

Aminotroponimine [ATI]H **10 π–electron system**

Figure 4.2: A representation of the conjugated electron system of an aminotroponimine ligand.

[20] Nishinaga, T., Aono, T., Isomura, E., Watanabe, S., Miyake, Y., Miyazaki, A., Enoki, T., Miyasaka, H., Otani, H. & Iyoda, M. (2010). *Dalton Transactions*, **39**, 2293-2300.
[21] Dochnahl, M., Löhnwitz, K., Pissarek, J., Biyikal, M., Schulz, S., Schön, S., Meyer, N., Roesky, P. & Blechert, S. (2007). *Chemistry - A European Journal*, **13**(23), 6654-6666.
[22] Dias, H. V. R., Jin, W. & Ratcliff, R. E. (1995). *Inorganic Chemistry*, **34**(24), 6100-6105.

Chapter 4

The tropolonoid ligand systems used in this study are chosen for some of its unique features:[23]

- It forms a five-membered chelated ring with a metal centre.
- The large, planar, seven-membered conjugated ring significantly stabilizes the metal complex.
- In the 2-(alkylamino)tropone ligand systems, the negative charge mainly accumulates on the nitrogen atom and they contain an enolic hydroxyl group as in a β-diketone.

In the design of these ligand systems the *N*-alkyl substituents as well as different combinations are varied to probe the different properties and the effect thereof on the metal chelating and coordinating abilities. The following characteristics of the substituents can be used to modify the properties of the resulting ligands:[21]

- Different aliphatic chain lengths and steric effects to alter the stability and coordinating ability of a ligand.
- Different linker chains could be varied in macrocyclic ligands (not applicable in this study) to change the chelation properties of a ligand.
- The basicity and donor strength of the nitrogen atoms to modify the ligand's electronic properties.

The aim is to synthesize and characterize the following ligand systems (Figure 4.3) and its Re(I) tricarbonyl complexes (Figure 4.4):

- Five *N,O* bidentate ligand systems - (2-alkylamino)tropones:
    - 2-(Methylamino)tropone (TropNHMe)
    - 2-(Ethylamino)tropone (TropNHEt)
    - 2-(2-Fluoroethylamino)tropone (TropNHEtF)
    - 2-(Phenethylamino)tropone (TropNHEtPh)
    - 2-(Benzylamino)tropone (TropNHBn)

[23] Dwivedi, A. D., Binnani, C., Tyagi, D., Rawat, K. S., Li, P., Zhao, Y., Mobin, S. M., Pathak, B. & Singh, S. K. (2016). *Inorganic Chemistry*, **55**(13), 6739-6749.

Chapter 4

- Nine *N,N'* bidentate ligand systems - aminotroponimines:
  - *N*-Methyl-2-(methylamino)troponimine ([$(Me)_2$ATI]H)
  - *N*-Ethyl-2-(ethylamino)troponimine ([$(Et)_2$ATI]H)
  - *N*-2-Fluoroethyl-2-(2-fluoroethylamino)troponimine ([$(EtF)_2$ATI]H)
  - *N*-Phenethyl-2-(phenethylamino)troponimine ([$(EtPh)_2$ATI]H)
  - *N*-Benzyl-2-(benzylamino)troponimine ([$(Bn)_2$ATI]H)
  - *N*-Methyl-2-(benzylamino)troponimine ([(Me,Bn)ATI]H)
  - *N*-Ethyl-2-(benzylamino)troponimine ([(Et,Bn)ATI]H)
  - *N*-2-Fluoroethyl-2-(benzylamino)troponimine ([(EtF,Bn)ATI]H)
  - *N*-Phenethyl-2-(benzylamino)troponimine ([(EtPh,Bn)ATI]H)
- Five *fac*-Re(I) tricarbonyl complexes of the type *fac*-[$Re(CO)_3(H_2O)$(*N,O*)]:
  - *fac*-[$Re(CO)_3(H_2O)$(TropNMe)]
  - *fac*-[$Re(CO)_3(H_2O)$(TropNEt)]
  - *fac*-[$Re(CO)_3(H_2O)$(TropNEtF)]
  - *fac*-[$Re(CO)_3(H_2O)$(TropNEtPh)]
  - *fac*-[$Re(CO)_3(H_2O)$(TropNBn)]
- Nine *fac*-Re(I) tricarbonyl complexes of the type *fac*-[$Re(CO)_3(H_2O)$(*N,N'*)]:
  - *fac*-[$Re(CO)_3(H_2O)$($(Me)_2$ATI)]
  - *fac*-[$Re(CO)_3(H_2O)$($(Et)_2$ATI)]
  - *fac*-[$Re(CO)_3(H_2O)$($(EtF)_2$ATI)]
  - *fac*-[$Re(CO)_3(H_2O)$($(EtPh)_2$ATI)]
  - *fac*-[$Re(CO)_3(H_2O)$($(Bn)_2$ATI)]
  - *fac*-[$Re(CO)_3(H_2O)$((Me,Bn)ATI)]
  - *fac*-[$Re(CO)_3(H_2O)$((Et,Bn)ATI)]
  - *fac*-[$Re(CO)_3(H_2O)$((EtF,Bn)ATI)]
  - *fac*-[$Re(CO)_3(H_2O)$((EtPh,Bn)ATI)]

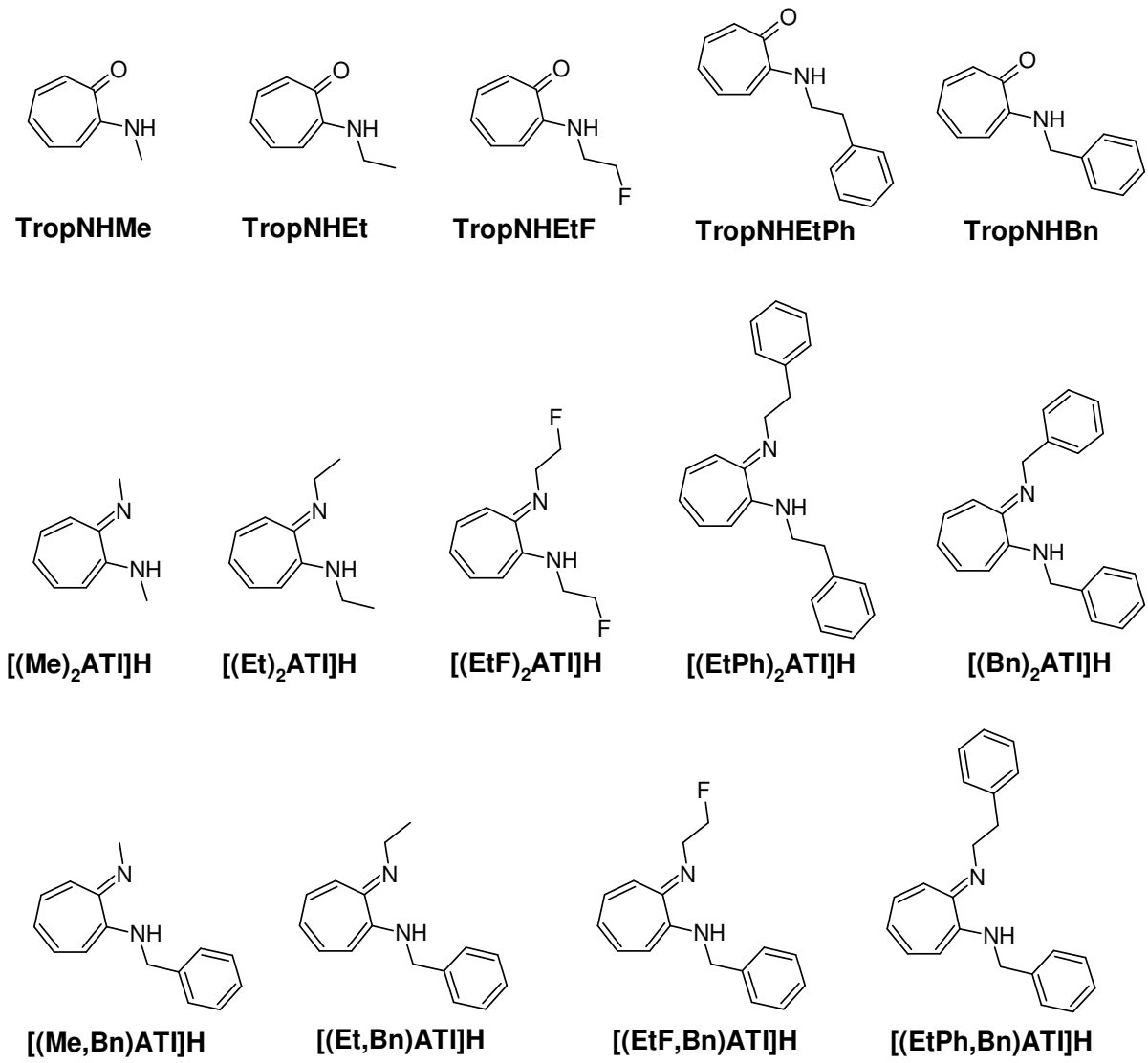

Figure 4.3: The chemical structures of 2-(alkylamino)tropone (1st row) and aminotroponimine (2nd and 3rd row) ligand systems synthesized in this study.

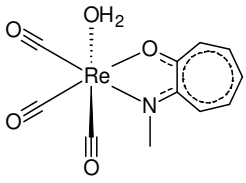

***fac*-[Re(CO)$_3$(H$_2$O)(TropNMe)]**

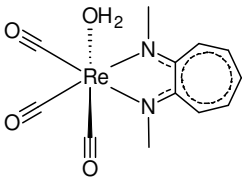

***fac*-[Re(CO)$_3$(H$_2$O)((Me)$_2$ATI)]**

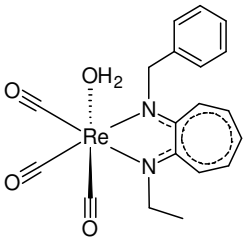

***fac*-[Re(CO)$_3$(H$_2$O)((Me,Bn)ATI)]**

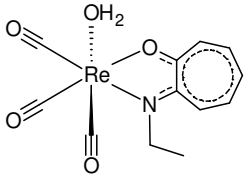

***fac*-[Re(CO)$_3$(H$_2$O)(TropNEt)]**

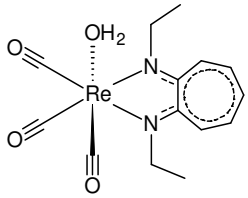

***fac*-[Re(CO)$_3$(H$_2$O)((Et)$_2$ATI)]**

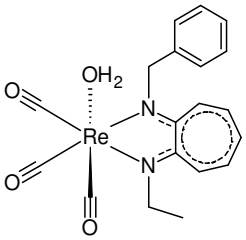

***fac*-[Re(CO)$_3$(H$_2$O)((Et,Bn)ATI)]**

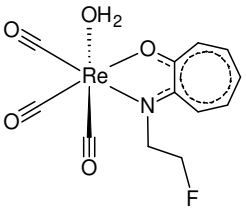

***fac*-[Re(CO)$_3$(H$_2$O)(TropNEtF)]**

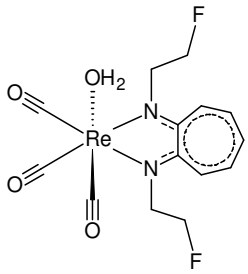

***fac*-[Re(CO)$_3$(H$_2$O)((EtF)$_2$ATI)]**

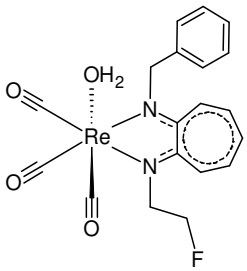

***fac*-[Re(CO)$_3$(H$_2$O)((EtF,Bn)ATI)]**

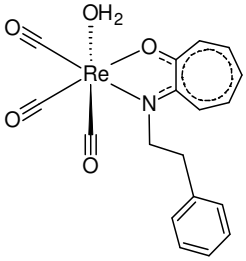

***fac*-[Re(CO)$_3$(H$_2$O)(TropNEtPh)]**

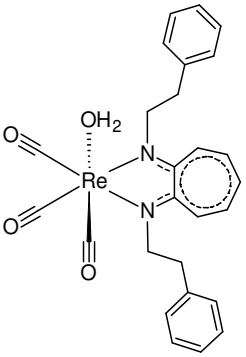

***fac*-[Re(CO)$_3$(H$_2$O)((EtPh)$_2$ATI)]**

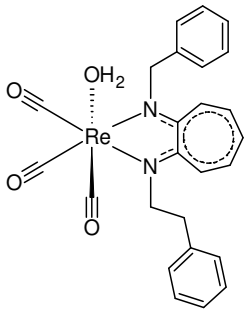

***fac*-[Re(CO)$_3$(H$_2$O)((EtPh,Bn)ATI)]**

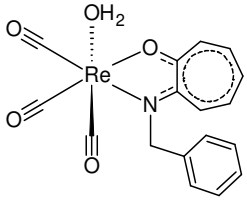

***fac*-[Re(CO)$_3$(H$_2$O)(TropNBn)]**

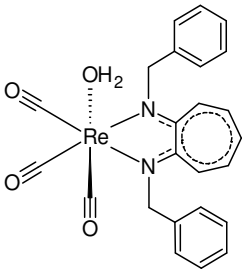

***fac*-[Re(CO)$_3$(H$_2$O)((Bn)$_2$ATI)]**

Figure 4.4: The chemical structures of the *fac*-Re(I) tricarbonyl complexes with *N,O* (1st column) and *N,N'* (2nd and 3rd column) bidentate ligands synthesized in this study.

4.2 Chemicals and apparatus

Unless stated otherwise, all chemicals and solvents used in the synthesis and characterization are of commercial grade and were purchased from Sigma Aldrich and Merck, South Africa. Reagents were used as received, without further purification. Rhenium pentacarbonyl bromide was purchased from Strem Chemicals, Newburyport (US). The pH of some reaction mixtures was adjusted, either with HNO_3 or NaOH. In reactions with water as solvent, distilled water was used. All reactions were performed under aerobic conditions with different solvents that are specified in each procedure.

All the infrared (IR) spectra of the precursors, ligands and complexes were collected at room temperature on a Bruker Tensor 27 Standard System spectrophotometer with a laser range of 4000 - 370 cm^{-1}, coupled to a computer.

The UV/Vis spectra were recorded on a Varian Cary 50 Conc UV/Visible Spectrophotometer, equipped with a Julabo F12-mV temperature cell regulator (accurate within 0.1 °C) in a 1.000(1) cm quartz cuvette cell.

All ^{1}H and ^{13}C NMR spectra were obtained on a Bruker 300 MHz or a Bruker 400 MHz nuclear magnetic resonance spectrometer. Chemical shifts (δ) of ^{1}H and ^{13}C spectra are referenced to $(CD_3)_2CO$ at 2.05 ppm and 29.8 ppm and $CDCl_3$ at 7.24 ppm and 77.2 ppm, respectively, and are reported in ppm. The deuterated solvent used is specified in each procedure.

4.3 Synthetic procedures

4.3.1 Synthesis of the precursor for ligand systems

4.3.1.1 Synthesis of 2-tosyloxytropone (TropOTs)

Tropolone (2.068 g, 17.082 mmol) and *p*-toluenesulfonyl chloride (3.228 g, 16.932 mmol) were dissolved in 20 mL dry pyridine and stirred for 2 hours. The reaction mixture was filtered, and the insoluble product was washed with cold water and dried.

Yield: 3.782 g, 81 %. IR (cm^{-1}): ν_{CO} = 1629, ν_{SO} = 1363. UV/Vis: λ_{max} = 305 nm (ε = 18 454 $Lmol^{-1}cm^{-1}$). ^{1}H NMR (300.18 MHz, $(CD_3)_2CO$): δ = 7.9 (d, 2H, *J* = 8.4 Hz), 7.5 (d, 2H, *J* = 8.1 Hz), 7.4 - 7.1 (m, 5H), 2.5 (s, 3H). ^{13}C NMR

(75.48 MHz, $(CD_3)_2CO$): δ = 206, 180, 156, 147, 142, 138, 136, 135, 132, 131, 129, 22.

4.3.2 Synthesis of *N,O* bidentate ligands

4.3.2.1 Synthesis of 2-(methylamino)tropone (TropNHMe)

2-Tosyloxytropone (2.000 g, 7.238 mmol) was dissolved in 40 mL dichloromethane and 10 mL of a 40 % methylamine solution (116 mmol) was added. The reaction mixture was stirred overnight at room temperature. The layers were separated, and the aqueous layer was extracted with dichloromethane. The combined organic layers were washed with water and dried over $MgSO_4$. DCM was removed under reduced pressure and the product was recrystallized from hexane to yield yellow crystals.

Yield: 0.647 g, 66 %. IR (cm^{-1}): ν_{NH} = 3305, ν_{CO} = 1596, 1529, ν_{CC} = 1503. UV/Vis: λ_{max} = 340, 410 nm (ε = 22 600, 17 700 $Lmol^{-1}cm^{-1}$). ^1H NMR (300.18 MHz, $CDCl_3$): δ = 7.8 (s, 1H), 7.3 - 7.2 (m, 2H), 6.9 (d, 1H, *J* = 11.7 Hz), 6.6 (t, 1H, *J* = 9.6 Hz), 6.5 (d, 1H, *J* = 10.8 Hz), 2.9 (d, 3H, *J* = 5.4 Hz). ^{13}C NMR (75.48 MHz, $CDCl_3$): δ = 177, 157, 138, 136, 129, 122, 108, 30.

4.3.2.2 Synthesis of 2-(ethylamino)tropone (TropNHEt)

2-Tosyloxytropone (5.000 g, 18.096 mmol) was dissolved in 100 mL dichloromethane and 25 mL of a 70 % aqueous ethylamine (309 mmol) solution was added. The reaction mixture was stirred overnight at room temperature. The layers were separated, and the aqueous layer was extracted with dichloromethane. The combined organic layers were washed with water and dried over $MgSO_4$. DCM was removed under reduced pressure and the product was obtained from pentane as a crystalline yellow precipitate.

Yield: 1.156 g, 43 %. IR (cm^{-1}): ν_{NH} = 3244, ν_{CO} = 1590, 1546, ν_{CC} = 1505. UV/Vis: λ_{max} = 340, 410 nm (ε = 26 500, 21 800 $Lmol^{-1}cm^{-1}$). ^1H NMR (400.13 MHz, $CDCl_3$): δ = 7.5 (s, 1H), 7.2 - 7.1 (m, 3H), 6.6 (t, 1H, *J* = 9.6 Hz), 6.4 (d, 1H, *J* = 10.4 Hz), 3.3 (dt, 2H, *J* = 12.8, 7.2 Hz), 1.3 (t, 3H, *J* = 7.2 Hz). ^{13}C NMR (100.61 MHz, $CDCl_3$): δ = 177, 156, 137, 136, 129, 122, 109, 38, 14.

4.3.2.3 Synthesis of 2-(2-fluoroethylamino)tropone (TropNHEtF)

2-Tosyloxytropone (2.500 g, 9.048 mmol) was dissolved in ethanol. To this solution were added 2-fluoroethylamine hydrochloride (1.000 g, 10.046 mmol) and triethylamine (6.5 mL, 47 mmol). The solution was refluxed for 24 h. The reaction mixture was dried *in vacuo*. The oily residue was extracted with DCM. The combined organic layers were washed with water and dried over $MgSO_4$. DCM was removed under reduced pressure. The product was obtained as yellow needles from a hexane solution.

Yield: 0.330 g, 22 %. IR (cm^{-1}): ν_{NH} = 3240, ν_{CO} = 1590, 1546, ν_{CC} = 1509. UV/Vis: λ_{max} = 340, 405 nm (ε = 22 200, 17 500 $Lmol^{-1}cm^{-1}$). ^1H NMR (400.13 MHz, $CDCl_3$): δ = 7.3 (s, 1H), 7.2 - 7.1 (m, 3H), 6.7 (t, 1H, *J* = 9.6 Hz), 6.5 (d, 1H, *J* = 10.4 Hz), 4.6 (dt, 2H, *J* = 47.2, 5.2 Hz), 3.6 (ddt, 2H, *J* = 25.2, 10.8, 5.6 Hz). ^{13}C NMR (100.61 MHz, $CDCl_3$): δ = 177, 138, 136, 130, 123, 109, 82, 81, 43.

4.3.2.4 Synthesis of 2-(phenethylamino)tropone (TropNHEtPh)

2-Tosyloxytropone (1.000 g, 3.619 mmol) was dissolved in 50 mL ethanol. To this solution were added phenethylamine (0.5 mL, 4 mmol) and triethylamine (5 mL, 36 mmol). The solution was refluxed for 24 h. The reaction mixture was dried *in vacuo*. The oily residue was extracted with DCM. The combined organic layers were washed with water and dried over $MgSO_4$. DCM was removed under reduced pressure. The product was obtained as yellow needles from a hexane solution.

Yield: 0.410 g, 50 %. IR (cm^{-1}): ν_{NH} = 3247, ν_{CO} = 1595, 1548, ν_{CC} = 1444. UV/Vis: λ_{max} = 340, 410 nm (ε = 23 500, 19 000 $Lmol^{-1}cm^{-1}$). ^1H NMR (400.13 MHz, $CDCl_3$): δ = 7.4 (s, 1H), 7.4 - 7.3 (m, 5H), 7.2 (d, 2H, *J* = 9.2 Hz), 7.0 (d, 1H, *J* = 12.0 Hz), 6.7 (d, 1H, *J* = 10.4 Hz), 6.6 (t, 1H, *J* = 9.6 Hz), 3.7 (t, 2H, *J* = 4.4 Hz), 3.1 (t, 2H, *J* = 7.6 Hz. ^{13}C NMR (100.61 MHz, $CDCl_3$): δ = 176, 155, 139, 137, 136, 129, 128, 127, 126, 121, 108, 43, 34.

4.3.2.5 Synthesis of 2-(benzylamino)tropone (TropNHBn)

2-Tosyloxytropone (4.395 g, 15.906 mmol) was dissolved in 150 mL ethanol. To this solution were added benzylamine (5.25 mL, 48 mmol) and triethylamine (11 mL, 79 mmol). The solution was refluxed for 24 h. The reaction mixture was dried *in vacuo*. The oily residue was extracted with DCM. The combined organic layers were washed with water and dried over $MgSO_4$. DCM was removed under reduced

pressure. The product was obtained as a yellow precipitate from an acetone solution.

Yield: 2.254 g, 59 %. IR (cm^{-1}): ν_{NH} = 3282, ν_{CO} = 1589, 1542, ν_{CC} = 1509. UV/Vis: λ_{max} = 340, 410 nm (ε = 23 431, 18 821 $Lmol^{-1}cm^{-1}$). ^1H NMR (400.13 MHz, $CDCl_3$): δ = 7.5 (s, 1H), 7.3 - 7.2 (m, 6H), 7.1 - 7.1 (m, 2H), 6.6 (t, 1H, *J* = 9.6 Hz), 6.5 (d, 1H, *J* = 10.4 Hz), 4.5 (d, 2H, *J* = 6.0 Hz). ^{13}C NMR (100.61 MHz, $CDCl_3$): δ = 177, 156, 138, 137, 136, 130, 129, 128, 127, 123, 109, 47.

4.3.3 Synthesis of *N,N'* bidentate ligands

4.3.3.1 Synthesis of *N*-methyl-2-(methylamino)troponimine ([(Me)$_2$ATI]H)

$Et_3O{\bullet}BF_4$ (464 mg, 2.442 mmol) in 5 mL dichloromethane was slowly added to a solution of 2-(methylamino)tropone (300 mg, 2.220 mmol) in 5 mL dichloromethane. After stirring for 24 hours, 0.5 mL of a 40 % methylamine solution (6 mmol) and 5 mL triethylamine (36 mmol) was added, and the solution was refluxed for 7 days. The reaction mixture was dried *in vacuo* and the residue was extracted with ethyl acetate and dried to obtain the product as an orange crystalline solid.

Yield: 0.243 g, 74 %. IR (cm^{-1}): ν_{NH} = 3424, ν_{CN} = 1606, ν_{CC} = 1518. UV/Vis: λ_{max} = 350, 425 nm (ε = 15 005, 12 227 $Lmol^{-1}cm^{-1}$). ^1H NMR (400.13 MHz, $CDCl_3$): δ = 9.9 (s, 1H), 7.6 (t, 2H, *J* = 10.8 Hz), 7.0 (t, 1H, *J* = 9.6 Hz), 6.9 (d, 2H, *J* = 11.2 Hz, 3.2 (d, 6H, *J* = 3.6 Hz). ^{13}C NMR (100.61 MHz, $CDCl_3$): δ = 152, 140, 126, 118, 31.

4.3.3.2 Synthesis of *N*-ethyl-2-(ethylamino)troponimine ([(Et)$_2$ATI]H)

$Et_3O{\bullet}BF_4$ (420 mg, 2.211 mmol) in 5 mL dichloromethane was slowly added to a solution of 2-(ethylamino)tropone (300 mg, 2.011 mmol) in 5 mL dichloromethane. After stirring for 24 hours, 0.5 mL of a 70 % ethylamine solution (6 mmol) and 5 mL triethylamine (36 mmol) was added, and the solution was refluxed for 7 days. The reaction mixture was dried *in vacuo* and the residue was extracted with chloroform and dried to obtain the product as an orange oil.

Yield: 0.074 g, 22 %. IR (cm^{-1}): ν_{NH} = 3147, ν_{CN} = 1601, ν_{CC} = 1515. UV/Vis: λ_{max} = 350, 410 nm (ε = 23 501, 17 332 $Lmol^{-1}cm^{-1}$). ^1H NMR (400.13 MHz, $CDCl_3$):

δ = 7.6 (t, 2H, *J* = 10.4 Hz), 7.5 (s, 1H), 7.0 (t, 2H, *J* = 9.2 Hz), 7.0 (d, 1H, *J* = 11.6 Hz), 3.5 (q, 4H, *J* = 7.2 Hz), 1.4 (t, 6H, *J* = 7.2 Hz). ^{13}C NMR (100.61 MHz, $CDCl_3$): δ = 152, 140, 126, 117, 30, 13.

4.3.3.3 Synthesis of *N*-2-fluoroethyl-2-(2-fluoroethylamino)troponimine ([(EtF)$_2$ATI]H)

$Et_3O•BF_4$ (250 mg, 1.316 mmol) in 3 mL dichloromethane was slowly added to a solution of 2-(2-fluoroethylamino)tropone (200 mg, 1.196 mmol) in 3 mL dichloromethane. After stirring for 24 hours, 10 mL of an ethanolic solution of 2-fluoroethylamine hydrochloride (238.2 mg, 2.393 mmol) and 5 mL triethylamine (36 mmol) was added, and the solution was refluxed for 7 days. The reaction mixture was dried *in vacuo* and the residue was extracted with pentane and the product was obtained as yellow crystals at -21 ˚C.

Yield: 0.061 g, 24 %. IR (cm^{-1}): ν_{NH} = 2922, ν_{CN} = 1602, ν_{CC} = 1517. UV/Vis: λ_{max} = 340, 405 nm (ε = 21 755, 14 645 $Lmol^{-1}cm^{-1}$). ^{1}H NMR (400.13 MHz, $CDCl_3$): δ = 7.3 (s, 1H), 7.2 - 7.2 (m, 3H), 6.6 (t, 1H, *J* = 9.6 Hz), 6.5 (d, 1H, *J* = 10.4 Hz), 4.7 - 4.6 (m, 4H), 3.7 - 3.5 (m, 4H). ^{13}C NMR (100.61 MHz, $CDCl_3$): δ = 153, 140, 128, 118, 81, 45.

4.3.3.4 Synthesis of *N*-phenethyl-2-(phenethylamino)troponimine ([(EtPh)$_2$ATI]H)

$Et_3O•BF_4$ (174 mg, 0.916 mmol) in 3 mL dichloromethane was slowly added to a solution of 2-(phenethylamino)tropone (187 mg, 0.830 mmol) in 3 mL dichloromethane. After stirring for 24 hours, 0.25 mL phenethylamine (2 mmol) and 2 mL triethylamine (14 mmol) was added, and the solution was refluxed for 7 days. The reaction mixture was dried *in vacuo* and the residue was extracted with hexane and dried to obtain the product as an orange solid.

Yield: 0.083 g, 30 %. IR (cm^{-1}): ν_{NH} = 3175, ν_{CN} = 1604, ν_{CC} = 1514. UV/Vis: λ_{max} = 345, 410 nm (ε = 20 677, 15 829 $Lmol^{-1}cm^{-1}$). ^{1}H NMR (400.13 MHz, $CDCl_3$): δ = 7.9 (s, 1H), 7.3 - 7.2 (m, 10H), 6.7 (t, 2H, *J* = 10.4 Hz), 6.3 (d, 2H, *J* = 10.8 Hz), 6.1 (t, 1H, *J* = 9.2 Hz), 3.6 (t, 4H, *J* = 7.6 Hz), 3.0 (t, 4H, *J* = 7.6 Hz). ^{13}C NMR (100.61 MHz, $CDCl_3$): δ = 153, 140, 133, 126, 122, 118, 111, 48, 37.

4.3.3.5 Synthesis of *N*-benzyl-2-(benzylamino)troponimine ([(Bn)$_2$ATI]H)

$Et_3O•BF_4$ (396 mg, 2.084 mmol) in 5 mL dichloromethane was slowly added to a solution of 2-(benzylamino)tropone (400 mg, 1.893 mmol) in 5 mL dichloromethane. After stirring for 24 hours, 0.5 mL benzylamine (5 mmol) and 4.5 mL triethylamine (32 mmol) was added, and the solution was refluxed for 7 days. The reaction mixture was dried *in vacuo* and the residue was extracted with pentane and dried to obtain the product as a yellow solid.

Yield: 0.200 g, 35 %. IR (cm^{-1}): ν_{NH} = 3244, ν_{CN} = 1590, ν_{CC} = 1504. UV/Vis: λ_{max} = 360, 425 nm (ε = 19 025, 14 319 $Lmol^{-1}cm^{-1}$). ^{1}H NMR (400.13 MHz, $CDCl_3$): δ = 7.6 (s, 1H), 7.4 - 7.3 (m, 6H), 7.3 - 7.2 (m, 4H), 6.8 (t, 2H, *J* = 10.4 Hz), 6.4 (d, 2H, *J* = 10.8 Hz), 6.2 (t, 1H, *J* = 9.2 Hz), 4.6 (s, 4H). ^{13}C NMR (100.61 MHz, $CDCl_3$): δ = 154, 140, 134, 129, 128, 127, 119, 111, 50.

4.3.3.6 Synthesis of *N*-methyl-2-(benzylamino)troponimine ([(Me,Bn)ATI]H)

$Et_3O•BF_4$ (396 mg, 2.084 mmol) in 5 mL dichloromethane was slowly added to a solution of 2-(benzylamino)tropone (400 mg, 1.893 mmol) in 5 mL dichloromethane. After stirring for 24 hours, 0.4 mL of a 40 % methylamine solution (5 mmol) and 5 mL triethylamine (36 mmol) was added, and the solution was refluxed for 7 days. The reaction mixture was dried *in vacuo* and the residue was extracted with chloroform and dried to obtain the product as an orange solid.

Yield: 0.174 g, 41 %. IR (cm^{-1}): ν_{NH} = 3149, ν_{CN} = 1597, ν_{CC} = 1516. UV/Vis: λ_{max} = 345, 410 nm (ε = 33 645, 26 916 $Lmol^{-1}cm^{-1}$). ^{1}H NMR (400.13 MHz, $CDCl_3$): δ = 7.6 (s, 1H), 7.3 - 7.2 (m, 6H), 7.2 (t, 2H, *J* = 10.0 Hz), 7.0 (d, 1H, *J* = 11.6 Hz), 6.6 (t, 1H, *J* = 9.6 Hz), 4.6 (d, 2H, *J* = 6.4 Hz), 3.1 (s, 3H). ^{13}C NMR (75.48 MHz, $CDCl_3$): δ = 177, 153, 140, 137, 135, 128, 126, 119, 109, 47, 46, 30, 8.

4.3.3.7 Synthesis of *N*-ethyl-2-(benzylamino)troponimine ([(Et,Bn)ATI]H)

$Et_3O•BF_4$ (396 mg, 2.084 mmol) in 5 mL dichloromethane was slowly added to a solution of 2-(benzylamino)tropone (400 mg, 1.893 mmol) in 5 mL dichloromethane. After stirring for 24 hours, 0.4 mL of a 70 % ethylamine solution (5 mmol) and 5 mL

triethylamine (36 mmol) was added, and the solution was refluxed for 7 days. The reaction mixture was dried *in vacuo* and the residue was extracted with chloroform and dried to obtain the product as a brown oil.

Yield: 0.152 g, 34 %. IR (cm^{-1}): ν_{NH} = 3139, ν_{CN} = 1597, ν_{CC} = 1514. UV/Vis: λ_{max} = 340, 405 nm (ε = 28 520, 22 736 $Lmol^{-1}cm^{-1}$). ^1H NMR (400.13 MHz, $CDCl_3$): δ = 7.8 (s, 1H), 7.4 - 7.3 (m, 4H), 7.3 - 7.3 (m, 2H), 7.2 (t, 1H, *J* = 10.0 Hz), 7.0 (d, 1H, *J* = 11.6 Hz), 6.6 (t, 1H, *J* = 9.2 Hz), 6.6 (d, 1H, *J* = 10.4 Hz), 4.7 (d, 2H, *J* = 6.0 Hz), 3.4 (q, 2H, *J* = 6.8 Hz), 1.1 (t, 3H, *J* = 6.8 Hz). ^{13}C NMR (100.61 MHz, $CDCl_3$): δ = 177, 155, 152, 140, 137, 136, 129, 127, 123, 117, 109, 47, 30, 13.

4.3.3.8 Synthesis of *N*-2-fluoroethyl-2-(benzylamino)troponimine ([(EtF,Bn)ATI]H)

$Et_3O{\bullet}BF_4$ (396 mg, 2.084 mmol) in 5 mL dichloromethane was slowly added to a solution of 2-(benzylamino)tropone (400 mg, 1.893 mmol) in 5 mL dichloromethane. After stirring for 24 hours, a 10 mL ethanolic solution of 2-fluoroethylamine hydrochloride (377 mg, 3.787 mmol) and 5 mL triethylamine (36 mmol) was added, and the solution was refluxed for 7 days. The reaction mixture was dried *in vacuo* and the residue was extracted with chloroform and dried to obtain the product as a yellow solid.

Yield: 0.134 g, 28 %. IR (cm^{-1}): ν_{NH} = 3153, ν_{CN} = 1589, ν_{CC} = 1511. UV/Vis: λ_{max} = 340, 405 nm (ε = 26 716, 21 196 $Lmol^{-1}cm^{-1}$). ^1H NMR (400.13 MHz, $CDCl_3$): δ = 8.2 (s, 1H), 7.4 - 7.3 (m, 4H), 7.3 - 7.2 (m, 2H), 7.2 (t, 1H, *J* = 10.0 Hz), 7.0 (d, 1H, *J* = 11.2 Hz), 6.6 (t, 1H, *J* = 9.6 Hz), 6.6 (d, 1H, *J* = 10.4 Hz), 4.8 (s, 2H), 4.9 (dt, 2H, *J* = 19.2, 4.8 Hz), 3.9 (dt, 2H, *J* = 42.8, 4.8 Hz). ^{13}C NMR (100.61 MHz, $CDCl_3$): δ = 177, 156, 152, 141, 138, 137, 129, 127, 123, 119, 110, 47, 30, 9.

4.3.3.9 Synthesis of *N*-phenethyl-2-(benzylamino)troponimine ([(EtPh,Bn)ATI]H)

$Et_3O{\bullet}BF_4$ (396 mg, 2.084 mmol) in 5 mL dichloromethane was slowly added to a solution of 2-(benzylamino)tropone (400 mg, 1.893 mmol) in 5 mL dichloromethane. After stirring for 24 hours, 0.5 mL phenethylamine (4 mmol) and 5 mL triethylamine (36 mmol) was added, and the solution was refluxed for 7 days. The reaction mixture was dried *in vacuo* and the residue was extracted with hexane and dried to obtain the product as a yellow solid.

Yield: 0.252 g, 39 %. IR (cm^{-1}): ν_{NH} = 3144, ν_{CN} = 1602, ν_{CC} = 1518. UV/Vis: λ_{max} = 360, 405 nm (ε = 32 916, 25 448 $Lmol^{-1}cm^{-1}$). ^{1}H NMR (400.13 MHz, $CDCl_3$): δ = 8.0 (s, 1H), 7.4 - 7.2 (m, 10H), 6.8 - 6.7 (m, 2H), 6.5 - 6.3 (m, 2H), 6.2 (t, 1H, *J* = 9.2 Hz), 4.5 (s, 2H), 3.6 (t, 2H, *J* = 7.2 Hz), 3.0 (t, 2H, *J* = 7.2 Hz). ^{13}C NMR (75.48 MHz, $CDCl_3$): δ = 177, 156, 152, 138, 137, 136, 129, 128, 127, 109, 123, 53, 47, 34, 30, 8.

4.3.4 Synthesis of the starting synthon $[NEt_4]_2[ReBr_3(CO)_3]$ (ReAA) for the synthesis of *fac*-Re(I) tricarbonyl complexes

4.3.4.1 Synthesis of $[NEt_4]_2[ReBr_3(CO)_3]$ (ReAA)

Finely ground $(NEt_4)Br$ (5.250 g, 0.025 mol) was dried under vacuum for 24 hours. 2,5,8-Trioxanone diglyme (150 mL) was added to the $(NEt_4)Br$ under a dry nitrogen atmosphere and stirred at 80 °C for 30 minutes. The system was evacuated and purged with N_2 several times. $Re(CO)_5Br$ (5 g, 0.0123 mol) was added as a solid to the mixture and stirred at 115 °C for 15 hours. The reaction mixture was cooled down to room temperature. The reaction mixture was filtered; the product as a colourless precipitate was dried. The product was washed several times with cold ethanol, filtered and washed with dry, cold dichloromethane.

Yield: 9.132 g, 96 %, IR (cm^{-1}): ν_{CO} = 1997, 1847.

4.3.5 Synthesis of Re(I) tricarbonyl complexes of the type *fac*-$[Re(CO)_3(H_2O)(N,O)]$

4.3.5.1 Synthesis of *fac*-$[Re(CO)_3(H_2O)(TropNMe)]$

ReAA (200 mg, 0.260 mmol) was dissolved in water at pH 2.2 (adjusted with HNO_3). Silver nitrate (134 mg, 0.789 mmol) was added to the solution and the reaction mixture was stirred at room temperature for 24 hours. The AgBr was filtered off, 2-(methylamino)tropone (33 mg, 0.244 mmol) was added and the pH was adjusted to 6.0 with NaOH. The solution was refluxed for 72 hours, cooled to room temperature, and filtered to yield the product as a dark orange powder.

Yield: 0.068 g, 66 %. IR (cm^{-1}): ν_{CO} = 1997, 1851. UV/Vis: λ_{max} = 340, 410 nm (ε = 24 865, 21 024 $Lmol^{-1}cm^{-1}$). ^{1}H NMR (400.13 MHz, $CDCl_3$): δ = 7.3 - 7.2

(m, 2H), 6.9 (d, 1H, *J* = 12.0 Hz), 6.6 (t, 1H, *J* = 9.6 Hz), 6.5 (d, 1H, *J* = 10.4 Hz), 2.9 (d, 3H, *J* = 5.2 Hz). ^{13}C NMR (100.61 MHz, $CDCl_3$): δ = 176, 156, 138, 135, 127, 121, 108, 29.

4.3.5.2 Synthesis of *fac*-[Re(CO)$_3$(H$_2$O)(TropNEt)]

ReAA (200 mg, 0.260 mmol) was dissolved in water at pH 2.2 (adjusted with HNO_3). Silver nitrate (134 mg, 0.789 mmol) was added to the solution and the reaction mixture was stirred at room temperature for 24 hours. The AgBr was filtered off, 2-(ethylamino)tropone (35 mg, 0.235 mmol) was added and the pH was adjusted to 6.0 with NaOH. The solution was refluxed for 72 hours, cooled to room temperature, and filtered to yield the product as a dark orange powder.

Yield: 0.070 g, 68 %. IR (cm^{-1}): ν_{CO} = 1997, 1866. UV/Vis: λ_{max} = 340, 410 nm (ε = 25 194, 22 317 $Lmol^{-1}cm^{-1}$). ^{1}H NMR (400.13 MHz, $CDCl_3$): δ = 7.3 - 7.2 (m, 3H), 7.1 (t, 1H, *J* = 10.0 Hz), 6.8 (d, 1H, *J* = 10.0 Hz), 4.0 - 3.9 (m, 2H), 1.2 (t, 3H, *J* = 6.8 Hz). ^{13}C NMR (100.61 MHz, $CDCl_3$): δ = 176, 155, 137, 136, 127, 121, 108, 37, 13.

4.3.5.3 Synthesis of *fac*-[Re(CO)$_3$(H$_2$O)(TropNEtF)]

ReAA (200 mg, 0.260 mmol) was dissolved in water at pH 2.2 (adjusted with HNO_3). Silver nitrate (134 mg, 0.789 mmol) was added to the solution and the reaction mixture was stirred at room temperature for 24 hours. The AgBr was filtered off, 2-(2-fluoroethylamino)tropone (41 mg, 0.245 mmol) was added and the pH was adjusted to 6.0 with NaOH. The solution was refluxed for 72 hours, cooled to room temperature and filtered to yield the product as a dark orange powder.

Yield: 0.078 g, 70 %. IR (cm^{-1}): ν_{CO} = 1999, 1870. UV/Vis: λ_{max} = 340, 405 nm (ε = 20 548, 17 189 $Lmol^{-1}cm^{-1}$). ^{1}H NMR (400.13 MHz, $CDCl_3$): δ = 7.3 - 7.1 (m, 3H), 6.8 (d, 1H, *J* = 10.4 Hz), 6.7 (t, 1H, *J* = 9.2 Hz), 4.7 (dt, 2H, *J* = 47.2, 5.2 Hz), 3.7 (dq, 2H, *J* = 26.4, 5.2 Hz). ^{13}C NMR (100.61 MHz, $CDCl_3$): δ = 176, 156, 137, 136, 128, 122, 108, 83, 43.

4.3.5.4 Synthesis of *fac*-[Re(CO)$_3$(H$_2$O)(TropNEtPh)]

ReAA (200 mg, 0.260 mmol) was dissolved in water at pH 2.2 (adjusted with HNO_3). Silver nitrate (134 mg, 0.789 mmol) was added to the solution and the reaction mixture was stirred at room temperature for 24 hours. The AgBr was filtered off and the filtrate was freeze-dried. The residue was dissolved in dichloromethane and

2-(phenethylamino)tropone (55 mg, 0.244 mmol) was added. The solution was stirred at room temperature for 24 hours after which it was washed with water to remove excess counter ions. The dried residue was washed with hexane to remove the unreacted 2-(phenethylamino)tropone. The product was obtained as a brown solid.

Yield: 0.094 g, 75 %. IR (cm^{-1}): ν_{CO} = 2002, 1876. UV/Vis: λ_{max} = 340, 410 nm (ε = 13 996, 10 743 $Lmol^{-1}cm^{-1}$). ^{1}H NMR (400.13 MHz, $CDCl_3$): δ = 7.2 - 7.0 (m, 6H), 6.9 (d, 2H, *J* = 10.0 Hz), 6.6 (t, 1H, *J* = 9.6 Hz), 6.5 (d, 1H, *J* = 10.4 Hz), 4.1 (t, 2H, *J* = 8.0 Hz), 3.5 (q, 2H, *J* = 6.8 Hz). ^{13}C NMR (100.61 MHz, $CDCl_3$): δ = 177, 156, 137, 136, 129, 127, 123, 120, 109, 57, 53, 44, 35.

4.3.5.5 Synthesis of *fac*-[Re(CO)$_3$(H$_2$O)(TropNBn)]

ReAA (200 mg, 0.260 mmol) was dissolved in water at pH 2.2 (adjusted with HNO_3). Silver nitrate (134 mg, 0.789 mmol) was added to the solution and the reaction mixture was stirred at room temperature for 24 hours. The AgBr was filtered off, 2-(benzylamino)tropone (52 mg, 0.246 mmol) was added and the pH was adjusted to 6.0 with NaOH. The solution was refluxed for 72 hours, cooled to room temperature, and filtered to yield the product as a dark orange powder.

Yield: 0.085 g, 69 %. IR (cm^{-1}): ν_{CO} = 1996, 1854. UV/Vis: λ_{max} = 340, 405 nm (ε = 22 947, 19 881 $Lmol^{-1}cm^{-1}$). ^{1}H NMR (400.13 MHz, $CDCl_3$): δ = 7.4 - 7.3 (m, 6H), 7.2 - 7.1 (m, 2H), 6.6 (t, 1H, *J* = 9.6 Hz), 6.6 (d, 1H, *J* = 10.8 Hz), 4.6 (d, 2H, *J* = 6.4 Hz). ^{13}C NMR (100.61 MHz, $CDCl_3$): δ = 177, 172, 151, 134, 133, 132, 125, 124, 123, 118, 105, 41.

4.3.6 Synthesis of Re(I) tricarbonyl complexes of the type *fac*-[Re(CO)$_3$(H$_2$O)(*N,N'*)]

4.3.6.1 Synthesis of *fac*-[Re(CO)$_3$(H$_2$O)((Me)$_2$ATI)]

ReAA (100 mg, 0.123 mmol) was dissolved in water at pH 2.2 (adjusted with HNO_3). Silver nitrate (67 mg, 0.394 mmol) was added to the solution and the reaction mixture was stirred at room temperature for 24 hours. The AgBr was filtered off and the filtrate was freeze-dried. The residue was dissolved in dichloromethane and *N*-methyl-2-(methylamino)troponimine (18 mg, 0.121 mmol) was added. The solution was stirred at room temperature for 24 hours after which it was washed with

water to remove excess counter ions. The dried residue was washed with ethyl acetate to remove the unreacted *N*-methyl-2-(methylamino)troponimine. The product was obtained as a dark red solid.

Yield: 0.049 g, 93 %. IR (cm^{-1}): ν_{CO} = 2017, 1882. UV/Vis: λ_{max} = 350, 425 nm (ε = 12 371, 9 105 $Lmol^{-1}cm^{-1}$). ^{1}H NMR (400.13 MHz, $CDCl_3$): δ = 7.7 (t, 2H, *J* = 10.4 Hz), 7.1 (t, 1H, *J* = 9.6 Hz), 7.0 (d, 2H, *J* = 11.6 Hz), 3.2 (d, 6H, *J* = 4.8 Hz). ^{13}C NMR (100.61 MHz, $CDCl_3$): δ = 153, 141, 127, 117, 32.

4.3.6.2 Synthesis of *fac*-[$Re(CO)_3(H_2O)((Et)_2ATI)$]

ReAA (100 mg, 0.123 mmol) was dissolved in water at pH 2.2 (adjusted with HNO_3). Silver nitrate (67 mg, 0.394 mmol) was added to the solution and the reaction mixture was stirred at room temperature for 24 hours. The AgBr was filtered off and the filtrate was freeze-dried. The residue was dissolved in dichloromethane and *N*-ethyl-2-(ethylamino)troponimine (21 mg, 0.119 mmol) was added. The solution was stirred at room temperature for 24 hours after which it was washed with water to remove excess counter ions. The dried residue was washed with ethyl acetate to remove the unreacted *N*-ethyl-2-(ethylamino)troponimine. The product was obtained as a dark orange solid.

Yield: 0.044 g, 80 %. IR (cm^{-1}): ν_{CO} = 2015, 1884. UV/Vis: λ_{max} = 355, 425 nm (ε = 19 409, 15 643 $Lmol^{-1}cm^{-1}$). ^{1}H NMR (400.13 MHz, $CDCl_3$): δ = 7.5 (t, 2H, *J* = 10.4 Hz), 7.0 (d, 1H, *J* = 13.6 Hz), 6.9 (t, 2H, *J* = 15.6 Hz), 3.5 (dq, 4H, *J* = 12.4, 7.2 Hz), 1.4 (t, 6H, *J* = 7.2 Hz). ^{13}C NMR (100.61 MHz, $CDCl_3$): δ = 152, 140, 126, 117, 30, 13.

4.3.6.3 Synthesis of *fac*-[$Re(CO)_3(H_2O)((EtF)_2ATI)$]

ReAA (100 mg, 0.123 mmol) was dissolved in water at pH 2.2 (adjusted with HNO_3). Silver nitrate (67 mg, 0.394 mmol) was added to the solution and the reaction mixture was stirred at room temperature for 24 hours. The AgBr was filtered off and the filtrate was freeze-dried. The residue was dissolved in dichloromethane and *N*-2-fluoroethyl-2-(2-fluoroethylamino)troponimine (26 mg, 0.123 mmol) was added. The solution was stirred at room temperature for 24 hours after which it was washed with water to remove excess counter ions. The dried residue was washed with ethyl acetate to remove the unreacted *N*-2-fluoroethyl-2-(2-fluoroethylamino)troponimine. The product was obtained as a dark orange solid.

Yield: 0.045 g, 73 %. IR (cm^{-1}): ν_{CO} = 2012, 1889. UV/Vis: λ_{max} = 350, 420 nm (ε = 17 182, 12 986 $Lmol^{-1}cm^{-1}$). ^1H NMR (400.13 MHz, $CDCl_3$): δ = 7.6 (t, 2H, *J* = 10.8 Hz), 7.2 (d, 2H, *J* = 11.2 Hz), 7.1 (t, 1H, *J* = 9.2 Hz), 4.8 (dt, 4H, *J* = 46.8, 4.8 Hz), 3.9 (dd, 4H, *J* = 25.2, 3.6 Hz) ^{13}C NMR (100.61 MHz, $CDCl_3$): δ = 153, 141, 129, 118, 82, 45.

4.3.6.4 Synthesis of *fac*-[$Re(CO)_3(H_2O)((EtPh)_2ATI)$]

ReAA (100 mg, 0.123 mmol) was dissolved in water at pH 2.2 (adjusted with HNO_3). Silver nitrate (67 mg, 0.394 mmol) was added to the solution and the reaction mixture was stirred at room temperature for 24 hours. The AgBr was filtered off and the filtrate was freeze-dried. The residue was dissolved in dichloromethane and *N*-phenethyl-2-(phenethylamino)troponimine (40 mg, 0.122 mmol) was added. The solution was stirred at room temperature for 24 hours after which it was washed with water to remove excess counter ions. The dried residue was washed with ethyl acetate to remove the unreacted *N*-phenethyl-2-(phenethylamino)troponimine. The product was obtained as a brown solid.

Yield: 0.070 g, 93 %. IR (cm^{-1}): ν_{CO} = 2002, 1881. UV/Vis: λ_{max} = 355, 425 nm (ε = 16 829, 13 648 $Lmol^{-1}cm^{-1}$). ^1H NMR (400.13 MHz, $CDCl_3$): δ = 7.5 (t, 2H, *J* = 10.4 Hz), 7.4 - 7.2 (m, 10H), 7.0 (t, 1H, *J* = 9.6 Hz), 6.9 (d, 2H, *J* = 11.2 Hz), 3.8 - 3.7 (m, 4H), 3.2 (t, 4H, *J* = 8.0 Hz). ^{13}C NMR (100.61 MHz, $CDCl_3$): δ = 152, 140, 138, 129, 127, 117, 53, 47, 34, 8.

4.3.6.5 Synthesis of *fac*-[$Re(CO)_3(H_2O)((Bn)_2ATI)$]

ReAA (100 mg, 0.123 mmol) was dissolved in water at pH 2.2 (adjusted with HNO_3). Silver nitrate (67 mg, 0.394 mmol) was added to the solution and the reaction mixture was stirred at room temperature for 24 hours. The AgBr was filtered off and the filtrate was freeze-dried. The residue was dissolved in dichloromethane and *N*-benzyl-2-(benzylamino)troponimine (37 mg, 0.123 mmol) was added. The solution was stirred at room temperature for 24 hours after which it was washed with water to remove excess counter ions. The dried residue was washed with ethyl acetate to remove the unreacted *N*-benzyl-2-(benzylamino)troponimine. The product was obtained as a brown solid.

Yield: 0.068 g, 94 %. IR (cm^{-1}): ν_{CO} = 2008, 1886. UV/Vis: λ_{max} = 350, 425 nm (ε = 14 495, 11 557 $Lmol^{-1}cm^{-1}$). ^1H NMR (400.13 MHz, $CDCl_3$): δ = 7.5 (t, 2H,

J = 10.4 Hz), 7.4 - 7.3 (m, 10H), 7.0 (d, 2H, *J* = 11.6 Hz), 7.0 (t, 1H, *J* = 9.2 Hz), 4.8 (d, 4H, *J* = 3.6 Hz). ^{13}C NMR (100.61 MHz, $CDCl_3$): δ = 153, 140, 135, 129, 127, 119, 53, 49, 8.

4.3.6.6 Synthesis of *fac*-[Re(CO)$_3$(H$_2$O)((Me,Bn)ATI)]

ReAA (100 mg, 0.123 mmol) was dissolved in water at pH 2.2 (adjusted with HNO_3). Silver nitrate (67 mg, 0.394 mmol) was added to the solution and the reaction mixture was stirred at room temperature for 24 hours. The AgBr was filtered off and the filtrate was freeze-dried. The residue was dissolved in dichloromethane and *N*-methyl-2-(benzylamino)troponimine (27 mg, 0.120 mmol) was added. The solution was stirred at room temperature for 24 hours after which it was washed with water to remove excess counter ions. The dried residue was washed with ethyl acetate to remove the unreacted *N*-methyl-2-(benzylamino)troponimine. The product was obtained as a dark red solid.

Yield: 0.034 g, 55 %. IR (cm^{-1}): ν_{CO} = 2003, 1875. UV/Vis: λ_{max} = 340, 405 nm (ε = 21 446, 18 003 $Lmol^{-1}cm^{-1}$). ^{1}H NMR (400.13 MHz, $CDCl_3$): δ = 7.6 - 7.4 (m, 3H), 7.2 - 6.9 (m, 5H), 6.6 (t, 1H, *J* = 9.2 Hz), 6.6 (d, 1H, *J* = 10.4 Hz), 4.7 (d, 2H, *J* = 4.4 Hz), 3.2 (d, 3H, *J* = 7.2 Hz). ^{13}C NMR (100.61 MHz, $CDCl_3$): δ = 176, 155, 141, 135, 129, 128, 127, 118, 52, 47, 32, 30, 7.

4.3.6.7 Synthesis of *fac*-[Re(CO)$_3$(H$_2$O)((Et,Bn)ATI)]

ReAA (100 mg, 0.123 mmol) was dissolved in water at pH 2.2 (adjusted with HNO_3). Silver nitrate (67 mg, 0.394 mmol) was added to the solution and the reaction mixture was stirred at room temperature for 24 hours. The AgBr was filtered off and the filtrate was freeze-dried. The residue was dissolved in dichloromethane and *N*-ethyl-2-(benzylamino)troponimine (29 mg, 0.122 mmol) was added. The solution was stirred at room temperature for 24 hours after which it was washed with water to remove excess counter ions. The dried residue was washed with ethyl acetate to remove the unreacted *N*-ethyl-2-(benzylamino)troponimine. The product was obtained as a dark red solid.

Yield: 0.036 g, 56 %. IR (cm^{-1}): ν_{CO} = 2002, 1871. UV/Vis: λ_{max} = 340, 405 nm (ε = 19 001, 16 374 $Lmol^{-1}cm^{-1}$). ^{1}H NMR (400.13 MHz, $CDCl_3$): δ = 7.6 - 7.4 (m, 3H), 7.4 - 7.3 (m, 4H), 7.0 (t, 3H, *J* = 12.8 Hz), 4.7 (d, 2H, *J* = 5.6 Hz), 3.1

(dq, 2H, *J* = 12.4, 7.2 Hz), 1.3 (t, 3H, *J* = 7.2 Hz). ^{13}C NMR (100.61 MHz, $CDCl_3$): δ = 176, 152, 140, 135, 129, 127, 117, 110, 52, 48, 40, 30, 13, 7.

4.3.6.8 Synthesis of *fac*-[Re(CO)$_3$(H$_2$O)((EtF,Bn)ATI)]

ReAA (100 mg, 0.123 mmol) was dissolved in water at pH 2.2 (adjusted with HNO_3). Silver nitrate (67 mg, 0.394 mmol) was added to the solution and the reaction mixture was stirred at room temperature for 24 hours. The AgBr was filtered off and the filtrate was freeze-dried. The residue was dissolved in dichloromethane and *N*-2-fluoroethyl-2-(benzylamino)troponimine (31 mg, 0.121 mmol) was added. The solution was stirred at room temperature for 24 hours after which it was washed with water to remove excess counter ions. The dried residue was washed with ethyl acetate to remove the unreacted *N*-2-fluoroethyl-2-(benzylamino)troponimine. The product was obtained as a brown solid.

Yield: 0.035 g, 53 %. IR (cm^{-1}): ν_{CO} = 2003, 1877. UV/Vis: λ_{max} = 345, 405 nm (ε = 13 589, 11 648 Lmol^{-1}cm^{-1}). ^{1}H NMR (400.13 MHz, $CDCl_3$): δ = 7.7 - 7.6 (m, 2H), 7.5 - 7.4 (m, 2H), 7.3 - 7.2 (m, 3H), 7.1 - 7.0 (m, 3H), 4.8 (dt, 2H, *J* = 12.0, 4.8 Hz), 4.7 (d, 2H, *J* = 5.2 Hz), 3.9 - 3.8 (m, 2H). ^{13}C NMR (100.61 MHz, $CDCl_3$): δ = 153, 152, 141, 138, 135, 129, 127, 119, 81, 52, 47, 9, 7.

4.3.6.9 Synthesis of *fac*-[Re(CO)$_3$(H$_2$O)((EtPh,Bn)ATI)]

ReAA (100 mg, 0.123 mmol) was dissolved in water at pH 2.2 (adjusted with HNO_3). Silver nitrate (67 mg, 0.394 mmol) was added to the solution and the reaction mixture was stirred at room temperature for 24 hours. The AgBr was filtered off and the filtrate was freeze-dried. The residue was dissolved in dichloromethane and *N*-phenethyl-2-(benzylamino)troponimine (38 mg, 0.121 mmol) was added. The solution was stirred at room temperature for 24 hours after which it was washed with water to remove excess counter ions. The dried residue was washed with ethyl acetate to remove the unreacted *N*-phenethyl-2-(benzylamino)troponimine. The product was obtained as a brown solid.

Yield: 0.041 g, 56 %. IR (cm^{-1}): ν_{CO} = 2001, 1867. UV/Vis: λ_{max} = 345, 405 nm (ε = 19 153, 16 746 Lmol^{-1}cm^{-1}). ^{11}H NMR (400.13 MHz, $CDCl_3$): δ = 7.5 - 7.3 (m, 2H 7.3 - 7.1 (m, 11H), 6.9 (d, 1H, *J* = 11.6 Hz), 6.8 (t, 1H, *J* = 11.6 Hz), 4.7 (d, 2H, *J* = 4.0 Hz), 3.7 – 3.6 (m, 2H), 3.1 - 3.0 (m, 2H). ^{13}C NMR (100.61 MHz, $CDCl_3$): δ = 177, 168, 157, 153, 152, 140, 138, 129, 128, 117, 52, 34, 30, 7.

4.4 Discussion

In this study, five *N,O* bidentate 2-(alkylamino)tropone and nine *N,N'* bidentate aminotroponimine ligand systems were successfully synthesized in yields ranging from 22 % to 74 % and characterized with UV/Vis, IR and NMR techniques. Two of the *N,O* and seven of the *N,N'* bidentate ligands are novel and have not been reported before in literature, and are illustrated in Figure 4.5.

The synthesis of these ligands is straightforward, although the synthesis of the aminotroponimine ligand systems is time consuming. The basicity of the ligands is an important property that was not determined in this study. It provides important information on the conditions for the synthesis of organometallic complexes as well as deprotonation at a specific pH in the body. Determination of the pKa's of the ligands will form part of future work. The novel ligand systems synthesized in this study are illustrated in Figure 4.5.

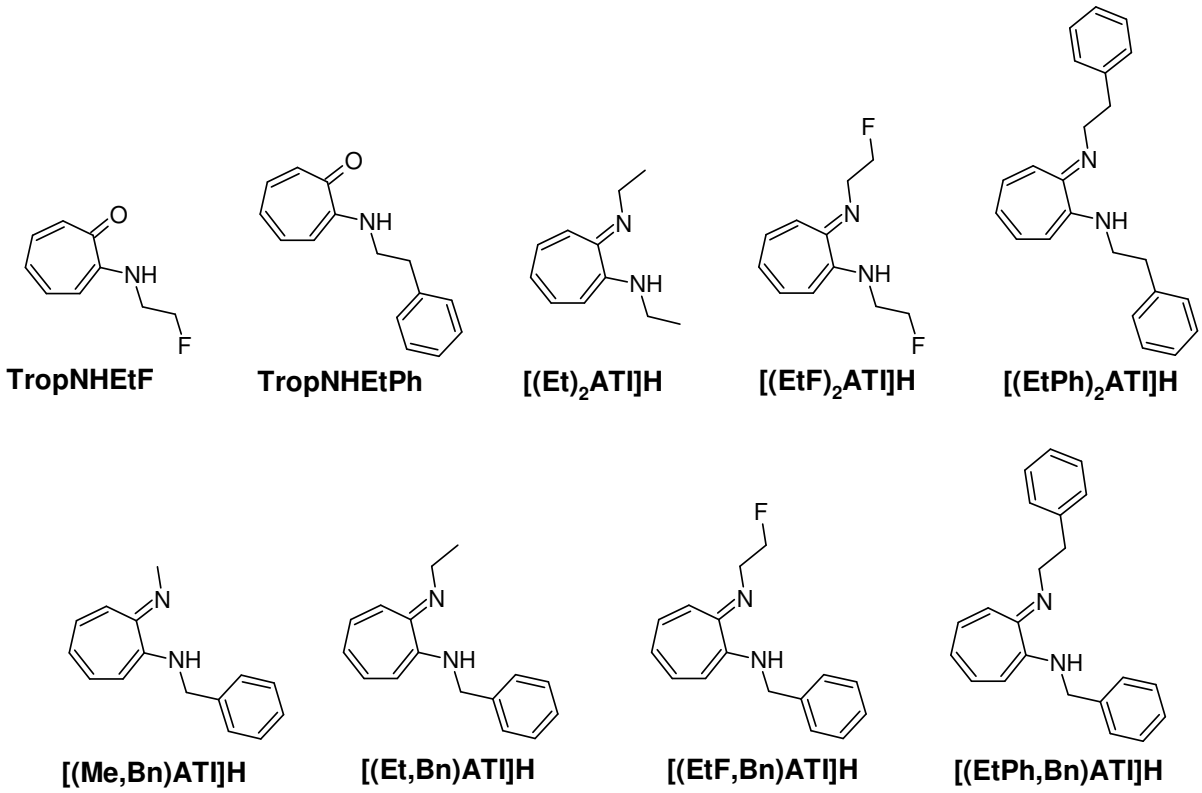

Figure 4.5: The chemical structures of novel *N,O* and *N,N'* bidentate ligands synthesized in this study.

Five of the ligands synthesized in this study have been reported before of which three have structure reports on the Cambridge Structural Database (CSD):[24] 2-(methylamino)tropone,[25] 2-(benzylamino)tropone[26] and *N*-methyl-2-(methylamino)troponimine.[27]

Five Re(I) tricarbonyl complexes of the type *fac*-[Re(CO)$_3$(H$_2$O)(*N,O*)] (*N,O* = different *N,O* bidentate ligands) and nine of the type *fac*-[Re(CO)$_3$(H$_2$O)(*N,N'*)] (*N,N'* = different *N,N'* bidentate ligands) were successfully synthesized in yields ranging from 53 % to 94 %. The synthesis of the complexes was also straightforward, although many of the ligands were not very soluble in water and dichloromethane was used as solvent instead. For this reason, the aqueous solutions were freeze-dried. The complexes were also characterized with UV/Vis, IR and NMR techniques. Structure searches on chemical databases yielded no records of Re(I) tricarbonyl complexes containing 2-(alkylamino)tropone or aminotroponimines ligand systems. However, many crystal structures of 2-(alkylamino)tropone and aminotroponimine ligands coordinated to various metal centres such as Al(III), Ni(II), Cu(II), As(III), Mn(III) Rh(I) and Pt(II) have been reported before.[28,29,30,31,32,33,34] Obtaining crystal structures of the synthesized Re(I) tricarbonyl metal complexes would significantly contribute to future studies on these complexes.

---

[24] Groom, C., Bruno, I., Lightfoot, M. & Ward, S. (2016). *Acta Crystallographica Section B Structural Science, Crystal Engineering and Materials*, **72**(2), 171-179.

[25] Jansen van Vuuren, L., Visser, H. & Schutte-Smith, M. (2019). *Acta Crystallographica Section E Crystallographic Communications*, **75**(8), 1128-1132.

[26] Barret, M., Bhatia, P., Kociok-Köhn, G. & Molloy, K. (2014). *Transition Metal Chemistry*, **39**(5), 543-551.

[27] Goldstein, P. & Trueblood, K. (1967). *Acta Crystallographica*, **23**(1), 148-156.

[28] Pappalardo, D., Mazzeo, M., Montefusco, P., Tedesco, C. & Pellecchia, C. (2004). *European Journal of Inorganic Chemistry*, **2004**(6), 1292-1298.

[29] Hicks, F., Jenkins, J. & Brookhart, M. (2003). *Organometallics*, **22**(17), 3533-3545.

[30] Villacorta, G., Gibson, D., Williams, I. & Lippard, S. (1985). *Journal of The American Chemical Society*, **107**(23), 6732-6734.

[31] Pop, L., Castel, A., Silaghi-Dumitrescu, L. & Saffon, N. (2011). *European Journal of Inorganic Chemistry*, **2011**(22), 3357-3364.

[32] Bartlett, M. & Palenik, G. (1970). *Journal of The Chemical Society D: Chemical Communications*, (7), 416.

[33] Villacorta, G. & Lippard, S. (1988). *Inorganic Chemistry*, **27**(1), 144-149.

[34] Traversa, E., Templeton, J., Cheng, H., Mohadjer Beromi, M., White, P. & West, N. (2013). *Organometallics*, **32**(6), 1938-1950.

The CO carbon atoms of the Re(I) tricarbonyl complexes are rarely visible on a ^{13}C NMR spectrum and are not reported for all complexes. ^{13}C NMR is not the preferred technique for the identification of the carbonyl peaks after coordination as it is very costly and time consuming. IR spectroscopy is a very useful technique when characterizing Re(I) tricarbonyl complexes and were used as the primary method of characterization thereof. Table 4.1 summarizes the CO stretching frequencies of the Re(I) tricarbonyl complexes.

Table 4.1: The CO stretching frequencies of the Re(I) tricarbonyl complexes obtained from its IR spectra.

Compound	ν_{CO} (cm^{-1})
Compounds containing *N,O* donor ligands	
fac-[$Re(CO)_3(H_2O)$(TropNMe)]	1997, 1851
fac-[$Re(CO)_3(H_2O)$(TropNEt)]	1997, 1866
fac-[$Re(CO)_3(H_2O)$(TropNEtF)]	1999, 1870
fac-[$Re(CO)_3(H_2O)$(TropNEtPh)]	2002, 1876
fac-[$Re(CO)_3(H_2O)$(TropNBn)]	1996, 1854
Compounds containing *N,N'* donor ligands	
fac-[$Re(CO)_3(H_2O)((Me)_2ATI)$]	2017, 1882
fac-[$Re(CO)_3(H_2O)((Et)_2ATI)$]	2015, 1884
fac-[$Re(CO)_3(H_2O)((EtF)_2ATI)$]	2012, 1889
fac-[$Re(CO)_3(H_2O)((EtPh)_2ATI)$]	2002, 1881
fac-[$Re(CO)_3(H_2O)((Bn)_2ATI)$]	2008, 1886
fac-[$Re(CO)_3(H_2O)$((Me,Bn)ATI)]	2003, 1875
fac-[$Re(CO)_3(H_2O)$((Et,Bn)ATI)]	2002, 1871
fac-[$Re(CO)_3(H_2O)$((EtF,Bn)ATI)]	2003, 1877
fac-[$Re(CO)_3(H_2O)$((EtPh,Bn)ATI)]	2001, 1867

The carbonyl group is polarized, and the dipole moment is influenced by any vibrational stretching of the carbonyl group. The distinct absorption peaks of symmetric stretching of the C≡O appear at lower frequencies than that of the asymmetric stretching because it requires more energy.

When the electron density is increased on the Re(I) metal centre, the π-backbonding from the CO ligands increase which results in a shorter Re-CO distance and an IR

vibration at lower frequency. The stretching frequencies of the complexes containing *N,O* bidentate ligands are slightly lower than those containing *N,N'* bidentate ligands, except for *fac*-[Re(CO)$_3$(H$_2$O)(TropNEtPh)]. This confirms that the *N,O* donor bidentate ligand systems are more electron donating than the *N,N'* donor bidentate ligands.

In the complexes containing *N,N'* bidentate ligands, it is observed that the stretching frequencies of *fac*-[Re(CO)$_3$(H$_2$O)((EtPh)$_2$ATI)], *fac*-[Re(CO)$_3$(H$_2$O)((Bn)$_2$ATI)], *fac*-[Re(CO)$_3$(H$_2$O)((Me,Bn)ATI)], *fac*-[Re(CO)$_3$(H$_2$O)((Et,Bn)ATI)], *fac*-[Re(CO)$_3$(H$_2$O)((EtF,Bn)ATI)] and *fac*-[Re(CO)$_3$(H$_2$O)((EtPh,Bn)ATI)] are notably lower than those of *fac*-[Re(CO)$_3$(H$_2$O)((Me)$_2$ATI)], *fac*-[Re(CO)$_3$(H$_2$O)((Et)$_2$ATI)] and *fac*-[Re(CO)$_3$(H$_2$O)((EtF)$_2$ATI)]. This is possibly due to the extra phenyl ring present in the first group of complexes mentioned which increases the electron density on the metal centre and decrease the stretching frequency. *fac*-[Re(CO)$_3$(H$_2$O)((Me)$_2$ATI)], *fac*-[Re(CO)$_3$(H$_2$O)((Et)$_2$ATI)] and *fac*-[Re(CO)$_3$(H$_2$O)((EtF)$_2$ATI)] display higher stretching frequencies. The high stretching frequency of *fac*-[Re(CO)$_3$(H$_2$O)((EtF)$_2$ATI)] is possibly due to the electron withdrawing effects of the 2-fluoroethyl substituents. The high stretching frequencies of *fac*-[Re(CO)$_3$(H$_2$O)((Me)$_2$ATI)] and *fac*-[Re(CO)$_3$(H$_2$O)((Et)$_2$ATI)] are unexpected since the methyl and ethyl substituents are electron donating.

The determination of crystal structures is an important method of characterization of ligands and compounds. Crystal structures were obtained of the synthesized intermediate 2-tosyloxytropone and two 2-(alkylamino)tropone ligands, namely 2-(methylamino)tropone and 2-(2-fluoroethylamino)tropone and are reported and discussed in the next chapter.

5

CRYSTALLOGRAPHIC STUDY OF SELECTED LIGAND SYSTEMS

5.1 Introduction

Tropolone and its derivatives are non-benzenoid aromatic compounds found in numerous naturally occurring biological products.[1] These compounds exhibit antibacterial, anti-fungal, anti-tumor and anti-viral biological activities and are of interest when investigating new or improved chemical compounds for medical applications.[2] The two ligand system types chosen for this study, namely 2-(alkylamino)tropones and aminotroponimines, are *N,O* and *N,N'* bidentate ligands respectively with good chelating properties.[3] Investigations involving these ligand systems have yielded compounds with possible applications in anticancer therapy.[4,5,6,7,8,9]

Among hundreds of crystal structure reports of *N,O* bidentate ligands found on the Cambridge Structural Database (CSD),[10] only eight of these structures are of the group of ligands called 2-(alkylamino)tropones of which two, namely

[1] Balachandra, C. & Sharma, N. (2017). *Dyes and Pigments*, **137**, 532-538.
[2] Liu, N., Song, W., Schienebeck, C., Zhang, M. & Tang, W. (2014). *Tetrahedron*, **70**(49), 9281-9305.
[3] Dochnahl, M., Löhnwitz, K., Pissarek, J., Biyikal, M., Schulz, S., Schön, S., Meyer, N., Roesky, P. & Blechert, S. (2007). *Chemistry - A European Journal*, **13**(23), 6654-6666.
[4] Mendiguchia, B. S., Pucci, D., Mastropietro, T. F., Ghedini, M. & Crispini, A. (2013). *Dalton Transactions*, **42**, 6768-6774.
[5] Liu, S. & Yamauchi, H. (2006). *Biochemical and Biophysical Research Communications*, **351**(1), 26-32.
[6] Haney, S. L., Allen, C., Varney, M. L., Dykstra, K. M., Falcone, E. R., Colligan, S. H., Hu, Q., Aldridge, A. M., Wright, D. L., Wiemer, A. J. & Holstein, S. A. (2017). *Oncotarget*, **8**(44), 76085-76098.
[7] Jayakumar, T., Liu, C., Wu, G., Lee, T., Manubolu, M., Hsieh, C., Yang, C. & Sheu, J. (2018). *International Journal of Molecular Sciences*, **19**(4), 939-952.
[8] Balsa, L., Ruiz, M., Santa Maria de la Parra, L., Baran, E. & León, I. (2020). *Journal of Inorganic Biochemistry*, **204**, 110975.
[9] Ononye, S., VanHeyst, M., Oblak, E., Zhou, W., Ammar, M., Anderson, A. & Wright, D. (2013). *ACS Medicinal Chemistry Letters*, **4**(8), 757-761.
[10] Groom, C., Bruno, I., Lightfoot, M. & Ward, S. (2016). The Cambridge Structural Database. *Acta Crystallographica Section B Structural Science, Crystal Engineering and Materials*, **72**(2), 171-179.

2-(isopropylamino)tropone[11] and 2-(4-fluoroanilino)tropone[12] are illustrated as examples in Figure 5.1.

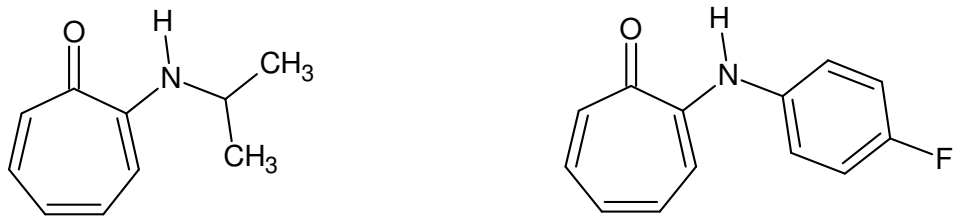

Figure 5.1: The chemical structures of 2-(isopropylamino)tropone and 2-(4-fluoroanilino)tropone, examples of 2-(alkylamino)tropones reported in literature.

The same is true for crystal structure reports of *N,N'* bidentate ligands - there are plenty reported on the CSD, but there are only nine structures of the group aminotroponimines. Two of these, namely *N*-methyl-2-(methylamino)troponimine[13] and *N*-(2,6-diisopropylanilino)-2-(butylamino)troponimine[14] are illustrated in Figure 5.2 as examples.

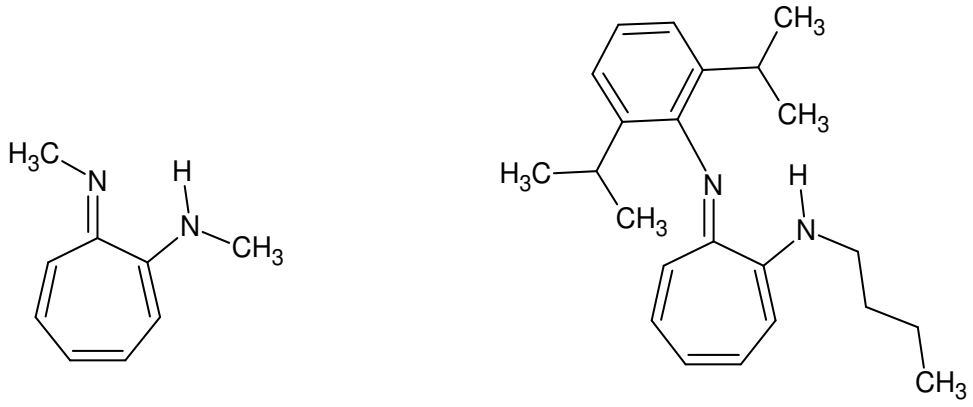

Figure 5.2: The chemical structures of *N*-methyl-2-(methylamino)troponimine and *N*-(2,6-diisopropylanilino)-2-(butylamino)troponimine, examples of aminotroponimines ligands in literature.

[11] Roesky, P. & Bürgstein, M. (1999). *Inorganic Chemistry*, **38**(24), 5629-5632.
[12] Steyl, G. (2007). *Acta Crystallographica Section E Structure Reports Online*, **63**(11), o4353-o4353.
[13] Goldstein, P. & Trueblood, K. (1967). *Acta Crystallographica*, **23**(1), 148-156.
[14] Szuromi, E., Klosin, J. & Abboud, K. (2011). *Organometallics*, **30**(17), 4589-4597.

Many crystal structures of 2-(alkylamino)tropone and aminotroponimine ligands coordinated to various metal centres such as Al(III), Ni(II), Cu(II), As(III), Mn(III) Rh(I) and Pt(II) have been reported in literature.[15,16,17,18,19,20,21]

One of the aims of this study was to obtain crystal structures of the synthesized 2-(alkylamino)tropone and aminotroponimine ligand systems as well as the Re(I) tricarbonyl complexes thereof. Unfortunately, we were only able to obtain crystal data for one intermediate, 2-tosyloxytropone (TropOTs) and two ligand systems, 2-(methylamino)tropone (TropNHMe) and 2-(2-fluoroethylamino)tropone (TropNHEtF) (Figure 5.3). The isolation of crystal structures of the Re(I) tricarbonyl complexes will form part of future work.

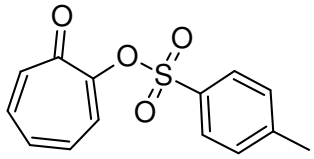

TropOTs

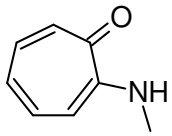

TropNHMe

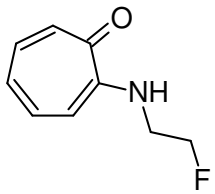

TropNHEtF

Figure 5.3: The chemical structure of the starting material TropOTs and ligand systems, TropNHMe and TropNHEtF of which crystal structure data were obtained.

[15] Pappalardo, D., Mazzeo, M., Montefusco, P., Tedesco, C. & Pellecchia, C. (2004). *European Journal of Inorganic Chemistry*, **2004**(6), 1292-1298.
[16] Hicks, F., Jenkins, J. & Brookhart, M. (2003). *Organometallics*, **22**(17), 3533-3545.
[17] Villacorta, G., Gibson, D., Williams, I. & Lippard, S. (1985). *Journal of The American Chemical Society*, **107**(23), 6732-6734.
[18] Pop, L., Castel, A., Silaghi-Dumitrescu, L. & Saffon, N. (2011). *European Journal of Inorganic Chemistry*, **2011**(22), 3357-3364.
[19] Bartlett, M. & Palenik, G. (1970). *Journal of The Chemical Society D: Chemical Communications*, (7), 416.
[20] Villacorta, G. & Lippard, S. (1988). *Inorganic Chemistry*, **27**(1), 144-149.
[21] Traversa, E., Templeton, J., Cheng, H., Mohadjer Beromi, M., White, P. & West, N. (2013). *Organometallics*, **32**(6), 1938-1950.

5.2 Experimental

The reflection data for the structure determinations were collected on a Bruker X8 ApexII 4K and a Bruker D8 Quest Eco Chi Photon II CPAD diffractometer with φ and ω-scans at 100 K. Graphite monochromated Mo *K*α radiation with wavelength λ = 0.71073 Å was used. The cell refinement and data reduction were done with SAINT-Plus[22] with XPREP[23] included. Absorption corrections were obtained by using the multi-scan technique and the SADABS software package.[22,24] The structures were solved by using the SHELXS-97, SHELXT, and the SIR-2014 package and refined with SHELXL-2014 and WinGX.[25,26,27,28] All the molecular graphics and presentation of crystal structures were done with DIAMOND.[29] All structures are presented with thermal ellipsoids drawn at 50 % probability level, unless otherwise stated. All non-hydrogen atoms were refined anisotropically. Methyl, aromatic and methylene hydrogen atoms were placed in geometrically idealized positions (C-H = 0.95 - 0.98 Å for methyl and aromatic and C-H = 0.99 Å for methylene hydrogen atoms) and constrained to ride on their parent atoms (U_{iso}(H) = 1.5U_{eq}(C) for methyl and 1.2U_{eq}(C) for aromatic and methylene hydrogen atoms). The N-H hydrogen atoms were located from a Fourier electron-density map and freely refined.

[22] Bruker (2016). *APEX3*, *SAINT* and *SADABS*. Bruker AXS Inc., Madison, Wisconsin, USA
[23] Bruker (2005). *XPREP* (Version 2005/2), Bruker AXS Inc., Madison, Wisconsin, USA.
[24] Bruker (2012). *SADABS* (version 2012/1), BrukerAXS Inc., Madison, Wisconsin, USA.
[25] Sheldrick, G. M. (2008). *Acta Crystallographica Section A,* A**64**, 112-122.
[26] Sheldrick, G. M. (2015). *Acta Crystallographica Section A,* A**71**, 3-8.
[27] Sheldrick, G. M. (2015). *Acta Crystallographica Section C,* C**71**, 3-8.
[28] Farrugia, L. J. (2012). *Journal of Applied Crystallography,* **45**, 849-854.
[29] Brandenburg, K. (2014). *DIAMOND*. Crystal Impact GbR, Bonn, Germany.

Table 5.1: Crystal data for 2-tosyloxytropone (TropOTs) and 2-(methylamino)tropone (TropNHMe).

Compound	TropOTs	TropNHMe
Empirical formula	C_{14} H_{12} O_4 S	C_8 H_9 N O
Formula weight (g.mol^{-1})	276.31	135.16
Temperature	100(2) K	100(2) K
Wavelength	0.71073 Å	0.71073 Å
Crystal system	Monoclinic	Monoclinic
Space group	*Cc*	*P*2$_1$/*c*
Unit cell dimensions	a = 7.882(3) Å α = 90° b = 14.943(5) Å β = 96.135(12)° c = 10.762(4) Å γ = 90°	a = 17.635(5) Å α = 90° b = 7.817(2) Å β = 110.639(9)° c = 16.718(4) Å γ = 90°
Volume (Å^3)	1260.3(8)	2156.8(10)
Z	4	12
Density (calculated) (mg/m^3)	1.541	1.249
Absorption coefficient (mm^{-1})	0.274	0.083
F(000)	608	864
Crystal size (mm^3)	0.350 x 0.310 x 0.210	0.578 x 0.304 x 0.277
Theta range for data collection (°)	3.326 to 28.000	3.704 to 27.994
Index ranges	-10<=h<=10 -19<=k<=19 -14<=l<=14	-23<=h<=23 -10<=k<=10 -20<=l<=22
Reflections collected	6934	33879
Independent reflections	2956 [R(int) = 0.0378]	5192 [R(int) = 0.0462]
Completeness to theta = 25.242°	99.7 %	99.6 %
Refinement method	Full-matrix least-squares on F^2	Full-matrix least-squares on F^2
Data / restraints / parameters	2956 / 2 / 173	5192 / 0 / 283
Goodness-of-fit on F^2	1.014	1.044
Final R indices [I>2sigma(I)]	R_1 = 0.0405, wR_2 = 0.1137	R_1 = 0.0420, wR_2 = 0.0924
R indices (all data)	R_1 = 0.0517, wR_2 = 0.1560	R_1 = 0.0708, wR_2 = 0.1107
Extinction coefficient	n/a	0.0113(9)
Largest diff. peak and hole (e.Å^{-3})	0.283 and -0.391	0.140 and -0.194

Table 5.2: Crystal data for 2-(2-fluoroethylamino)tropone (TropNHEtF).

Compound	**TropNHEtF**	
Empirical formula	$C_9 H_{10} F N O$	
Formula weight (g.mol^{-1})	167.18	
Temperature	100(2) K	
Wavelength	0.71073 Å	
Crystal system	Monoclinic	
Space group	$P2_1/n$	
Unit cell dimensions	a = 9.822(3) Å b = 4.9893(15) Å c = 16.857(5) Å	α= 90° β= 99.718(9)° γ = 90°
Volume (Å^3)	814.2(4)	
Z	4	
Density (calculated) (mg/m^3)	1.364	
Absorption coefficient (mm^{-1})	0.105	
F(000)	352	
Crystal size (mm^3)	0.209 x 0.108 x 0.053	
Theta range for data collection (°)	2.452 to 27.000°	
Index ranges	-12<=h<=12 -6<=k<=6 -21<=l<=21	
Reflections collected	9945	
Independent reflections	1773 [R(int) = 0.0933]	
Completeness to theta = 25.242°	99.9 %	
Refinement method	Full-matrix least-squares on F^2	
Data / restraints / parameters	1773 / 0 / 113	
Goodness-of-fit on F^2	1.083	
Final R indices [I>2sigma(I)]	R_1 = 0.0729, wR_2 = 0.1334	
R indices (all data)	R_1 = 0.1517, wR_2 = 0.1681	
Extinction coefficient	n/a	
Largest diff. peak and hole (e.Å^{-3})	0.253 and -0.217	

5.3 Crystal structure of 2-tosyloxytropone (TropOTs)

5.3.1 Introduction

The title compound was synthesized according to the procedure reported in Paragraph 4.3.1. Colourless crystals suitable for single crystal XRD were obtained from deuterated acetone. Table 5.1 summarizes the general crystal data and Figure 5.4 illustrates the molecular diagram and numbering scheme of the structure of TropOTs. Selected bond distances and bond and torsion angles are presented in Table 5.3 and the discussion of the structure with a comparison to crystal structures of the same compound will follow in Paragraph 5.3.2. Atomic coordinates, anisotropic displacement parameters, all bond distances and angles and hydrogen coordinates are given in the supplementary data (Appendix A, Tables A.1 - A.6).

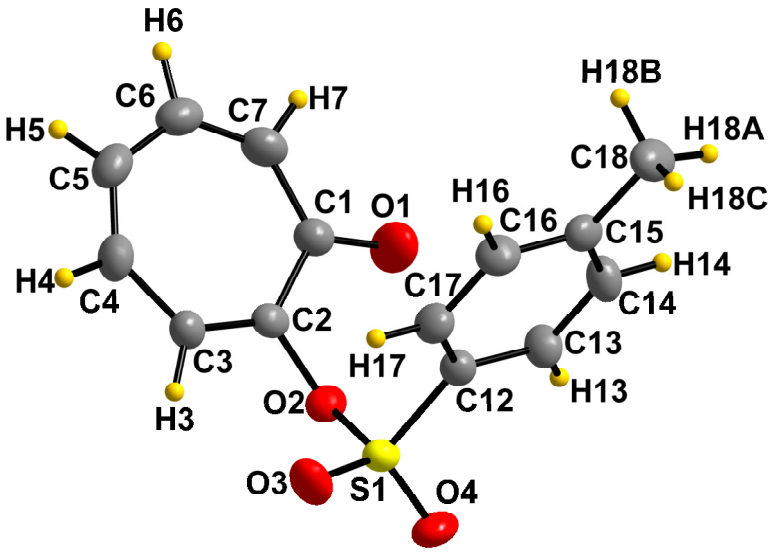

Figure 5.4: Molecular presentation of 2-tosyloxytropone indicating the numbering scheme with ellipsoids drawn at 50 % probability level.

5.3.2 Results and discussion

2-Tosyloxytropone crystallized in the monoclinic *Cc* space group. Two crystal structures of the same compound, both also in the *Cc* space group, were deposited to the Cambridge Structural Database (CSD)[10] in 2000 by Roesky & Bürgstein[11] and in 2006 by Steyl & Roodt.[30]

Table 5.3: Selected bond distances [Å] and bond and torsion angles [°] for 2-tosyloxytropone reported in this study compared to two other structure reports of this compound.

	This study	Roesky & Bürgstein[11]	Steyl & Roodt[30]
Selected bond distances [Å]			
C1-O1	1.241(7)	1.230(4)	1.234(2)
C2-O2	1.402(5)	1.403(3)	1.403(2)
C12-S1	1.752(5)	1.751(2)	1.7483(17)
O2-S1	1.604(3)	1.596(2)	1.6014(12)
Selected bond angles [°]			
O1-C1-C2	118.8(5)	119.3(8)	119.00(17)
O2-C2-C1	110.7(4)	110.2(2)	110.66(14)
C2-O2-S1	121.9(3)	121.40(14)	121.30(10)
O2-S1-C12	105.22(19)	104.96(10)	105.14(7)
Selected torsion angles [°]			
O1-C1-C2-O2	-6.4(6)	-6.683(334)	-6.3(2)

All the selected bond distances and angles of the three structures agree well with each other. The O1-C1-C2 angles are close to 120˚ which is expected in a structure containing a carbonyl group. The O2-C2-C1 bond angles are smaller than the expected 120˚, possibly due to hydrogen bonding interactions (Figure 5.5) causing the molecule to fold and twist to a certain extent as well as steric influences of the phenyl ring.

[30] Steyl, G. & Roodt, A. (2006). *CSD Communication*.

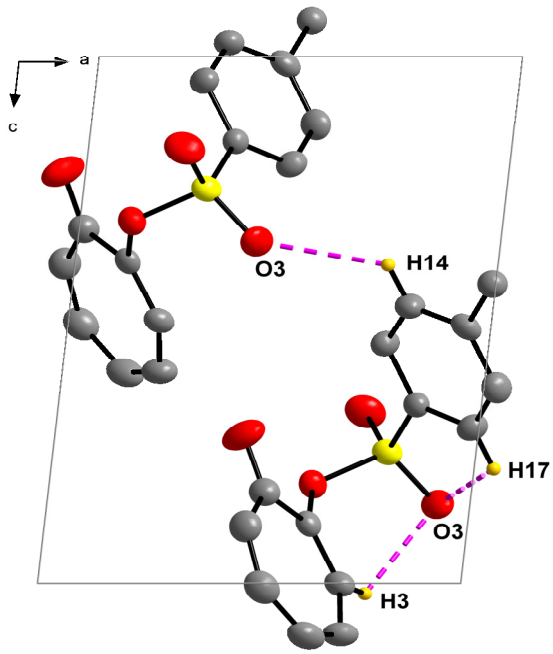

Figure 5.5: Hydrogen bonding interactions observed in the structure of TropOTs when viewed along the b-axis and indicated in pink dashed lines. The hydrogen atoms not taking part in interactions are omitted for clarity.

Three C-H…O hydrogen bonding interactions, two intramolecular and one intermolecular, are observed in the structure of TropOTs and is presented in Figure 5.5. The bonds are bifurcated on the O3 atom which contributes to the way the molecules fold and twist intramolecularly and pack in the unit cell. The contact distances and angles of the hydrogen bonding interactions are presented in Table 5.4.

Table 5.4: Hydrogen bonding interactions observed in 2-tosyloxytropone [Å and °].

D-H...A	d(D-H)	d(H...A)	d(D...A)	<(DHA)
C3-H3...O3	0.95	2.47	3.028(6)	117.6
C17-H17...O3	0.95	2.56	2.925(6)	103.2
C14-H14...O3[1]	0.95	2.55	3.162(6)	122.6

Symmetry transformations used to generate equivalent atoms:

[1] x-1/2,-y+1/2,z-1/2

A weak π-π interaction with a centroid to centroid distance of 3.923(1) Å is observed between the six-membered ring (C12-C13-C14-C15-C16-C17) of one molecule and the seven-membered ring (C1-C2-C3-C4-C5-C6-C7) of a neighbouring molecule (-1/2+x, 1/2-y,1/2+z) and is illustrated in Figure 5.6. The dihedral angle between the planes of the two rings are 13.84(13)˚.

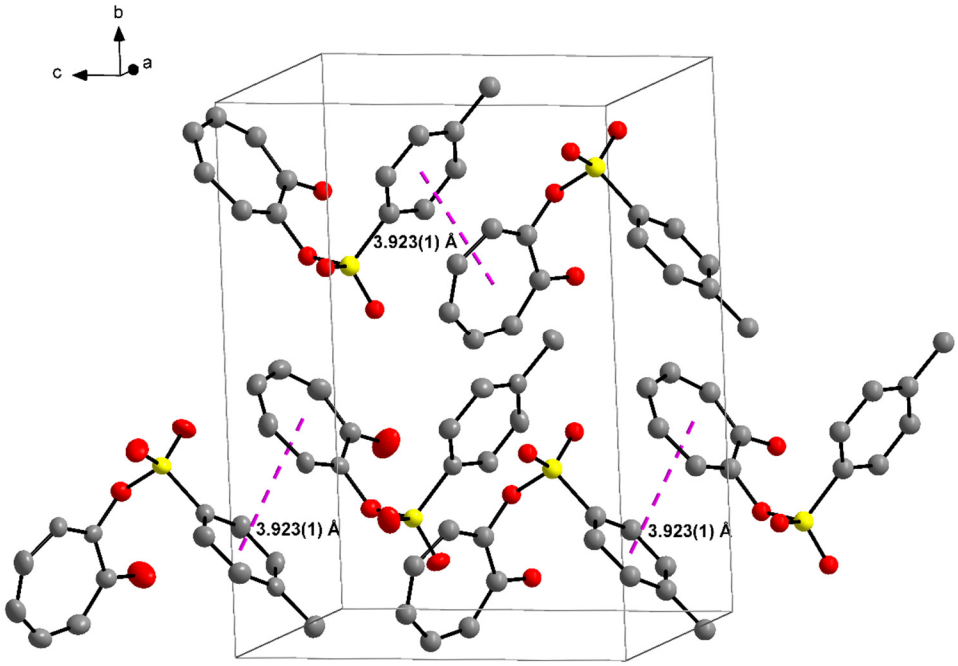

Figure 5.6: Illustration of the weak π-π interaction (indicated in a pink dashed line) observed between molecules of TropOTs. Hydrogen atoms are omitted for clarity.

The hydrogen bonding interactions and the π-interactions lead to the inverted head-to-tail packing of molecules in the unit cell when viewed along the a-axis as illustrated in Figure 5.7.

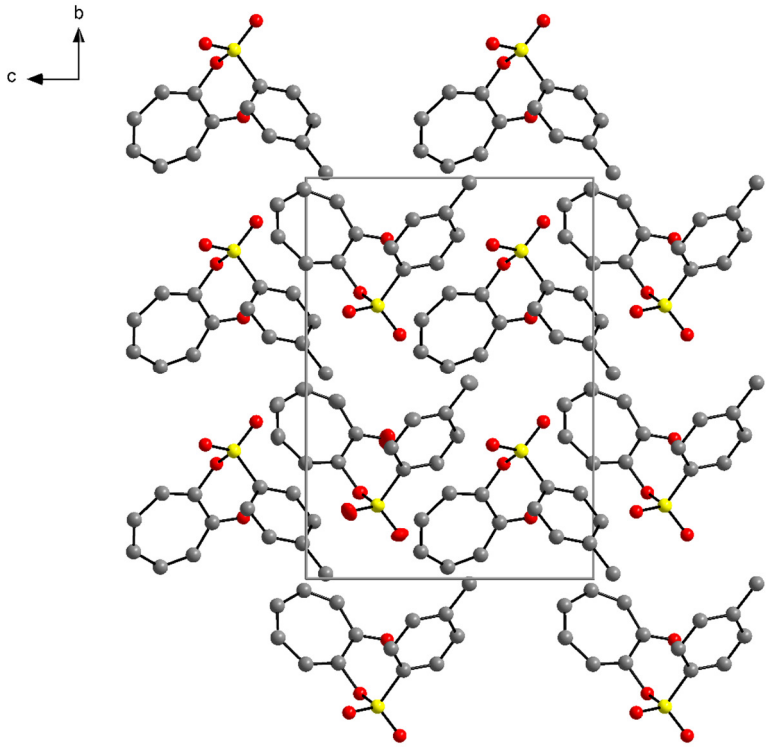

Figure 5.7: Packing of TropOTs in the unit cell viewed along the bc plane. Hydrogen atoms are omitted for clarity.

5.4 Crystal structure of 2-(methylamino)tropone (TropNHMe)

5.4.1 Introduction

2-(Methylamino)tropone, one of the *N,O* bidentate ligands used in this study, was synthesized according to the procedure reported in Paragraph 4.3.2.1. Yellow crystals suitable for single crystal XRD were obtained from an acetone solution.[31] The general crystal data is summarized in Table 5.1 and in Figure 5.8 the molecular diagram and numbering scheme of TropNHMe is presented. In Table 5.5 selected bond distances and bond and torsion angles are presented and the discussion and comparison of the three independent molecules will follow in Paragraph 5.4.2. Atomic coordinates, anisotropic displacement parameters, all bond distances and angles and hydrogen coordinates are given in the supplementary data (Appendix B, Tables B.1 - B.6).

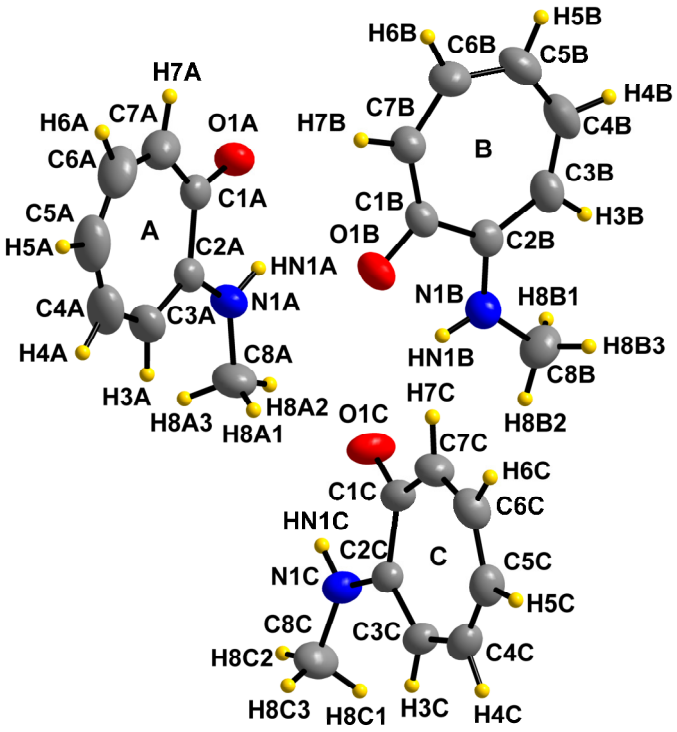

Figure 5.8: Molecular presentation of 2-(methylamino)tropone indicating the numbering scheme of molecules A, B and C in the asymmetric unit with ellipsoids drawn at 50 % probability level.

[31] Jansen van Vuuren, L., Visser, H. G. & Schutte-Smith, M. (2019). *Acta Crystallographica Section E Crystallographic Communications*, **75**(8), 1128-1132.

5.4.2 Results and discussion

2-(Methylamino)tropone crystallized in the monoclinic $P2_1/c$ space group with three molecules in the asymmetric unit. Similar compounds reported in literature include 2-(benzylamino)tropone,[32] 2-(isopropylamino)tropone[11] and tropolone[33] and these also crystallized in the $P2_1/c$ space group. Other similar compounds, 2-(cyclohexylamino)tropone[34] and 2-(*t*-butylamino)tropone[35] crystallized in the $P2_1/n$ and $P2_12_12_1$ space groups, respectively. The selected bond distances and angles of TropNHMe are within normal range and also agree well with similar structures in literature.[11,32,33,34,35] The bond distances and bond angles of the three molecules in the asymmetric unit also agree well with each other. The selected bond angles involving the carbonyl group namely O1-C1-C7 and O1-C1-C2 are close to 120˚ (119.73(12)˚ - 119.87(12)˚ and 116.31(12)˚ - 116.84(12)˚), the general size of the angle in trigonal planar geometries. The C2-N1-C8 bond angle is slightly larger than the usual 120˚ with reported angles of 125.70(13)˚, 125.25(13)˚ and 125.07(13)˚ for molecule A, B and C, respectively, possibly due to the methyl (C8) substituent's steric influence.

Table 5.5: Selected bond distances [Å] and bond and torsion angles [°] for 2-(methylamino)tropone.

	Selected bond distances [Å]		
	Molecule A	**Molecule B**	**Molecule C**
C8-N1	1.4518(19)	1.4474(18)	1.4492(18)
N1-C2	1.3370(18)	1.3446(18)	1.3424(17)
O1-C1	1.2521(17)	1.2564(16)	1.2540(16)
	Selected bond angles [°]		
C2-N1-C8	125.70(13)	125.25(13)	125.07(13)
O1-C1-C7	119.84(14)	119.87(12)	119.73(12)
O1-C1-C2	116.31(12)	116.38(12)	116.84(12)
N1-C2-C3	120.90(13)	121.28(13)	120.27(12)
N1-C2-C1	112.24(12)	112.31(11)	112.83(11)
	Selected torsion angles [°]		
C8-N1-C2-C3	-0.8(2)	2.3(2)	7.7(2)
O1-C1-C2-N1	1.89(17)	4.67(17)	-7.19(17)

[32] Barret, M., Bhatia, P., Kociok-Köhn, G. & Molloy, K. (2014). *Transition Metal Chemistry*, **39**(5), 543-551.

[33] Shimanouchi, H. & Sasada, Y. (1973). *Acta Crystallographica Section B,* B**29**, 81-90.

[34] Dwivedi, A. D., Binnani, C., Tyagi, D., Rawat, K. S., Li, P., Zhao, Y., Mobin, S. M., Pathak, B. & Singh, S. K. (2016). *Inorganic Chemistry*, **55**(13), 6739-6749.

[35] Siwatch, R., Kundu, S., Kumar, D. & Nagendran, S. (2011). *Organometallics*, **30**(7), 1998-2005.

The torsion angles (C8-N1-C2-C3 and O1-C1-C2-N1) seem to differ among the three molecules. This is observed especially in molecule C with reported torsion angles of -0.8(2), 2.3(2) and 7.7(2) for C8-N1-C2-C3 and 1.89(17), 4.67(17) and -7.19(17) for O1-C1-C2-N1 in molecule A, B and C respectively. A plane fitted through the seven ring carbons (C1-C2-C3-C4-C5-C6-C7) of the three molecules in the asymmetric unit indicates that the molecules are almost planar with root-mean-square deviations from the planes of 0.0141(12), 0.0261(11) and 0.0345(11) Å, for molecules A, B and C respectively. The small deviations from planarity and the difference in the torsion angles could possibly be ascribed to the intermolecular hydrogen bonding interactions. The almost planar seven-membered aromatic ring of similar ligands have proved to contribute to the stability of the complex formed with transition metals.[34]

Six intramolecular and three intermolecular hydrogen bonding interactions, three C-H…O and six N-H…O, are observed in the structure of TropNHMe and are illustrated in Figure 5.9. Bifurcation of the interactions are also observed, with some branches being intramolecular and some intermolecular, forming hydrogen-bonded pairs of molecules A and B which increases the stability of the structure. This same phenomenon (bonded pairs) is described for the crystal structure of the starting material, tropolone, by Shimanouchi and Sasada (1973). In the structure of TropNHMe, some of the hydrogen bonding interactions link molecules together to form infinite chains with base vector [0 0 1]. The interactions clearly contribute to the way in which the molecules arrange themselves in the unit cell. The two hydrogen bonding interactions to the carbonyl oxygen (O1) could enhance the polarization $>C^{\delta+}\text{-}O^{\delta-}$. The contact distances and angles of the hydrogen bonding interactions are presented in Table 5.6.

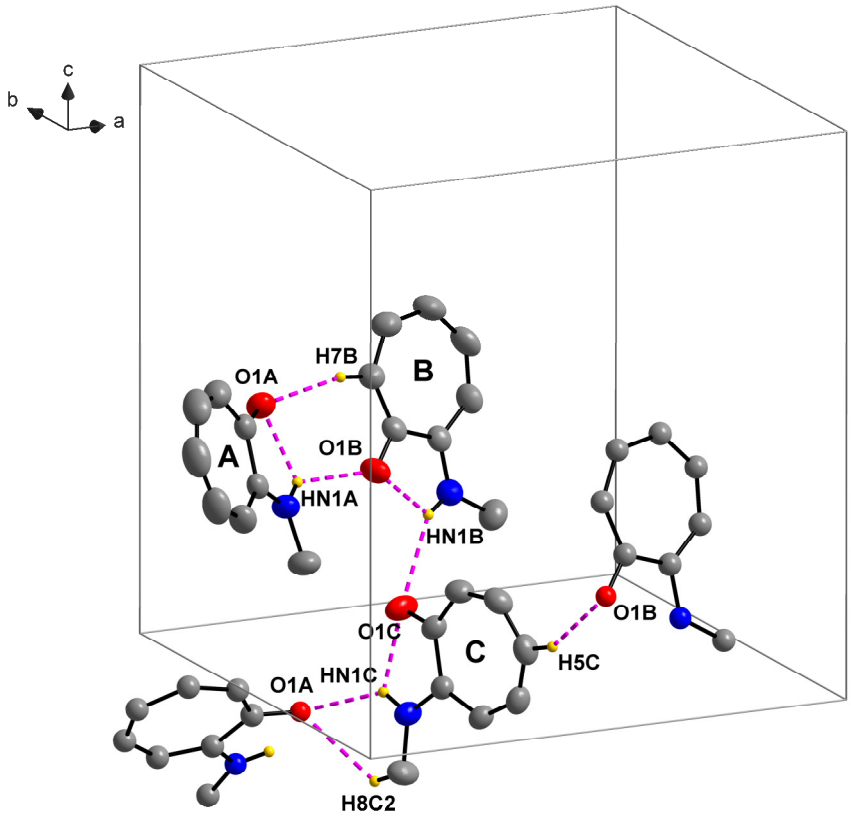

Figure 5.9: Hydrogen bonding interactions (indicated in pink dashed lines) observed in the structure of TropNHMe. Some hydrogen atoms are omitted for clarity.

Table 5.6: Summary of the hydrogen bonding interactions observed in the structure of 2-(methylamino)tropone [Å and °].

D-H...A	d(D-H)	d(H...A)	d(D...A)	<(DHA)
N1A-HN1A...O1A	0.880(18)	2.099(17)	2.5455(16)	110.6(13)
N1A-HN1A...O1B	0.880(18)	2.254(17)	2.9376(17)	134.4(15)
N1B-HN1B...O1B	0.893(15)	2.087(15)	2.5513(16)	111.4(12)
N1B-HN1B...O1C	0.893(15)	2.384(16)	3.1560(18)	144.8(13)
N1C-HN1C...O1C	0.891(16)	2.132(16)	2.5776(16)	110.1(13)
N1C-HN1C...O1A[1]	0.891(16)	2.310(16)	2.9759(17)	131.4(13)
C5C-H5C...O1B[2]	0.95	2.42	3.2914(19)	152.8
C8C-H8C...O1A[1]	0.98	2.56	3.178(2)	120.7
C7B-H7B...O1A	0.95	2.42	3.3441(19)	164.5

Symmetry transformations used to generate equivalent atoms:

[1] x, -y+3/2, z-1/2 [2] x, y-1, z

One π-π interaction is observed in the structure of TropNHMe (Figure 5.10), with a centroid to centroid distance of 3.4462(19) Å between the overlapping aromatic rings of two inversion-related B molecules (1-x, 1-y, 1-z). The molecules pack diagonally in a head-to-tail fashion across the ac plane with the aromatic rings overlapping, forming stacked 'columns' when viewed along the b-axis. The C molecules in each asymmetric unit pack in an almost perpendicular direction to the A and B molecules (Figure 5.11).

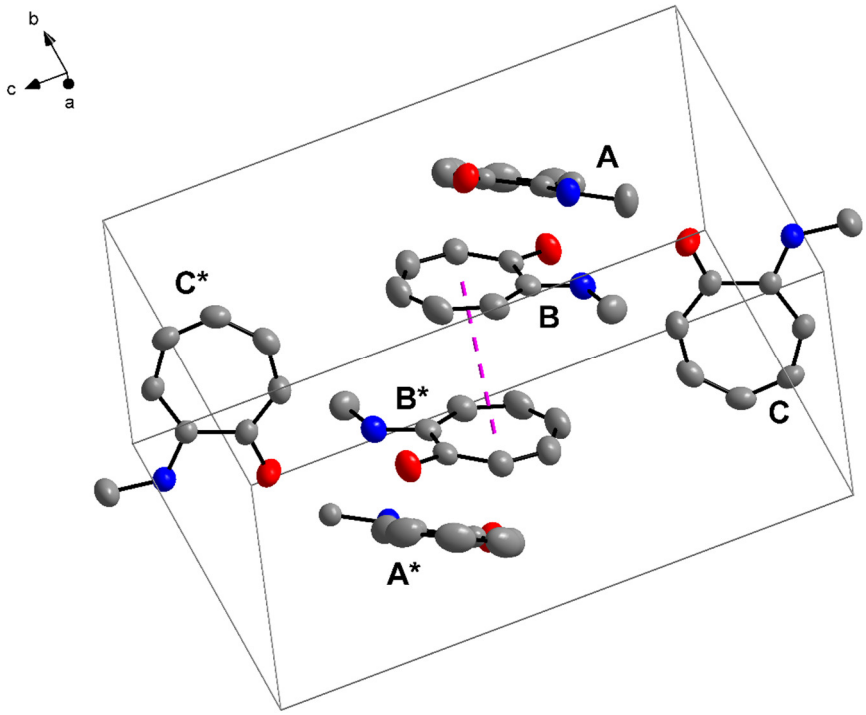

Figure 5.10: A π-π interaction (indicated by the pink dashed line) observed in the structure of TropNHMe between overlapping aromatic rings of molecule B, where B and B* are related through inversion. Hydrogen atoms are omitted for clarity.

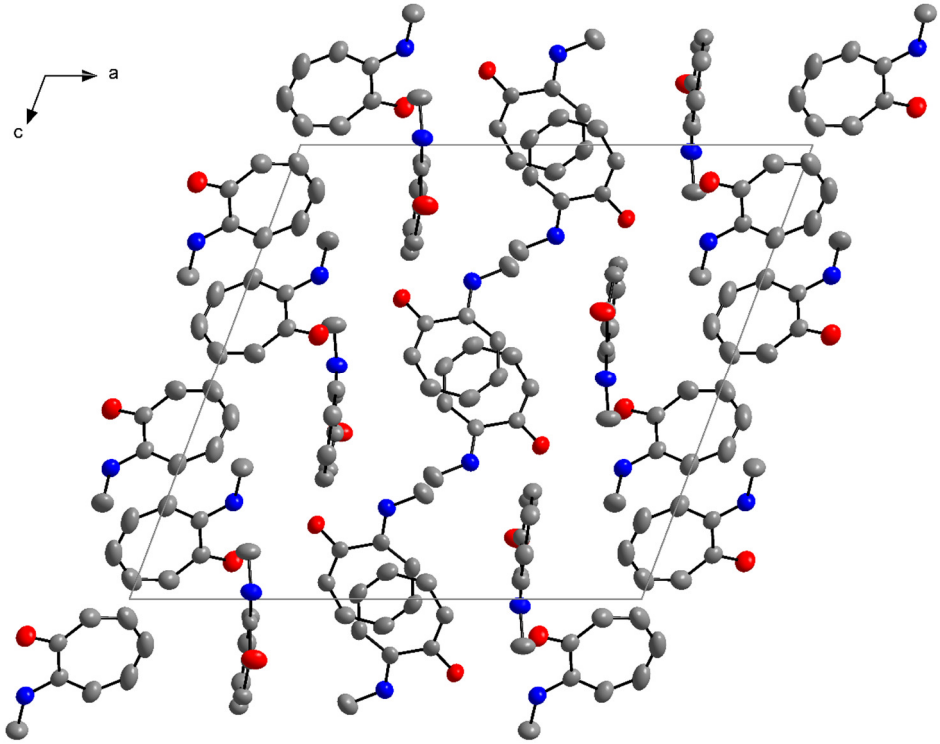

Figure 5.11: Packing of TropNHMe in the unit cell when viewed along the ac plane. Hydrogen atoms are omitted for clarity.

5.5 Crystal structure of 2-(2-fluoroethylamino)tropone (TropNHEtF)

5.5.1 Introduction

2-(2-Fluoroethylamino)tropone was synthesized according to the procedure reported in Paragraph 4.3.2.3. Yellow crystals suitable for single crystal XRD were obtained from pentane at -21 ˚C. The general crystal data is summarized in Table 5.2 and Figure 5.12 illustrates the molecular diagram and numbering scheme of the structure. Selected bond distances and bond and torsion angles are presented in Table 5.7. In Paragraph 5.5.2 the structural and supramolecular features of TropNHEtF will be discussed. Atomic coordinates, anisotropic displacement parameters, all bond distances and angles and hydrogen coordinates are given in the supplementary data (Appendix C, Tables C.1 - C.6).

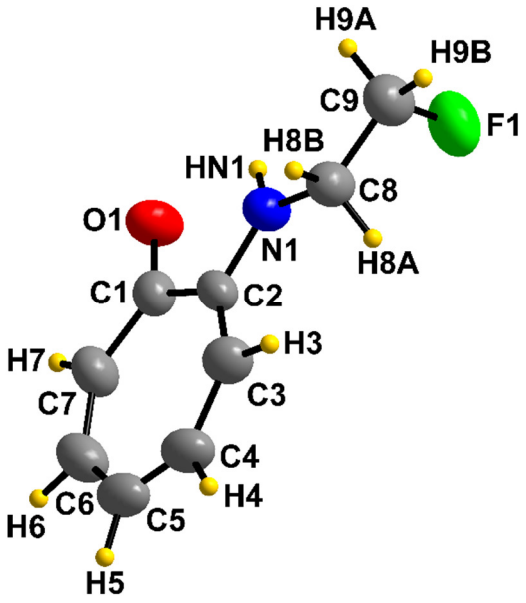

Figure 5.12: Molecular representation of 2-(2-fluoroethylamino)tropone indicating the numbering scheme with ellipsoids drawn at 50 % probability level.

5.5.2 Results and discussion

2-(2-Fluoroethylamino)tropone crystallized in the $P2_1/n$ space group with one molecule in the asymmetric unit. The selected bond distances and angles of TropNHEtF are within normal range for structures of this type and agree with those of similar compounds such as 2-(benzylamino)tropone,[32] 2-(isopropylamino)tropone,[11] tropolone,[33] 2-(cyclohexylamino)tropone,[34] 2-(*t*-butylamino)tropone[35] and 2-(methylamino)tropone[31] reported in literature. The trigonal geometry surrounding both the O1 and N1 atoms contain bond angles close to 120˚ as expected. The C2-N1-C8 bond angles of the abovementioned 2-(alkylamino)tropones of 125.09(12)˚,[32] 127.6(3)˚,[11] 128.62(13)˚,[34] 131.9(2)˚,[35] and 125.34(13)˚,[31] respectively, differ due to the steric influences of the various alkyl substituents on N1. The torsion angles of TropNHEtF are small and indicate no significant deviation from planarity with the root-mean-square deviation of the seven-membered ring system from the plane being 0.0079 Å.

Table 5.7: Selected bond distances [Å] and bond and torsion angles [°] for 2-(2-fluoroethylamino)tropone.

Selected bond distances [Å]	
C1-O1	1.248(4)
C2-N1	1.342(4)
C8-N1	1.439(4)
Selected bond angles [°]	
O1-C1-C7	119.8(3)
O1-C1-C2	116.8(3)
N1-C2-C3	121.3(3)
N1-C2-C1	112.3(3)
C2-N1-C8	125.3(3)
Selected torsion angles [°]	
O1-C1-C2-N1	-1.0(4)
C3-C2-N1-C8	-2.7(5)

Three hydrogen bonding interactions, two N-H…O and one C-H…O are observed in the structure of TropNHEtF with the interactions on the O1 atom being bifurcated. This contributes to the alignment of the molecules towards each other to form pairs as illustrated in Figure 5.13. The contact distances and angles are presented in Table 5.8.

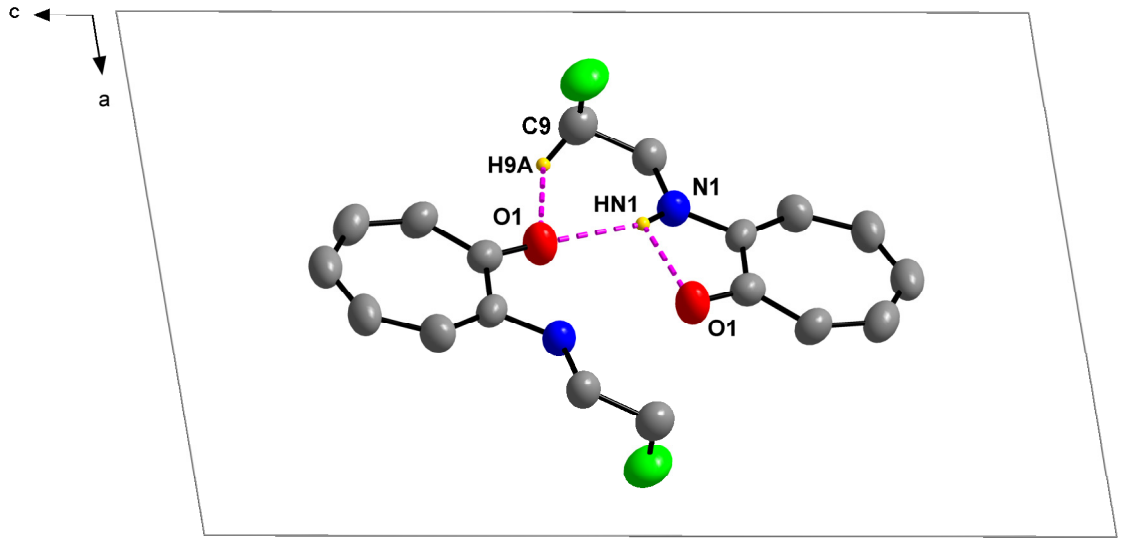

Figure 5.13: Hydrogen bonding interactions observed in 2-(2-fluoroethylamino)tropone when viewed along the b-axis. Hydrogen atoms not part of hydrogen bonding interactions are omitted for clarity.

Table 5.8: Summary of hydrogen bonding interactions for 2-(2-fluoroethylamino)tropone [Å and °].

D-H...A	d(D-H)	d(H...A)	d(D...A)	<(DHA)
N1-HN1...O1	0.94(3)	2.05(3)	2.552(4)	112(2)
N1-HN1...O1[1]	0.94(3)	2.14(3)	3.027(4)	156(3)
C9-H9B...O1[1]	0.99	2.55	3.236(5)	126.4

Symmetry transformations used to generate equivalent atoms:

[1] -x+1, -y, -z+1

The molecules in the unit cell pack diagonally in a head-to-tail manner in alternating directions when viewed along the ac plane and is illustrated in Figure 5.14. No ring overlap or π-interactions are observed in the structure of TropNHEtF.

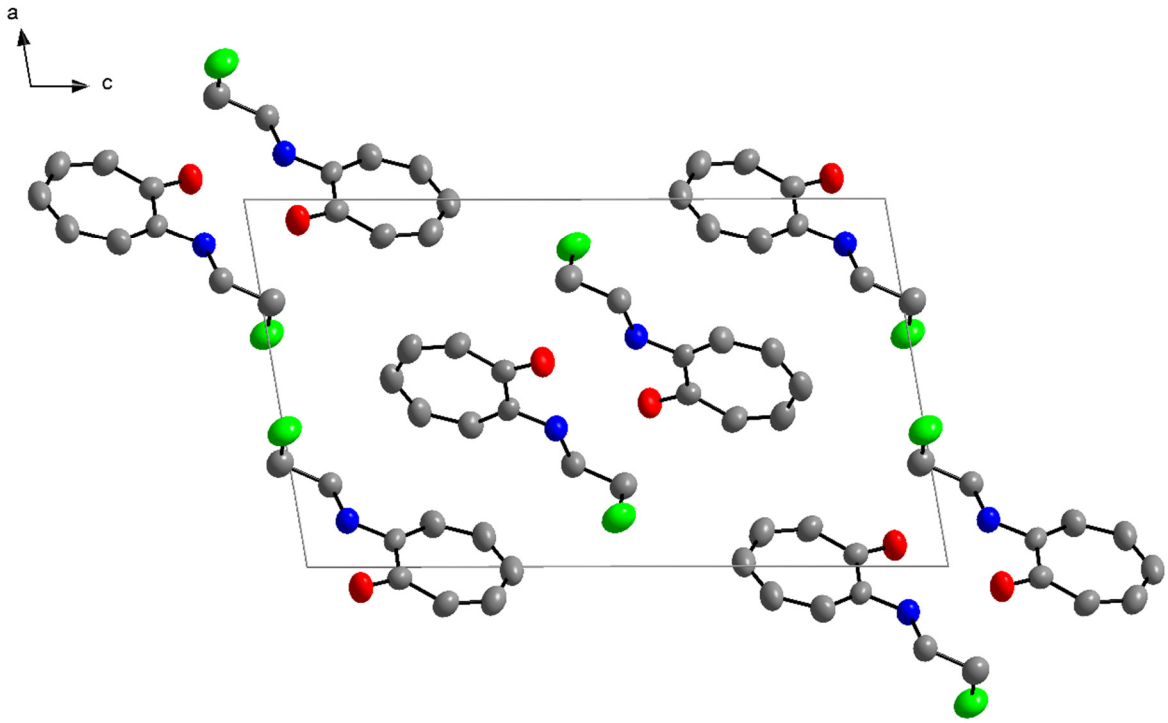

Figure 5.14: Packing of molecules of TropNHEtF in the unit cell when viewed along the ac plane with hydrogen atoms omitted for clarity.

5.6 Conclusion

The structures of TropOTs, TropNHMe and TropNHEtF all show interesting packing patterns in their unit cells. TropNHMe has three molecules in its asymmetric unit where TropOTs and TropNHEtF have only one. In all three structures hydrogen bonding interactions are observed, but only in TropNHMe do these interactions form one-dimensional infinite chains. TropNHEtF is the only structure not displaying π-π interactions, with hydrogen bonding interactions possibly leading to the packing pattern observed in the unit cell.

The solid-state crystal structures of the abovementioned three molecules were successfully determined and evaluated. The results of the cytotoxicity evaluations will be discussed in the next chapter.

6
CYTOTOXICITY

6.1 Introduction

Cytotoxicity is the ability of a chemical compound to damage a living tissue cell and consequently inhibit cell growth or induce cell death.[1] Evaluation of the cytotoxicity and mechanism of action of organic molecules or metal complexes is an important step when investigating it as possible medicinal agents, especially in chemotherapy and photodynamic therapy. Various *in vitro* cytotoxicity and cell viability assays are used for testing chemicals and for drug screening because it is simple, fast and has a high sensitivity.[1,2,3]

The methods of cytotoxicity assays are mainly based on the evaluation of healthy and damaged cells after chemicals of a certain concentration had been administered for a specific period. Cell growth, reproduction and the morphological effects of the chemical compounds on the cells are then observed.[3] Evaluation of drug-induced cytotoxicity are performed on various cancer cell lines such as an estrogen receptor-positive breast cancer (MCF7), non-small cell lung cancer (A549) and human cervical adenocarcinoma (HeLa) cells to investigate the specificity of the compound to certain types of cancers.[4,5] In some studies, healthy human cells such as retinal pigment epithelial (RPE-1) cells are also used to determine the extent of the damage on normal cells and in this way predict possible side effects.[5] A cytotoxic evaluation is also important in determining the cytotoxicity of possible photosensitizers (PS) in photodynamic therapy (PDT),[6] which is a form of treatment where a non-toxic drug or dye known as a photosensitizer (PS) is administered. When the specific tumor

[1] Aslantürk, Ö. (2018). *Genotoxicity - A Predictable Risk to Our Actual World*. doi: 10.5772/intechopen.71923
[2] Riss, T. & Moravec, R. (2004). *ASSAY and Drug Development Technologies*, **2**(1), 51-62.
[3] Li, W., Zhou, J. & Xu, Y. (2015). *Biomedical Reports*, **3**(5), 617-620.
[4] Hynds, R., Vladimirou, E. & Janes, S. (2018). *Disease Models and Mechanisms*, **11**(11), dmm037366.
[5] Kamao, H., Miki, A. & Kiryu, J. (2019). *Journal of Ophthalmology*, **2019**, 1-10.
[6] Robertson, C., Evans, D. & Abrahamse, H. (2009). *Journal of Photochemistry and Photobiology B: Biology*, **96**(1), 1-8.

site is irradiated with red visible light (620-690 nm), cytotoxic species are generated in the presence of oxygen and this leads to cell destruction.[6]

The cytotoxicity of different compounds could be compared by their half maximal inhibitory concentration (IC_{50}) values. The IC_{50} value is a quantitative measure of the molar (M) concentration at which a compound inhibits a specific biological or biochemical process *in vitro* by 50 %.[7]

In a recent study by Gantsho *et al*.[8] the cytotoxicity of four Re(I) tricarbonyl compounds containing tropolone as an O,O' bidentate ligand was evaluated. The results proved the selective nature of these compounds towards cancerous cells.[8] When tested against HeLa cells all except one compound proved to have anticancer activity. Two of the compounds had IC_{50} values comparable to those of cisplatin, the positive control in the study. The toxicity towards RPE-1 cells were only slightly lower. One compound had an IC_{50} value higher than 100 μM against HeLa and RPE-1 cell lines, while another compound was much less toxic towards the non-cancerous (RPE-1) cells compared to HeLa cells.[8] These results suggest the diversity and versatility of these type of compounds, depending on certain ligand systems; the Re(I) tricarbonyl compounds containing tropolone-derivatives as ligands are therefore interesting compounds to conduct cytotoxicity evaluations on.

[7] Stewart, M. & Watson, I. (1983). *British Journal of Clinical Pharmacology*, **16**(1), 3-7.
[8] Gantsho, V., Dotou, M., Jakubaszek, M., Goud, B., Gasser, G., Visser, H. & Schutte-Smith, M. (2020). *Dalton Transactions*, **49**(1), 35-46.

6.2 *In vitro* testing of synthesized ligands and compounds

In this study the cytotoxicity of five (2-alkylamino)tropone ligands (*N,O*), nine aminotroponimine ligands (*N,N'*) and four *fac*-Re(I) tricarbonyl complexes were evaluated. The structures of these compounds are presented in Figure 6.1 and the synthetic procedures of these compounds are reported in Chapter 4.

***N,O* bidentate ligands - (2-alkylamino)tropones:**

- 2-(Methylamino)tropone (TropNHMe)
- 2-(Ethylamino)tropone (TropNHEt)
- 2-(2-Fluoroethylamino)tropone (TropNHEtF)
- 2-(Benzylamino)tropone (TropNHBn)
- 2-(Phenethylamino)tropone (TropNHEtPh)

***N,N'* bidentate ligands - aminotroponimines:**

- *N*-Methyl-2-(methylamino)troponimine ([$(Me)_2$ATI]H)
- *N*-Ethyl-2-(ethylamino)troponimine ([$(Et)_2$ATI]H)
- *N*-2-Fluoroethyl-2-(2-fluoroethylamino)troponimine ([$(EtF)_2$ATI]H)
- *N*-Phenethyl-2-(phenethylamino)troponimine ([$(EtPh)_2$ATI]H)
- *N*-Benzyl-2-(benzylamino)troponimine ([$(Bn)_2$ATI]H)
- *N*-Methyl-2-(benzylamino)troponimine ([(Me,Bn)ATI]H)
- *N*-Ethyl-2-(benzylamino)troponimine ([(Et,Bn)ATI]H)
- *N*-2-Fluoroethyl-2-(benzylamino)troponimine ([(EtF,Bn)ATI]H)
- *N*-Phenethyl-2-(benzylamino)troponimine ([(EtPh,Bn)ATI]H)

***fac*-Re(I) tricarbonyl complexes:**

- *fac*-[$Re(CO)_3(H_2O)$(TropNMe)]
- *fac*-[$Re(CO)_3(H_2O)$(TropNEt)]
- *fac*-[$Re(CO)_3(H_2O)$(TropNEtF)]
- *fac*-[$Re(CO)_3(H_2O)$(TropNBn)]

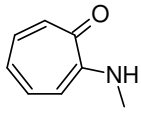

TropNHMe

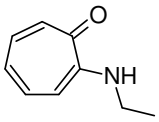

TropNHEt

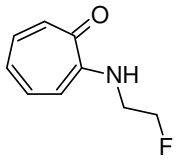

TropNHEtF

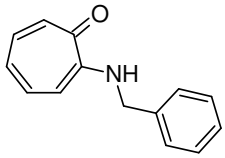

TropNHBn

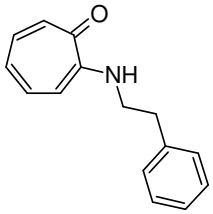

TropNHEtPh

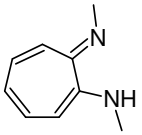

[(Me)$_2$ATI]H

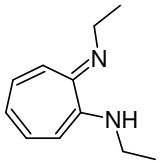

[(Et)$_2$ATI]H

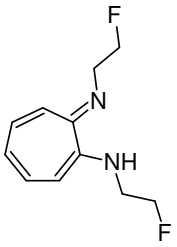

[(EtF)$_2$ATI]H

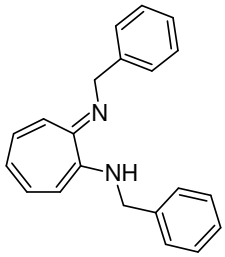

[(Bn)$_2$ATI]H

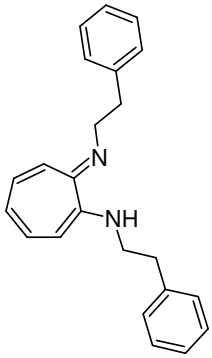

[(EtPh)$_2$ATI]H

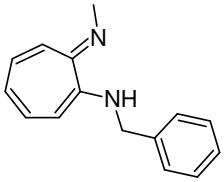

[(Me,Bn)ATI]H

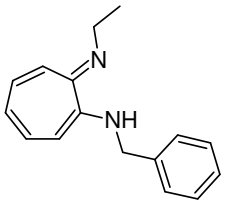

[(Et,Bn)ATI]H

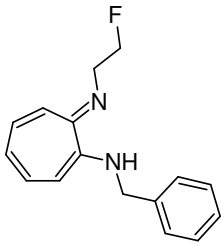

[(EtF,Bn)ATI]H

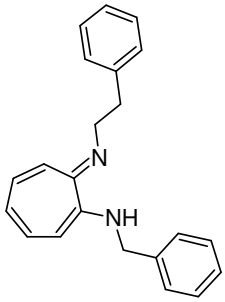

[(EtPh,Bn)ATI]H

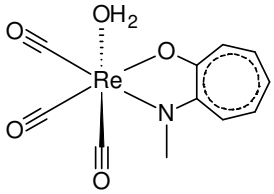

***fac*-[Re(CO)$_3$(H$_2$O)(TropNMe)]**

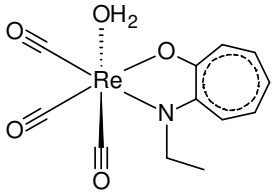

***fac*-[Re(CO)$_3$(H$_2$O)(TropNEt)]**

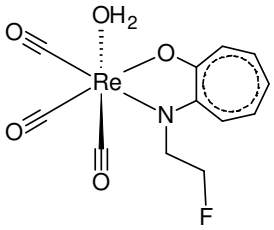

***fac*-[Re(CO)$_3$(H$_2$O)(TropNEtF)]**

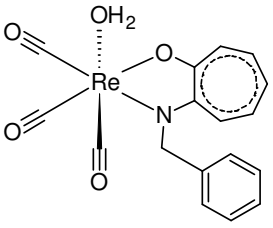

***fac*-[Re(CO)$_3$(H$_2$O)(TropNBn)]**

Figure 6.1: The chemical structures of the ligand systems and compounds evaluated for its anticancer activity.

These ligands and complexes were tested against HeLa cells and its IC_{50} values were calculated.

6.3 Experimental procedure

6.3.1 Cell culture

HeLa cells (human cervical cancer cell line) were cultured in Dulbecco's modified eagle medium (DMEM) supplemented with 10 % fetal calf serum and 1 % penicillin/streptomycin. The cells were incubated at 37.0 ˚C in a humid atmosphere with 5 % carbon dioxide (CO_2).

6.3.2 Cytotoxicity assay

The sulforhodamine B (SRB) assay was used to perform the tests.[9] Monolayer cells were dissociated using trypsin and suspended in 1 mL growth medium. The cell count was altered to 0.5 x 10^5 mL and 0.1 mL dilute cell suspension was added to each well of a 96 well microplate. The cells were allowed to adhere to the plate during a one-hour incubation period. To each well was added 0.1 mL of the ligand solutions with concentrations ranging from 0.01 µM to 100 µM. The plates were incubated at 37.0 ˚C for 7 days in a 5 % CO_2 atmosphere. A 50 % trichloroacetic acid solution (0.05 mL) was added to each well and the plates were incubated overnight at 4 ˚C. The plates were rinsed under running tap water and dried for one hour at 50 ˚C. To each well was added SRB stain (0.1 mL) and the plates were stored in the dark for one hour. The plates were washed four times with a 1 % acetic acid solution (0.1 mL) and dried again. The dyes were solubilized by the addition of 0.1 mL of a 10 mM tris(hydroxymethyl) aminomethane solution (Tris buffer) to each of the wells. The plates were gently shaken for one hour and the optical density measured at 510 nm. The growth inhibition of the ligands was determined as a percentage of the optical density of the control group. IC_{50} values were calculated by ANOVA with Dunnett's post-test using GraphPad Prism[10] and the data was fitted to a nonlinear regression against a normalized response.

[9] Vichai, V. & Kirtikara, K. (2006). *Nature Protocols*, **1**(3), 1112-1116.
[10] GraphPad Prism version 5.00 for Windows, GraphPad Software, San Diego, California, USA.

6.4 Results and discussion

The *in vitro* cytotoxicity evaluation of the fourteen ligands and four complexes yielded the following IC_{50} values (Table 6.1 and Figure 6.2) in μM concentration:

Table 6.1: The IC_{50} values of ligands and complexes tested against HeLa cells.

Compound	IC_{50} (μM)*
***N,O* bidentate ligands**	
TropNHBn	19.8
TropNHEtF	21.2
TropNHMe	24.5
TropNHEtPh	27.6
TropNHEt	36.1
***N,N'* bidentate ligands**	
[(EtPh,Bn)ATI]H	0.45
[(Me,Bn)ATI]H	0.66
[(Et,Bn)ATI]H	1.10
$[(EtPh)_2ATI]H$	2.4
$[(Bn)_2ATI]H$	7.4
$[(Et)_2ATI]H$	17.2
[(EtF,Bn)ATI]H	18.2
$[(EtF)_2ATI]H$	33.8
$[(Me)_2ATI]H$	35.9
Re(I) tricarbonyl complexes	
fac-$[Re(CO)_3(H_2O)(TropNMe)]$	47.0
fac-$[Re(CO)_3(H_2O)(TropNEt)]$	52.1
fac-$[Re(CO)_3(H_2O)(TropNBn)]$	73.2
fac-$[Re(CO)_3(H_2O)(TropNEtF)]$	77.4
Cisplatin (positive control)	
Cisplatin	3.26

*The IC_{50} values presented in the table are the average values of the results of the tests done in triplicate.

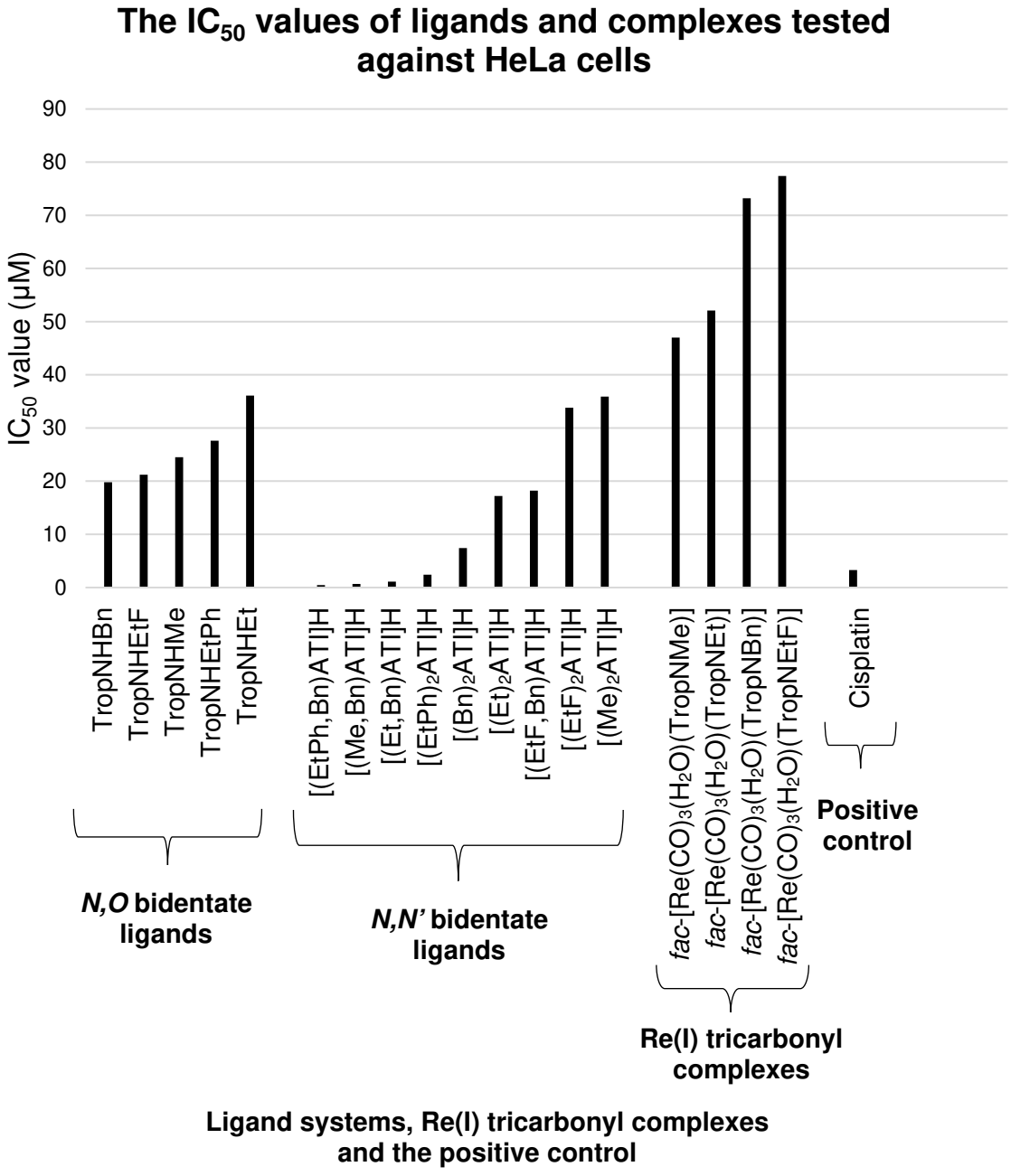

Figure 6.2: The IC_{50} values of the ligand systems, Re(I) tricarbonyl complexes and a positive control, cisplatin.

The IC_{50} values of the *N,N'* bidentate ligands proved to be generally lower than that of the *N,O* bidentate ligands except for $[(Me)_2ATI]H$ and $[(EtF)_2ATI]H$. Four of the *N,N'* bidentate ligands are even more cytotoxic than cisplatin which was used as the control in all of the tests; [(EtPh,Bn)ATI]H, [(Me,Bn)ATI]H, [(Et,Bn)ATI]H and $[(EtPh)_2ATI]H$ yielded IC_{50} values of 0.45, 0.66, 1.10 and 2.4 μM respectively with cisplatin having an IC_{50} value of 3.26 μM. The chemical structures of these ligands are presented in Figure 6.3. It is interesting to note that the compounds with two of

the same substituents appear to be less toxic than those where different substituents are combined. An especially interesting observation is that the IC_{50} values of $[(Bn)_2ATI]H$ and $[(EtPh)_2ATI]H$, although both very low, are higher than that of the compound with a combination of the two phenyl substituents, [(EtPh,Bn)ATI]H. These ligands only differ in the chain lengths of the *N*-subsituents.

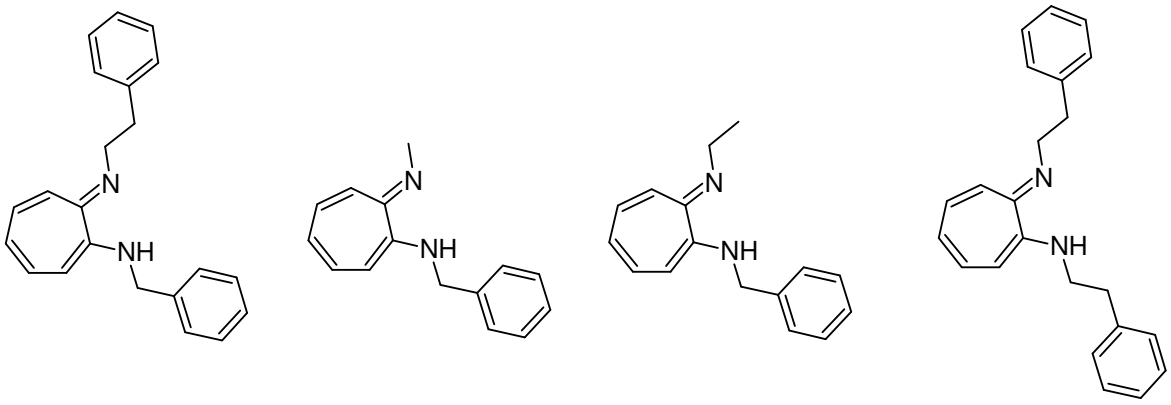

[(EtPh,Bn)ATI]H **0.45 μM** | **[(Me,Bn)ATI]H** **0.66 μM** | **[(Et,Bn)ATI]H** **1.10 μM** | **$[(EtPh)_2ATI]H$** **2.4 μM**

Figure 6.3: The chemical structures of the four ligands, [(EtPh,Bn)ATI]H, [(Me,Bn)ATI]H, [(Et,Bn)ATI]H and $[(EtPh)_2ATI]H$, with IC_{50} values lower than that of cisplatin.

The *fac*-Re(I) tricarbonyl complexes of four of the *N,O* bidentate ligands are soluble in dimethyl sulfoxide and exhibited much lower cytotoxicity than their corresponding ligands, with higher IC_{50} values of 47.0, 52.1, 73.2 and 77.4 μM compared to the ligands' 24.5, 36.1, 19.8 and 21.2 μM, respectively. A phenomenon like this was also observed by Carreño and co-workers[11] in their study with *N,N'* bidentate ligands such as bipyridine coordinated to the *fac*-Re(I) tricarbonyl core. The ancillary ligand as well as the cell model tested have an effect on the cytotoxicity of these compounds. The decreased cytotoxicity of the compounds compared to the ligands is a desired trait for imaging and photoluminescent purposes.[11]

El-Boraey and El-Gammal synthesized a novel tetraamide (N_4) macrocyclic 15-membered ligand, naphthyl-dibenzo[1,5,9,12]tetraazacyclopen-tadecine-6,10,11,15-tetraone and its Fe(II), Co(II), Ni(II), Cu(II), Ru(III) and Pd(II) transition

[11] Carreño, A., Solís-Céspedes, E., Zúñiga, C., Nevermann, J., Rivera-Zaldívar, M. M., Gacitúa, M., Ramírez-Osorio, A., Páez-Hernández, D., Arratia-Pérez, R. & Fuentes, J. A. (2019). *Chemical Physics Letters*, **715**, 231-238.

metal complexes.[12] The ligand and its metal complexes were evaluated for their anticancer activity against human breast cancer cell lines (MCF-7) and human hepatocarcinoma (HepG2) cells. The ligand showed moderate anticancer activity with IC_{50} values of 13 μM against MCF-7 and 26 μM against HepG2 cells. Five complexes, one of each metal species showed excellent cytotoxicity against MCF-7 cells with IC_{50} values of 2.27 - 2.7 μM. Their cytotoxicity varied against the HepG2 cells with IC_{50} values of 8.33, 24.5, 30.5 and 31.1 μM for the Fe(II), Cu(II), Ru(III) and Pd(II) complexes, respectively. The Ni(II) complex showed no activity against the HepG2 cells. Contradicting the study of Carreño *et al*., these results suggest that the cytotoxic activity can be enhanced upon coordination of a ligand to a metal center. This improvement may be ascribed to the increase in conjugation in the ligand moiety on complexation.[12,13]

6.6 Conclusion

All the synthesized ligands show good cytotoxic activity against HeLa cells and the four Re(I) complexes yielded IC_{50} values higher than those of their corresponding ligands, but still lower than 100 μM. A few of the aminotroponimine ligands exhibited extremely low IC_{50} values which creates an opportunity for further evaluation of these specific ligands as well as their complexes which have not yet been evaluated.

Unfortunately, not all the Re(I) tricarbonyl complexes could be tested in this project due to time constraints. The ligands and compounds were not tested against normal cells or other cancer cell lines as the on-site lab only has HeLa cells available for testing. Although some compounds prove to have possible anticancer properties, further conclusions can only be made when the toxicity to normal cells are known. This will form part of future investigations of these ligand systems and compounds.

The novel ligands synthesized in this study namely TropNHEtF, TropNHEtPh, [(EtPh,Bn)ATI]H, [(Me,Bn)ATI]H, [(Et,Bn)ATI]H, [(EtF,Bn)ATI]H, $[(EtPh)_2ATI]H$ and $[(EtF)_2ATI]H$ yielded excellent IC_{50} values and will be explored further. These results are one of the major successes of this study.

[12] El-Boraey, H. & El-Gammal, O. (2015). *Spectrochimica Acta Part A: Molecular and Biomolecular Spectroscopy*, **138**, 553-562.
[13] Atta, E., Hegab, K., Abdelgawad, A. & Youssef, A. (2019). *Saudi Pharmaceutical Journal*, **27**(4), 584-592.

7
PHOTOLUMINESCENCE

7.1 Introduction

Photoluminescence can shortly be described as a process in which a molecule absorbs a photon in the visible region, exciting one of its electrons to a higher electronic energy state, after which it emits a photon as it returns to a lower energy state.[1]

The activation of prodrugs by light is an important part of oncological research and can be divided into two categories:[2]

- Photoactivated chemotherapy (PACT)
- Photodynamic therapy (PDT)

PACT allows for better control over when and where a drug is activated. This treatment method uses a chemotherapeutic agent with no biological activity and low toxicity which only becomes activated once exposed to light of a specific wavelength.[3,4] PACT uses different mechanisms to activate the compound and consequently induce cell death, such as ligand ejection, DNA crosslinking and caging techniques.[2,3,4]

PDT is a modern, minimally toxic and non-invasive treatment method for cancer and other diseases. PDT uses a photosensitizer and light of a specific wavelength. The photosensitizer in the form of a drug becomes light activated and reacts with molecular oxygen to produce reactive oxygen species (ROS) and radicals.[2,5] The ROS and radicals are toxic species that can interact with cell components to biochemically disrupt the cell, eventually destroying it. Photoluminescence is responsible for the generation of the toxic reactive oxygen species (ROS) called

[1] Atkins, P. & De Paula, J. (2010). *Physical Chemistry* (9th ed.). Oxford: Oxford University Press.
[2] Mari, C., Pierroz, V., Ferrari, S. & Gasser, G. (2015). *Chemical Science*, **6**(5), 2660-2686.
[3] Farrer, N., Salassa, L. & Sadler, P. (2009). *Dalton Transactions*, (48), 10690-10701.
[4] Bonnet, S. (2018). *Dalton Transactions*, **47**(31), 10330-10343.
[5] Josefsen, L. & Boyle, R. (2008). *Metal-Based Drugs*, **2008**, 1-23.

singlet oxygen ($^1O_2$) in PDT.[2,5] Examples of PDT agents currently in use are Photofrin®, Foscan®, Lutex®, Tookad®, Purlytin®, Visudyne® and Laserphyrin®.[6]

Photoluminescence is also very important in cell imaging, where the generally used fluorescent probes are organic dyes which present various limitations, leading to investigations towards alternative types of fluorescent probes, especially those with versatile metal cores.[7,8]

7.2 Experimental

The ligands and complexes were synthesized according to the procedures discussed in Chapter 4. The UV/Vis measurements in this study were conducted on a Varian Cary 50 Conc. Spectrometer, equipped with a Julabo F12-mV temperature cell regulator accurate within 0.1 ˚C. A 1.000(1) cm tandem quartz cuvette was used for the absorbance spectra measurements. The solvent used for the UV/Vis absorbance measurements was liquid chromatography grade chloroform ($CHCl_3$). An Edinburgh Instruments FLS980 series Fluorescence Spectrometer was used to conduct photoluminescence measurements. The samples were excited with a continuous xenon lamp (Xe1) with a 450W arc lamp light source. The single photon counting technique was used to acquire the data. The luminescence was measured in solution using a 1.000(1) cm quartz cuvette with solvent correction scans taken at each excitation wavelength. The solvent used for the photoluminescence measurements was liquid chromatography grade chloroform ($CHCl_3$).

7.3 Results and discussion

The photoluminescence (PL) studies yielded results that are presented in Figure 7.1 - 7.17 below. In each graph the excitation (blue) and emission (orange) spectra are shown for the ligands and the compounds. The emission spectra (green) of the solvent, chloroform, is also included in each graph and its emission is regarded as negligible.

---

[6] Baskaran, R., Lee, J. & Yang, S. (2018). *Biomaterials Research*, **22**(1). doi: 10.1186/s40824-018-0140-z

[7] Yang, Y., Zhao, Q., Feng, W. & Li, F. (2013). *Chemical Reviews*, **113**(1), 192-270.

[8] Kuil, J., Steunenberg, P., Chin, P. T. K., Oldenburg, K., Jalink, J., Velders, A. & van Leeuwen, F. W. B. (2011). *ChemBioChem*, **12**, 1897-1903.

7.3.1 Analysis of 2-(alkylamino)tropone ligands and its Re(I) tricarbonyl complexes

The excitation and emission spectra of the synthesized *N,O* bidentate ligands and its Re(I) tricarbonyl complexes are reported in this section.

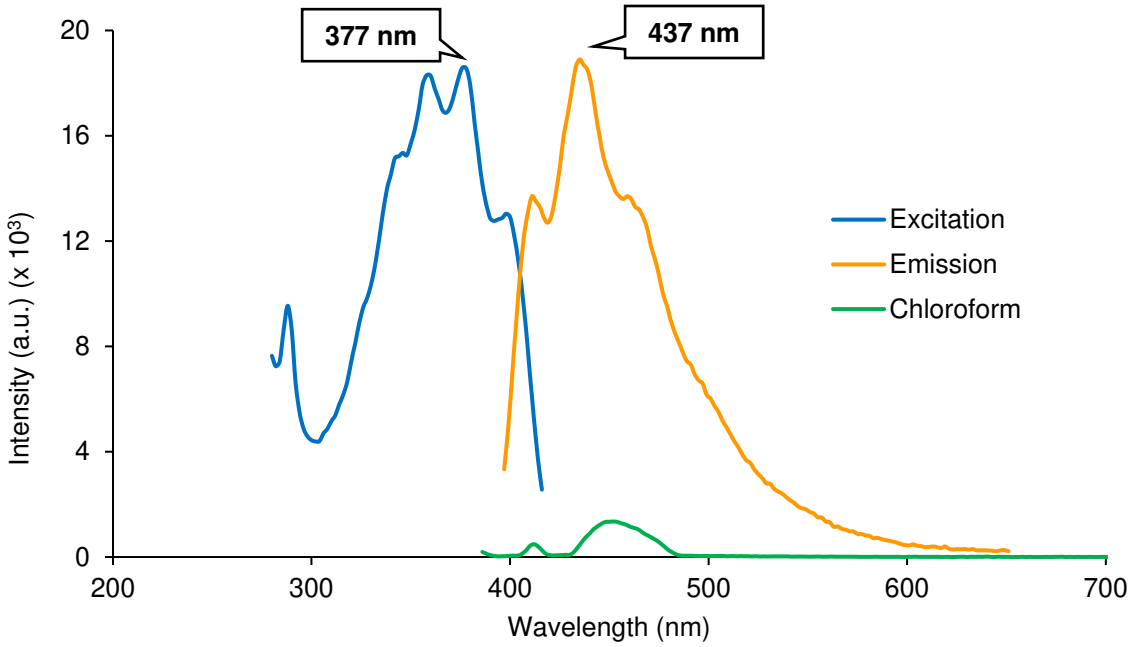

Figure 7.1: The excitation and emission spectra of 2-(methylamino)tropone (1.0×10^{-5} M) in chloroform.

2-(Methylamino)tropone (TropNHMe) exhibits multiple excitation wavelengths in solution and is called a multi-emitter. The most prominent excitation peak is at 377 nm and the corresponding maximum emission peak at 437 nm as illustrated in Figure 7.1. The emission spectrum between 390 and 700 nm indicated in a green line was obtained for pure chloroform.

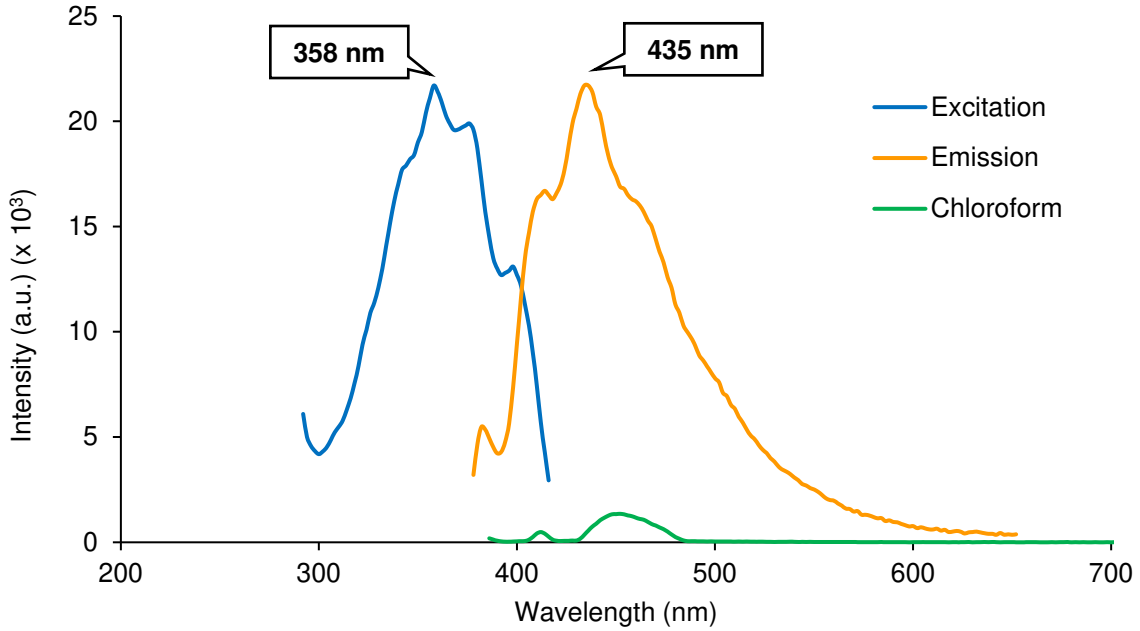

Figure 7.2: The excitation and emission spectra of *fac*-[Re(CO)$_3$(H$_2$O)(TropNMe)] (1.0 x 10^{-5} M) in chloroform.

fac-[Re(CO)$_3$(H$_2$O)(TropNMe)] is also a multi-emitter and the most prominent excitation peak is at 358 nm with the corresponding maximum emission peak at 435 nm, both depicted in Figure 7.2.

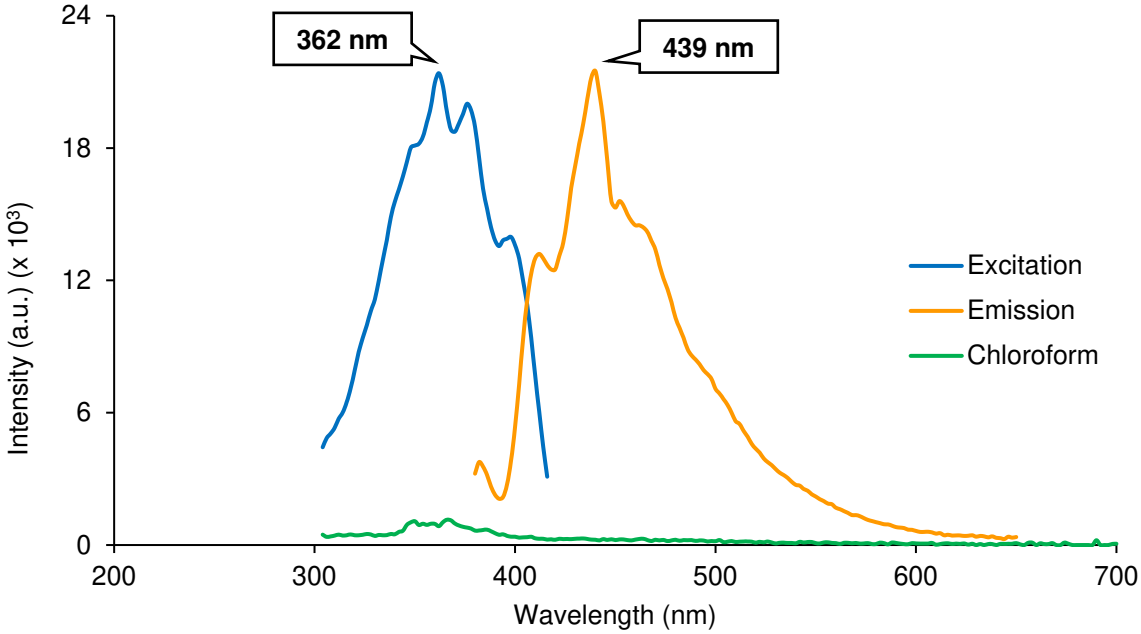

Figure 7.3: The excitation and emission spectra of 2-(ethylamino)tropone (1.0 x 10^{-5} M) in chloroform.

2-(Ethylamino)tropone (TropNHEt) displays multiple emissions with the highest emission at 439 nm from an excitation wavelength of 362 nm as seen in Figure 7.3. The shoulders seen on the emission spectrum can be attributed to noise.

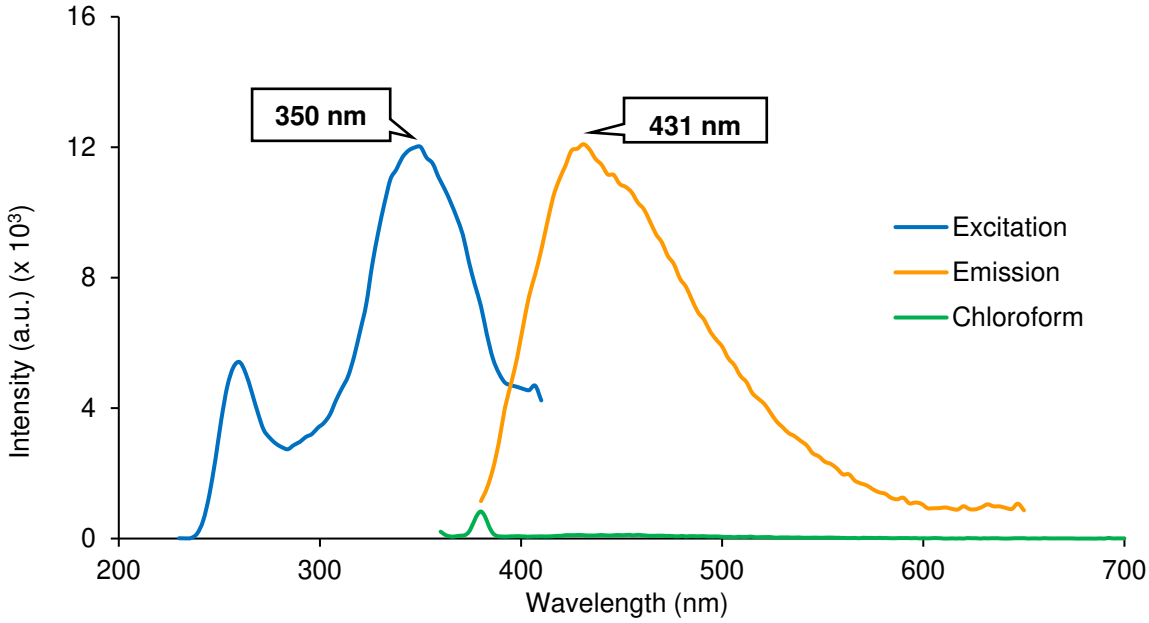

Figure 7.4: The excitation and emission spectra of *fac*-[Re(CO)$_3$(H$_2$O)(TropNEt)] (1.0 x 10^{-5} M) in chloroform.

fac-[Re(CO)$_3$(H$_2$O)(TropNEt)] exhibits multi-emission and the excitation peak at 350 nm gives rise to the emission peak at 431 nm as seen in Figure 7.4.

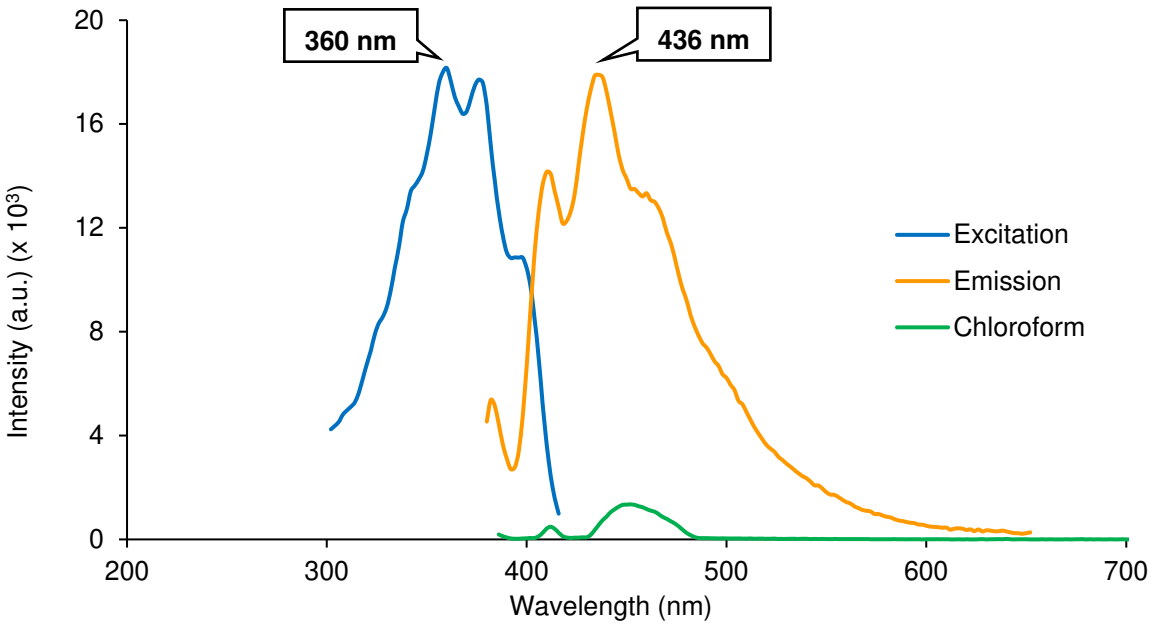

Figure 7.5: The excitation and emission spectra of 2-(2-fluoroethylamino)tropone (1.0 x 10^{-5} M) in chloroform.

The excitation peak of 2-(2-fluoroethylamino)tropone (TropNHEtF) at 360 nm results in a maximum emission at 436 nm. These are the most prominent excitation and emission peaks and are illustrated in Figure 7.5.

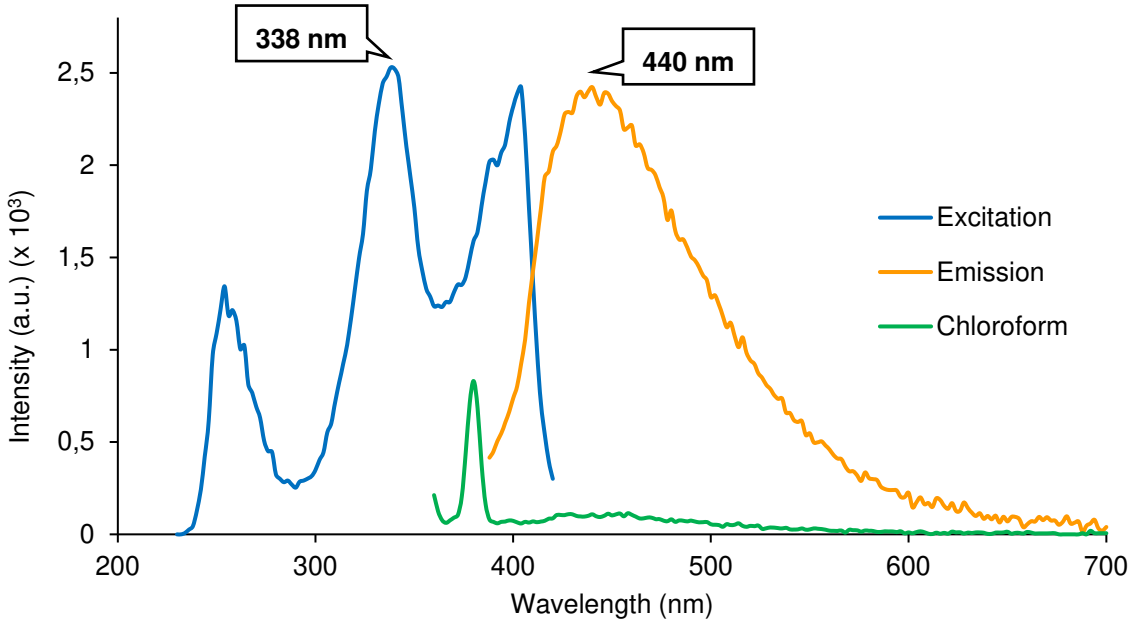

Figure 7.6: The excitation and emission spectra of *fac*-[Re(CO)$_3$(H$_2$O)(TropNEtF)] (1.0 x 10^{-5} M) in chloroform.

The excitation of *fac*-[Re(CO)$_3$(H$_2$O)(TropNEtF)] in solution at a wavelength of 338 nm gives rise to an emission peak at 440 nm as illustrated in Figure 7.6. The multiple excitation wavelengths can also be seen in Figure 7.6, but only the most prominent emission peak at 338 nm excitation wavelength is illustrated.

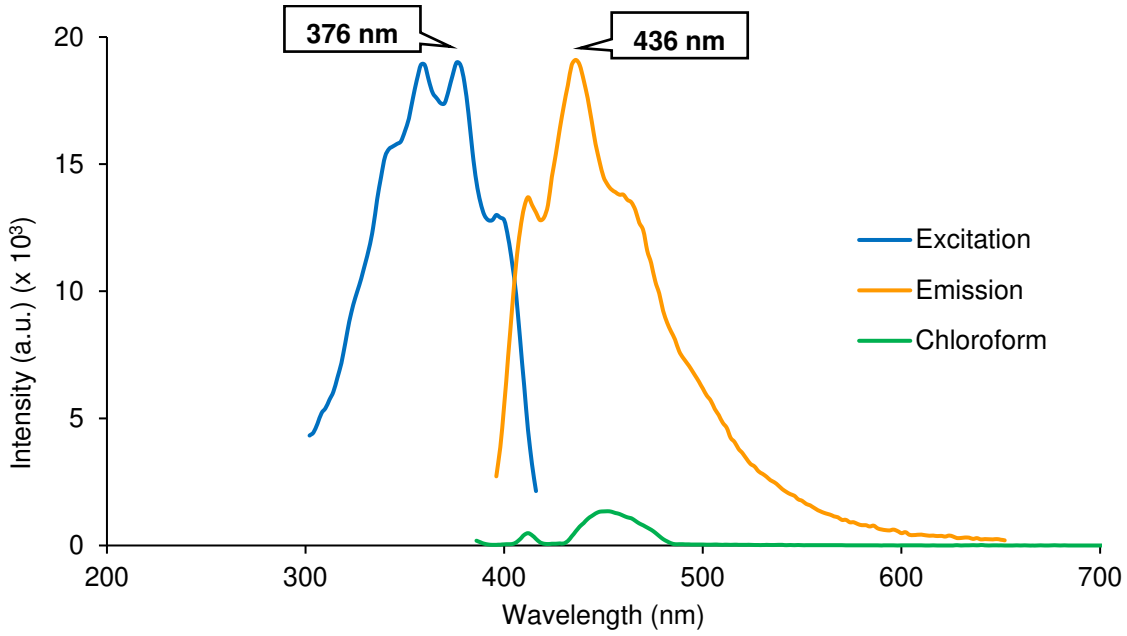

Figure 7.7: The excitation and emission spectra of 2-(benzylamino)tropone (1.0 x 10^{-5} M) in chloroform.

In Figure 7.7 it is seen that 2-(benzylamino)tropone (TropNHBn) is also a multi-emitter with the most prominent excitation and emission wavelengths at 376 nm and 436 nm, respectively.

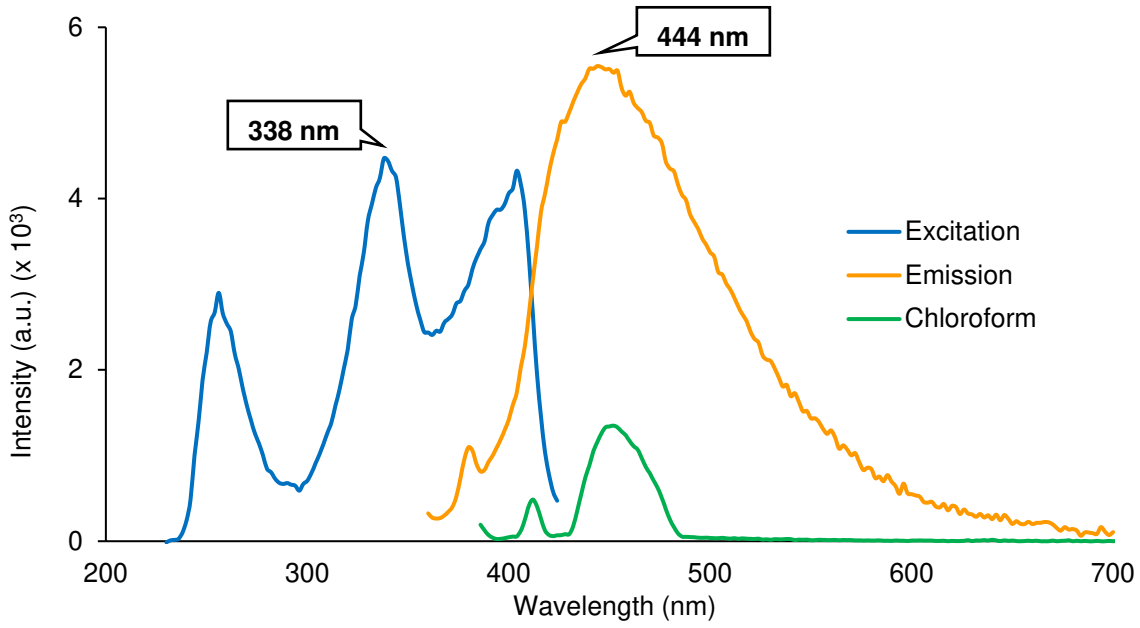

Figure 7.8: The excitation and emission spectra of *fac*-[$Re(CO)_3(H_2O)$(TropNBn)] (1.0 x 10^{-5} M) in chloroform using a 420 nm long-pass filter.

fac-[Re(CO)$_3$(H$_2$O)(TropNBn)] is another multi-emitter. The most prominent excitation peak is at 338 nm and gives rise to an emission peak at 444 nm (Figure 7.8). A 420 nm long-pass filter was used to reduce the noise at these low intensities.

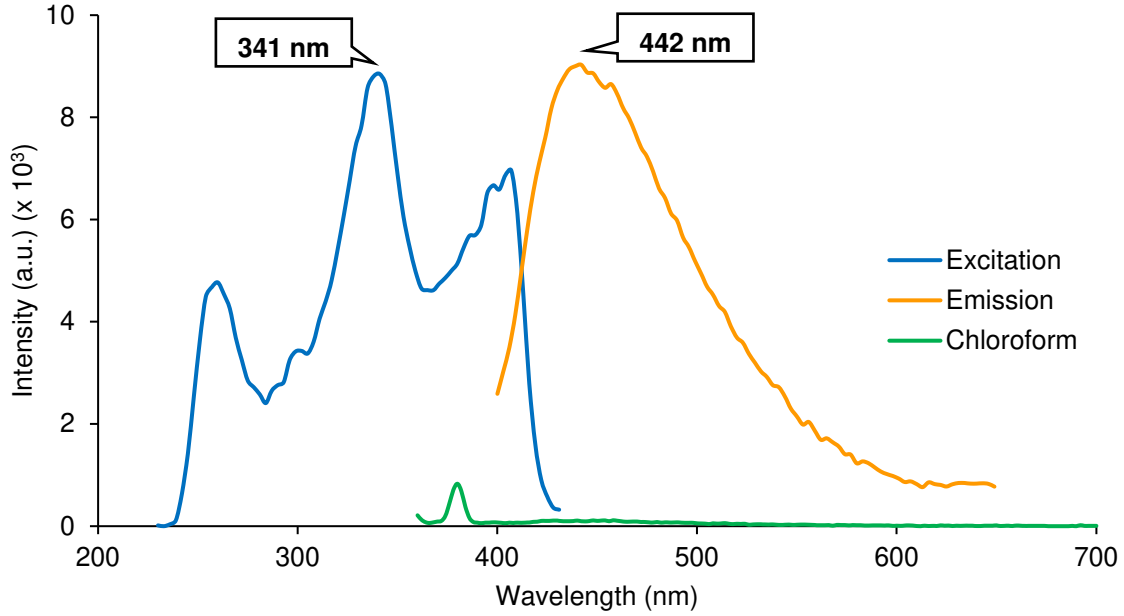

Figure 7.9: The excitation and emission spectra of 2-(phenethylamino)tropone (1.0 x 10^{-5} M) in chloroform.

2-(Phenethylamino)tropone (TropNHEtPh) exhibits multi-emission with the most prominent excitation wavelength of 341 nm giving rise to an emission peak at 442 nm (Figure 7.9).

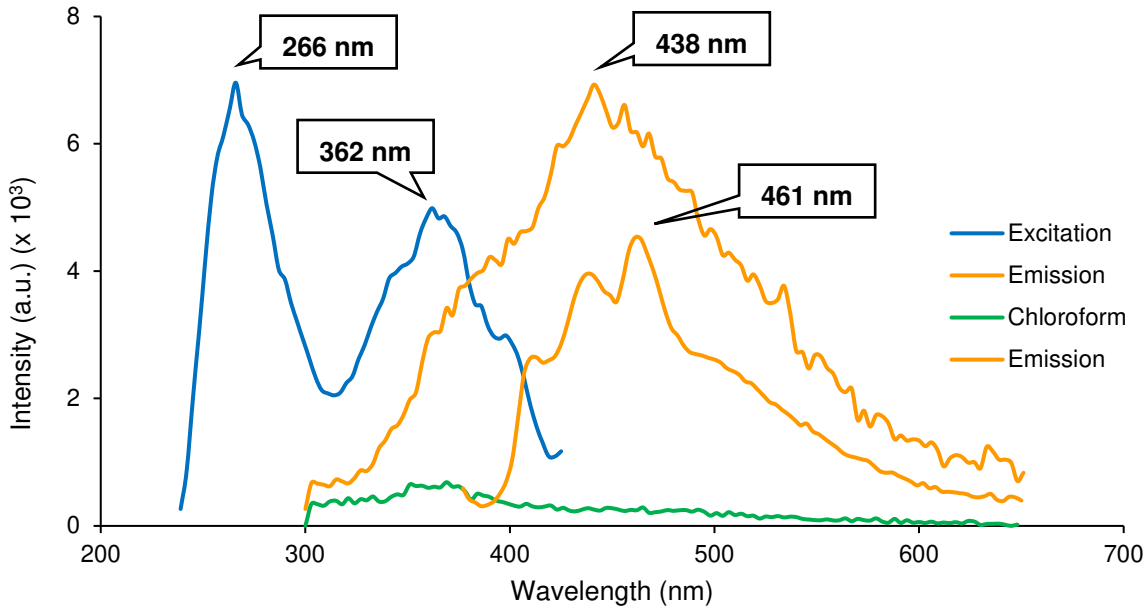

Figure 7.10: The excitation and emission spectra of *fac*-[Re(CO)$_3$(H$_2$O)(TropNEtPh)] (1.0 x 10^{-5} M) in chloroform.

fac-[Re(CO)$_3$(H$_2$O)(TropNEtPh)] also exhibits multi-emission with the most prominent excitation wavelength of 266 nm giving rise to an emission peak at 438 nm (Figure 7.10). To be able to compare the spectra of *fac*-[Re(CO)$_3$(H$_2$O)(TropNEtPh)] with that of 2-(phenethylamino)tropone, the free ligand, the emission spectrum with a peak at 461 nm from the excitation at 362 nm, the closest excitation wavelength to that of the free ligand (341 nm) is also illustrated in Figure 7.10. The shoulders on the spectra could be attributed to noise.

7.3.2 Analysis of aminotroponimine ligands and its Re(I) tricarbonyl complexes

The excitation and emission spectra of the synthesized *N,N'* bidentate ligands and its Re(I) tricarbonyl complexes are reported in this section.

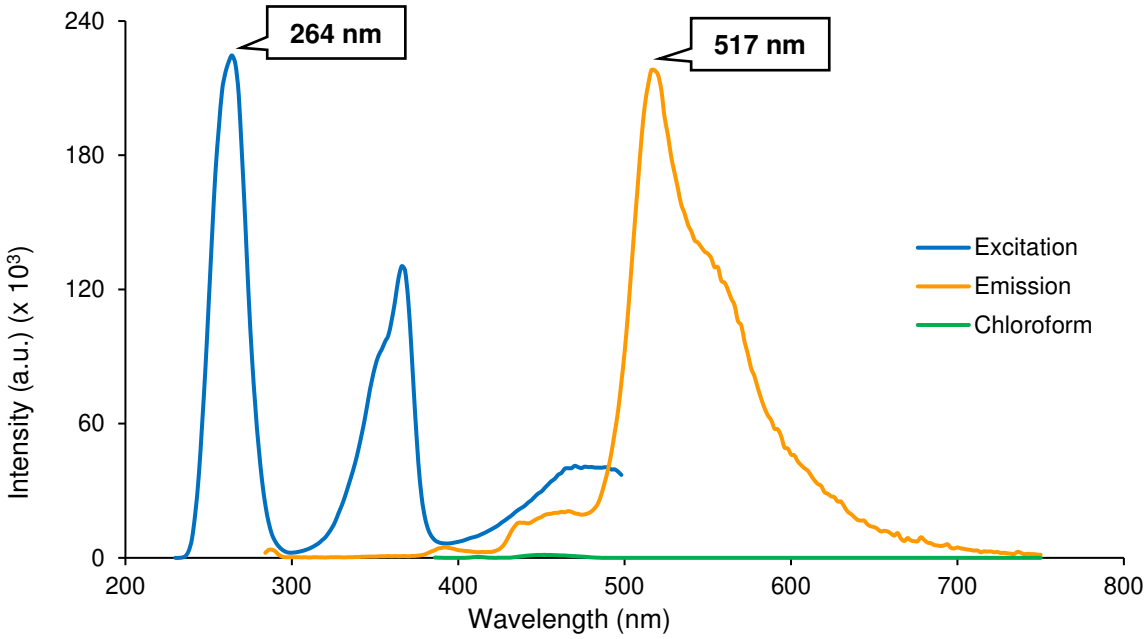

Figure 7.11: The excitation and emission spectra of *N*-methyl-2-(methylamino)troponimine (1.0 x 10^{-5} M) in chloroform.

N-Methyl-2-(methylamino)troponimine ([(Me)$_2$ATI]H) is also a multi-emitter just like the preceding *N,O* bidentate ligands and their Re(I) tricarbonyl complexes. This ligand, however, yielded intensities about tenfold higher than some of the *N,O* ligands and its compounds. The most prominent excitation peak at 264 nm gave rise to an emission peak at 517 nm as seen in Figure 7.11.

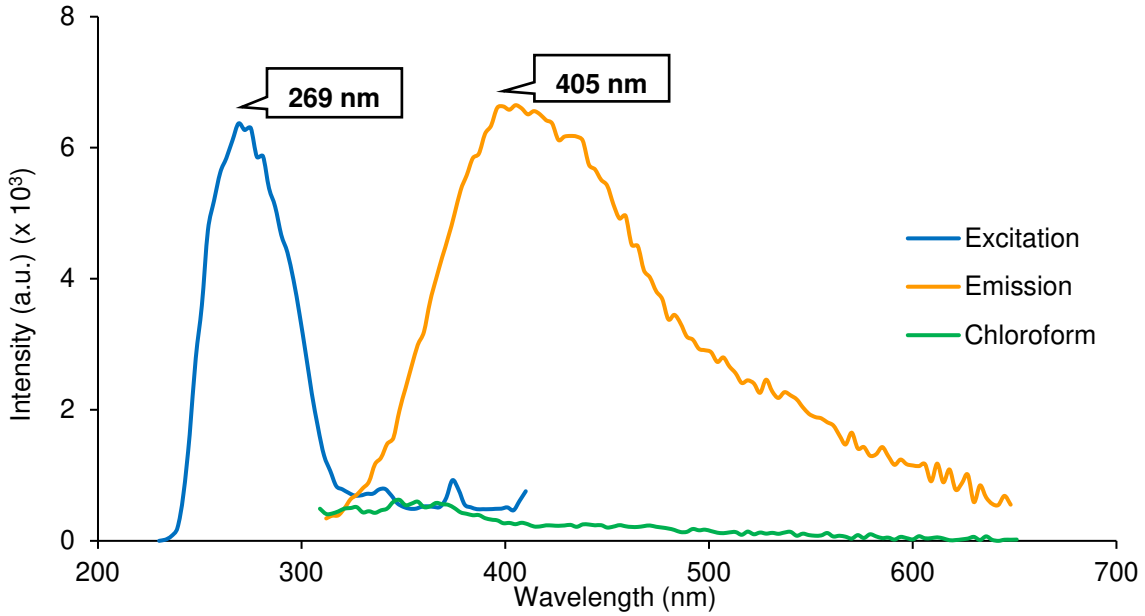

Figure 7.12: The excitation and emission spectra of *fac*-[Re(CO)$_3$(H$_2$O)((Me)$_2$ATI)] (1.0 x 10^{-5} M) in chloroform.

In Figure 7.12, *fac*-[Re(CO)$_3$(H$_2$O)((Me)$_2$ATI)] shows an excitation wavelength of 269 nm which gives rise to an emission peak at 405 nm.

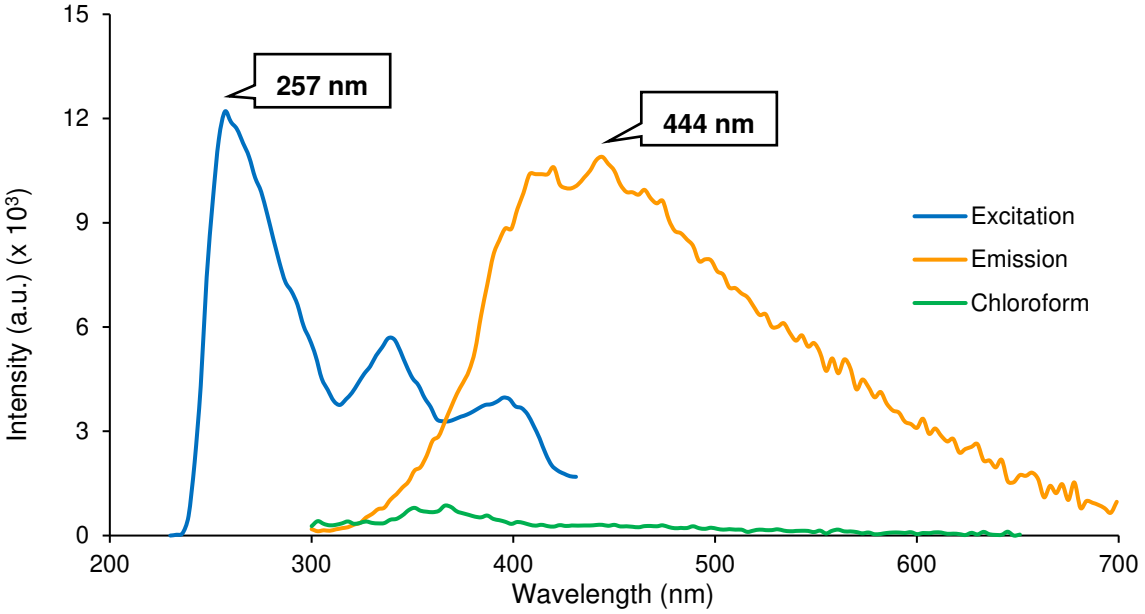

Figure 7.13: The excitation and emission spectra of *N*-benzyl-2-(benzylamino)troponimine (1.0 x 10^{-5} M) in chloroform.

N-Benzyl-2-(benzylamino)troponimine ([(Bn)$_2$ATI]H) displays multiple emission wavelengths and has its most prominent excitation peak at 257 nm with the corresponding emission peak at 444 nm (Figure 7.13).

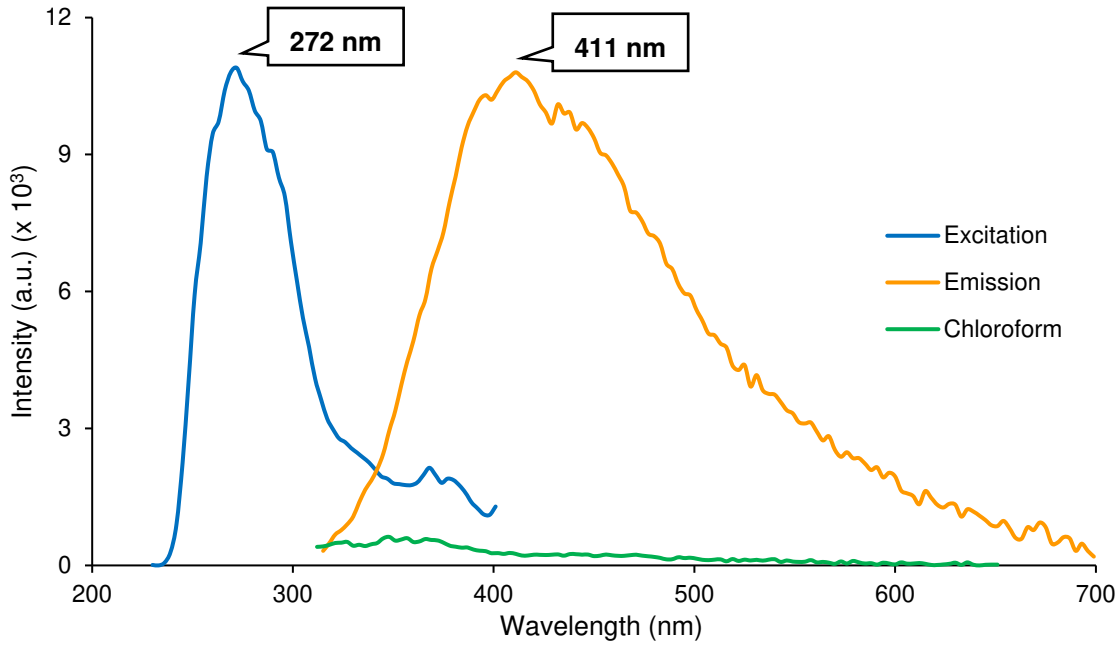

Figure 7.14: The excitation and emission spectra of *fac*-[Re(CO)$_3$(H$_2$O)((Bn)$_2$ATI)] (1.0 x 10^{-5} M) in chloroform.

The complex *fac*-[Re(CO)$_3$(H$_2$O)((Bn)$_2$ATI)] displays an emission peak at 411 nm when excited at 272 nm, as seen in Figure 7.14.

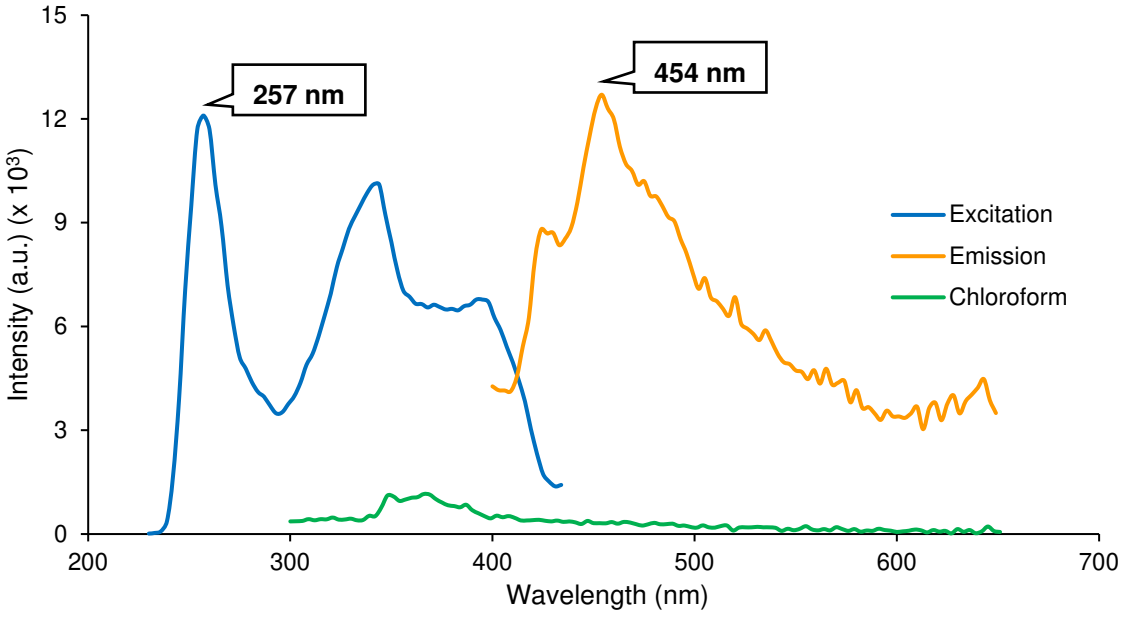

Figure 7.15: The excitation and emission spectra of *N*-phenethyl-2-(phenethylamino)troponimine (1.0 x 10^{-5} M) in chloroform.

N-Phenethyl-2-(phenethylamino)troponimine ([(EtPh)$_2$ATI]H) displays multiple excitation and emission wavelengths. The most prominent excitation peak (257 nm) and its corresponding emission peak (454 nm) are illustrated in Figure 7.15.

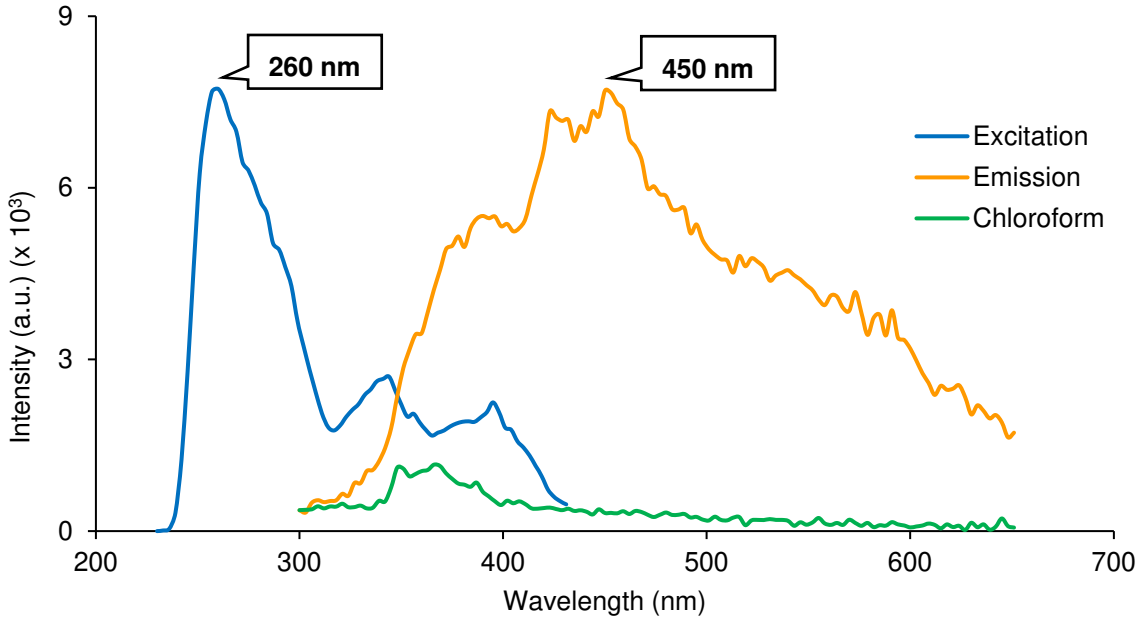

Figure 7.16: The excitation and emission spectra of *fac*-[Re(CO)$_3$(H$_2$O)((EtPh)$_2$ATI)] (1.0 x 10^{-5} M) in chloroform.

fac-[Re(CO)$_3$(H$_2$O)((EtPh)$_2$ATI)] displays a very prominent excitation peak at 260 nm and this gives rise to an emission peak at 450 nm (Figure 7.16). The shoulders on the spectrum could be attributed to noise.

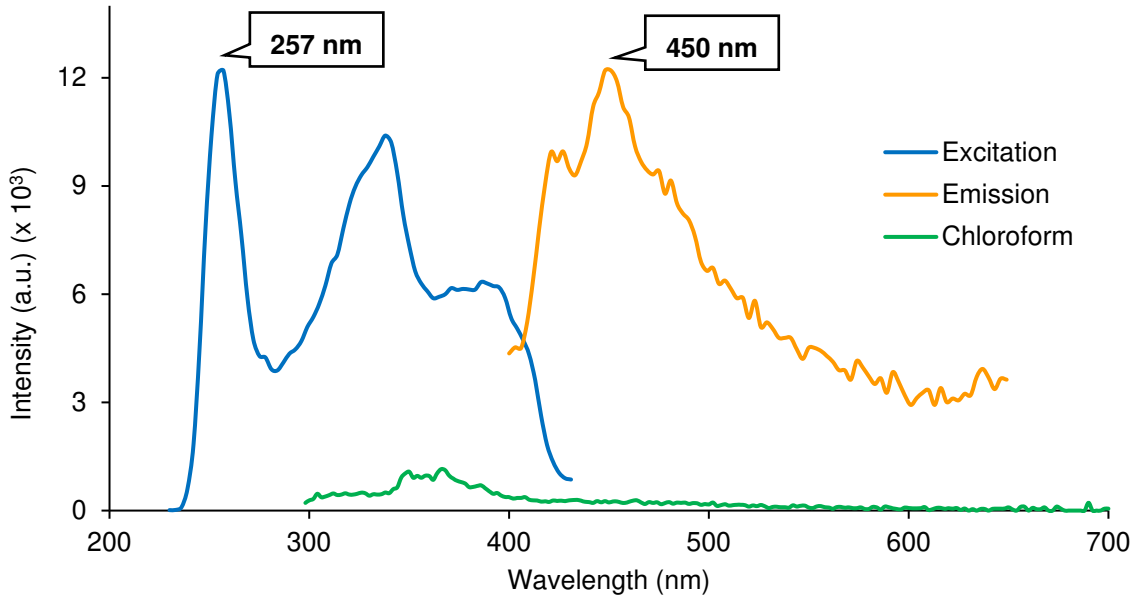

Figure 7.17: The excitation and emission spectra of *N*-phenethyl-2-(benzylamino)troponimine (1.0 x 10^{-5} M) in chloroform.

N-Phenethyl-2-(benzylamino)troponimine ([(EtPh,Bn)ATI]H) also exhibits multi-emission with the most prominent excitation and emission peaks at 257 nm and 450 nm, respectively. The photoluminescence study of the Re(I) tricarbonyl complex containing this ligand was not performed and will form part of future work.

The quantum yields of the evaluated ligands and complexes could not be determined on account of the low intensities obtained.

7.3.3 Discussion

Table 7.1 summarizes the UV/Vis absorbance wavelengths as well as the excitation and emission wavelengths from the photoluminescence studies of the ligands and complexes evaluated.

Table 7.1: The absorbance, excitation and emission wavelengths of the selected 2-(alkylamino)tropone and aminotroponimine ligand systems as well as their Re(I) tricarbonyl complexes.

Ligand/Complex	$\lambda_{Absorbance}$ (nm)	$\lambda_{Excitation}$ (nm)	$\lambda_{Emission}$ (nm)
TropNHMe	340, 410	377	437
***fac*-[Re(CO)$_3$(H$_2$O)(TropNMe)]**	340, 410	358	435
TropNHEt	340, 410	362	439
***fac*-[Re(CO)$_3$(H$_2$O)(TropNEt)]**	340, 410	350	431
TropNHEtF	340, 405	360	436
***fac*-[Re(CO)$_3$(H$_2$O)(TropNEtF)]**	340, 405	338	440
TropNHBn	340, 410	376	436
***fac*-[Re(CO)$_3$(H$_2$O)(TropNBn)]**	340, 405	338	444
TropNHEtPh	340, 410	341	442
***fac*-[Re(CO)$_3$(H$_2$O)(TropNEtPh)]**	340, 410	266; 362	438; 461
[(Me)$_2$ATI]H	350, 420	264	517
***fac*-[Re(CO)$_3$(H$_2$O)([(Me)$_2$ATI]H)]**	350, 425	269	405
[(Bn)$_2$ATI]H	360, 425	257	444
***fac*-[Re(CO)$_3$(H$_2$O)([(Bn)$_2$ATI]H)]**	350, 425	272	411
[(EtPh)$_2$ATI]H	345, 410	257	454
***fac*-[Re(CO)$_3$(H$_2$O)([(EtPh)$_2$ATI]H)]**	355, 425	260	450
[(EtPh,Bn)ATI]H	360, 405	257	450

Chapter 7

The selected ligand systems and complexes used in this study all show photoluminescent properties. As seen from Table 7.1 the excitation wavelengths of the evaluated ligands and complexes range from 257 nm - 377 nm and the emission wavelengths from 405 - 517 nm. The emission in intensities range from 2.37 x 10^3 to 21.5 x 10^3 arbitrary units with $[(Me)_2ATI]H$ being the only exception with a high intensity value of 218.0 x 10^3 arbitrary units. Except for *fac*-$[Re(CO)_3(H_2O)(TropNEtPh)]$, the 2-(alkylamino)tropone ligands and its complexes have longer excitation wavelengths than that of the aminotroponimines ligands and its complexes. There is no significant trend or differences in the emission wavelengths of these two types of ligands and complexes, except for the 517 nm emission wavelength of $[(Me)_2ATI]H$, which is discussed later in this paragraph.

The free ligand TropNHMe is excited at 377 nm, a little higher than the 358 nm for its Re(I) tricarbonyl complex, *fac*-$[Re(CO)_3(H_2O)(TropNMe)]$. A hypsochromic shift of only 2 nm is observed between the emission wavelengths of TropNHMe (437 nm) and *fac*-$[Re(CO)_3(H_2O)(TropNMe)]$ (435 nm) with a small increase in intensity. For TropNHEt and its complex *fac*-$[Re(CO)_3(H_2O)(TropNEt)]$ with excitation wavelengths of 362 nm and 350 nm, respectively, the hypsochromic (blue) shift is 8 nm from 439 nm to 431 nm with a significant decrease in intensity. One of the three pairs of ligands and complexes showing a bathochromic (red) shift is TropNHEtF and its complex *fac*-$[Re(CO)_3(H_2O)(TropNEtF)]$. TropNHEtF and *fac*-$[Re(CO)_3(H_2O)(TropNEtF)]$ have excitation wavelengths of 360 nm and 338 nm, yielding emission wavelengths of 436 nm and 440 nm, respectively. This results in a 4 nm red shift with a major decrease in intensity. The emission wavelengths of the TropNHBn (376 nm) and *fac*-$[Re(CO)_3(H_2O)(TropNBn)]$ (338 nm) ligand-complex-pair is also red-shifted with 8 nm and a large decrease in intensity. The third pair that exhibits a red shift (19 nm) for the emission wavelength of 461 nm but also a small blue shift of 4 nm for an emission wavelength of 438 nm is TropNHEtPh and its complex *fac*-$[Re(CO)_3(H_2O)(TropNEtPh)]$.

In Figure 7.10 two sets of spectra is seen for the complex *fac*-$[Re(CO)_3(H_2O)(TropNEtPh)]$, which is a multi-emitter. The most prominent excitation peak is at 266 nm and gives rise to an emission peak at 438 nm, a 4 nm blue-shift compared to the free ligand and only a slight decrease in intensity.

However, when excitation takes place at a wavelength (362 nm) much closer to the excitation wavelength of the free ligand (341 nm), an emission peak is obtained at 461 nm and a 19 nm red shift is observed, but a larger decrease in intensity is seen. Although this second emission wavelength is at a lower intensity than the first, the red shift is a more desirable outcome.

The free aminotroponimine ligand $[(Me)_2ATI]H$ emits at the longest wavelength of 517 nm with a very high intensity of 218.0 x 10^3 arbitrary units. This is the ligand with the best results in this study since the long wavelength and high intensity are desired properties. The Re(I) complex *fac*-$[Re(CO)_3(H_2O)([(Me)_2ATI]H)]$ emits at 405 nm resulting in a 112 nm blue shift and more than 10-fold decrease in intensity. The excitation peaks of the free ligand [(Bn)2ATI]H and its complex *fac*-$[Re(CO)_3(H_2O)([(Bn)_2ATI]H)]$ at 257 nm and 272 nm, respectively, leads to emission peaks at 444 nm and 411 nm with a 33 nm blue shift and no significant change in intensity. The free ligand $[(EtPh)_2ATI]H$ and its complex *fac*-$[Re(CO)_3(H_2O)([(EtPh)_2ATI]H)]$ have excitation wavelengths of 257 nm and 260 nm, respectively. The emission wavelengths of 454 nm for the ligand and 450 nm for the complex shows a small blue shift of 4 nm with a decrease in intensity. The free ligand [(EtPh,Bn)ATI]H has an excitation and emission wavelength of 257 nm and 450 nm. The complex of this ligand was not evaluated due to time constraints and will form part of future work to relate the photoluminescent properties of the ligand and the complex to eachother.

The ligand with the best photoluminescent properties in terms of both wavelength and intensity is the free aminotroponimine ligand $[(Me)_2ATI]H$. The metal complex with the best results in terms of wavelength is *fac*-$[Re(CO)_3(H_2O)(TropNEtPh)]$ and in terms of intensity *fac*-$[Re(CO)_3(H_2O)(TropNMe)]$. It is interesting to note that there are no significant trends with regards to the properties of the ligands and complexes containing different *N*-substituents, for instance; TropNHMe and its complex have close emission wavelengths with a slight difference in intensity, where the $[(Me)_2ATI]H$ ligand has a much longer wavelength and intensity than TropNHMe and its complex has a much shorter wavelength and lower intensity than $[(Me)_2ATI]H$ and *fac*-$[Re(CO)_3(H_2O)([(Me)_2ATI]H)]$; TropNHBn, *fac*-$[Re(CO)_3(H_2O)(TropNBn)]$, [(Bn)2ATI]H and *fac*-$[Re(CO)_3(H_2O)([(Bn)_2ATI]H)]$ emits at wavelengths close to each other; the intensity of emission of *fac*-$[Re(CO)_3(H_2O)(TropNBn)]$ is much lower

than that of the free ligand TropNHBn; the intensity of emission of the ligand $[(Bn)_2ATI]H$ is also lower than that of TropNHBn, but only slightly higher than that of its complex. Contrary to this, the ligand TropNHEtPh has a lower intensity than $[(EtPh)_2ATI]H$ and both the ligands have slightly higher intensities than their complexes. Another interesting observation lies in the properties of the free ligands $[(Bn)_2ATI]H$, $[(EtPh)_2ATI]H$ and [(EtPh,Bn)ATI]H. In terms of cytotoxicity (Chapter 6) [(EtPh,Bn)ATI]H has a lower IC_{50} value than $[(Bn)_2ATI]H$ and $[(EtPh)_2ATI]H$. With regards to the photoluminescent properties, the intensity as well as the wavelength of emission is more or less in between that of $[(Bn)_2ATI]H$ and $[(EtPh)_2ATI]H$.

The ligand systems and complexes in this study all contain a troponato ring system and absorb in the range of 340 - 425 nm. When compared to the precursor tropolone and tropolonato complexes in literature, the absorbance wavelengths are slightly longer. Complexes of rhodium containing tropolonato as a bidentate ligand have been synthesized by Kunkely *et al*.[9] The study of the optical properties of the ligands and complexes revealed that the free ligand tropolone in ethanol absorbs at wavelengths of 402, 368, 351 and 319 nm. The absorption spectrum of $Rh(phpy)_2(tro)$ (where phpy = deprotonated 2-phenylpyridine and tro = deprotonated tropolone) displays its longest-wavelength spin-allowed band at 400 nm. A very weak absorption might occur near 450 nm due to an additional spin-forbidden transition.[9]

The higher absorption energy of the complexes in the wavelength range of 340 - 360 nm most likely correspond to intra-ligand π–π* transitions and are therefore expected to be only dependent on the nature of the aminotroponimine ligands. The lower energy absorption energy of the complexes in the wavelength range of 405 - 425 nm could correspond to metal-to-ligand-charge-transfer (MLCT) transitions which generally dominates the photochemical properties of Re(I) tricarbonyl complexes.[10] The MLCT transition state energy is mostly independent of the nature of the ligand in the sixth position. This means that differences in the MLCT bands can mainly be ascribed to differences in the ligand π* orbitals.

[9] Kunkely, H., Pawlowski, V. & Vogler, A. (2008). *Zeitschrift Für Naturforschung B*, **63**(8), 963-967.

[10] Marker, S., MacMillan, S., Zipfel, W., Li, Z., Ford, P. & Wilson, J. (2018). *Inorganic Chemistry*, **57**(3), 1311-1331.

fac-[Re(CO)$_3$(*N,N'*)L] complexes (where *N,N'* is a bidendate ligand and L an ancillary ligand or halide) are attractive candidates for bioimaging probes because they usually exhibit long-lived emission from triplet metal-to-ligand-charge-transfer ($_3$MLCT) excited states.[11] The photophysical and bioimaging properties of the complexes such as absorption, emission, biomolecular specificity, cellular uptake and cytotoxicity can easily be modified through variation of the coordinating ligands.[11]

Although all the ligands and complexes show photoluminescent properties, none of them emit at long enough wavelengths to be promoted as photosensitizers in PDT. One ligand, [(Me)$_2$ATI]H, emits at a long wavelength of 517 nm and shows that the ligands have the potential to reach higher wavelengths. This could be achieved by modifying the chemical structures with better electron acceptor properties to achieve emission at longer wavelengths.[12]

[11] Gabr, M. & Pigge, F. (2017). *Dalton Transactions*, **46**(43), 15040-15047.
[12] Kamecka, A., Prachnio, K. & Kapturkiewicz, A. (2018). *Journal of Luminescence*, **203**, 409-419.

8

CRITICAL EVALUATION AND FUTURE RESEARCH

8.1 Results obtained

The objectives of this study were to synthesize and fully characterize a range of *N,O* and *N,N'* donor bidentate ligands and the Re(I) tricarbonyl complexes thereof, to evaluate the synthesized compounds' anticancer activity and to study the photoluminescent properties of the compounds.

Five *N,O* bidentate ligand systems (2-(alkylamino)tropones) were successfully synthesized and characterized, namely 2-(methylamino)tropone, 2-(ethylamino)tropone, 2-(2-fluoroethylamino)tropone, 2-(benzylamino)tropone and 2-(phenethylamino)tropone. The products were obtained in yields ranging from 22 to 66 %. Nine *N,N'* bidentate ligand systems (aminotroponimines) were successfully synthesized and characterized, namely *N*-methyl-2-(methylamino)troponimine, *N*-ethyl-2-(ethylamino)troponimine, *N*-2-fluoroethyl-2-(2-fluoroethylamino)troponimine, *N*-phenethyl-2-(phenethylamino)troponimine, *N*-benzyl-2-(benzylamino)troponimine, *N*-methyl-2-(benzylamino)troponimine, *N*-ethyl-2-(benzylamino)troponimine, *N*-2-fluoroethyl-2-(benzylamino)troponimine, *N*-phenethyl-2-(benzylamino)troponimine. The products were obtained in yields ranging from 22 to 74 %. Five Re(I) tricarbonyl complexes of the type *fac*-[$Re(CO)_3(H_2O)(N,O)$] (*N,O* = different *N,O* bidentate ligands) namely *fac*-[$Re(CO)_3(H_2O)$(TropNMe)], *fac*-[$Re(CO)_3(H_2O)$(TropNEt)], *fac*-[$Re(CO)_3(H_2O)$(TropNEtF)], *fac*-[$Re(CO)_3(H_2O)$(TropNBn)], *fac*-[$Re(CO)_3(H_2O)$(TropNEtPh)] and nine of the type *fac*-[$Re(CO)_3(H_2O)(N,N')$] (*N,N'* = different *N,N'* bidentate ligands) namely *fac*-[$Re(CO)_3(H_2O)$([$(Me)_2$ATI]H)], *fac*-[$Re(CO)_3(H_2O)$([$(Et)_2$ATI]H)], *fac*-[$Re(CO)_3(H_2O)$([$(EtF)_2$ATI]H)], *fac*-[$Re(CO)_3(H_2O)$([$(Bn)_2$ATI]H)], *fac*-[$Re(CO)_3(H_2O)$([$(EtPh)_2$ATI]H)], *fac*-[$Re(CO)_3(H_2O)$([(Me,Bn)ATI]H)], *fac*-[$Re(CO)_3(H_2O)$([(Et,Bn)ATI]H)], *fac*-[$Re(CO)_3(H_2O)$([(EtF,Bn)ATI]H)], *fac*-[$Re(CO)_3(H_2O)$([(EtPh,Bn)ATI]H)] were successfully synthesized and characterized. The complexes were obtained in yields ranging from 53 % to 94 %.

The solid-state crystal structures of one intermediate, 2-tosyloxytropone and two 2-(alkylamino)tropone ligands, namely 2-(methylamino)tropone and 2-(2-fluoroethylamino)tropone were successfully determined and reported in Chapter 5. The structures have final R-indices of R_1 = 0.0405 and wR_2 = 0.1137 for 2-tosyloxy)tropone, R_1 = 0.0420 and wR_2 = 0.0924 for 2-(methylamino)tropone and R_1 = 0.0729 and wR_2 = 0.1334 for 2-(2-fluoroethylamino)tropone. No crystal structures were obtained for Re(I) tricarbonyl complexes.

In vitro cytotoxicity studies were performed on the synthesized ligands and on four of the *fac*-[Re(CO)$_3$(H_2O)(*N,O*)] (*N,O* = different *N,O* bidentate ligands) complexes and the results were discussed in Chapter 6. In summary, the ligands yielded IC_{50} values ranging from 0.45 - 36.1 µM and the complexes yielded higher IC_{50} values between 47.0 µM and 77.4 µM. Four of the *N,N'* bidentate ligands, namely [(EtPh,Bn)ATI]H, [(Me,Bn)ATI]H, [(Et,Bn)ATI]H and [(EtPh)$_2$ATI]H have IC_{50} values of 0.45, 0.66, 1.10 and 2.4 µM, respectively, which are lower than that of cisplatin, the control in this study, with an IC_{50} value of 3.26 µM. The remainder of the synthesized Re(I) tricarbonyl complexes were not evaluated due to time constraints and will be included in future endeavors.

The photoluminescent properties of all the synthesized ligands and complexes were successfully determined and the results were reported in Chapter 7. Good results were obtained for the evaluated ligands and complexes, which include excitation wavelengths ranging from 257 nm - 377 nm and emission wavelengths from 405 - 517 nm. The emissions vary in intensity ranging from 2.37 x 10^3 to 21.5 x 10^3 arbitrary units with [(Me)$_2$ATI]H having a very high intensity of emission of 218.0 x 10^3 arbitrary units. The quantum yields of the compounds could unfortunately not be determined successfully due to the low intensities of the emissions.

In conclusion, the aims of this study were achieved to a great extent.

8.2 Future research

The synthesized Re(I) tricarbonyl complexes have an H_2O molecule as the substituent in the 6th position. The substitution kinetics of these reactions could be investigated to obtain information regarding the reactivity and *in vivo* behaviour of the compounds as well as its intermediates.

Chapter 8

The results of the cytotoxicity evaluations of the remainder of the Re(I) tricarbonyl complexes would provide important information regarding the nature of these metal complexes, since the anticancer activities of the various ligands proved to differ substantially. In addition to this, it is important to test these compounds against non-cancerous cells to determine the selectivity of the compounds and their potential as chemotherapeutic agents.

Several factors contribute to the photoluminescent properties of compounds. These factors will be taken into consideration when synthesizing new compounds with the goal of increasing their quantum yields. An increase in the degree of conjugation of a compound as well as the incorporation of electron-withdrawing substituents could increase its fluorescence and quantum yield.

APPENDIX A

Table A.1: Atomic coordinates (x 10^4) and equivalent isotropic displacement parameters ($Å^2$ x 10^3) for 2-(tosyloxy)tropone. U(eq) is defined as one third of the trace of the orthogonalized U^{ij} tensor.

	x	y	z	U(eq)
C(1)	5110(6)	3602(3)	8273(5)	34(1)
C(2)	6235(6)	2906(3)	8882(4)	27(1)
C(3)	7140(6)	2873(3)	10016(4)	32(1)
C(4)	7296(7)	3532(4)	10984(5)	41(1)
C(5)	6486(8)	4327(4)	11009(5)	43(1)
C(6)	5310(7)	4709(4)	10080(6)	42(1)
C(7)	4757(7)	4406(4)	8929(5)	41(1)
C(12)	8458(5)	2727(3)	6612(4)	28(1)
C(13)	7547(6)	2878(4)	5455(4)	33(1)
C(14)	8029(6)	3576(4)	4743(4)	36(1)
C(15)	9410(6)	4120(3)	5137(4)	32(1)
C(16)	10301(7)	3958(4)	6292(5)	37(1)
C(17)	9842(7)	3261(3)	7045(5)	34(1)
C(18)	9921(8)	4877(4)	4323(6)	45(1)
O(1)	4457(6)	3476(3)	7186(4)	58(1)
O(2)	6229(4)	2141(2)	8126(3)	31(1)
O(3)	9232(5)	1667(3)	8510(4)	43(1)
O(4)	7269(5)	1095(2)	6742(4)	45(1)
S(1)	7898(1)	1821(1)	7517(1)	30(1)

Table A.2: Bond distances [Å] and angles [°] for 2-(tosyloxy)tropone.

Bond	Bond distance	Bond angle	Angle
C(1)-O(1)	1.241(7)	**O(1)-C(1)-C(7)**	120.5(5)
C(1)-C(7)	1.435(7)	**O(1)-C(1)-C(2)**	118.8(5)
C(1)-C(2)	1.474(7)	**C(7)-C(1)-C(2)**	120.8(5)
C(2)-C(3)	1.347(7)	**C(3)-C(2)-O(2)**	117.7(4)
C(2)-O(2)	1.402(5)	**C(3)-C(2)-C(1)**	131.5(4)
C(3)-C(4)	1.429(7)	**O(2)-C(2)-C(1)**	110.7(4)
C(3)-H(3)	0.9500	**C(2)-C(3)-C(4)**	129.2(5)
C(4)-C(5)	1.350(9)	**C(2)-C(3)-H(3)**	115.4
C(4)-H(4)	0.9500	**C(4)-C(3)-H(3)**	115.4
C(5)-C(6)	1.409(9)	**C(5)-C(4)-C(3)**	128.0(5)
C(5)-H(5)	0.9500	**C(5)-C(4)-H(4)**	116.0
C(6)-C(7)	1.347(8)	**C(3)-C(4)-H(4)**	116.0
C(6)-H(6)	0.9500	**C(4)-C(5)-C(6)**	128.3(5)
C(7)-H(7)	0.9500	**C(4)-C(5)-H(5)**	115.9
C(12)-C(13)	1.387(6)	**C(6)-C(5)-H(5)**	115.9
C(12)-C(17)	1.392(7)	**C(7)-C(6)-C(5)**	129.8(5)
C(12)-S(1)	1.752(5)	**C(7)-C(6)-H(6)**	115.1
C(13)-C(14)	1.372(7)	**C(5)-C(6)-H(6)**	115.1
C(13)-H(13)	0.9500	**C(6)-C(7)-C(1)**	132.3(5)
C(14)-C(15)	1.389(7)	**C(6)-C(7)-H(7)**	113.9
C(14)-H(14)	0.9500	**C(1)-C(7)-H(7)**	113.9
C(15)-C(16)	1.382(8)	**C(13)-C(12)-C(17)**	121.3(4)
C(15)-C(18)	1.512(7)	**C(13)-C(12)-S(1)**	119.2(4)
C(16)-C(17)	1.390(7)	**C(17)-C(12)-S(1)**	119.5(4)
C(16)-H(16)	0.9500	**C(14)-C(13)-C(12)**	118.5(4)
C(17)-H(17)	0.9500	**C(14)-C(13)-H(13)**	120.7
C(18)-H(18A)	0.9800	**C(12)-C(13)-H(13)**	120.7
C(18)-H(18B)	0.9800	**C(13)-C(14)-C(15)**	122.0(4)
C(18)-H(18C)	0.9800	**C(13)-C(14)-H(14)**	119.0
O(2)-S(1)	1.604(3)	**C(15)-C(14)-H(14)**	119.0
O(3)-O(3)	0.000(12)	**C(16)-C(15)-C(14)**	118.6(4)
O(3)-S(1)	1.435(4)	**C(16)-C(15)-C(18)**	120.8(5)
O(4)-S(1)	1.424(4)	**C(14)-C(15)-C(18)**	120.7(5)
		C(15)-C(16)-C(17)	121.1(5)
		C(15)-C(16)-H(16)	119.4

	C(17)-C(16)-H(16)	119.4
	C(16)-C(17)-C(12)	118.5(5)
	C(16)-C(17)-H(17)	120.7
	C(12)-C(17)-H(17)	120.7
	C(15)-C(18)-H(18A)	109.5
	C(15)-C(18)-H(18B)	109.5
	H(18A)-C(18)-H(18B)	109.5
	C(15)-C(18)-H(18C)	109.5
	H(18A)-C(18)-H(18C)	109.5
	H(18B)-C(18)-H(18C)	109.5
	C(2)-O(2)-S(1)	121.9(3)
	O(3)-O(3)-S(1)	0(10)
	O(4)-S(1)-O(3)	119.7(2)
	O(4)-S(1)-O(3)	119.7(2)
	O(3)-S(1)-O(3)	0.0(4)
	O(4)-S(1)-O(2)	102.5(2)
	O(3)-S(1)-O(2)	108.1(2)
	O(3)-S(1)-O(2)	108.1(2)
	O(4)-S(1)-C(12)	110.8(2)
	O(3)-S(1)-C(12)	109.2(2)
	O(3)-S(1)-C(12)	109.2(2)
	O(2)-S(1)-C(12)	105.22(19)

Table A.3: Anisotropic displacement parameters ($Å^2$ x 10^3) for 2-(tosyloxy)tropone. The anisotropic displacement factor exponent takes the form: $-2\pi^2[h^2a^{*2}U^{11} + ... + 2hka^*b^*U^{12}]$.

	U^{11}	U^{22}	U^{33}	U^{23}	U^{13}	U^{12}
C(1)	37(2)	31(2)	35(2)	2(2)	5(2)	2(2)
C(2)	26(2)	25(2)	31(2)	3(2)	8(2)	-1(2)
C(3)	36(2)	33(2)	28(2)	3(2)	7(2)	5(2)
C(4)	49(3)	47(3)	27(2)	-2(2)	3(2)	-2(2)
C(5)	55(3)	40(3)	36(3)	-9(2)	12(2)	-9(2)
C(6)	50(3)	30(2)	49(3)	-3(2)	14(2)	0(2)
C(7)	40(3)	35(2)	46(3)	5(2)	4(2)	8(2)
C(12)	26(2)	29(2)	28(2)	1(2)	3(2)	3(2)
C(13)	31(2)	38(3)	30(2)	1(2)	1(2)	-6(2)
C(14)	35(2)	44(3)	27(2)	5(2)	2(2)	1(2)
C(15)	37(2)	30(2)	32(2)	-1(2)	14(2)	2(2)
C(16)	35(3)	33(2)	43(3)	-2(2)	6(2)	-7(2)
C(17)	35(2)	34(2)	32(2)	-4(2)	-2(2)	-2(2)
C(18)	56(3)	37(3)	46(3)	5(2)	23(3)	-3(2)
O(1)	64(3)	62(3)	43(2)	-5(2)	-17(2)	21(2)
O(2)	30(2)	28(2)	36(2)	-2(1)	6(1)	-4(1)
O(3)	40(2)	49(2)	39(2)	11(2)	2(2)	17(2)
O(4)	64(3)	26(2)	47(2)	-10(2)	12(2)	-2(2)
S(1)	35(1)	24(1)	31(1)	0(1)	6(1)	5(1)

Table A.4: Hydrogen coordinates (x 10^4) and isotropic displacement parameters ($Å^2$ x 10^3) for 2-(tosyloxy)tropone.

	x	y	z	U(eq)
H(3)	7762	2336	10199	38
H(4)	8066	3394	11699	49
H(5)	6740	4673	11746	52
H(6)	4836	5264	10299	51
H(7)	3986	4799	8461	49
H(13)	6611	2506	5163	40
H(14)	7398	3690	3956	43
H(16)	11243	4328	6576	45
H(17)	10460	3153	7838	41
H(18A)	9152	4892	3545	67
H(18B)	9847	5446	4766	67
H(18C)	11095	4784	4129	67

Table A.5: Torsion angles [°] for 2-(tosyloxy)tropone.

Torsion angle	Angle
O(1)-C(1)-C(2)-C(3)	177.7(5)
C(7)-C(1)-C(2)-C(3)	-3.1(8)
O(1)-C(1)-C(2)-O(2)	-6.4(6)
C(7)-C(1)-C(2)-O(2)	172.8(4)
O(2)-C(2)-C(3)-C(4)	-176.7(5)
C(1)-C(2)-C(3)-C(4)	-1.1(9)
C(2)-C(3)-C(4)-C(5)	4.1(9)
C(3)-C(4)-C(5)-C(6)	-1.2(10)
C(4)-C(5)-C(6)-C(7)	-3.2(11)
C(5)-C(6)-C(7)-C(1)	2.2(11)
O(1)-C(1)-C(7)-C(6)	-178.7(6)
C(2)-C(1)-C(7)-C(6)	2.1(9)
C(17)-C(12)-C(13)-C(14)	-0.6(7)
S(1)-C(12)-C(13)-C(14)	-178.3(4)
C(12)-C(13)-C(14)-C(15)	1.1(7)
C(13)-C(14)-C(15)-C(16)	-1.1(7)
C(13)-C(14)-C(15)-C(18)	179.2(5)
C(14)-C(15)-C(16)-C(17)	0.5(7)
C(18)-C(15)-C(16)-C(17)	-179.8(5)
C(15)-C(16)-C(17)-C(12)	0.0(7)
C(13)-C(12)-C(17)-C(16)	0.1(7)
S(1)-C(12)-C(17)-C(16)	177.8(4)
C(3)-C(2)-O(2)-S(1)	-69.4(5)
C(1)-C(2)-O(2)-S(1)	114.0(4)
O(3)-O(3)-S(1)-O(4)	0.0(7)
O(3)-O(3)-S(1)-O(2)	0.0(8)
O(3)-O(3)-S(1)-C(12)	0.0(8)
C(2)-O(2)-S(1)-O(4)	-174.2(3)
C(2)-O(2)-S(1)-O(3)	58.4(4)
C(2)-O(2)-S(1)-O(3)	58.4(4)
C(2)-O(2)-S(1)-C(12)	-58.2(4)
C(13)-C(12)-S(1)-O(4)	32.4(4)
C(17)-C(12)-S(1)-O(4)	-145.4(4)
C(13)-C(12)-S(1)-O(3)	166.3(4)
C(17)-C(12)-S(1)-O(3)	-11.4(4)

C(13)-C(12)-S(1)-O(3)	166.3(4)
C(17)-C(12)-S(1)-O(3)	-11.4(4)
C(13)-C(12)-S(1)-O(2)	-77.8(4)
C(17)-C(12)-S(1)-O(2)	104.5(4)

Table A.6: Hydrogen bonds for 2-(tosyloxy)tropone [Å and °].

D-H...A	d(D-H)	d(H...A)	d(D...A)	<(DHA)
C(3)-H(3)...O(3)	0.95	2.47	3.028(6)	117.6
C(17)-H(17)...O(3)	0.95	2.56	2.925(6)	103.2
C(14)-H(14)...O(3)[1]	0.95	2.55	3.162(6)	122.6

Symmetry transformations used to generate equivalent atoms:

[1] x-1/2, -y+1/2, z-1/2

APPENDIX B

Table B.1: Atomic coordinates (x 10^4) and equivalent isotropic displacement parameters ($Å^2$ x 10^3) for 2-(methylamino)tropone. U(eq) is defined as one third of the trace of the orthogonalized U^{ij} tensor.

	x	y	z	U(eq)
C(8A)	1233(1)	5412(2)	2112(1)	62(1)
C(8B)	4967(1)	4930(2)	2681(1)	58(1)
C(8C)	1972(1)	2657(2)	-1038(1)	58(1)
N(1A)	1328(1)	6414(2)	2873(1)	45(1)
N(1B)	4353(1)	5549(2)	3000(1)	45(1)
N(1C)	2325(1)	3172(2)	-151(1)	44(1)
O(1A)	1746(1)	8358(1)	4178(1)	52(1)
O(1B)	3097(1)	6182(1)	3371(1)	51(1)
O(1C)	2881(1)	4604(1)	1332(1)	57(1)
C(1B)	3746(1)	6701(2)	3922(1)	37(1)
C(2B)	4500(1)	6308(2)	3761(1)	37(1)
C(3B)	5287(1)	6622(2)	4313(1)	47(1)
C(4B)	5574(1)	7385(2)	5119(1)	54(1)
C(5B)	5163(1)	8101(2)	5592(1)	55(1)
C(6B)	4326(1)	8237(2)	5360(1)	51(1)
C(7B)	3725(1)	7642(2)	4643(1)	43(1)
C(1C)	2796(1)	3014(2)	1352(1)	39(1)
C(2C)	2528(1)	2103(2)	520(1)	34(1)
C(3C)	2494(1)	340(2)	394(1)	40(1)
C(4C)	2618(1)	-998(2)	974(1)	45(1)
C(5C)	2794(1)	-966(2)	1841(1)	49(1)
C(6C)	2920(1)	487(2)	2357(1)	49(1)
C(7C)	2928(1)	2181(2)	2151(1)	45(1)
C(1A)	1073(1)	7648(2)	4029(1)	41(1)
C(2A)	790(1)	6522(2)	3268(1)	39(1)
C(3A)	56(1)	5652(2)	2957(1)	53(1)
C(4A)	-565(1)	5510(2)	3281(1)	64(1)
C(5A)	-645(1)	6213(3)	3993(1)	70(1)
C(6A)	-101(1)	7312(3)	4571(1)	70(1)
C(7A)	630(1)	7941(2)	4583(1)	58(1)

Appendix B

Table B.2: Bond distances [Å] and angles [°] for 2-(methylamino)tropone.

Bond	Bond distance	Bond angle	Angle
C(8A)-N(1A)	1.4516(19)	**N(1A)-C(8A)-H(8A1)**	109.5
C(8A)-H(8A1)	0.9800	**N(1A)-C(8A)-H(8A2)**	109.5
C(8A)-H(8A2)	0.9800	**H(8A1)-C(8A)-H(8A2)**	109.5
C(8A)-H(8A3)	0.9800	**N(1A)-C(8A)-H(8A3)**	109.5
C(8B)-N(1B)	1.4473(18)	**H(8A1)-C(8A)-H(8A3)**	109.5
C(8B)-H(8B1)	0.9800	**H(8A2)-C(8A)-H(8A3)**	109.5
C(8B)-H(8B2)	0.9800	**N(1B)-C(8B)-H(8B1)**	109.5
C(8B)-H(8B3)	0.9800	**N(1B)-C(8B)-H(8B2)**	109.5
C(8C)-N(1C)	1.4491(18)	**H(8B1)-C(8B)-H(8B2)**	109.5
C(8C)-H(8C1)	0.9800	**N(1B)-C(8B)-H(8B3)**	109.5
C(8C)-H(8C2)	0.9800	**H(8B1)-C(8B)-H(8B3)**	109.5
C(8C)-H(8C3)	0.9800	**H(8B2)-C(8B)-H(8B3)**	109.5
N(1A)-C(2A)	1.3370(18)	**N(1C)-C(8C)-H(8C1)**	109.5
N(1A)-HN1A	0.878(18)	**N(1C)-C(8C)-H(8C2)**	109.5
N(1B)-C(2B)	1.3447(18)	**H(8C1)-C(8C)-H(8C2)**	109.5
N(1B)-HN1B	0.894(15)	**N(1C)-C(8C)-H(8C3)**	109.5
N(1C)-C(2C)	1.3423(17)	**H(8C1)-C(8C)-H(8C3)**	109.5
N(1C)-HN1C	0.890(16)	**H(8C2)-C(8C)-H(8C3)**	109.5
O(1A)-O(1A)	0.000(3)	**C(2A)-N(1A)-C(8A)**	125.71(13)
O(1A)-C(1A)	1.2520(17)	**C(2A)-N(1A)-HN1A**	115.1(11)
O(1B)-O(1B)	0.000(2)	**C(8A)-N(1A)-HN1A**	118.7(11)
O(1B)-C(1B)	1.2566(16)	**C(2B)-N(1B)-C(8B)**	125.24(13)
O(1C)-O(1C)	0.000(2)	**C(2B)-N(1B)-HN1B**	114.5(10)
O(1C)-C(1C)	1.2539(16)	**C(8B)-N(1B)-HN1B**	120.3(10)
C(1B)-O(1B)	1.2566(15)	**C(2C)-N(1C)-C(8C)**	125.08(13)
C(1B)-C(7B)	1.4237(19)	**C(2C)-N(1C)-HN1C**	114.7(10)
C(1B)-C(2B)	1.4777(18)	**C(8C)-N(1C)-HN1C**	119.5(10)
C(2B)-C(3B)	1.3919(19)	**O(1A)-O(1A)-C(1A)**	0(10)
C(3B)-C(4B)	1.395(2)	**O(1B)-O(1B)-C(1B)**	0(10)
C(3B)-H(3B)	0.9500	**O(1C)-O(1C)-C(1C)**	0(10)
C(4B)-C(5B)	1.366(2)	**O(1B)-C(1B)-O(1B)**	0.00(11)
C(4B)-H(4B)	0.9500	**O(1B)-C(1B)-C(7B)**	119.86(12)
C(5B)-C(6B)	1.392(2)	**O(1B)-C(1B)-C(7B)**	119.86(12)
C(5B)-H(5B)	0.9500	**O(1B)-C(1B)-C(2B)**	116.38(12)
C(6B)-C(7B)	1.372(2)	**O(1B)-C(1B)-C(2B)**	116.38(12)

C(6B)-H(6B)	0.9500	**C(7B)-C(1B)-C(2B)**	123.75(12)
C(7B)-H(7B)	0.9500	**N(1B)-C(2B)-C(3B)**	121.27(13)
C(1C)-O(1C)	1.2539(16)	**N(1B)-C(2B)-C(1B)**	112.31(11)
C(1C)-C(7C)	1.4291(19)	**C(3B)-C(2B)-C(1B)**	126.40(13)
C(1C)-C(2C)	1.4834(18)	**C(2B)-C(3B)-C(4B)**	130.76(14)
C(2C)-C(3C)	1.3924(18)	**C(2B)-C(3B)-H(3B)**	114.6
C(3C)-C(4C)	1.3912(19)	**C(4B)-C(3B)-H(3B)**	114.6
C(3C)-H(3C)	0.9500	**C(5B)-C(4B)-C(3B)**	130.44(14)
C(4C)-C(5C)	1.372(2)	**C(5B)-C(4B)-H(4B)**	114.8
C(4C)-H(4C)	0.9500	**C(3B)-C(4B)-H(4B)**	114.8
C(5C)-C(6C)	1.395(2)	**C(4B)-C(5B)-C(6B)**	126.63(14)
C(5C)-H(5C)	0.9500	**C(4B)-C(5B)-H(5B)**	116.7
C(6C)-C(7C)	1.370(2)	**C(6B)-C(5B)-H(5B)**	116.7
C(6C)-H(6C)	0.9500	**C(7B)-C(6B)-C(5B)**	129.40(15)
C(7C)-H(7C)	0.9500	**C(7B)-C(6B)-H(6B)**	115.3
C(1A)-O(1A)	1.2520(17)	**C(5B)-C(6B)-H(6B)**	115.3
C(1A)-C(7A)	1.426(2)	**C(6B)-C(7B)-C(1B)**	132.21(14)
C(1A)-C(2A)	1.4816(19)	**C(6B)-C(7B)-H(7B)**	113.9
C(2A)-C(3A)	1.3907(19)	**C(1B)-C(7B)-H(7B)**	113.9
C(3A)-C(4A)	1.387(2)	**O(1C)-C(1C)-O(1C)**	0.00(10)
C(3A)-H(3A)	0.9500	**O(1C)-C(1C)-C(7C)**	119.73(12)
C(4A)-C(5A)	1.362(3)	**O(1C)-C(1C)-C(7C)**	119.73(12)
C(4A)-H(4A)	0.9500	**O(1C)-C(1C)-C(2C)**	116.85(12)
C(5A)-C(6A)	1.392(3)	**O(1C)-C(1C)-C(2C)**	116.85(12)
C(5A)-H(5A)	0.9500	**C(7C)-C(1C)-C(2C)**	123.38(12)
C(6A)-C(7A)	1.373(2)	**N(1C)-C(2C)-C(3C)**	120.27(12)
C(6A)-H(6A)	0.9500	**N(1C)-C(2C)-C(1C)**	112.84(11)
C(7A)-H(7A)	0.9500	**C(3C)-C(2C)-C(1C)**	126.87(12)
		C(4C)-C(3C)-C(2C)	130.58(13)
		C(4C)-C(3C)-H(3C)	114.7
		C(2C)-C(3C)-H(3C)	114.7
		C(5C)-C(4C)-C(3C)	130.16(13)
		C(5C)-C(4C)-H(4C)	114.9
		C(3C)-C(4C)-H(4C)	114.9
		C(4C)-C(5C)-C(6C)	126.53(14)
		C(4C)-C(5C)-H(5C)	116.7
		C(6C)-C(5C)-H(5C)	116.7

C(7C)-C(6C)-C(5C)	130.17(14)
C(7C)-C(6C)-H(6C)	114.9
C(5C)-C(6C)-H(6C)	114.9
C(6C)-C(7C)-C(1C)	131.53(13)
C(6C)-C(7C)-H(7C)	114.2
C(1C)-C(7C)-H(7C)	114.2
O(1A)-C(1A)-O(1A)	0.00(10)
O(1A)-C(1A)-C(7A)	119.85(14)
O(1A)-C(1A)-C(7A)	119.85(14)
O(1A)-C(1A)-C(2A)	116.31(12)
O(1A)-C(1A)-C(2A)	116.31(12)
C(7A)-C(1A)-C(2A)	123.84(13)
N(1A)-C(2A)-C(3A)	120.89(13)
N(1A)-C(2A)-C(1A)	112.24(12)
C(3A)-C(2A)-C(1A)	126.86(13)
C(4A)-C(3A)-C(2A)	130.68(16)
C(4A)-C(3A)-H(3A)	114.7
C(2A)-C(3A)-H(3A)	114.7
C(5A)-C(4A)-C(3A)	130.38(17)
C(5A)-C(4A)-H(4A)	114.8
C(3A)-C(4A)-H(4A)	114.8
C(4A)-C(5A)-C(6A)	126.66(17)
C(4A)-C(5A)-H(5A)	116.7
C(6A)-C(5A)-H(5A)	116.7
C(7A)-C(6A)-C(5A)	130.17(17)
C(7A)-C(6A)-H(6A)	114.9
C(5A)-C(6A)-H(6A)	114.9
C(6A)-C(7A)-C(1A)	131.29(17)
C(6A)-C(7A)-H(7A)	114.4
C(1A)-C(7A)-H(7A)	114.4

Appendix B

Table B.3: Anisotropic displacement parameters ($Å^2$ x 10^3) for 2-(methylamino)tropone. The anisotropic displacement factor exponent takes the form: $-2\pi^2[h^2a^{*2}U^{11} + ... + 2hka^*b^*U^{12}]$.

	U^{11}	U^{22}	U^{33}	U^{23}	U^{13}	U^{12}
C(8A)	63(1)	73(1)	47(1)	-17(1)	16(1)	-3(1)
C(8B)	64(1)	62(1)	58(1)	3(1)	34(1)	10(1)
C(8C)	75(1)	57(1)	37(1)	2(1)	13(1)	0(1)
N(1A)	41(1)	50(1)	43(1)	-9(1)	11(1)	-5(1)
N(1B)	43(1)	52(1)	42(1)	1(1)	17(1)	2(1)
N(1C)	58(1)	37(1)	38(1)	-1(1)	16(1)	-1(1)
O(1A)	48(1)	48(1)	58(1)	-14(1)	13(1)	-7(1)
O(1B)	35(1)	71(1)	44(1)	-6(1)	9(1)	-6(1)
O(1C)	86(1)	36(1)	49(1)	-7(1)	23(1)	-8(1)
C(1B)	36(1)	40(1)	35(1)	7(1)	10(1)	-2(1)
C(2B)	38(1)	37(1)	39(1)	9(1)	14(1)	-1(1)
C(3B)	35(1)	56(1)	51(1)	9(1)	16(1)	0(1)
C(4B)	35(1)	66(1)	52(1)	8(1)	4(1)	-8(1)
C(5B)	51(1)	63(1)	42(1)	-2(1)	5(1)	-14(1)
C(6B)	57(1)	53(1)	42(1)	-5(1)	18(1)	-6(1)
C(7B)	40(1)	49(1)	41(1)	2(1)	16(1)	-1(1)
C(1C)	40(1)	38(1)	41(1)	-6(1)	16(1)	-2(1)
C(2C)	32(1)	36(1)	36(1)	-1(1)	14(1)	0(1)
C(3C)	44(1)	36(1)	41(1)	-5(1)	16(1)	0(1)
C(4C)	47(1)	33(1)	57(1)	-1(1)	19(1)	2(1)
C(5C)	48(1)	42(1)	56(1)	12(1)	16(1)	4(1)
C(6C)	46(1)	58(1)	39(1)	7(1)	12(1)	-2(1)
C(7C)	49(1)	50(1)	37(1)	-5(1)	14(1)	-5(1)
C(1A)	39(1)	36(1)	41(1)	3(1)	8(1)	6(1)
C(2A)	36(1)	34(1)	41(1)	3(1)	7(1)	4(1)
C(3A)	40(1)	50(1)	62(1)	-6(1)	8(1)	-4(1)
C(4A)	39(1)	59(1)	90(1)	6(1)	17(1)	-4(1)
C(5A)	44(1)	79(1)	91(1)	25(1)	31(1)	9(1)
C(6A)	66(1)	88(1)	68(1)	17(1)	37(1)	24(1)
C(7A)	60(1)	64(1)	50(1)	-2(1)	19(1)	11(1)

Table B.4: Hydrogen coordinates (x 10^4) and isotropic displacement parameters ($Å^2$ x 10^3) for 2-(methylamino)tropone.

	x	y	z	U(eq)
H(8A1)	1137	4212	2217	93
H(8A2)	1726	5499	1972	93
H(8A3)	771	5848	1634	93
H(8B1)	5308	5888	2634	87
H(8B2)	4706	4410	2117	87
H(8B3)	5304	4074	3077	87
H(8C1)	2347	1891	-1180	87
H(8C2)	1870	3672	-1405	87
H(8C3)	1460	2058	-1130	87
HN1A	1799(11)	6890(20)	3145(11)	63(5)
HN1B	3828(10)	5398(19)	2694(10)	51(4)
HN1C	2346(9)	4280(20)	-17(10)	56(5)
H(3B)	5698	6256	4107	56
H(4B)	6147	7410	5382	65
H(5B)	5481	8552	6134	66
H(6B)	4145	8829	5756	61
H(7B)	3193	7907	4624	52
H(3C)	2366	-5	-184	48
H(4C)	2573	-2110	732	55
H(5C)	2834	-2041	2119	59
H(6C)	3016	266	2943	58
H(7C)	3041	2937	2623	54
H(3A)	-36	5058	2435	64
H(4A)	-1006	4809	2954	77
H(5A)	-1120	5923	4107	83
H(6A)	-261	7685	5029	84
H(7A)	885	8706	5040	69

Table B.5: Torsion angles [°] for 2-(methylamino)tropone.

Torsion angle	Angle
O(1B)-O(1B)-C(1B)-C(7B)	0.00(8)
O(1B)-O(1B)-C(1B)-C(2B)	0.00(12)
C(8B)-N(1B)-C(2B)-C(3B)	2.3(2)
C(8B)-N(1B)-C(2B)-C(1B)	-176.59(13)
O(1B)-C(1B)-C(2B)-N(1B)	4.67(17)
O(1B)-C(1B)-C(2B)-N(1B)	4.67(17)
C(7B)-C(1B)-C(2B)-N(1B)	-174.08(12)
O(1B)-C(1B)-C(2B)-C(3B)	-174.11(13)
O(1B)-C(1B)-C(2B)-C(3B)	-174.11(13)
C(7B)-C(1B)-C(2B)-C(3B)	7.1(2)
N(1B)-C(2B)-C(3B)-C(4B)	179.81(15)
C(1B)-C(2B)-C(3B)-C(4B)	-1.5(2)
C(2B)-C(3B)-C(4B)-C(5B)	-2.5(3)
C(3B)-C(4B)-C(5B)-C(6B)	-0.2(3)
C(4B)-C(5B)-C(6B)-C(7B)	3.2(3)
C(5B)-C(6B)-C(7B)-C(1B)	0.8(3)
O(1B)-C(1B)-C(7B)-C(6B)	174.25(15)
O(1B)-C(1B)-C(7B)-C(6B)	174.25(15)
C(2B)-C(1B)-C(7B)-C(6B)	-7.0(2)
O(1C)-O(1C)-C(1C)-C(7C)	0.0(2)
O(1C)-O(1C)-C(1C)-C(2C)	0.00(18)
C(8C)-N(1C)-C(2C)-C(3C)	7.7(2)
C(8C)-N(1C)-C(2C)-C(1C)	-173.99(13)
O(1C)-C(1C)-C(2C)-N(1C)	-7.19(17)
O(1C)-C(1C)-C(2C)-N(1C)	-7.19(17)
C(7C)-C(1C)-C(2C)-N(1C)	170.44(12)
O(1C)-C(1C)-C(2C)-C(3C)	170.98(13)
O(1C)-C(1C)-C(2C)-C(3C)	170.98(13)
C(7C)-C(1C)-C(2C)-C(3C)	-11.4(2)
N(1C)-C(2C)-C(3C)-C(4C)	-174.99(14)
C(1C)-C(2C)-C(3C)-C(4C)	7.0(2)
C(2C)-C(3C)-C(4C)-C(5C)	1.4(3)
C(3C)-C(4C)-C(5C)-C(6C)	-2.5(3)
C(4C)-C(5C)-C(6C)-C(7C)	-2.3(3)
C(5C)-C(6C)-C(7C)-C(1C)	1.4(3)

O(1C)-C(1C)-C(7C)-C(6C)	-175.91(15)
O(1C)-C(1C)-C(7C)-C(6C)	-175.91(15)
C(2C)-C(1C)-C(7C)-C(6C)	6.5(2)
O(1A)-O(1A)-C(1A)-C(7A)	0.00(3)
O(1A)-O(1A)-C(1A)-C(2A)	0.00(2)
C(8A)-N(1A)-C(2A)-C(3A)	-0.8(2)
C(8A)-N(1A)-C(2A)-C(1A)	179.77(13)
O(1A)-C(1A)-C(2A)-N(1A)	1.89(17)
O(1A)-C(1A)-C(2A)-N(1A)	1.89(17)
C(7A)-C(1A)-C(2A)-N(1A)	-177.80(13)
O(1A)-C(1A)-C(2A)-C(3A)	-177.44(14)
O(1A)-C(1A)-C(2A)-C(3A)	-177.44(14)
C(7A)-C(1A)-C(2A)-C(3A)	2.9(2)
N(1A)-C(2A)-C(3A)-C(4A)	176.29(16)
C(1A)-C(2A)-C(3A)-C(4A)	-4.4(3)
C(2A)-C(3A)-C(4A)-C(5A)	1.6(3)
C(3A)-C(4A)-C(5A)-C(6A)	1.5(3)
C(4A)-C(5A)-C(6A)-C(7A)	-0.6(3)
C(5A)-C(6A)-C(7A)-C(1A)	-1.7(3)
O(1A)-C(1A)-C(7A)-C(6A)	-178.89(17)
O(1A)-C(1A)-C(7A)-C(6A)	-178.89(17)
C(2A)-C(1A)-C(7A)-C(6A)	0.8(3)

Table B.6: Hydrogen bonds for 2-(methylamino)tropone [Å and °].

D-H...A	d(D-H)	d(H...A)	d(D...A)	<(DHA)
N(1A)-HN1A...O(1A)	0.878(18)	2.102(17)	2.5455(16)	110.5(13)
N(1A)-HN1A...O(1B)	0.878(18)	2.254(17)	2.9376(17)	134.6(15)
N(1B)-HN1B...O(1B)	0.894(15)	2.086(15)	2.5512(16)	111.4(12)
N(1B)-HN1B...O(1C)	0.894(15)	2.383(16)	3.1558(18)	144.8(13)
N(1C)-HN1C...O(1C)	0.890(16)	2.130(16)	2.5776(16)	110.3(13)
N(1C)-HN1C...O(1A)[1]	0.890(16)	2.312(16)	2.9759(17)	131.3(13)
C(5C)-H(5C)...O(1B)[2]	0.95	2.42	3.2915(19)	152.8
C(7B)-H(7B)...O(1A)	0.95	2.42	3.3443(19)	164.5
C(8C)-H(8C2)...O(1A)[1]	0.98	2.56	3.178(2)	121.2

Symmetry transformations used to generate equivalent atoms:

[1] x, -y+3/2, z-1/2 [2] x, y-1, z

APPENDIX C

Table C.1: Atomic coordinates (x 10^4) and equivalent isotropic displacement parameters ($Å^2$ x 10^3) for 2-(2-fluoroethylamino)tropone. U(eq) is defined as one third of the trace of the orthogonalized U^{ij} tensor.

	x	y	z	U(eq)
F(1)	8689(2)	2534(5)	5009(1)	72(1)
O(1)	4439(2)	-203(5)	5782(1)	50(1)
N(1)	6240(3)	3463(6)	5748(2)	36(1)
C(2)	5722(3)	3310(7)	6434(2)	34(1)
C(1)	4697(3)	1135(7)	6415(2)	38(1)
C(3)	6152(3)	5048(7)	7070(2)	41(1)
C(8)	7221(3)	5430(7)	5575(2)	42(1)
C(6)	4090(4)	1608(8)	7822(2)	48(1)
C(9)	7828(4)	4760(8)	4855(2)	50(1)
C(4)	5801(4)	5202(8)	7834(2)	47(1)
C(5)	4891(4)	3714(8)	8180(2)	49(1)
C(7)	4001(4)	541(7)	7069(2)	46(1)

Appendix C

Table C.2: Bond distances [Å] and angles [°] for 2-(2-fluoroethylamino)tropone.

Bond	Bond distance	Bond angle	Angle
F(1)-C(9)	1.394(4)	**C(2)-N(1)-C(8)**	125.3(3)
O(1)-C(1)	1.248(4)	**C(2)-N(1)-HN1**	113.2(19)
N(1)-C(2)	1.342(4)	**C(8)-N(1)-HN1**	121.5(19)
N(1)-C(8)	1.439(4)	**N(1)-C(2)-C(3)**	121.3(3)
N(1)-HN1	0.94(3)	**N(1)-C(2)-C(1)**	112.3(3)
C(2)-C(3)	1.388(5)	**C(3)-C(2)-C(1)**	126.4(3)
C(2)-C(1)	1.477(5)	**O(1)-C(1)-C(7)**	119.8(3)
C(1)-C(7)	1.423(5)	**O(1)-C(1)-C(2)**	116.8(3)
C(3)-C(4)	1.391(4)	**C(7)-C(1)-C(2)**	123.4(3)
C(3)-H(3)	0.9500	**C(2)-C(3)-C(4)**	131.2(4)
C(8)-C(9)	1.478(4)	**C(2)-C(3)-H(3)**	114.4
C(8)-H(8A)	0.9900	**C(4)-C(3)-H(3)**	114.4
C(8)-H(8B)	0.9900	**N(1)-C(8)-C(9)**	112.9(3)
C(6)-C(7)	1.366(5)	**N(1)-C(8)-H(8A)**	109.0
C(6)-C(5)	1.388(5)	**C(9)-C(8)-H(8A)**	109.0
C(6)-H(6)	0.9500	**N(1)-C(8)-H(8B)**	109.0
C(9)-H(9B)	0.9900	**C(9)-C(8)-H(8B)**	109.0
C(9)-H(9A)	0.9900	**H(8A)-C(8)-H(8B)**	107.8
C(4)-C(5)	1.366(5)	**C(7)-C(6)-C(5)**	129.9(4)
C(4)-H(4)	0.9500	**C(7)-C(6)-H(6)**	115.1
C(5)-H(5)	0.9500	**C(5)-C(6)-H(6)**	115.1
C(7)-H(7)	0.9500	**F(1)-C(9)-C(8)**	110.0(3)
		F(1)-C(9)-H(9B)	109.7
		C(8)-C(9)-H(9B)	109.7
		F(1)-C(9)-H(9A)	109.7
		C(8)-C(9)-H(9A)	109.7
		H(9B)-C(9)-H(9A)	108.2
		C(5)-C(4)-C(3)	130.4(4)
		C(5)-C(4)-H(4)	114.8
		C(3)-C(4)-H(4)	114.8
		C(4)-C(5)-C(6)	126.2(3)
		C(4)-C(5)-H(5)	116.9
		C(6)-C(5)-H(5)	116.9
		C(6)-C(7)-C(1)	132.5(4)

C(6)-C(7)-H(7)	113.8
C(1)-C(7)-H(7)	113.8

Table C.3: Anisotropic displacement parameters ($Å^2$ x 10^3) for 2-(2-fluoroethylamino)tropone. The anisotropic displacement factor exponent takes the form: $-2\pi^2[h^2a^{*2}U^{11} + ... + 2hka^*b^*U^{12}]$.

	U^{11}	U^{22}	U^{33}	U^{23}	U^{13}	U^{12}
F(1)	61(2)	80(2)	81(2)	-6(1)	28(1)	10(1)
O(1)	61(2)	55(2)	35(1)	-9(1)	11(1)	-17(1)
N(1)	38(2)	40(2)	31(2)	-2(1)	6(1)	-3(1)
C(2)	30(2)	39(2)	32(2)	4(2)	7(1)	7(2)
C(1)	35(2)	45(2)	36(2)	3(2)	7(2)	3(2)
C(3)	44(2)	44(2)	36(2)	-4(2)	7(2)	2(2)
C(8)	42(2)	48(2)	37(2)	1(2)	7(2)	-9(2)
C(6)	55(2)	56(2)	39(2)	6(2)	21(2)	13(2)
C(9)	49(2)	55(3)	47(2)	4(2)	11(2)	-4(2)
C(4)	50(2)	52(2)	36(2)	-6(2)	2(2)	10(2)
C(5)	55(2)	60(3)	31(2)	-1(2)	9(2)	20(2)
C(7)	41(2)	51(2)	50(2)	0(2)	17(2)	-3(2)

Table C.4: Hydrogen coordinates (x 10^4) and isotropic displacement parameters ($Å^2$ x 10^3) for 2-(2-fluoroethylamino)tropone.

	x	y	z	U(eq)
H(3)	6798	6362	6964	50
H(8A)	7972	5587	6045	51
H(8B)	6756	7193	5492	51
H(6)	3516	782	8152	58
H(9B)	7081	4372	4397	60
H(9A)	8364	6307	4707	60
H(4)	6270	6559	8169	56
H(5)	4798	4163	8715	58
H(7)	3348	-871	6961	55
HN1	5890(30)	2140(60)	5370(19)	37(9)

Table C.5: Torsion angles [°] for 2-(2-fluoroethylamino)tropone.

Torsion angle	Angle
C(8)-N(1)-C(2)-C(3)	-2.7(5)
C(8)-N(1)-C(2)-C(1)	177.7(3)
N(1)-C(2)-C(1)-O(1)	-1.0(4)
C(3)-C(2)-C(1)-O(1)	179.4(3)
N(1)-C(2)-C(1)-C(7)	179.6(3)
C(3)-C(2)-C(1)-C(7)	0.1(5)
N(1)-C(2)-C(3)-C(4)	-177.5(3)
C(1)-C(2)-C(3)-C(4)	2.0(6)
C(2)-N(1)-C(8)-C(9)	167.6(3)
N(1)-C(8)-C(9)-F(1)	-69.1(4)
C(2)-C(3)-C(4)-C(5)	-2.0(6)
C(3)-C(4)-C(5)-C(6)	0.6(6)
C(7)-C(6)-C(5)-C(4)	-0.5(6)
C(5)-C(6)-C(7)-C(1)	1.9(7)
O(1)-C(1)-C(7)-C(6)	178.5(4)
C(2)-C(1)-C(7)-C(6)	-2.1(6)

Table C.6: Hydrogen bonds for 2-(2-fluoroethylamino)tropone [Å and °].

D-H...A	d(D-H)	d(H...A)	d(D...A)	<(DHA)
N(1)-HN1...O(1)	0.94(3)	2.05(3)	2.552(4)	112(2)
N(1)-HN1...O(1)[1]	0.94(3)	2.14(3)	3.027(4)	156(3)
C(9)-H(9B)...O(1)[1]	0.99	2.55	3.236(5)	126.4

Symmetry transformations used to generate equivalent atoms:

[1] -x+1, -y, -z+1

APPENDIX D

Checkcif: 2-tosyloxytropone (TropOTs)

checkCIF/PLATON report

Structure factors have been supplied for datablock(s) I

THIS REPORT IS FOR GUIDANCE ONLY. IF USED AS PART OF A REVIEW PROCEDURE FOR PUBLICATION, IT SHOULD NOT REPLACE THE EXPERTISE OF AN EXPERIENCED CRYSTALLOGRAPHIC REFEREE.

No syntax errors found. CIF dictionary Interpreting this report

Datablock: I

```
Bond precision:  C-C = 0.0074 A          Wavelength=0.71073

Cell:            a=7.882(3)     b=14.943(5)          c=10.762(4)
                 alpha=90       beta=96.135(12)      gamma=90
Temperature:     100 K

                 Calculated                Reported
Volume           1260.3(8)                 1260.3(8)
Space group      C c                       C c
Hall group       C -2yc                    C -2yc
Moiety formula   C14 H12 O4 S              C14 H12 O4 S1
Sum formula      C14 H12 O4 S              C14 H12 O4 S
Mr               276.30                    276.30
Dx,g cm-3        1.456                     1.541
Z                4                         4
Mu (mm-1)        0.264                     0.274
F000             576.0                     608.0
F000'            576.80
h,k,lmax         10,19,14                  10,19,14
Nref             3045[ 1527]               2956
Tmin,Tmax        0.909,0.944               0.909,0.944
Tmin'            0.909

Correction method= # Reported T Limits: Tmin=0.909 Tmax=0.944
AbsCorr = MULTI-SCAN

Data completeness= 1.94/0.97       Theta(max)= 28.000

R(reflections)= 0.0405( 2586)      wR2(reflections)= 0.1560( 2956)

S = 1.014                  Npar= 173
```

The following ALERTS were generated. Each ALERT has the format
test-name_ALERT_alert-type_alert-level.
Click on the hyperlinks for more details of the test.

Appendix D

Alert level B

```
DENSD01_ALERT_1_B  The ratio of the submitted crystal density and that
           calculated from the formula is outside the range 0.95 <> 1.05
           Crystal density given    =      1.541
           Calculated crystal density =      1.456
PLAT044_ALERT_1_B Calculated and Reported Density Dx  Differ by ..      0.0848 Check
PLAT046_ALERT_1_B Reported Z, MW and D(calc) are Inconsistent ....       1.456 Check
PLAT934_ALERT_3_B Number of (Iobs-Icalc)/Sigma(W) > 10 Outliers ..           6 Check
```

Alert level C

```
ABSMU01_ALERT_1_C  The ratio of given/expected absorption coefficient lies
              outside the range 0.99 <> 1.01
           Calculated value of mu =     0.264
           Value of mu given      =     0.274
PLAT068_ALERT_1_C Reported F000 Differs from Calcd (or Missing)...     Please Check
PLAT340_ALERT_3_C Low Bond Precision on  C-C Bonds ...............    0.00736 Ang.
PLAT918_ALERT_3_C Reflection(s) with I(obs) much Smaller I(calc) .          6 Check
PLAT939_ALERT_3_C Large Value of Not (SHELXL) Weight Optimized S .      59.26 Check
```

Alert level G

```
PLAT066_ALERT_1_G Predicted and Reported Tmin&Tmax Range Identical          ? Check
PLAT072_ALERT_2_G SHELXL First  Parameter in WGHT  Unusually Large       0.11 Report
PLAT093_ALERT_1_G No s.u.'s on H-positions, Refinement Reported as      mixed Check
PLAT380_ALERT_4_G Incorrectly? Oriented X(sp2)-Methyl Moiety .....        C18 Check
PLAT779_ALERT_4_G Suspect or Irrelevant (Bond) Angle(s) in CIF . #         47 Check
             O3   -O3   -S1      1.555   1.555   1.555             0.00 Deg.
PLAT779_ALERT_4_G Suspect or Irrelevant (Bond) Angle(s) in CIF . #         50 Check
             O3   -S1   -O3      1.555   1.555   1.555             0.00 Deg.
PLAT882_ALERT_1_G No Datum for _diffrn_reflns_av_unetI/netI ......     Please Do !
PLAT910_ALERT_3_G Missing # of FCF Reflection(s) Below Theta(Min).          2 Note
PLAT916_ALERT_2_G Hooft y and Flack x Parameter Values Differ by .       0.43 Check
PLAT933_ALERT_2_G Number of OMIT Records in Embedded .res File ...          3 Note
PLAT941_ALERT_3_G Average HKL Measurement Multiplicity ...........        4.5 Low
PLAT978_ALERT_2_G Number C-C Bonds with Positive Residual Density.          2 Info
```

```
   0 ALERT level A = Most likely a serious problem - resolve or explain
   4 ALERT level B = A potentially serious problem, consider carefully
   5 ALERT level C = Check. Ensure it is not caused by an omission or oversight
  12 ALERT level G = General information/check it is not something unexpected

   8 ALERT type 1 CIF construction/syntax error, inconsistent or missing data
   4 ALERT type 2 Indicator that the structure model may be wrong or deficient
   6 ALERT type 3 Indicator that the structure quality may be low
   3 ALERT type 4 Improvement, methodology, query or suggestion
   0 ALERT type 5 Informative message, check
```

Appendix D

Publication of your CIF

You should attempt to resolve as many as possible of the alerts in all categories. Often the minor alerts point to easily fixed oversights, errors and omissions in your CIF or refinement strategy, so attention to these fine details can be worthwhile. In order to resolve some of the more serious problems it may be necessary to carry out additional measurements or structure refinements. However, the nature of your study may justify the reported deviations from journal submission requirements and the more serious of these should be commented upon in the discussion or experimental section of a paper or in the "special_details" fields of the CIF. *checkCIF* was carefully designed to identify outliers and unusual parameters, but every test has its limitations and alerts that are not important in a particular case may appear. Conversely, the absence of alerts does not guarantee there are no aspects of the results needing attention. It is up to the individual to critically assess their own results and, if necessary, seek expert advice.

If you wish to submit your CIF for publication in Acta Crystallographica Section C or E, you should upload your CIF via the web. If you wish to submit your CIF for publication in IUCrData you should upload your CIF via the web. If your CIF is to form part of a submission to another IUCr journal, you will be asked, either during electronic submission or by the Co-editor handling your paper, to upload your CIF via our web site.

PLATON version of 18/09/2020; check.def file version of 20/08/2020

Datablock I - ellipsoid plot

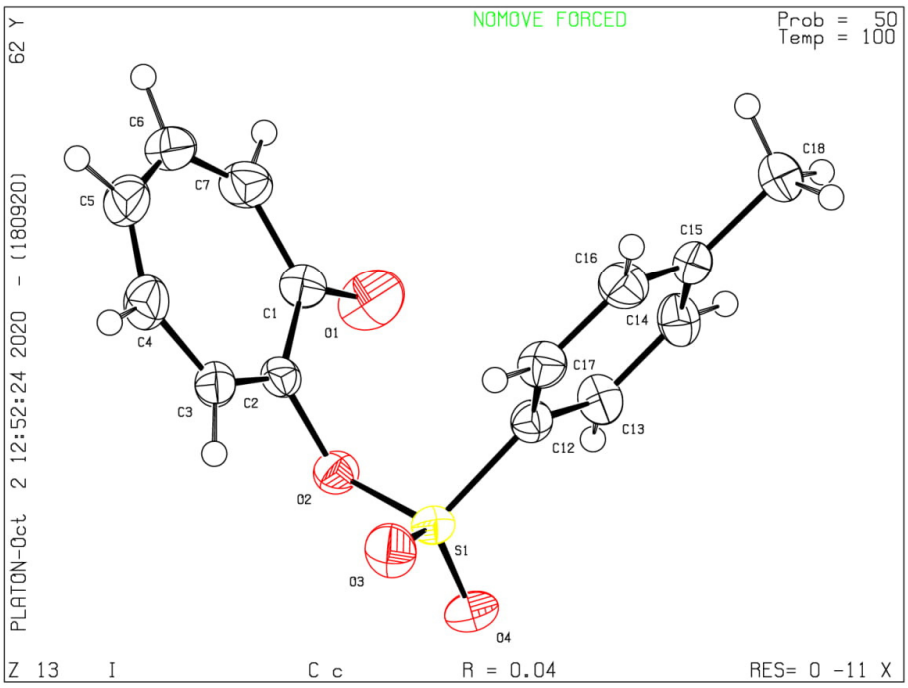

Appendix D

Checkcif: 2-(methylamino)tropone (TropNHMe)

checkCIF/PLATON report

Structure factors have been supplied for datablock(s) I

THIS REPORT IS FOR GUIDANCE ONLY. IF USED AS PART OF A REVIEW PROCEDURE FOR PUBLICATION, IT SHOULD NOT REPLACE THE EXPERTISE OF AN EXPERIENCED CRYSTALLOGRAPHIC REFEREE.

No syntax errors found. CIF dictionary Interpreting this report

Datablock: I

```
Bond precision:  C-C = 0.0021 A          Wavelength=0.71073

Cell:            a=17.635(5)     b=7.817(2)          c=16.718(4)
                 alpha=90        beta=110.639(9)     gamma=90
Temperature:     100 K

                Calculated               Reported
Volume          2156.7(10)               2156.8(10)
Space group     P 21/c                   P 21/c
Hall group      -P 2ybc                  -P 2ybc
Moiety formula  C8 H9 N O                C8 H9 N1 O1
Sum formula     C8 H9 N O                C8 H9 N O
Mr              135.16                   135.16
Dx,g cm-3       1.249                    1.249
Z               12                       12
Mu (mm-1)       0.083                    0.083
F000            864.0                    864.0
F000'           864.36
h,k,lmax        23,10,22                 23,10,22
Nref            5206                     5192
Tmin,Tmax       0.970,0.977              0.970,0.977
Tmin'           0.953

Correction method= # Reported T Limits: Tmin=0.970 Tmax=0.977
AbsCorr = MULTI-SCAN

Data completeness= 0.997          Theta(max)= 27.994

R(reflections)= 0.0394( 3575)     wR2(reflections)= 0.1036( 5192)

S = 1.026                 Npar= 287
```

The following ALERTS were generated. Each ALERT has the format
test-name_ALERT_alert-type_alert-level.
Click on the hyperlinks for more details of the test.

Appendix D

Alert level B

```
PLAT910_ALERT_3_B Missing # of FCF Reflection(s) Below Theta(Min).         15 Note
```

Alert level C

```
PLAT230_ALERT_2_C Hirshfeld Test Diff for    C5A      --C6A      .        6.3 s.u.
PLAT905_ALERT_3_C Negative K value in the Analysis of Variance ...     -0.076 Report
```

Alert level G

```
PLAT066_ALERT_1_G Predicted and Reported Tmin&Tmax Range Identical          ? Check
PLAT720_ALERT_4_G Number of Unusual/Non-Standard Labels .........          12 Note
PLAT779_ALERT_4_G Suspect or Irrelevant (Bond) Angle(s) in CIF . #         28 Check
              O1A  -O1A  -C1A     1.555   1.555   1.555              0.00 Deg.
PLAT779_ALERT_4_G Suspect or Irrelevant (Bond) Angle(s) in CIF . #         29 Check
              O1B  -O1B  -C1B     1.555   1.555   1.555              0.00 Deg.
PLAT779_ALERT_4_G Suspect or Irrelevant (Bond) Angle(s) in CIF . #         30 Check
              O1C  -O1C  -C1C     1.555   1.555   1.555              0.00 Deg.
PLAT779_ALERT_4_G Suspect or Irrelevant (Bond) Angle(s) in CIF . #         31 Check
              O1B  -C1B  -O1B     1.555   1.555   1.555              0.00 Deg.
PLAT779_ALERT_4_G Suspect or Irrelevant (Bond) Angle(s) in CIF . #         55 Check
              O1C  -C1C  -O1C     1.555   1.555   1.555              0.00 Deg.
PLAT779_ALERT_4_G Suspect or Irrelevant (Bond) Angle(s) in CIF . #         79 Check
              O1A  -C1A  -O1A     1.555   1.555   1.555              0.00 Deg.
PLAT882_ALERT_1_G No Datum for _diffrn_reflns_av_unetI/netI ......     Please Do !
PLAT933_ALERT_2_G Number of OMIT Records in Embedded .res File ...         13 Note
PLAT960_ALERT_3_G Number of Intensities with I  <   - 2*sig(I) ...          4 Check
PLAT978_ALERT_2_G Number C-C Bonds with Positive Residual Density.          8 Info
PLAT992_ALERT_5_G Repd & Actual _reflns_number_gt Values Differ by          2 Check
```

```
   0 ALERT level A = Most likely a serious problem - resolve or explain
   1 ALERT level B = A potentially serious problem, consider carefully
   2 ALERT level C = Check. Ensure it is not caused by an omission or oversight
  13 ALERT level G = General information/check it is not something unexpected

   2 ALERT type 1 CIF construction/syntax error, inconsistent or missing data
   3 ALERT type 2 Indicator that the structure model may be wrong or deficient
   3 ALERT type 3 Indicator that the structure quality may be low
   7 ALERT type 4 Improvement, methodology, query or suggestion
   1 ALERT type 5 Informative message, check
```

Appendix D

Publication of your CIF

You should attempt to resolve as many as possible of the alerts in all categories. Often the minor alerts point to easily fixed oversights, errors and omissions in your CIF or refinement strategy, so attention to these fine details can be worthwhile. In order to resolve some of the more serious problems it may be necessary to carry out additional measurements or structure refinements. However, the nature of your study may justify the reported deviations from journal submission requirements and the more serious of these should be commented upon in the discussion or experimental section of a paper or in the "special_details" fields of the CIF. *checkCIF* was carefully designed to identify outliers and unusual parameters, but every test has its limitations and alerts that are not important in a particular case may appear. Conversely, the absence of alerts does not guarantee there are no aspects of the results needing attention. It is up to the individual to critically assess their own results and, if necessary, seek expert advice.

If you wish to submit your CIF for publication in Acta Crystallographica Section C or E, you should upload your CIF via the web. If you wish to submit your CIF for publication in IUCrData you should upload your CIF via the web. If your CIF is to form part of a submission to another IUCr journal, you will be asked, either during electronic submission or by the Co-editor handling your paper, to upload your CIF via our web site.

PLATON version of 18/09/2020; check.def file version of 20/08/2020

Datablock I - ellipsoid plot

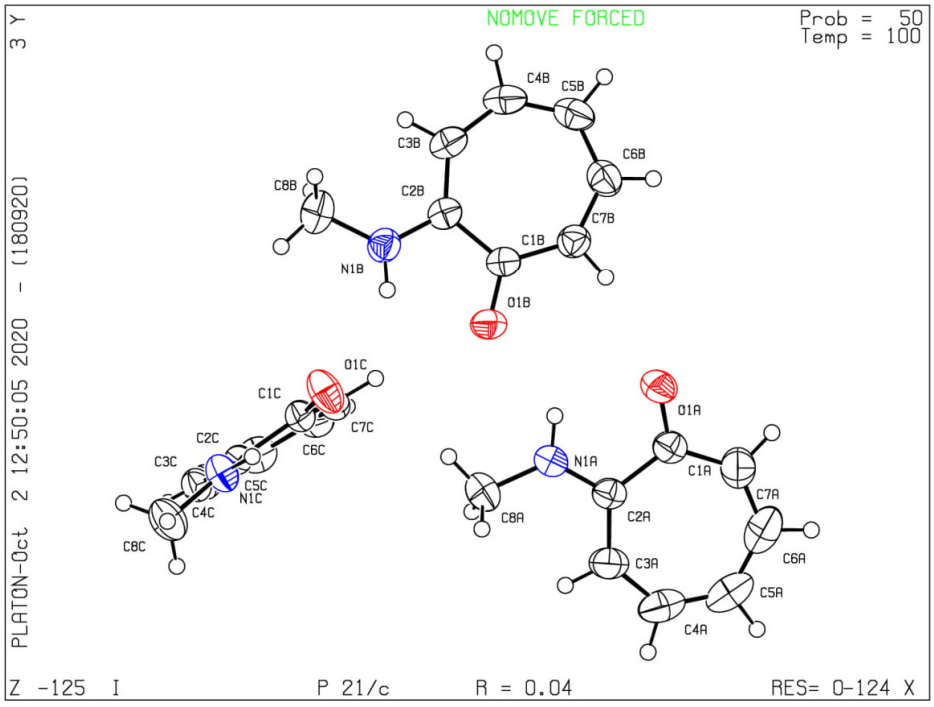

Appendix D

Checkcif: 2-(2-fluoroethylamino)tropone (TropNHEtF)

checkCIF/PLATON report

Structure factors have been supplied for datablock(s) I

THIS REPORT IS FOR GUIDANCE ONLY. IF USED AS PART OF A REVIEW PROCEDURE FOR PUBLICATION, IT SHOULD NOT REPLACE THE EXPERTISE OF AN EXPERIENCED CRYSTALLOGRAPHIC REFEREE.

No syntax errors found. CIF dictionary Interpreting this report

Datablock: I

```
Bond precision:  C-C = 0.0050 A          Wavelength=0.71073

Cell:             a=9.822(3)     b=4.9893(15)        c=16.857(5)
                  alpha=90       beta=99.718(9)      gamma=90
Temperature:      100 K

                Calculated                Reported
Volume          814.2(4)                  814.2(4)
Space group     P 21/n                    P 21/n
Hall group      -P 2yn                    -P 2yn
Moiety formula  C9 H10 F N O              C9 H10 N1 O1 F1
Sum formula     C9 H10 F N O              C9 H10 F N O
Mr              167.18                    167.18
Dx,g cm-3       1.364                     1.364
Z               4                         4
Mu (mm-1)       0.105                     0.105
F000            352.0                     352.0
F000'           352.20
h,k,lmax        12,6,21                   12,6,21
Nref            1782                      1773
Tmin,Tmax       0.986,0.994               0.986,0.994
Tmin'           0.978

Correction method= # Reported T Limits: Tmin=0.986 Tmax=0.994
AbsCorr = MULTI-SCAN

Data completeness= 0.995          Theta(max)= 27.000

R(reflections)= 0.0729( 925)      wR2(reflections)= 0.1681( 1773)

S = 1.083                 Npar= 113
```

The following ALERTS were generated. Each ALERT has the format
test-name_ALERT_alert-type_alert-level.
Click on the hyperlinks for more details of the test.

Alert level C

```
PLAT340_ALERT_3_C Low Bond Precision on  C-C Bonds ..............      0.005 Ang.
PLAT906_ALERT_3_C Large K Value in the Analysis of Variance ......      9.034 Check
```

Alert level G

```
PLAT042_ALERT_1_G Calc. and Reported MoietyFormula Strings  Differ     Please Check
PLAT066_ALERT_1_G Predicted and Reported Tmin&Tmax Range Identical          ? Check
PLAT720_ALERT_4_G Number of Unusual/Non-Standard Labels ..........          1 Note
PLAT882_ALERT_1_G No Datum for _diffrn_reflns_av_unetI/netI ......     Please Do !
PLAT910_ALERT_3_G Missing # of FCF Reflection(s) Below Theta(Min).          1 Note
PLAT912_ALERT_4_G Missing # of FCF Reflections Above STh/L=  0.600          7 Note
PLAT960_ALERT_3_G Number of Intensities with I  <   - 2*sig(I) ...          1 Check
PLAT978_ALERT_2_G Number C-C Bonds with Positive Residual Density.          0 Info
```

0 **ALERT level A** = Most likely a serious problem - resolve or explain
0 **ALERT level B** = A potentially serious problem, consider carefully
2 **ALERT level C** = Check. Ensure it is not caused by an omission or oversight
8 **ALERT level G** = General information/check it is not something unexpected

3 ALERT type 1 CIF construction/syntax error, inconsistent or missing data
1 ALERT type 2 Indicator that the structure model may be wrong or deficient
4 ALERT type 3 Indicator that the structure quality may be low
2 ALERT type 4 Improvement, methodology, query or suggestion
0 ALERT type 5 Informative message, check

checkCIF publication errors

Alert level A

```
PUBL012_ALERT_1_A  _publ_section_abstract is missing.
            Abstract of paper in English.
```

Alert level G

```
PUBL017_ALERT_1_G The _publ_section_references section is missing or
            empty.
```

1 **ALERT level A** = Data missing that is essential or data in wrong format
1 **ALERT level G** = General alerts. Data that may be required is missing

Appendix D

Publication of your CIF

You should attempt to resolve as many as possible of the alerts in all categories. Often the minor alerts point to easily fixed oversights, errors and omissions in your CIF or refinement strategy, so attention to these fine details can be worthwhile. In order to resolve some of the more serious problems it may be necessary to carry out additional measurements or structure refinements. However, the nature of your study may justify the reported deviations from journal submission requirements and the more serious of these should be commented upon in the discussion or experimental section of a paper or in the "special_details" fields of the CIF. *checkCIF* was carefully designed to identify outliers and unusual parameters, but every test has its limitations and alerts that are not important in a particular case may appear. Conversely, the absence of alerts does not guarantee there are no aspects of the results needing attention. It is up to the individual to critically assess their own results and, if necessary, seek expert advice.

If level A alerts remain, which you believe to be justified deviations, and you intend to submit this CIF for publication in a journal, you should additionally insert an explanation in your CIF using the Validation Reply Form (VRF) below. This will allow your explanation to be considered as part of the review process.

Validation response form

Please find below a validation response form (VRF) that can be filled in and pasted into your CIF.

```
# start Validation Reply Form
_vrf_PUBL012_GLOBAL
;
PROBLEM: _publ_section_abstract is missing.
RESPONSE: ...
;
# end Validation Reply Form
```

If you wish to submit your CIF for publication in Acta Crystallographica Section C or E, you should upload your CIF via the web. If you wish to submit your CIF for publication in IUCrData you should upload your CIF via the web. If your CIF is to form part of a submission to another IUCr journal, you will be asked, either during electronic submission or by the Co-editor handling your paper, to upload your CIF via our web site.

PLATON version of 18/09/2020; check.def file version of 20/08/2020

Appendix D

Datablock I - ellipsoid plot